Hiroyuki Kajimoto
Dongjun Lee
Sang-Youn Kim
Masashi Konyo
Ki-Uk Kyung *Editors*

Haptic Interaction

Perception, Devices and Algorithms

Springer

Lecture Notes in Electrical Engineering

Volume 535

The book series *Lecture Notes in Electrical Engineering* (LNEE) publishes the latest developments in Electrical Engineering - quickly, informally and in high quality. While original research reported in proceedings and monographs has traditionally formed the core of LNEE, we also encourage authors to submit books devoted to supporting student education and professional training in the various fields and applications areas of electrical engineering. The series cover classical and emerging topics concerning:

- Communication Engineering, Information Theory and Networks
- Electronics Engineering and Microelectronics
- Signal, Image and Speech Processing
- Wireless and Mobile Communication
- Circuits and Systems
- Energy Systems, Power Electronics and Electrical Machines
- Electro-optical Engineering
- Instrumentation Engineering
- Avionics Engineering
- Control Systems
- Internet-of-Things and Cybersecurity
- Biomedical Devices, MEMS and NEMS

For general information about this book series, comments or suggestions, please contact leontina.dicecco@springer.com.

To submit a proposal or request further information, please contact the Publishing Editor in your country:

China

Jasmine Dou, Associate Editor (jasmine.dou@springer.com)

India

Swati Meherishi, Executive Editor (swati.meherishi@springer.com)
Aninda Bose, Senior Editor (aninda.bose@springer.com)

Japan

Takeyuki Yonezawa, Editorial Director (takeyuki.yonezawa@springer.com)

South Korea

Smith (Ahram) Chae, Editor (smith.chae@springer.com)

Southeast Asia
Ramesh Nath Premnath, Editor (ramesh.premnath@springer.com)

USA, Canada:

Michael Luby, Senior Editor (michael.luby@springer.com)

All other Countries:
Leontina Di Cecco, Senior Editor (leontina.dicecco@springer.com)
Christoph Baumann, Executive Editor (christoph.baumann@springer.com)

** Indexing: The books of this series are submitted to ISI Proceedings, EI-Compendex, SCOPUS, MetaPress, Web of Science and Springerlink **

More information about this series at http://www.springer.com/series/7818

Hiroyuki Kajimoto · Dongjun Lee ·
Sang-Youn Kim · Masashi Konyo ·
Ki-Uk Kyung
Editors

Haptic Interaction

Perception, Devices and Algorithms

Springer

Editors
Hiroyuki Kajimoto
Department of Informatics
The University of Electro-Communications
Chofu, Tokyo, Japan

Sang-Youn Kim
Korea University of Technology
and Education
Cheonan-si, Ch´ungch´ong-namdo,
Korea (Republic of)

Ki-Uk Kyung
Department of Mechanical Engineering
Korea Advanced Institute of Science
and Technology
Daejeon, Korea (Republic of)

Dongjun Lee
School of Mechanical and Aerospace
Engineering
Seoul National University
Seoul, Korea (Republic of)

Masashi Konyo
Tohoku University
Miyagi, Miyagi, Japan

Preface

Welcome to the proceedings of the third international conference, AsiaHaptics 2018, held in Incheon, Korea, during 14–16 November.

AsiaHaptics is a new type of international conference for the haptics fields, featuring interactive presentations with demos. The conference became the place to experience more than 90 demonstrations of haptics research.

While the haptics-related research field is huge, this book divided into six parts.

Part 1 is composed of eight chapters, treating perception and psychophysics of haptics. They are undoubtedly the basis of the haptics research.

Part 2 is composed of nine chapters, treating rendering methods. They treat important steps toward practical application of haptics, such as how to convert recorded vibration, force, and thermal information for haptic display.

Part 3 is composed of 12 chapters, treating haptic technology. These are somewhat in-between science and application, giving novel schemes to convey haptic information.

Part 4 is composed of 28 chapters, treating novel devices. Haptics is still an immature and rapidly growing field, and intensive research is required for device development.

Part 5 is composed of 13 chapters, treating haptic application, especially focusing on real-world interaction, such as controlling robots, e-commerce, and welfare.

Part 6 is composed of seven chapters, treating application of haptics to virtual reality, which is an intensively studied area of haptics.

This book helps not only active haptic researchers, but also general readers to understand what is going on in this interdisciplinary area of science and technology. All papers have accompanied videos available online. Therefore, readers can easily understand the concept of the work with the supplemental videos.

November 2018
Sang-Youn Kim
Masashi Konyo
Ki-Uk Kyung
Hiroyuki Kajimoto
Dongjun Lee

Contents

Haptic Technology

Haptic Application

Haptics in Virtual Reality

Haptic Perception and Science

Midair Ultrasound Haptic Display with Large Workspace

Shun Suzuki[✉], Masahiro Fujiwara, Yasutoshi Makino, and Hiroyuki Shinoda

Graduate School of Frontier Sciences,
University of Tokyo, Tokyo, Chiba, Japan
suzuki@hapis.k.u-tokyo.ac.jp, Masahiro_Fujiwara@ipc.i.u-tokyo.ac.jp,
{Yasutoshi_Makino,Hiroyuki_Shinoda}@k.u-tokyo.ac.jp

Abstract. Midair haptic display using airborne ultrasound enables to give tactile feedback to a human body without wearing any devices. In the conventional ultrasound midair haptics system, the workspace was limited to the space of about 30 cm cube. In this paper, we integrate multiple ultrasound display units to achieve a large workspace. Our prototype system enables visuo-tactile interaction with AR images in a space of about 2 m cube.

Keywords: Midair haptics · Visuo-haptic interaction · Mixed reality

1 Introduction

The Airborne Ultrasound Tactile Display (AUTD) originating from the study by Iwamoto et al. [1] enabled non-contact haptic feedback to the human body surface. Such midair haptic display devices have been studied to provide haptic feedback in a VR, AR and MR environment. The advantage of midair haptics is that the user does not have to wear any devices and the movement of the user is not limited. However, in the conventional midair haptic system using ultrasound such as HaptoMime [2] and HaptoClone [3], the workspace is limited to a space of 30 cm cube at most, and the movement of the user is limited to this space. This is because ultrasonic waves are highly attenuated in the air.

To obtain the desired convergence of ultrasound in a large workspace, the workspace should be surrounded by many transducers. The problem is to digitize the position and posture of these transducers. The practical way is to surround the workspace with multiple phased array units (AUTD units) with a convenient size. By arranging multiple AUTD Unit, we can design a large workspace flexibly.

In this paper, we achieve a system that enables visuo-haptic interaction in a space of 2 m cube, where the user can freely move both hands while standing. Figure 1 shows a picture of the proposed system. The system monitors the motion of user by depth sensors and displays visual and haptic feedback when the user touches a 3D image.
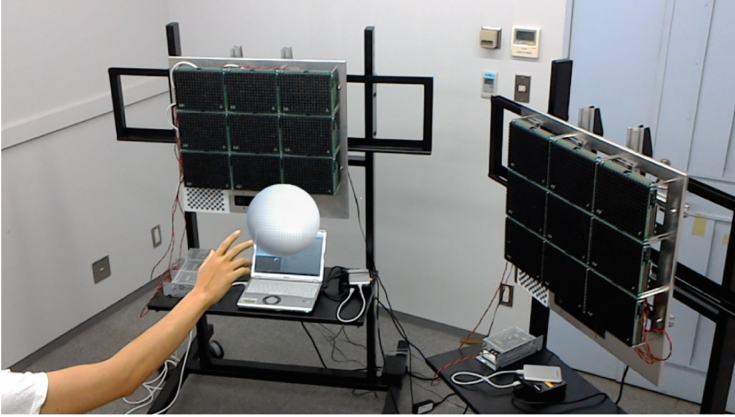
Fig. 1. Multiple phased array system. A user can touch and interact with an AR image.

2   Prototype System

The system configuration used in this study is shown in Fig. 2. Each AUTD unit has a depth sensor (Kinect v2, Microsoft Corp.) for three-dimensional measurement, a slave PC and nine AUTD subunits. The slave PC is connected to the master PC via the LAN. All units are synchronized, three-dimensional measurement is performed simultaneously and point cloud data is transmitted to the master PC. The master PC obtain the position and posture of the AUTD units and controls the AUTD units based on the information from the depth sensor.
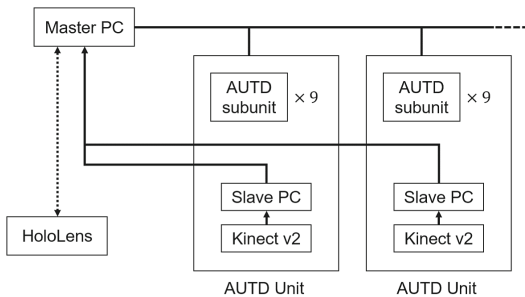
Fig. 2. Proposed system configuration.

The appearance of the AUTD unit is shown in Fig. 3. Nine AUTD subunits are fixed to the aluminum frame. One AUTD subunit has 249 ultrasonic transducers and the AUTD unit has 2241 transducers in total. The depth sensor is also fixed to the frame. The positional relationship between the AUTD subunit and the depth sensor is measured in advance.
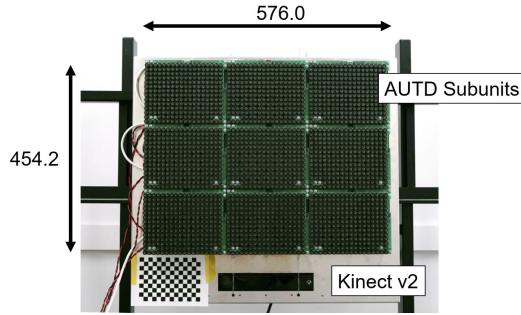
Fig. 3. Photograph of AUTD Unit. Dimensions are in mm.

Stereoscopic 3D image is drawn by MR device (HoloLens, Microsoft Corp.). Calibration between MR device and AUTD unit is performed by using calibration pattern attached to AUTD unit. Since HoloLens has a self-position estimating function, calibration is performed only once at the beginning. Calibrations of multiple AUTD Units are also performed by using this function.

3   Conclusion

In this paper, we proposed a visuo-haptic interactive system, whose workspace is over 2 m cube. In the proposed system, a standing user can move hands freely and interact with a 3D image with tactile feedback. The system configuration of the prototype was shown. The objective evaluation of the effect of midair haptics in such large space remains as a future study.

References

1. Iwamoto, T., Tatezono, M., Shinoda, H.: Non-contact method for producing tactile sensation using airborne ultrasound. In: Proceedings Eurohaptics 2008, pp. 504–513 (2008)
2. Monnai, Y., Hasegawa, K., Fujiwara, M., Yoshino, K., Inoue, S., Shinoda, S.: HaptoMime: mid-air haptic interaction with a floating virtual screen. In: Proceedings 27th Annual ACM Symposium User Interface Software Technology, pp. 663–667 (2014)
3. Makino, Y., Furuyama, Y., Inoue, S., Shinoda, H.: HaptoClone (Haptic-Optical Clone) for mutual tele-environment by real-time 3D image transfer with midair force feedback. In: Proceedings 2016 CHI Conference Human Factors Computure System, pp. 1980–1990 (2016)

Efficiency of Haptic Search Facilitated by the Scale Division

Hirotsugu Kaga[✉] and Tetsuya Watanabe

University of Niigata, Ikarashi 2-no-cho, Nishi-ku, Niigata, Japan
hkaga@eng.niigata-u.ac.jp

Abstract. An experiment was conducted to reveal the efficiency of haptic search facilitated by the division of the searchable area. Tactile maps with five different numbers of divisions were presented to 16 blind participants and they were instructed to find the target. The results show that the search time became minimal at the 4×5 condition, but there was no significant difference between any pair of conditions.

Keywords: Haptic search · Scale division · Search time · Tactile map · Blind people

1 Introduction

Scales provided around tactile maps can shorten the search time for tactile symbols on the map [1]. However, the optimum number of divisions has not been found yet. In our prior study, an experiment was conducted in which tactile maps with five different numbers of divisions were presented to blindfolded sighted participants, and the results indicate that scales with 3×4 divisions minimize the search time [2]. In the current study, the same protocol as in the prior study was applied to blind participants.

2 Experiment

The tactile maps consisted of B4 sized swell paper with scales, roads (1 mm solid lines), and target stimuli (a circle of 9 mm). Scales with a line length of 5 mm and a width of 1 mm were added around the map, so as not to be confused with the lines of the streets (see Fig. 1). The number of divisions of the length and width were changed through the experiment, 2×3, 3×4, 4×5, 5×6, respectively (length $\times$ width). Maps without scales were prepared as a comparison.

Sixteen early blind people (9 male and 7 female, with a mean age of 28.7 years) participated in the experiment. They were informed of the divided area that contained the target before each trial. In addition, the number of divisions for the next trial was explained before starting the search. The participants used both hands for the searching task. All five conditions were shown to each of the participants in a different order of the stimuli. Ten tactile maps were used for one condition, which is one set, and the map was shown randomly. The participant's searching time was recorded by a stopwatch and the finger motion was recorded by a motion capture system (OptiTrack, V120: Trio).
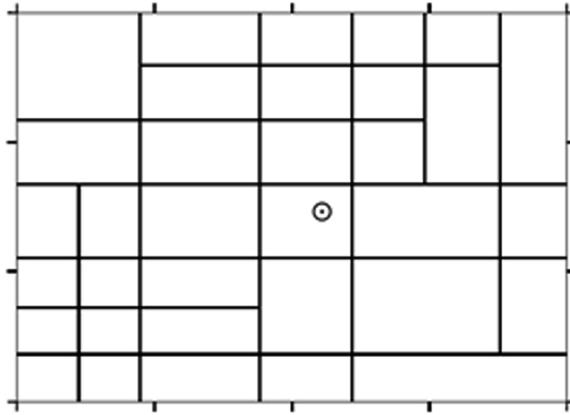
Fig. 1. An example of the target on the map with 3 × 4 divisions (the target was placed in the 2–3 area).

The study protocol was reviewed and approved by the institutional review boards of the University of Niigata.

3   Results

Figure 2 shows the relationship between the number of divisions and search time. The search time became minimal at the 4 × 5 condition. On the other hand, some trials that involved searching failures and the starting over of scale-counting took extremely long times at the 2 × 3 and 5 × 6 conditions. In comparison with blindfolded sighted participants, the search times became shorter at all conditions, and the entire search time was halved [2].
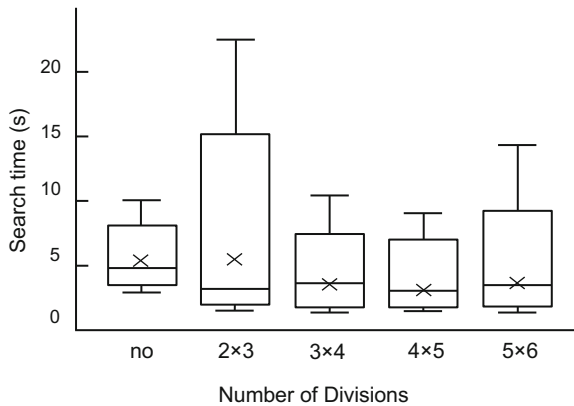
Fig. 2. Quantiles of the search time by the number of divisions. X-marks represent the average.

A Friedman test showed a significant difference among the five conditions (χ^2 (4) = 12.25, $p < .05$). However, multiple comparison using the Ryan's procedure showed no significant difference between any pair of conditions ($p > .05$).

4   Conclusion

In this study, the haptic search experiment using a tactile map with five different scale conditions was conducted in order to reveal the efficacy of the divided area. The results indicate the 4 × 5 divisions minimize the search time, and the relationship between the number of divisions and search time was not monotonic. Contrary to the hypothesis, the search time in the 2 × 3 condition was longer than in the non-scale condition. This could be the participants searched the entire map carefully in the non-scale condition and that led to short search times, on the other hand they searched only the divided area that had the target in the 2 × 3 condition but failed. Then they had to start over the search and that led to long search times. In contrast, the median searching time over the 3 × 4 and 5 × 6 conditions had no large difference. It is assumed that the effect of the divided area on efficiency of the haptic searching has a limitation from a certain size. Therefore, for the future prospect, we should conduct a study of the different sizes of tactile maps in order to reveal the relationship between search time and the size of the map.

This finding should be utilized for the optimization of automated tactile map creation system.

References

1. Watanabe, K., et al.: Development of an embossed map automated creation system and evaluation of the legibility of the maps produced. IEICE Trans. D **J95-D**(4), 948–959 (2012)
2. Kaga, H., et al.: Haptic search in divided areas: optimizing the number of divisions. Jpn. Psychol. Res. **59**(2), 144–151 (2017)

Body-Ownership Illusion by Gazing at a Blurred Fake Hand Image

Hikaru Hasegawa[1](✉), Shogo Okamoto[1], Nader Rajaei[1], Masayuki Hara[2],
Noriaki Kanayama[3], Yasuhiro Akiyama[1],
and Yoji Yamada[1]

[1] School of Engineering, Nagoya University, Nagoya, Japan
`hasegawa.hikaru@c.mbox.nagoya-u.ac.jp`
[2] School of Science and Engineering, Saitama University, Saitama, Japan
[3] Human Informatics Research Institute, National Institute of Advanced Industrial
Science and Technology (AIST), Tsukuba, Japan

Abstract. Feeling body ownership over a fake body image in video
games or virtual environments may enhance the immersion and feeling
of presence in them. In these situation, the sharpness of the image may
influence the induction of the body-ownership illusion. In this study, we
investigated the effect of blurring the image on the rubber hand illusion
experience under seven levels of blur intensity. The results showed that
blurring the image within the limits of hand recognizability may induce
stronger body ownership of the fake hand but may not influence agency.
This indicates that body ownership of a body image can be controlled
by the sharpness of the presented image.

Keywords: Body ownership · Agency · Rubber hand illusion ·
Blurred image

1 Introduction

The induction of feeling as if a body image on a computer screen is part of
one's own body is expected to provide greater immersion and presence in the
virtual environments or video games. The feeling of a part of one's body (body
ownership) and the sense of authorship of body motion (body agency) [1,2] have
been investigated in the rubber hand illusion (RHI) paradigm [3]. The RHI is
an illusory experience one feels body ownership over a fake hand while gazing
at it being exposed to spatially and temporally congruent visuohaptic stimuli.

Many studies have attempted to induce the RHI through a computer
screen [4–7]. For instance, one study found that, when screen projection of the
camera image of the hand was delayed by more than 300 ms, the RHI becomes
weaker [4]. However, the conditions for inducing a body-ownership illusion has
not been investigated thoroughly. In this study, we focused on the sharpness of
the body image captured by a camera and projected on a computer screen, which
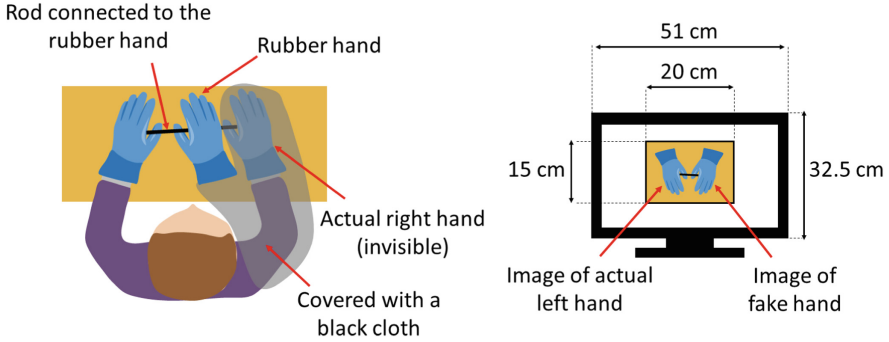
Fig. 1. Left: top view of the apparatus for inducing an active RHI. The right hand is covered with a black cloth. The movements of the actual and fake hands are synchronized by the rod. Right: specification of the screen and image used in the experiment.

is often restricted by the specification or performance of the camera, monitor, computer, and communication environment used. Determining the influence of image sharpness on the RHI contributes to the development of video games and virtual reality environments that employ the body-ownership illusion.

The influence of image sharpness on the RHI has not previously been investigated. Therefore, we investigated it in an RHI experiment where participants gaze at a fake hand image. Participants moved their own hand and the fake hand synchronously while gazing at seven images (each with a different level of blur) in a random order. Then, they answered to a questionnaire related to body ownership and agency. The results of this study are beneficial for controlling the body ownership of a fake body image on a computer screen.

2   Materials and Methods

2.1   Participants

Five university students (all right handed males aged between 21 and 23) who had no experience of the RHI participated in the experiment with informed consent. This experiment was approved by the ethical committee of the School of Engineering, Nagoya University (#17–12).

2.2   Experimental Setup for Inducing the RHI Through a Screen

Rubber gloves, an acrylic rod for synchronizing the hand motion, and a black cloth for covering the actual right hand and arm were used for inducing the RHI (Fig. 1 (left)). This apparatus was also used in [8]. Participants wore the rubber gloves and moved their hands synchronously with the fake hand by softly grasping the acrylic rod fixed to the fake hand.

The motion of the actual and fake hands was captured by a camera (HD WEBCAM C270, Logicool), and the camera image (15 cm × 20 cm, 408 × 544 pixel) was
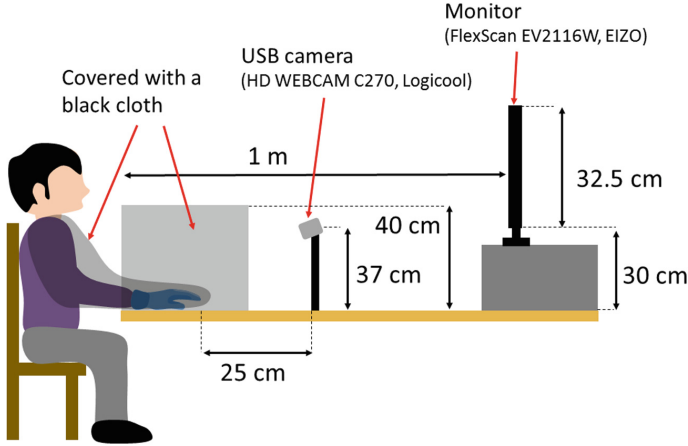
Fig. 2. Side view of the experimental setup for inducing RHI through a screen.

projected on a monitor (FlexScan EV2116W, EIZO) with a refresh rate of 59–61 Hz (Fig. 1 (right)). The captured image was flipped horizontally to give a mirror image [2]. The camera and monitor were located in front of the participant as shown in Fig. 2, and the captured image of their hands was shown on the monitor. The monitor height was same as the participant's eye level. The fake and actual hands were hidden by a frame covered with black cloth in order to prevent a direct view.

2.3   Methods

The camera images were blurred by an average filter. The blur levels were changed by the filter size, which had seven levels that range from not blurred (filter size: 0) to blurred beyond hand recognition (filter size: 75×75 pixel) in a geometrical series. The seven levels of blurred image are shown in Fig. 3.

2.4   Task

Before the experiment, participants tapped or rubbed the table with them on and experienced the RHI by gazing at the fake hand as shown in Fig. 1 (left), such that they could familiarize themselves with the rubber gloves. Then, participants experienced the RHI at seven levels of blurred image projected in a random order. The first four trials were used for practice. Then, 14 trials were conducted (each of the seven levels of blur was shown twice). Participants experienced the stimulus for one minute in each trail.

The magnitudes of body ownership and agency over the fake hand are rated by the questionnaire [1–3]. The questionnaire shown in Table 1 was a modified version of the one used by Botvinick and Cohen [3]. Q1 and Q2 are related to body ownership and agency, respectively, and the others are control items.

Level 1
(Not blurred)

Level 2
Filter size (10 × 10)

Level 3
Filter size (15 × 15)

Level 4
Filter size (22 × 22)

Level 5
Filter size (33 × 33)

Level 6
Filter size (50 × 50)

Level 7
Filter size (75 × 75)
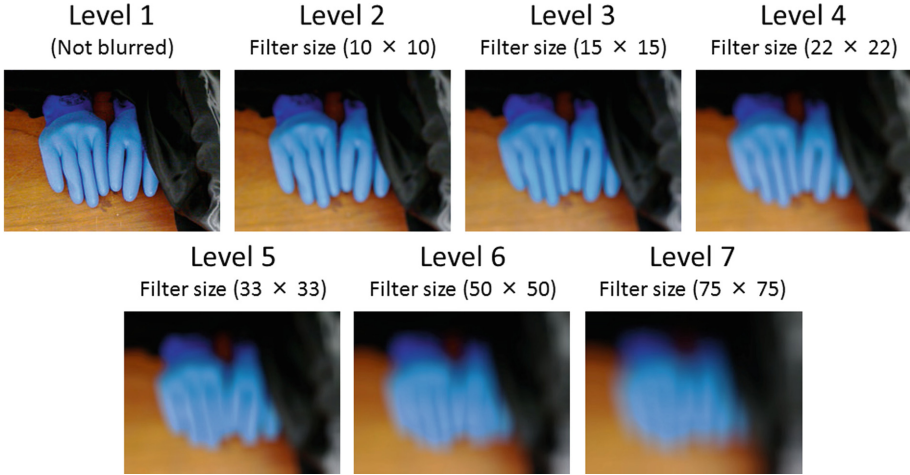
Fig. 3. Seven levels of blurred image used in the experiment. For the image of level 1, no filtering effect was applied. For levels 2–7, average filters of different sizes were applied.

Table 1. Questionnaire for evaluation of the RHI intensity

Q1	I felt as if the rubber hand was my own hand
Q2	It seemed like I was directly moving the rubber hand
Q3	It seemed as if I might have more than one right hand or arm
Q4	It felt as if my (real) hand was turning "rubbery"
Q5	It appeared (visually) as if the rubber hand was drifting towards the right (towards my real hand)
Q6	The rubber hand began to resemble my own (real) hand in terms of shape, size, or some other visual feature
Q7	I felt as if my (real) hand was drifting towards the left (towards the rubber hand)

Participants gave each question a score on a seven-level scale for each trial (-3 for strongly disagree up to $+3$ for strongly agree). A positive answer score indicates that the participant agreed with the question.

3   Results

The answer scores from each participant were averaged in each stimulus condition. Figure 4 shows the means and standard errors of the answer scores for each question and each blur level. The answer scores against Q3–Q7 (control items) were equally negative under all conditions, which denied the suggestibility of the setting. We applied a one-way ANOVA to the answer scores against Q1 and Q2, which are related to the RHI, by considering the blur levels as the factor to investigate the effect of blur process.
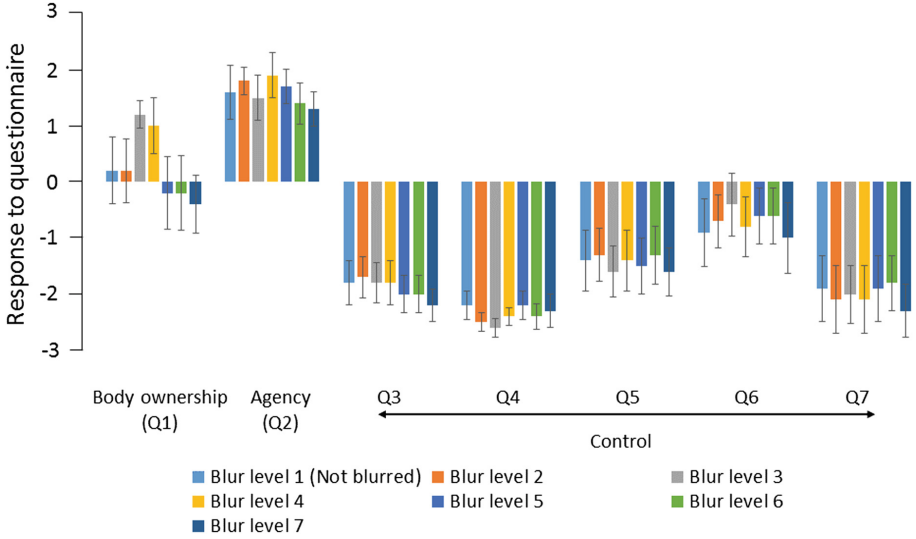
Fig. 4. The means and standard errors of the RHI questionnaire scores for each blur level.

The answer scores against Q1 (body ownership) were positive values for blur levels 1–4 and were negative values under stronger blurring conditions. Furthermore, they peak between blur levels 3 and 4. However, these were not significant results ($F(6, 63) = 1.27$, $p = 0.29$). The answer scores against Q2 (agency) were positive values under all blurring conditions and there was no significant difference among any conditions ($F(6, 63) = 0.35$, $p = 0.91$).

4   Discussion

Body ownership was reported in slightly blurred conditions (blur levels 3 and 4), but not in intensive blurring conditions where the hands become unrecognizable. Moreover, the answer scores against body ownership under blurring conditions within the limits of hands being recognizable (i.e., blur levels 3 and 4) were higher than under the unblurred condition. This result can be explained by the inverse effect [9], where the illusion, which is a multisensory integration of visuohaptic cues, might have been strengthened by degradation in the reliability of visual cues. Also, slightly blurred conditions (blur levels 3 and 4) may masked the visual difference between the fake and actual hands, and might have resulted in intensive illusions. However, given the limited number of participants, we could not achieve significant results and further investigation is required.

Although agency was reported regardless of the blurring intensity, the types of it differed between blur levels. Under blur levels 3 and 4, body agency may be induced since body ownership was also reported. On the other hand, under

stronger blurring conditions (blur levels 5–7), external agency [1] may be induced in the same way as when you use a tool or manipulate an object.

In this way, using an unclear image within the limits of hand recognizability may be effective for inducing body ownership on the fake hand image while remaining agency.

5   Conclusion

In this study, we investigated the effect of blurring a fake hand image on the RHI experience. Camera images of participants' hands were blurred to seven different extents and projected on a monitor in front of them. Participants answered a questionnaire related to illusion after moving their actual and fake hands synchronously while gazing at the blurred image. The results showed that blurring the image within the limits of hand recognizability induced stronger body ownership than under unblurred conditions. However, agency was induced equally under all blurring conditions. We suggest that the blurring process within the limits of hand recognizability may be effective for inducing body-ownership illusion with a fake hand image on a screen.

References

1. Kalckert, A., Ehrsson, H.: Moving a rubber hand that feels like your own: a dissociation of ownership and agency. Front. Hum. Neurosci. **6**(40), 1–14 (2012)
2. Jenkinson, M.P., Preston, C.: New reflections on agency and body ownership: the moving rubber hand illusion in the mirror. Conscious. Cogn. **33**, 432–442 (2015)
3. Botvinick, M., Cohen, J.: Rubber hands 'feel' touch that eyes see. Nature **391**, 756 (1988)
4. Shimada, S., Fukuda, K., Hiraki, K.: Rubber hand illusion under delayed visual feedback. PLoS One **4**, 1–5 (2009)
5. Hara, M., et al.: Voluntary self-touch increases body ownership. Front. Psychol. **6**(1509), 1–22 (2015)
6. IJsselsteijn, W.A., de Kort, Y.A.W., Haans, A.: Is this my hand I see before me? The rubber hand illusion in reality, virtual reality, and mixed reality. Presence: Teleoperators Virtual Environ. **15**(4), 455–464 (2006)
7. Slater, M., Pérez, M.D., Ehrsson, H., Sanchez-Vives, M.: Inducing illusory ownership of a virtual body. Front. Neurosci. **3**(2), 214–220 (2009)
8. Itoh, K., Okamoto, S., Hara, M., Yamada, Y.: An attempt to induce a strong rubber hand illusion under active-hand movement with tactile feedback and visuotactile stimulus. In: Bello, F., Kajimoto, H., Visell, Y. (eds.) Haptics: Perception, Devices, Control, and Applications. Lecture Notes in Computer Science, vol. 9775, pp. 346–353. Springer, Cham (2016)
9. Otto, T.U., Dassy, B., Mamassian, P.: Principles of multisensory behavior. Soc. Neurosci. **33**(17), 7463–7474 (2013)

A Soft Tactile Display Using Dielectric Elastomer Actuator for Fingertip Interaction

Jung-Hwan Youn [ID], Seung-Mo Jeong [ID], Young-Seok Choi [ID], and Ki-Uk Kyung$^{(\boxtimes)}$ [ID]

Korea Advanced Institute of Science and Technology, Daejeon, Korea
{jungwhan08lo, seungmoj, cjysk, kyungku}@kaist.ac.kr

Abstract. In this paper, we demonstrate a soft tactile display composed of a thin dielectric elastomer (DE) actuator coupled with silicone gel in a bubble shape, which can provide tactile stimulation to the skin. The design of the tactile display is referred from hydrostatically coupled DEA structures. We could observe the maximum force of the tactile actuator as 378 mN. In addition, the actuating module could provide exerting force higher than 250 mN in overall range of perceivable frequencies.

Keywords: Dielectric elastomer actuator · Soft · Tactile display · Haptic · HC-DEA

1 Introduction

So far, tactile feedback has been achieved through vibration or shape transformation [1, 2]. Nonetheless, more research needs to be done in order to create a thin, flexible, and safe tactile display.

Electro-active polymer (EAP) actuators, especially dielectric elastomer actuators (DEA), are emerging soft actuators that are characterized by its large area strain, fast response, high specific energy density, light weight, low cost and low power consumption [3, 4]. However, DEA still have challenges in producing sufficient amount of output force for using in tactile displays. Several researchers have tried to overcome this issue through hydrostatic coupling (0.8 N) [5, 6], and multi-layering (255 mN) [1].

In this demonstration, we implement a soft actuator for tactile display composed of DEA layers coupled with silicone gel in a bubble shape, which has been proposed as HC-DEA (Hydrostatically Coupled Dielectric Elastomer Actuator) [5, 6]. In order to verify applicability of the soft actuating mechanism as a tactile display in human perceivable range, we have conducted measurement of exerting force in accordance with frequency variation. The soft tactile actuator shows fast response, and sufficiently large output force (output force: >250 mN in frequency range: 0–300 Hz).

2 Experimental

2.1 Fabrication

The soft tactile display is composed of dielectric elastomer (DE) layers coupled with silicone gel. In this structure, the ball-shaped silicone gel lies within dielectric elastomer and passive layers. The dielectric elastomer membrane is made of 0.5 mm thick

3M VHB 4905 film, pre-stretched by a ratio of three. The active layer's diameter is 10 mm, and the frame's diameter is 18 mm. The working principle of the tactile actuator is as follows. First, voltage is input to the device. Then, due to induced electrical potential, the dielectric elastomer membrane (lower layer) undergoes expansion [3]. As a result, the DE membrane buckles and the ball-shaped silicone gel moves perpendicularly down. On the other hand, when voltage is turned off, the membrane contracts and the silicone gel moves up (Fig. 1).
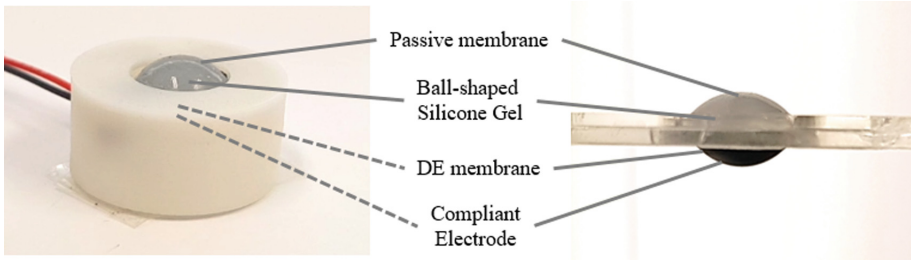
Fig. 1. Fabricated soft tactile display

2.2   Actuation Performance Test

The performance of soft tactile display is evaluated by measuring its output force. The load cell is made contact with the actuator's passive layer for an accurate force measurement. For the measurement, square waves of 4 kV amplitude at 0–300 Hz frequency are input to the display. Figure 2 shows the output force as a function of frequency.
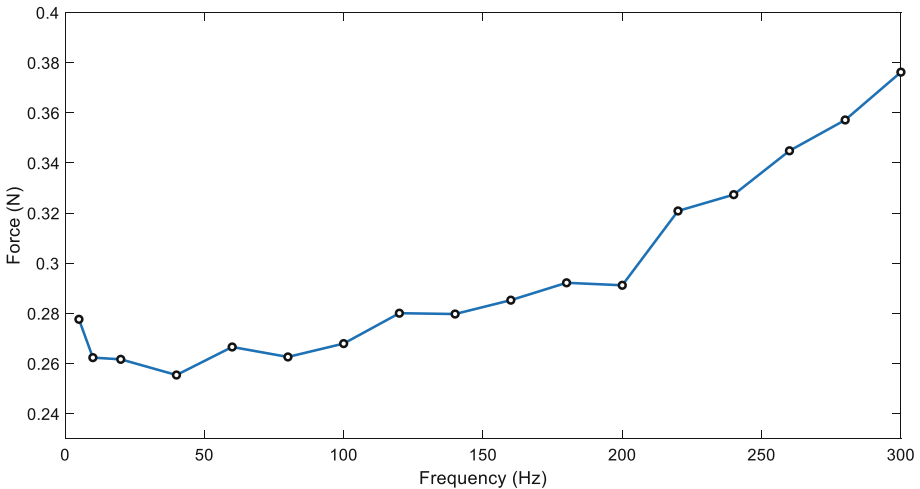
Fig. 2. Performance test of DEA under loading condition with input frequency sweep at 4 kV

The measured output force of soft tactile display is higher than 250 mN at all operating frequencies. The highest output force is measured as 378 mN at 300 Hz. As force perception threshold at fingertip is reported to be 1.7 mN in 320 Hz [7], the fabricated soft tactile display proves to be appropriate for human-machine applications.

3 Conclusion and Future Work

In this paper, the soft tactile display based on DEA coupled with silicone gel in a bubble shape has been demonstrated. The actuator recorded a maximum force of 378 mN at 300 Hz. In the low frequency zone, around 5 Hz, the output force is measured as 279 mN.

In the future, we will consider fabricating actuator applicable to wearable interfaces, such as fingertip tactile glove and forearm vibro-tactile band. Since the threshold of force perception in forearm is much higher than the fingertip, providing not only contact force, but also vibro-tactile stimulus to the skin is considered.

References

1. Mun, S., Yun, S., Nam, S., Park, S.K., Park, S., Park, B.J., Lim, J.M., Kyung, K.U.: Electroactive polymer based soft tactile interface for wearable devices. IEEE Trans. Haptics **11**(1), 15–21 (2018)
2. Matysek, M., Lotz, P., Winterstein, T., Schlaak, H.: Dielectric elastomer actuators for tactile displays. In: World Haptics 2009, pp. 290–295. IEEE, Salt Lake City (2009)
3. Gu, G.-Y., Zhu, J., Zhu, L.-M., Zhu, X.: A survey on dielectric elastomer actuators for soft robots. Bioinspir. Biomim. **12**(1) (2017)
4. Romasanta, L.J., Lopez-Manchado, M.A., Verdejo, R.: Increasing the performance of dielectric elastomer actuators: a review from the materials perspective. Prog. Polym. Sci. **51**(1), 188–211 (2015)
5. Frediani, G., Mazzei, D., De Rossi, D.E., Carpi, F.: Wearable wireless tactile display for virtual interactions with soft bodies. Front. Bioeng. Biotechnol. **2**(31) (2014)
6. Boys, H., Frediani, G., Ghilardi, M., Poslad, S., Busfield, J., Carpi, F.: Soft wearable nonvibratory tactile displays. In: 2018 IEEE International Conference on Soft Robotics, Robosoft, pp. 270–275. IEEE, Livorno (2018)
7. Hatzfeld, C., Cao, R.S., Kupnik, M.: Vibrotactile force perception – absolute and differential thresholds and external influences. IEEE Trans. Haptics **9**(4), 586–597 (2016)

Haptic Texture Authoring:
A Demonstration

Waseem Hassan[(✉)] , Arsen Abdulali , and Seokhee Jeon

Department of Computer Science and Engineering, Kyung Hee University,
Yongin, Republic of Korea
{waseem.h,abdulali,jeon}@khu.ac.kr

Abstract. We present a haptic texture authoring algorithm for synthe-
sizing new virtual textures by manipulating affective properties of exist-
ing real textures. Two different spaces are established: "affective space"
built from a series of psychophysical experiments and "haptic model
space" built on features from tool-surface contact vibrations. Another
space, called "authoring space" is formed by merging the two spaces,
whereby, features of model space that were highly correlated with affec-
tive space become axes of the space. Thus, new texture signal corre-
sponding to any point in authoring space can be synthesized by weighted
interpolation of nearest real surfaces in perceptually correct manner.

Keywords: Haptic texture · Interpolation · Texture perception ·
Texture rendering · Psychophysics

1 Introduction

In the field of texture perception, the relationship between visual perception
and physical characteristics of surfaces has received a high level of interest from
the research community, while, on the other hand, the relationship between tac-
tile perception and physical characteristics is a less trodden path. This can be
accredited to the difficulty in finding specific factors and characteristics of tactile
perception which can be controlled and manipulated independently. It is a well
known fact that vibrations originating from interaction with different surfaces
play a vital role in texture perception and identification. Various researchers
have successfully rendered virtual tactile sensations by reproducing vibrations
encountered during tactile interactions [3]. However, such studies did not succeed
in pointing out definitive characteristics that can be used to directly manipu-
late the perception or affective properties of textures. The process of directly
manipulating the affective properties is called as haptic texture authoring.

The main aim of haptic texture authoring is to provide a system where the
affective properties of textures are readily manipulated. This can be achieved if
a relationship is established between the physical properties of textures and its
affective properties. In this study, the physical properties are modelled using the
algorithm presented by Abdulali et al. in [1], whereas, the affective properties
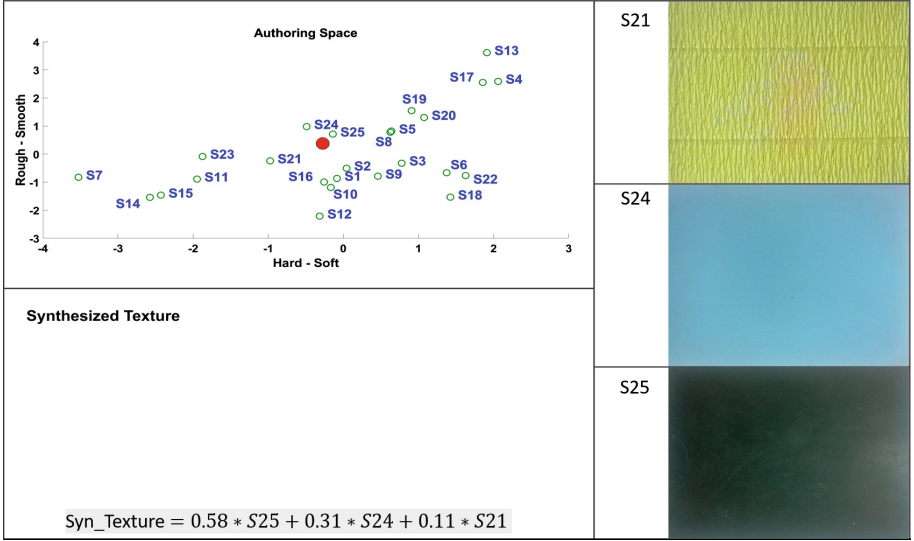
Fig. 1. A screen shot of the demonstration scenario for haptic texture authoring.

are captured by following methods similar to [4]. In the current study, we strive to find out this relationship, and then exploit it to alter the physical properties of surfaces by manipulating its affective properties.

In order to achieve haptic texture authoring, an affective space based on psychophysical experiments, and a haptic model space based on tool-surface interaction vibrations are established. Based on the relationship established between these two spaces an authoring space is established. Thus the authoring space inherits the physical properties and affective properties of textures. Creation of new haptic textures with user defined properties takes place by manipulating the affective properties which in turn changes the physical properties of surfaces. Rendering of the new virtual haptic textures is carried out using the method provided in [2].

2 Demonstration Scenario

The aim of this demonstration is to create various virtual textures with predefined affective properties. The user interface for the demonstration is shown in Fig. 1. A user can select any value of the affective properties by clicking inside the authoring space (within the convex hull of the given textures). A new virtual texture having the specified affective properties will be generated on the screen by interpolating its neighbors. Users can also compare the newly created texture with its parent real textures. A video for this demonstration is available at http://haptics.khu.ac.kr/Haptic_Texture_Authoring_AsiaHaptics2018.mp4.

References

1. Abdulali, A., Jeon, S.: Data-driven modeling of anisotropic haptic textures: data segmentation and interpolation. In: International Conference on Human Haptic Sensing and Touch Enabled Computer Applications, pp. 228–239. Springer (2016)
2. Abdulali, A., Jeon, S.: Data-driven rendering of anisotropic haptic textures. In: International AsiaHaptics Conference, pp. 401–407. Springer (2016)
3. Culbertson, H., Unwin, J., Kuchenbecker, K.J.: Modeling and rendering realistic textures from unconstrained tool-surface interactions. IEEE Trans. Haptics **7**(3), 381–393 (2014)
4. Hassan, W., Jeon, S.: Evaluating differences between bare-handed and tool-based interaction in perceptual space. In: 2016 IEEE Haptics Symposium (HAPTICS), pp. 185–191. IEEE (2016)

Reducing 3D Vibrations to 1D
in Real Time

Gunhyuk Park and Katherine J. Kuchenbecker^(✉)

Haptic Intelligence Department, Max Planck Institute for Intelligent Systems,
Heisenbergstr. 3, 70569 Stuttgart, Germany
{ghpark,kjk}@is.mpg.de

Abstract. For simple and realistic vibrotactile feedback, 3D accelerations from real contact interactions are usually rendered using a single-axis vibration actuator; this dimensional reduction can be performed in many ways. This demonstration implements a real-time conversion system that simultaneously measures 3D accelerations and renders corresponding 1D vibrations using a two-pen interface. In the demonstration, a user freely interacts with various objects using an In-Pen that contains a 3-axis accelerometer. The captured accelerations are converted to a single-axis signal, and an Out-Pen renders the reduced signal for the user to feel. We prepared seven conversion methods from the simple use of a single-axis signal to applying principal component analysis (PCA) so that users can compare the performance of each conversion method in this demonstration.

Keywords: Vibrotactile feedback · Signal processing ·
Dimensional reduction · User interface · Realistic vibration

1 Introduction

Vibrotactile feedback has contributed to a myriad of interfaces for improved and enriched user interactions [1]. Depending on the target application, vibrotactile patterns have been designed to be realistic for better user experiences [2,3] and rich tactile information [4] or to be nonrealistic for attracting user attentions [5] and encoding numerous tactile languages [6].

Realistic vibrotactile feedback can be synthesized through either a physics-based model designed by experts [7] or a data-driven model derived from 3D vibrations captured from real interactions [8]. Although both of these approaches can generate realistic 3D vibration signals that react to user input, the human hand cannot easily distinguish the direction of the vibrotactile output [9]. Furthermore, the commercial vibration actuators that are widely used in haptics output only single-axis vibrations. Haptics researchers thus often reduce 3D vibrations to 1D for rendering, a process that may lose some of the original information and may decrease the realism of the interaction.

We prepared a system that captures 3D accelerations using an In-Pen and simultaneously converts them to 1D vibrations that are rendered in real time

using an Out-Pen. In this demonstration, the participant can interact with surrounding objects using the In-Pen to capture 3D accelerations and feel the reduced 1D vibration from the Out-Pen. During the demonstration, the participant can choose between seven conversion methods and compare them to find his or her favorite method.
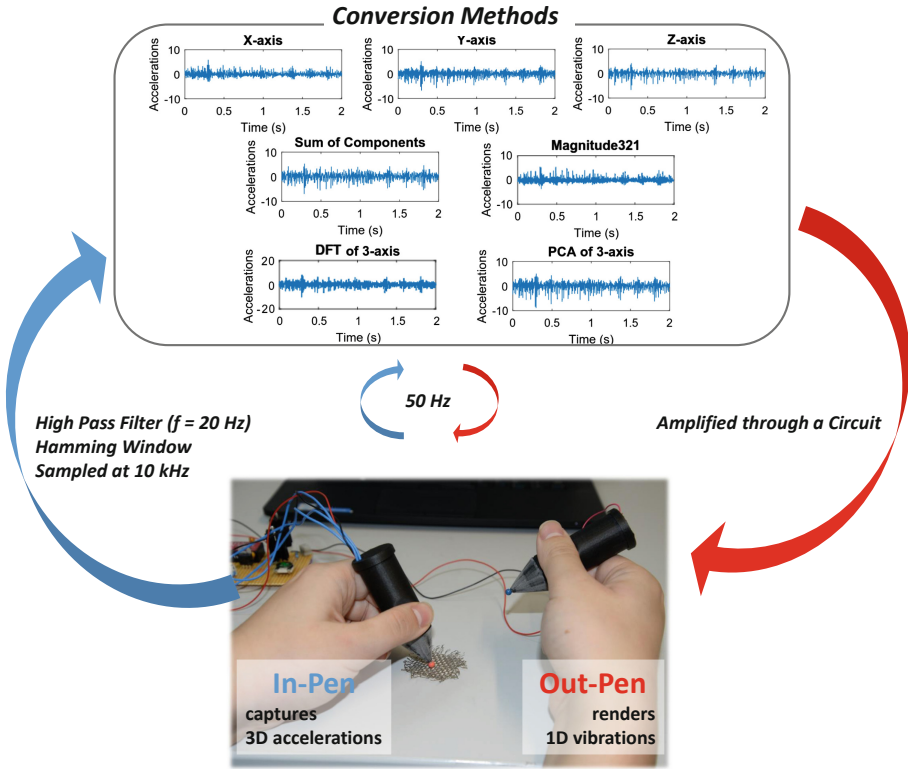
Fig. 1. The overall system structure of the demonstration. 3D accelerations measured from the In-Pen are captured every 20 ms and converted to corresponding 1D vibration signals. When a user interacts with surrounding objects using the In-Pen, the user simultaneously feels the converted vibration from the Out-Pen.

2   System Structure

We designed a two-pen interface for the real-time vibrotactile conversion system (see Fig. 1). The In-Pen that contains a 3-axis accelerometer (ADXL354CZ; Analog Devices) measures 3D accelerations caused by the user's interactions. A computer captures 200 acceleration samples on each axis from the In-Pen every

20 ms using a data acquisition board (USB-6343; National Instruments) and converts them to the single-axis vibration signal using the presently selected conversion method. The converted signals are amplified via a custom circuit (OPA544T; Texas Instruments), and the Out-Pen renders the vibrations using a voice-coil actuator (Haptuator Redesign; TactileLabs).

We showcase seven conversion methods that range from simple to complex. Landin et al. first derived versions of these approaches and applied them to several-second-long signals offline [10]. Landin et al. then estimated the spectral and temporal matching between the original signal and the reduced signal but performed no user validation. We implemented this demonstration to continuously convert signals using the methods in real time by applying a Hamming window on 50% overlapping samples that are 10 ms long.

Single Axis This method simply uses the x, y, or z-axis acceleration for the reduced vibration; there are no differences between the real-time and compiletime implementations. If the interaction axis matches the converting axis, then this method provides realistic feedback to the user. Generally, user interactions occur along various directions, so this method is not good at keeping the original spectral and temporal information.

Sum of Components Another simple approach to the dimensional reduction is adding up the three-axis acceleration vector components. This approach does not deal with possible negative correlations between axes; therefore, interactions in certain directions lead to the loss of spectral and temporal information. Despite these disadvantages, the sum of components usually captures important events and transfers them to users in real time [4].

Vector Magnitude One of the simplest ways to reduce vector signals into single-component signals is to take the square root of the sum of the squares of the components. This conversion distorts the spectral information of the original accelerations and is insensitive to 3D accelerations that have approximately constant magnitude and changing direction.

Discrete Fourier Transform This approach synthesizes single-axis vibrations to have the same spectral energy as the original three-axis accelerations together. As introduced in [10], the spectral magnitude of the frequency components and the corresponding average phase are calculated to accomplish the maximum spectral matching.

Principle Component Analysis Another way to solve this problem is finding the principal axis of the 3D accelerations and projecting the data onto this axis. This approach previously showed unsatisfactory results [10] when it was applied to long-duration signals because the main vibration direction changes over time. Real-time implementation calculates a new principal vibrating axis every 20 ms, thus adapting to directional changes.

In this demonstration, a user grasps the In-Pen and the Out-Pen with different hands. The user then touches objects using the In-Pen with various interaction methods including tapping, scratching, and hitting from the side. During the interactions, the user feels the corresponding 1D vibration from the Out-Pen.

The user can voluntarily select any of the seven conversion algorithms at anytime and compare them to determine his or her favorite method.

References

1. Choi, S., Kuchenbecker, K.J.: Vibrotactile display: perception, technology, and applications. Proc. IEEE **101**(9), 2093–2104 (2013)
2. Chen, H.Y., Park, J., Dai, S., Tan, H.Z.: Design and evaluation of identifiable key-click signals for mobile devices. IEEE Trans. Haptics **4**(4), 229–241 (2011)
3. Israr, A., Zhao, S., Schwalje, K., Klatzky, R., Lehman, J.: Feel effects: enriching storytelling with haptic feedback. ACM Trans. Appl. Percept. **11**(3), 11:1–11:17 (2014)
4. McMahan, W., Gewirtz, J., Standish, D., Martin, P., Kunkel, J.A., Lilavois, M., Wedmid, A., Lee, D.I., Kuchenbecker, K.J.: Tool contact acceleration feedback for telerobotic surgery. IEEE Trans. Haptics **4**(3), 210–220 (2011)
5. Korres, G., Jensen, C.B.F., Park, W., Bartsch, C., Eid, M.: A vibrotactile alarm system for pleasant awakening. IEEE Trans. Haptics **11**, 357–366 (2018)
6. Tan, H.Z., Reed, C.M., Durlach, N.I.: Optimum information-transfer rates for communication through haptic and other sensor modalities. IEEE Trans. Haptics **3**(2), 98–108 (2010)
7. Park, G., Choi, S.: A physics-based vibrotactile feedback library for collision events. IEEE Trans. Haptics **10**(3), 325–337 (2017)
8. Romano, J.M., Kuchenbecker, K.J.: Creating realistic virtual textures from contact acceleration data. IEEE Trans. Haptics **5**(2), 109–119 (2012)
9. Hwang, I., Seo, J., Kim, M., Choi, S.: Vibrotactile perceived intensity for mobile devices as a function of direction, amplitude, and frequency. IEEE Trans. Haptics **6**(3), 352–362 (2013)
10. Landin, N., Romano, J.M., McMahan, W., Kuchenbecker, K.J.: Dimensional reduction of high-frequency accelerations for haptic rendering. In: International Conference on Human Haptic Sensing and Touch Enabled Computer Applications, pp. 79–86. Springer (2010)

Haptic Rendering

Induced Pulling Sensation by Synthesis of Frequency Component for Voice-Coil Type Vibrators

Takeshi Tanabe[(✉)] [iD], Hiroaki Yano[(✉)], and Hiroo Iwata[(✉)]

University of Tsukuba, 1-1-1 Tennodai, Tsukuba, Ibaraki 305-8573, Japan
t_tanabe@vrlab.esys.tsukuba.ac.jp, yano@iit.tsukuba.ac.jp,
iwata@kz.tsukuba.ac.jp
http://intron.kz.tsukuba.ac.jp

Abstract. It is known that humans experience a kinesthetic illusion, such as a pulling sensation in a particular direction, when asymmetric vibrations are presented. In our previous experiment, it was suggested that the fundamental wave and the second harmonic of asymmetric vibration may contribute to this illusion. In this study, we verified whether this illusion can be induced by combining frequency components using three kinds of commercial vibrators through psychophysical experiments. The results confirmed that participants could perceive the correct direction of the pulling force with a correct answer rate of 83.3%.

Keywords: Illusory force perception · Asymmetric vibration · Non-grounded haptic interface

1 Introduction

It is reported that humans experience a kinesthetic illusion like a pulling sensation in a particular direction when asymmetric vibrations, in which strong and weak accelerations are exerted sequentially, are presented [1]. Moreover, in recent years, many methods for exerting the asymmetric vibrations to a user with a small voice-coil type vibrator to induce this pulling sensation have been proposed [2–6]. However, the physical quantity of the asymmetric vibration was not precisely controlled in these methods. Considering this, the characteristics of the vibrator are handled as black boxes, and although the input signal is operated, the output vibrations are not strictly controlled [2–5]. Input signals for which the illusion prominently occurs were chosen experimentally for each specific vibrator. On the other hand, Culbertson et al. modeled the characteristics of the vibrator [6]. However, they also did not control the output vibrations, and the input signals were not determined based on a targeted vibration. Therefore, it was difficult to generate the same phenomenon with other vibrators.

On the other hand, we confirmed that asymmetric vibrations in which this illusion is induced, and these vibrations, consisted of a few frequency components [4]. Moreover, in our previous experiment [7], using the vibrator that we

developed [8], it was suggested that the fundamental wave and the second harmonic of the asymmetric vibration may contribute to this illusion. Based on this finding, we hypothesized that this illusion can be induced by generating vibrations with two frequency components even with other commercial vibrators. If this hypothesis can be clarified, it may be possible to show a method with high reproducibility compared to the previous method that selects input signals experimentally for each specific vibrator [2–6]. In this study, we verified whether this illusion can be induced by combining frequency components using three kinds of commercial vibrators through psychophysical experiments.

2   Method

2.1   Stimulus

Figure 1 shows the asymmetric vibration that extracted only the fundamental wave and the second harmonic from the original asymmetric vibration observed in our previous study [4]. This data can be expressed using two order Fourier series as shown below.

$$\ddot{x}_{ref} = A_{peak} \sum_{n=1}^{2} a_n \cos(2\pi n f t) + b_n \sin(2\pi n f t) \tag{1}$$

In Eq. 1, the coefficients in the Fourier series were $a_{1,2} = 0.32$, 0.07 and $b_{1,2} = 0.38$, 0.51. A_{peak} represents the acceleration of the peak at the asymmetric vibration. The directions of the perceived pulling forces were controlled by changing the sign of A_{peak}. f indicates the frequency of the fundamental wave. In this experiment, $A_{peak} = 120\,\mathrm{m/s^2}$, and $f = 75\,\mathrm{Hz}$, which is the same frequency as in our previous study [4]. In this experiment, this asymmetric vibration was used as a stimulus, and the directions of the perceived pulling forces were leftward and rightward. This asymmetric vibration was generated using three kinds of commercial vibrators (Haptuator BM1C (referred to as vib.1), Haptuator Mark II (referred to as vib.2), and Haptuator MM3C (referred to as vib.3)) made by Tactile Labs Inc. (Fig. 2). The control method of asymmetric vibration is as follows. We proposed a control method for asymmetric vibration for the vibrator we developed [8], and this method was also applied to vibrators used in this experiment. McMahan et al. [9] and Culbertson et al. [6] considered the user's fingers and the vibrator as a linear system in case that gripping force keeps constant. And this system was modeled by the dynamic model of the mass-spring-damper system. Based on those knowledges, we modeled our system as follow. A transfer function when input was the current and the output were the vibration acceleration of participants' fingertip was identified. The acceleration data of the target asymmetric vibration is designed in advance. The input current was simulated from the target acceleration using the inverse function of the identified transfer function. The target asymmetric vibration is generated by sending the simulated current to the vibrators. The details are described in Ref. [8]. The signals to control the vibrators were generated by MATLAB R2018a (Math Works Inc.). These

signals were output from a personal computer (PC) using a USB audio adapter, amplified by an audio amplifier (Lepy, LP-2024A +), and then they served as input for the vibrators.
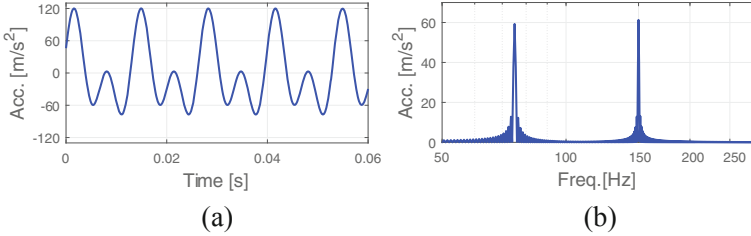
Fig. 1. Reference data of the asymmetric vibration for this illusion. (a) Time series variation. (b) Frequency spectrum.
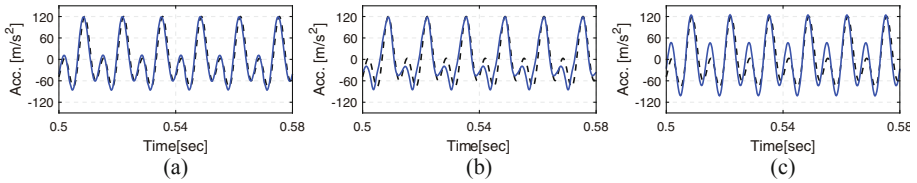
Fig. 2. Typical measurement result of asymmetric vibrations that were generated by the three vibrators used in the experiment. The solid line and the broken line indicate the mean of the measured data and the target data of asymmetric vibrations, respectively. (a) vib.1; (b) vib.2; and (c) vib.3.

2.2   Procedure

Six participants whose ages ranged from 22 to 25 years (5 males and 1 females) participated in this experiment. All participants were right-handed. This experiment was approved by University of Tsukuba, Faculty of Engineering, Information and Systems, Research Ethics Committee (approval number: 2018R213), and the procedures were performed in accordance with the Declaration of Helsinki. Informed consent was obtained from all individual participants included in the study.

A participant sat on a chair and grasped one of the three vibrators with his/her dominant hand, as shown in Fig. 3. Participants were instructed to keep the gripping force constant during the experiment. Participants were presented with the rightward or leftward pulling force by asymmetric vibration stimuli. If the participants could perceive the pulling force, they indicated the direction of

each force in terms of "to the right" or "to the left" using two alternative forced choices (2AFC). The correct answer rates were calculated by comparing them with the presented force directions and the answered directions. Each stimulus was presented for 1 s. The next vibration was presented after the participant indicated the force direction and took a 2 s break. There were 30 trials per set, as each direction (2 level) was tested 15 times. Two sets of trials were performed for each participant and each vibrator. These trials were performed with each vibrator (3 level). Therefore, 180 trials were performed for each participant. The vibrators were randomly selected to avoid a trial order effect. To address the fatigue of the participants, the participants were given a one-minute break between every set in a comfortable position. A gamepad (ELECOM Co., Ltd., JC-U3808TWH) was held by the non-dominant hand, and with its cross-key, the participants indicated the perceived force direction. Audiovisual information was suppressed by closing the eyes and a noise canceling headset (Sony Corp., WH-1000XM2) that output white noise.

(a)   (b)   (c)
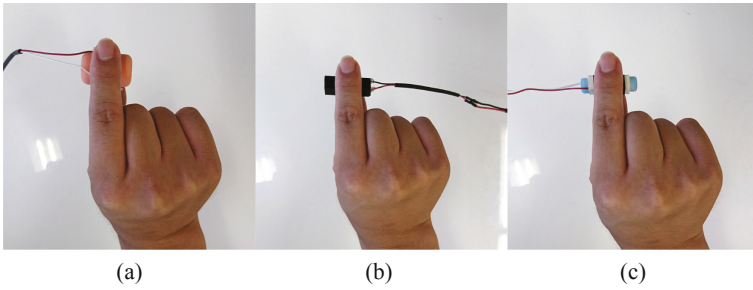
Fig. 3. Gripping state of vibrators: (a) vib.1; (b) vib.2; and (c) vib.3.
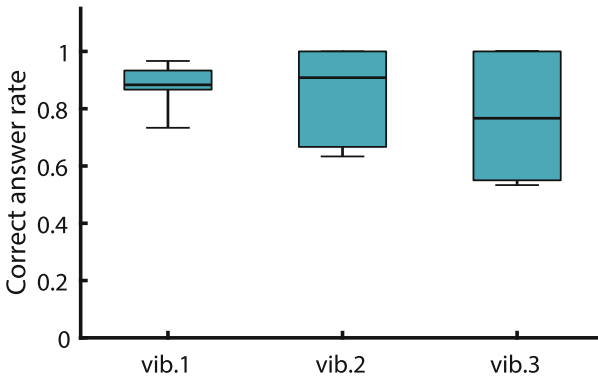
Fig. 4. Correct answer rates of all participants for each vibrator.

3   Result and Discussion

Figure 4 shows the correct answer rate of all participants for each vibrator. In Fig. 4, the top and bottom of the box indicate the lower quartile and the upper quartile of the correct answer rate, the whiskers indicate the minimum and maximum of the rate, and the horizontal bar indicates the median of the rate. The correct answer rate was higher than the chance level (50%) for all vibrators. Moreover, the average correct answer rate for all conditions was 83.3%. This means participants could perceive the correct directions of pulling force. Therefore, this result suggests that the kinesthetic illusion can be induced by generating asymmetric vibrations that consist of a fundamental wave and a second harmonic using commercial vibrators.

We conducted a two-way repeated measures ANOVA (analysis of variance) for the correct answer rate with the vibrator type and the directions of force as factors. A Mauchly's sphericity test was performed before the ANOVA, and the sphericity assumption was not rejected for all factors. The ANOVA showed that vibrator type $[F_{(2,10)} = 1.43, p = 0.28, \eta_p^2 = 0.22]$, direction of applied force $[F_{(1,5)} = 0.94, p = 0.37, \eta_p^2 = 0.15]$, and an interaction between the vibrator type and the direction of the applied force $[F_{(2,10)} = 1.41, p = 0.29, \eta_p^2 = 0.22]$ did not have a significant effect on the correct answer rate. Therefore, it was suggested that the illusion was not influenced by differences in the vibrator type and the directions of the applied force.

Although no significant differences were found in the correct answer rate between vibrators, the variance of the correct answer rate was different for each vibrator. In this experiment, vibration acceleration was controlled according to a concept of Amemiya et al. [1]. However, it is presumed that the forces that were applied to the fingertip by the vibrations were different because the sizes and weights of the vibrators were different. The weights of vib.1, vib.2, and vib.3 were 18.1 g, 9.2 g, and 9.5 g, respectively. It is considered that the strongest force was applied on the fingertips by the vibration generated from vib.1, as vib.1 had the largest mass, and the same acceleration profile was applied for each vibrator. The force applied to the fingertip in this illusion may be a factor.

4   Conclusion

In this study, we verified whether a kinesthetic illusion can be induced by combining the fundamental waves and second harmonics of vibrations generated by three kinds of commercial vibrators through psychophysical experiments. As a result, it was confirmed that participants could perceive the correct direction of the pulling force with a correct answer rate of 83.3%. In future works, it will be necessary to evaluate the illusion under the condition where a controlled force applied to the fingertip. Moreover, this illusion should be evaluated at other frequencies.

References

1. Amemiya, T., Ando, H., Maeda, T.: Lead me interface for a pulling sensation from handheld devices. ACM Trans. Appl. Percept. **5**(3), 1–17 (2008). Article 15
2. Rekimoto, J.: Traxion: a tactile interaction device with virtual force sensation. In: Proceedings of ACM Symposium on User Interface Software and Technology, pp. 427–431 (2013)
3. Amemiya, T., Gomi, H.: Distinct pseudo-attraction force sensation by a thumb-sized vibrator that oscillates asymmetrically. In: 2014 Proceedings of Euro Haptics, pp. 88–95 (2014)
4. Tanabe, T., Yano, H., Iwata, H.: Evaluation of the perceptual characteristics of a force induced by asymmetric vibrations. IEEE Trans. Haptics **11**(2), 220–231 (2018)
5. Kim, H., Yi, H., Lee, H., Lee, W.: HapCube: a wearable tactile device to provide tangential and normal pseudo-force feedback on a fingertip. In: Proceedings of ACM CHI 2018, pp. 501:1–501:13 (2018)
6. Culbertson, H., Walker, J.M., Okamura, A.M.: Modeling and design of asymmetric vibrations to induce ungrounded pulling sensation through asymmetric skin displacement. In: 2016 Proceedings of IEEE Haptics Symposium, pp. 27–33 (2016)
7. Tanabe, T., Yano, H., Iwata, H.: The perceptual characteristics of induced pulling illusion corresponding to the frequency spectrum of asymmetric vibrations. In: Proceedings of the Virtual Reality Society of Japan, Annual Conference 2018, 31A-3 (2018, in press). in Japanese
8. Tanabe, T., Yano, H., Iwata, H.: A control method of asymmetric vibrations for a quantitative evaluation of induced pulling sensation. In: 2018 Proceedings of IEEE Haptics Symposium, pp. 54–55 (2018)
9. McMahan, W., Kuchenbecker, K.J.: Dynamic modeling and control of voice-coil actuators for high-fidelity display of haptic vibrations. In: 2014 Proceedings of IEEE Haptics Symposium, pp. 115–122 (2014)

Estimation of Racket Grip Vibration from Tennis Video by Neural Network

Kentaro Yoshida[1(✉)], Yuuki Horiuchi[1], Tomohiro Ichiyama[1], Seki Inoue[1], Yasutoshi Makino[1,2], and Hiroyuki Shinoda[1,2]

[1] Graduate School of Information Science and Technology, The University of Tokyo, 7-3-1 Hongo, Bunkyo-ku, Tokyo, Japan
`yoshida@hapis.k.u-tokyo.ac.jp`
[2] Graduate School of Frontier Sciences, The University of Tokyo, 5-1-5 Kashiwanoha, Kashiwa-shi, Chiba, Japan
`http://www.hapis.k.u-tokyo.ac.jp/?lang=en`

Abstract. In this paper, vibrotactile perception of a person in a video is automatically estimated from the visual and audio information. We limit the video scene to the back view of a tennis player rallying, but other factors such as locations, a player's clothes, sound environments are arbitrary. We use tennis videos taken in three locations for neural network learning of the relation between the video and measured acceleration of the racket grip. Then we show the grip sensation can be successfully estimated from an unknown video. The quality of the produced vibrotactile sensation is evaluated by a subject experiment. The system is based on a similar concept to VibVid proposed by the authors. In this paper, we examine more general case than the previous research. . .

Keywords: Neural network · Signal generation · Video analysis · Multi modal · Vibrotactile stimulus

1 Introduction

Note: this study was demonstrated at IEEE Haptics Symposium 2018 [1].

Enormous number of videos are shared on the Internet and potential needs to create haptic experiences from such videos are emerging. Since an ordinary video with visual and auditory information includes no explicit haptic information, an approach is that a human designer edits the haptic stimulation heuristically being supported by authoring tools. Automatic production of haptic signals has also been tried in many researches, which was extensively reviewed by Danieau et al. [2] in 2013.

If we focus on automatic vibrotactile signal production from a video, the displayed information is divided into two categories. One is vibration seeking psychological effects where the faithfulness to actual haptic perception is not considered. The vibrations displayed by a seat or jacket reflecting the music

and sound can enhance the immersiveness, but such vibration is not necessarily faithful to the physical events [3–6].

The other one is vibration for realistic haptic experience. The vibration to a large body area reflecting the visual vibration of a first-person video can produce a body experience for the watcher. In the research of [7], the bike-handle vibration was reproduced from the overall visual vibration of a bike-riding first-person video. In [8], the quality of experience of the watcher improved by presenting tactile sensation based on the acceleration recorded simultaneously with the video. In most of the situations, it is theoretically impossible to recover the actual vibrations perfectly, but possible to produce effective vibration felt realistic.

In this research, we extend the realistic vibration recovery into more general events. Suppose a problem that a video watcher holding a tactile display experiences the tactile sensation of a person in the video. Automatic generation of such tactile sensation from video had been considered practically difficult since the computer must understand the event in the scene, but recent technological advancement of machine learning makes it realistic. In this paper, we try automatic recovery of racket vibration from a tennis video. We limit the video scene to the back view of a player but other factors of the environmental view, clothes of the players, and sounds from the environment are arbitrary. After reasonable term of machine-learning between the video and measured acceleration of the racket grip, we show the grip sensation can be successfully estimated from an unknown video.

The similar concept of the vibration recovery has already been published as VibVid in [9]. But the device was imperfect, and the experimental condition was limited. In this research, we improved the device and we verify the generalization ability of VibVid. Since the first-person video of a player was used in the previous research [9], the overall visual vibration was a too strong que of the shot moment. In this research, we use the videos from behind the player with a fixed camera. Furthermore, we take three different videos in different locations and we verify the performance to the video taken in a different place.

2   System

The outline of the proposed system is shown in Fig. 1. In order to learn the estimation model, videos (image frames and sound) and acceleration data are stored. Next, we synchronize the three kinds of data in time. After some preprocessings are done to the data input, an estimation model whose inputs are image frames and sound data, and an output is an acceleration data begins to be generated. We advance the model learning by using the acceleration measured as correct answer data. With this system, we aim to produce appropriate vibrotactile sense for a certain genre (tennis play here) of videos using the above estimation model on the acceleration. The details of the method is explained in following sections.
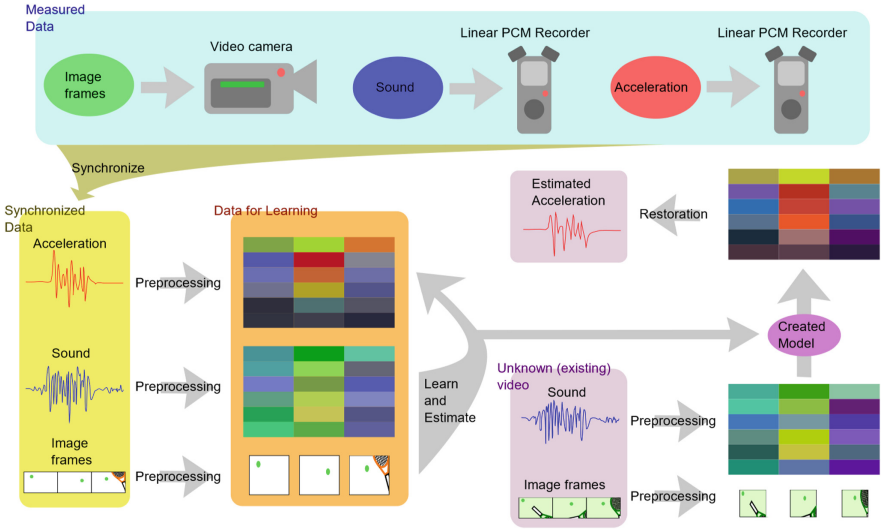
Fig. 1. System overview.

2.1   Recording Acceleration Data

First, we record the acceleration data simultaneously with the video. In order to richly generate vibrotactile signals, we must record acceleration data at a high frame rate [10]. Therefore, acceleration data is recorded using a recording device for audio. A design for simultaneously recording acceleration and sound is shown in Fig. 2. Data are recorded from a monaural microphone and a 1-axis acceleration sensor with stereo PCM (Pulse-Code Modulation) recorder. Here, the sound is recorded together because of the later synchronization processing.

In addition, it is conceivable that the video to be given the tactile sense might be a genre that is active and has a large movement of the photographer. So, not only the acceleration sensor, but also the circuit board and the like for driving and recording are necessary to be small and lightweight so that the photographer can wear entire devices for the record of acceleration.

2.2   Synchronization Among Image Frames, Sound, and Acceleration

Next, the data obtained individually are synchronized in time. The acceleration is recorded by the acceleration sensor as described above, the video (image frames) is recorded by a video camera, and the sound is by another audio recorder.

The data recorded separately on 3 devices are time-synchronized by the method shown in Fig. 3. The circuit including two metal rods shown in the right of Fig. 3 is made so that the LED turns on by bringing the rods into contact. By assuming the metal sound and the light of the LED appear at the exact same timing, synchronization is achieved.
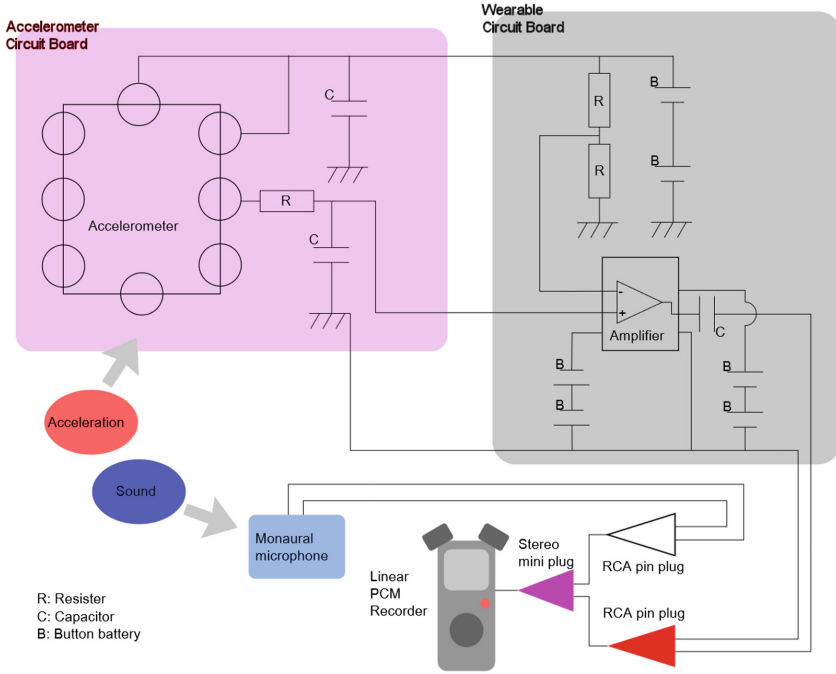
Fig. 2. Circuits for recording acceleration data with sound data.
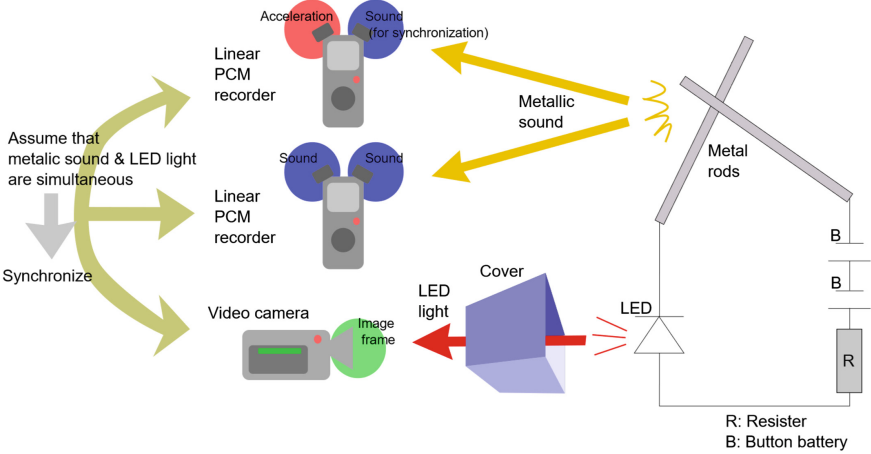
Fig. 3. Synchronization system overview.

2.3   Estimation Model

By using a machine learning framework, we construct a neural network that estimates acceleration data from image frames and sound data. Since the information contained in the video is enormous, its computational load is high.

In this method, in order to efficiently advance the learning, some preprocessing are performed on data, and then necessary information is extracted.

Both video and acceleration are time series data, and it is natural that the relevance (between video and acceleration) at the same time period is very high. Therefore, the time period corresponding to one image frame is defined as one block and the sound/image frame of N blocks centered on the very block is used to estimate the acceleration data of one block. For example, when $N = 3$, the model outputs acceleration data of #5 when inputting sound and image frame data from #4 to #6. The approximate shape of the neural network constructed by this method is shown in Fig. 4. As shown in Fig. 4, convolution layers and max pooling layers are applied only to image data, because they are 2D spacial data and have important information in shapes and colors rather than just positions of them. When only image frame is used for input, it is configured as a neural network with only the portions indicated by yellow and green in the Fig. 4. Similarly, when only sound is used for input, it becomes blue and green parts.
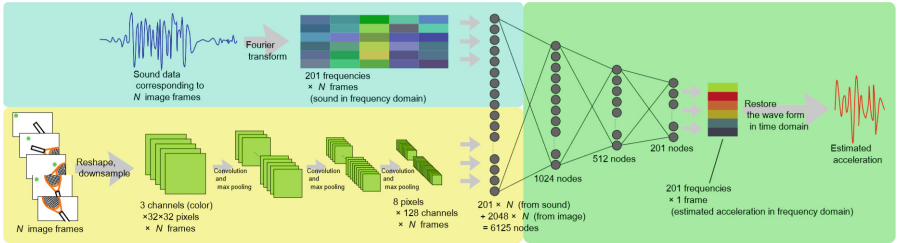
Fig. 4. Neural network for the estimation model.

The image frame was downsampled to 32×32 pixels and used as the image input of the neural network in order to decrease the calculation load.

Next, sound and acceleration, although these are one-dimensional quantities, the sampling rate is high and the amount of information is also large. There is also a method to calculate the time series sound data by directly placing it in the framework of machine learning, but it is known that the calculation load is large [11]. In this paper, we focus on the information on the amplitude and frequency of the waveform, so the data is converted into power spectrum from chronological order. Then, every 1 block of sound and acceleration data is converted into a power spectrum (one-dimensional vector) by using a Fourier transform.

The data organized by the above preprocessing is used into the neural network as inputs or a label, and a model is obtained through the learning. The neural network is implemented with a framework chainer. The layer structure is as shown in Fig. 4, the batch size is 100, the LeRU function is used for the activation function, and Adam [12] is used for the optimizer.

2.4 Waveform Restoration

After the learning, by applying the model to existing video (whose acceleration is unknown), we get a power spectrum of an estimated acceleration data. Then we must convert it to time series data of acceleration. The obtained data is a power spectrum in a time range corresponding to one block. Let the obtained one-dimensional vector

$$\mathbf{v} = (v_1, v_2, \ldots v_i, \ldots v_M) \tag{1}$$

represent the power spectrum of the acceleration data for discrete frequency,

$$f_i = i \times \Delta f. \tag{2}$$

Here, since this power spectrum is converted from a sample of 1 block by using discrete Fourier transform, f and time range for 1 block T_b have the following relationship,

$$f = T_b^{-1}. \tag{3}$$

Therefore, all waves with the frequency of the intensity represented by v can reproduce waves of exactly integral multiples within one block. Since v has no phase information, the phase shift of the acceleration signal within one block can not be restored. Here, ignoring the phase, a sine wave of the discrete frequencies that makes the start point and the end point (of one block) zero is generated. That is, the time series acceleration data $V(t)$ is reconstructed as

$$V(t) = \sum_{i=1}^{M} v_i \times \sin(2\pi f_i t). \tag{4}$$

Also, since humans are known not to be able to perceive vibrations with too high frequencies, here a frequency higher than $M \times \Delta f$ are ignored.

3 Implementation

Figure 5 shows what we made for this research. This time we implemented on the premise that we will record the vibration transmitted to the tennis racket. Therefore, the acceleration sensor was attached to the lower part of the face of the tennis racket. As shown in Fig. 5D, in order to attach the accelerometer, the frame was sandwiched between duralumin plates and rubber double-faced tapes, and strongly fixed with screws. The accelerometer base was fixed with screws on its lower face. This time we used ADXL250 (Analog Devices) as an accelerometer. A circuit for driving this accelerometer and connecting it to the

linear PCM recorder was mounted on the wristband as shown in Fig. 5A, B, C. In this implementation, LS-P2 (Olympus) was used as a linear PCM recorder.

Also, the device fabricated for synchronization is shown in Fig. 5E. In this case I used a triangle as metal rods and made a cover with black acrylic board.

Finally, a device for presenting vibration was constructed as shown in Fig. 5F. A duralumin board and a vibrator were attached with glue to the tennis racket cut at the grip part. We used MM3C-LF (Tactile Labs) as the vibrator.
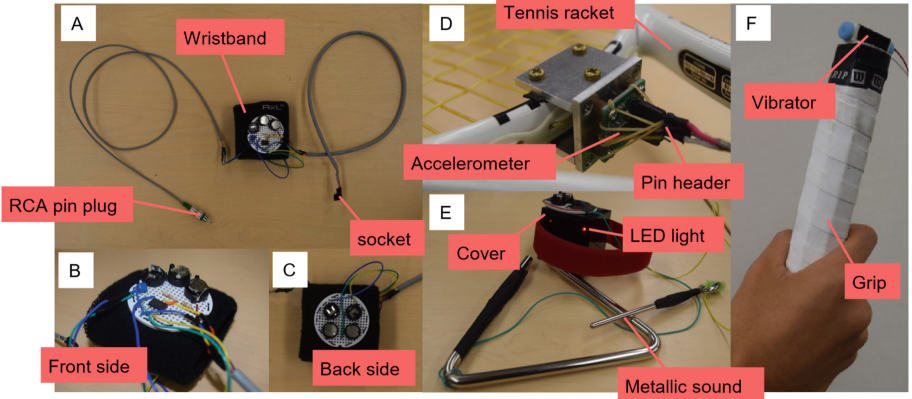
Fig. 5. A, B, C: implementation for recording acceleration transmitted to the tennis racket, D: the accelerometer fixed at the bottom of a face of a tennis racket, E: the devices for synchronization of three recorded data, and F: the device shaped tennis racket's grip for presenting vibrotactile signal.

4   Experiment

Next, we implement the estimation model by this method and conduct its evaluation experiment. Firstly, as shown in Fig. 6A, we recorded videos of tennis for the experiment. GoPro HERO 5 Session (Woodman Labs) was used for the video camera for image frame recording, LS-P2 (Olympus) was used for sound recording, and the device described in the previous section was used for acceleration recording. As shown in Fig. 7A, videos were taken for about 3 to 9 min each at four tennis courts at different places. The image used for the experiment is 1280 × 720 pixels, 120 fps. The contents of the video were two players rallying with strokes and the video camera was placed about 5 m behind the end line. We used videos at the three tennis courts shown in Fig. 7A-1, A-2, A-3 (about 18 min) for learning, and the video at one remaining tennis court in Fig. 7B (about 2 min) was used for testing. A player and photographer, a racket, and shoes were the same in four videos, but clothes and a hitting partner were different.
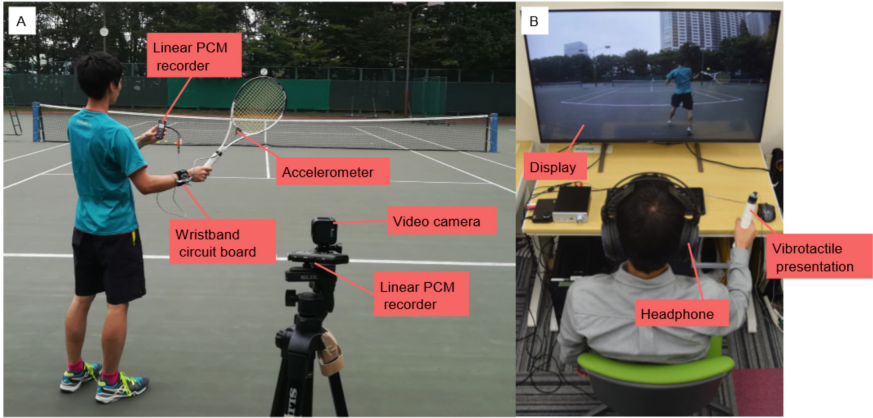
Fig. 6. A: Data recording from the back of a tennis player and photographer, B: the experiment of vibrotactile presentation while watching a tennis video.

PC used for machine learning loaded Intel Xeon E5-1620 v3 @ 3.50 GHz ×8, TITAN X (Pascal)/PCIe/SSE2. The time taken to the learning using 18 min video was about 12 to 24 h per one epoch, and the time taken to the estimation of vibrotactile signal from the unknown video by applying the model is about the same as the length of video being applied.

All procedures in this experiment involving human participants were in accordance with the ethical standards of the institutional research committee (The University of Tokyo) and with the 1964 Helsinki declaration and its later amendments or comparable ethical standards. Informed consent was also obtained from all individual participants.
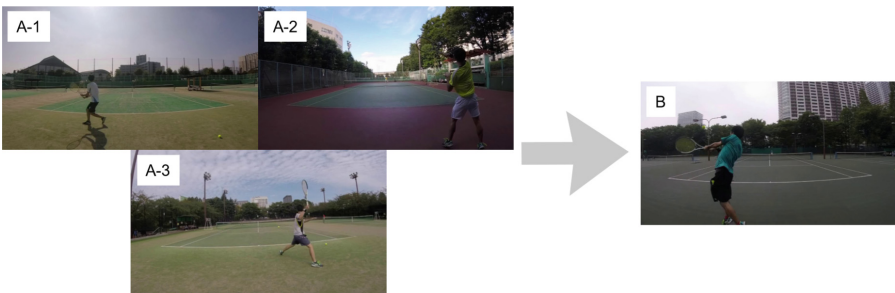
Fig. 7. A: Three videos taken at different locations for learning, and B: a video taken at a different location from the left three for testing.

4.1   Vibration Waveform Estimation

The model obtained by the learning was applied to the video taken at an different location which is shown in Fig. 7B, and a vibration waveform was estimated. We evaluated two estimation method, Sound-only method and Sound-image method. Sound-only method uses only sound data for the input, and Sound-image method uses both image frames and sound data for the input. We tried a method using only image frame for the input, but it did not generate any good waveforms, so it was not evaluated this time. We used the model of Sound-only method at 5th epoch and the model of Sound-image method at 1st epoch for the experiment, which were determined by checking root mean squared errors. The reason we didn't require many epochs is that the amount of input was sufficiently large compared to the diversity of the input.

Figure 8 shows the results about one of the video for testing. In Fig. 8, recorded sound waveform was shown as blue line, real measured acceleration waveform as black, acceleration waveform which lost phase information by being performed Fourier transform and inverse Fourier transform (Converted real acceleration) as gray, estimated waveform by Sound-only method as light blue, and estimated waveform by Sound-image method as orange.

Figure 9 shows an enlarged waveform at about 37 s in Fig. 8, and their spectrograms are shown in Fig. 10. The reason that there is less high frequency component in Converted real acceleration than Real is because frequencies that are too high are removed during processing as explained by the Eq. (4) of the method. In this example, $M = 9$, and vibration with frequency higher than 1080 Hz was removed.

4.2   User Experiment

User experiment was conducted as shown in Fig. 6B. We used two videos taken at the location for testing as shown in Fig. 7. Ten subjects from 20 years old to 24 years old participated the experiment. Among the subjects, six were male, two experienced tennis for over 5 years, all were right handed. We paid about 5 dollars for each subject as a reward. Subjects were presented with vibrations generated in three methods along with the videos, and evaluated it by 9 stages (from 0 to 8) after each video. Three methods are 1: measured real acceleration (Real), 2: acceleration estimated from sound only (Sound-only method), 3: acceleration estimated from images and sounds of 5 frames (Sound-image method). The reason that information of 5 frames were used in Sound-image method was that it was considered necessary to take motion information from multiple frames in order to extract vibration information from the image frame. Evaluation criteria are harmony ("Did the vibrations match to the video?"), fun/satisfaction ("Did the vibrations makes the video fun?"), immersiveness ("Did the vibration help you be immersed in the video?"), comfortableness/fatigue ("Did the vibrations feel comfortable to enjoy the video?"), and realism ("Did the vibration played back with the video seem consistent with your real-world experiences?"). Each vibration pattern was reproduced in random order, and they were repeated twice.
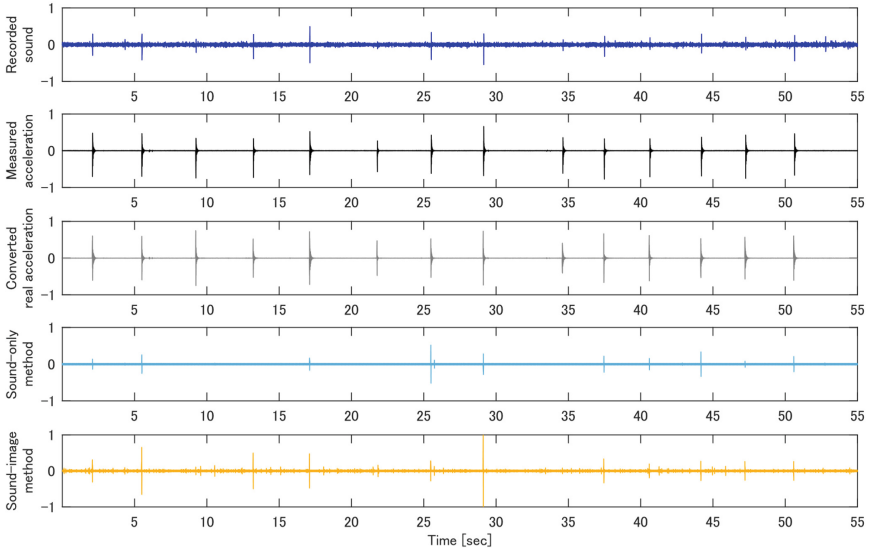
Fig. 8. Waveforms (blue: recorded sound, black: measured (real) acceleration, gray: converted real acceleration, light blue: estimated by Sound-only method, and orange: estimated by Sound-image method).
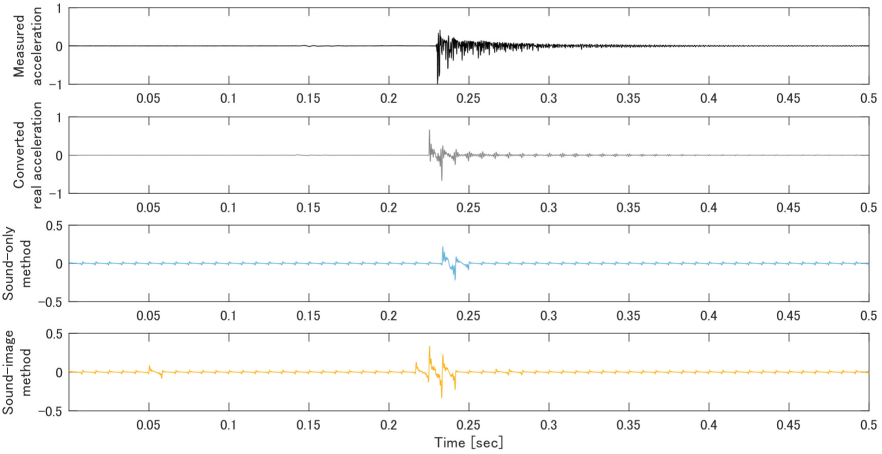
Fig. 9. A segment of acceleration waveforms. Black: measured (real) acceleration, gray: converted real acceleration, light blue: estimated by Sound-only method, and orange: estimated by Sound-image method.

Only the latter part was used for the evaluation. This experiment was conducted after the research ethics review by Graduate School of Information Science and Technology, The University of Tokyo. The result of one of the video is shown in Fig. 11.
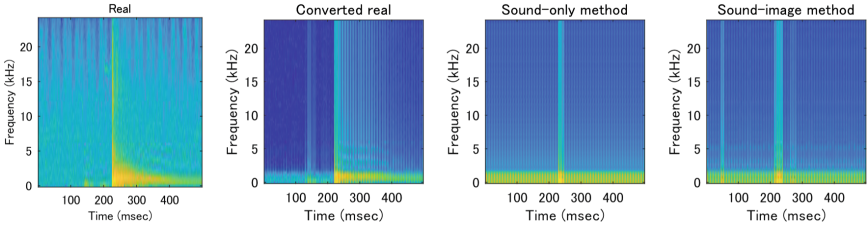
Fig. 10. Short time Fourier transform of Fig. 9 data.
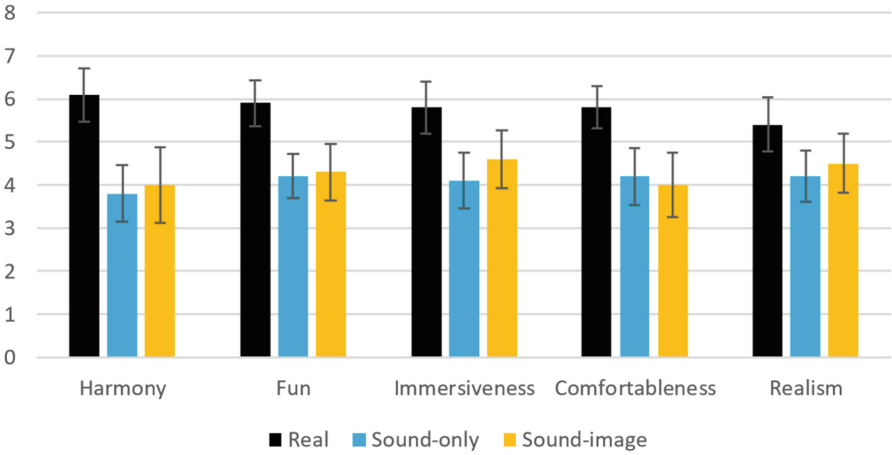
Fig. 11. User experiment results by three method (real, sound-only method, and sound-image method).

Multiple comparison was performed using Tukey's HSD analysis, but no statistical difference was found at the 5% significance level. As a trend, Real's vibration is best evaluated, and the two results of Sound-only method and Sound-image method seem to be not much different.

5   Discussion

The image used was taken at a public tennis court, and there were many general users on next courts and nearby road. Therefore, recorded sound data contained much noise that was not related to vibration or even tennis. Compared with the waveform of the sound, there was much less noise in the data of the recorded acceleration. The waveform in which the phase information was lost by performing the Fourier transform and the inverse Fourier transform on the recorded

acceleration is painted in gray in Fig. 8. In this way, even if the phase information is missing, there is no big influence on the waveform of vibration. Rather, in the experiment of [9], missing phase information showed a tendency better than actual acceleration in all evaluation indices. Therefore, we used this converted real waveform as a correct label of the machine learning.

In the waveform estimated by the Sound-only method, there were some detection errors. In the time axis 9 s and 22 s in Fig. 8, very weak (almost no) sound is recorded in the sound data, but the shot is done. With such recorded data, it is difficult to estimate the vibration from only sound data, and it was impossible to generate the vibration with the Sound-only method. However, since the image information is also used in the Sound-image method, a peak wave is generated by this method although it is a weak waveform.

When closely looking at a single shot wave as in Fig. 9, the Sound-image method generated vibrations for a longer time than the Sound-only method, and the timing was also closer to Converted real. However, in the Sound-image method, many unwanted vibrations were generated, which seemed to be an negative effect in subject experiments.

Looking at the measured acceleration, the sharpness of the amplitude decays progressively after a sudden strong impact like a spike at shot. The shape of this attenuation has not been successfully reproduced in the estimated waveforms as shown in Fig. 9. The reason why Real's score was always good in the results of subject experiments may be due to the difference in expression of waves of this attenuation.

As a result of examining the variance of the score for each subject, the variance value of the Sound-image method was the largest in all of the five evaluation indices. The vibrations by the Sound-image method tend to be strongly liked or disliked. We think the main reason of this individual difference is that some people like steady weak vibrations but the others don't. Since Sound-image method generated vibrations with some noises like steady weak vibrations, some people said that it was realistic feeling such as winds or movements but the others said that there were unnecessary vibrations.

As described above, generally-taken video includes various noises, and it is difficult to appropriately estimate the vibration from only the sound or only the image. Although there was no clear difference in the subject experiment, looking at the estimated waveform, it was clearly better to use both image frames and sound data.

6   Conclusions

Vibrotactile perception of a person in a tennis video was automatically estimated from the visual and audio information. The proposed system was an improved version of the neural network based system VibVid and it was applied to the videos taken in a different location.

The estimation results of Sound-only and Sound-image methods are compared. Although there was no big difference in a subject experiment, the Sound-image method was superior to the Sound-only method in the ability to generate vibration waveforms.

Since the proposed system successfully estimated the racket acceleration data from a video taken at a different location from the one for learning, it was confirmed that the system had generalization ability.

In the future, it is expected that the accuracy of these methods will be further improved by improving neural network structure and input/output data forms.

References

1. Yoshida, K., Horiuchi, Y., Ichiyama, T., Inoue, S., Makino, Y., Shinoda, H.: Estimation and presentation of racket grip vibration with tennis video. In: IEEE Haptics Symposium 2018, Demo 5, California, USA, San Francisco, 25–28 March 2018 (2018)
2. Danieau, F., Lecuyer, A., Guillotel, P., Fleureau, J., Mollet, N., Christie, M.: Enhancing audiovisual experience with haptic feedback: a survey on HAV. IEEE Trans. Haptics **6**(2), 193–205 (2013)
3. Kim, M., Lee, S., Choi, S.: Saliency-driven real-time video-to-tactile translation. IEEE Trans. Haptics **7**(3), 394–404 (2014)
4. Hwang, I., Choi, S.: Improved haptic music player with auditory saliency estimation. In: Auvray, M., Duriez C. (eds.) Haptics: Neuroscience, Devices, Modeling, and Applications, EuroHaptics 2014. Lecture Notes in Computer Science, vol. 8618. Springer, Heidelberg (2014)
5. Lee, J., Choi, S.: Real-time perception-level translation from audio signals to vibrotactile effects. In: Proceedings of the SIGCHI Conference on Human Factors in Computing Systems (CHI 2013), pp. 2567–2576. ACM, New York (2013)
6. Lee, J., Han, B., Choi, S.: Motion effects synthesis for 4D films. IEEE Trans. Vis. Comput. Graph. **22**(10), 2300–2314 (2016)
7. Gongora, D., Nagano, H., Konyo, M., Tadokoro, S.: Vibrotactile rendering of camera motion for bimanual experience of first-person view videos. In: 2017 IEEE World Haptics Conference (WHC), Munich, pp. 454–459 (2017)
8. Danieau, F., et al.: Framework for enhancing video viewing experience with haptic effects of motion. In: 2012 IEEE Haptics Symposium (HAPTICS), Vancouver, BC, pp. 541–546 (2012)
9. Yoshida, K., Inoue, S., Makino, Y., Shinoda, H.: VibVid: VIBration estimation from VIDeo by using neural network. In: Proceedings of the 27th International Conference on Artificial Reality and Telexistence and the 22st Eurographics Symposium on Virtual Environments (ICAT-EGVE 2017). Eurographics Association, Adelaide (in press)
10. Akahane, K., Hasegawa, S., Koike, Y., Sato, M.: A development of high definition haptic controller. In: First Joint Eurohaptics Conference and Symposium on Haptic Interfaces for Virtual Environment and Teleoperator Systems. World Haptics Conference, pp. 576–577 (2005)
11. Oord, A., Dieleman, S., Zen, H., Simonyan, K., Vinyals, O., Graves, A., Kalchbrenner, N., Senior, A.W., Kavukcuoglu, K.: WaveNet: a generative model for raw audio. CoRR, abs/1609.03499 (2016)
12. Kingma, D., Ba, J.: Adam: a method for stochastic optimization. CoRR, abs/1412.6980 (2014)

A Hand Wearable Device Used in Local Curvature Recovery

Tao Zeng[1,2(✉)] and Shizhen Huang[1,2]

[1] Department of Instrumental and Electrical Engineering, Xiamen University, Xiamen, China
tao.zeng@xmu.edu.cn
[2] Shenzhen Research Institute of Xiamen University, Shenzhen, China

Abstract. In virtual curvature perception, extrusion-type curvature reproduction that refers to extruding the fingertip by a plate to render skin and muscle deformation so as to obtain the sense of curvature, is the way that with favorable effects. However, as the extrusion stimulus is always a rigid plate, the contact surface between the finger and the plate is a plane, only height difference and attitude difference are considered but not the local curvature. This work presents a hand wearable device which is used to recover local curvature by lifting up or pressing down the finger according to touch position in the process of exploring, which is a supplement to traditional extrusion-type curvature reproduction.

Keywords: Curvature reproduction · Local curvature · Hand wearable device

1 Introduction

The three geometrical components of curvature are height difference, attitude difference and local curvature corresponding to zeroth-, first- and second-order information respectively, and the attitude difference is the dominant resource in curvature perception [1, 2]. In the present methods, extrusion-type curvature reproduction is a favorable one, which can truly render zeroth-order and first-order information. What's more, extrusion-type curvature reproduction can realize active and dynamic touch resulting in significant similarity compared to the real process [3]. However, a rigid plate is always used as the extrusion stimulus, the second-order information will definitely be recovered with deviation when the curvature is relatively large. As shown in Fig. 1(a), the length of local curvature is relatively longer when touching at a physical sinusoidal model than that when touching at an interactive plate. For recovery of contact length at the fingertip in extrusion process, we put forward a hand wearable device to lift up or press down the finger according to touch positions, in order to make local curvature compensation based on traditional extrusion-type curvature reproduction.
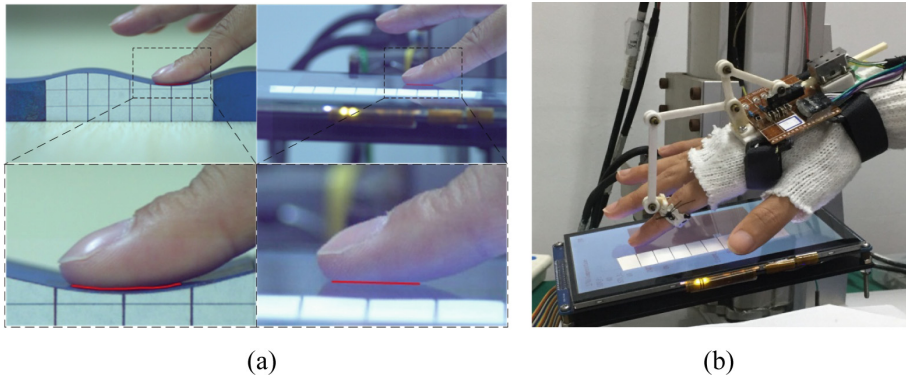
Fig. 1. (a) Difference of second-order information between touching at physical sinusoidal model and touching at interactive plate. (b) The hand wearable device and its application.

2 Device Design and Its Application

The hand wearable device, which is driven by a piezoelectric linear motor, can convert the linear movement of the motor into the finger movement of pressing down or lifting up. The interactive plate described in [3] is used as the extrusion stimulus, which can simulate the dominant cue for curvature perception. As shown in Fig. 1(b), the hand wearable device presses down or lifts up the finger according to compensation dosage in local curvature along with simultaneous the rotation of interactive plate, making that the contact length approximates to the real situation. The extrusion displacement compensation is the difference between the target and actual extrusion displacements of the finger touching the extrusion plate. The advantage of this method is that all the components of curvature are reproduced, including the height difference, attitude difference, and local curvature.

References

1. Pont, S.C., Kappers, A.M.L., Koenderink, J.J.: Similar mechanisms underlie curvature comparison by static and by dynamic touch. Percept. Psychophys. **61**(5), 874–894 (1999)
2. Wijntjes, M.W.A., Sato, A., Hayward, V., Kappers, A.M.L.: Local surface orientation dominates haptic curvature discrimination. IEEE Trans. Haptics **2**(2), 94–102 (2009)
3. Zeng, T., Chen, W., Li, N., He, L., Huang, L.: Haptic perception of macro texture. In: Asiahaptics 2016, pp. 9–11. Springer, Singapore (2016)

Random Forest for Modeling and Rendering of Viscoelastic Deformable Objects

Hojun Cha[✉], Amit Bhardwaj, Chaeyong Park, and Seungmoon Choi

Pohang University of Science and Technology (POSTECH),
Pohang, Republic of Korea
{hersammc,amitbhardwaj,pcy8201,choism}@postech.ac.kr

Abstract. In the recent past, data-driven approaches have gained importance for modeling and rendering of haptic properties of deformable objects. In this paper, we propose a new data-driven approach based on a well known machine learning technique: random forest. We train the random forest for regression for estimating the input-output mapping between discrete-time interaction data (position/displacement and force) collected on a homogeneous deformable object. Unlike currently existing data-driven approaches, we use at most 1% of the recorded interaction data for the training of the random forest. Even then, the trained random forest model reproduces all the interactions used for the training with a good accuracy. This also provides promising results on unseen data. When employed for haptic rendering, the model estimates smooth and stable interaction forces at an update rate more than 650 Hz.

Keywords: Viscoelasticity · Haptic modeling and rendering ·
Random forest

1 Introduction

In the recent past, data-driven techniques have gained importance for modeling and rendering of viscoelastic deformable objects [2,3]. Here non-parametric input-output mapping models are trained using measured discrete-time interaction data (position, velocity, acceleration, and force) and machine learning approaches. In [3,4], viscoelastic response of a deformable object is estimated using Radial Basis Functions (RBFs) trained on the measured data. In [6], Yim et al. extend this approach to inhomogeneous materials. The currently existing RBF-based approach quickly become computationally intractable when used on large datasets. In the very recent work [5], Matthias's group has tried to address

this problem. They have proposed a method for reducing the size of discrete-time dataset. Firstly, a low-dimensional compact feature space is generated in the frequency domain. Next, this feature space is used to reduce the size of the original discrete-time dataset with the help of feature-based learning. The reduced discrete-time dataset is used for training the RBFs.

In this work, we propose a new data-driven approach based on random forests, for modeling and rendering of the viscoelastic behavior of deformable objects. The proposed approach is capable of handling large datasets, unlike RBF-based approach. We train the random forest for regression estimating the relationship between the measured position (input data) and the response force (output data) signals. We acquire discrete-time interaction data (position/displacement and force) from many automated pushing interactions on a deformable object. Unlike the currently existing approach (the RBFs), we consider at most 1% of the measured data for training of the random forest. Even then, the trained forest model reproduces all the interactions used for the training with a good accuracy. On unseen data, the performance of the model is also promising. Subsequently, we employ the trained model for haptic rendering, and realize smooth and stable interactions in a virtual environment. In summary, our proposed approach for modeling and rendering is very simple and quite efficient in handling large datasets.
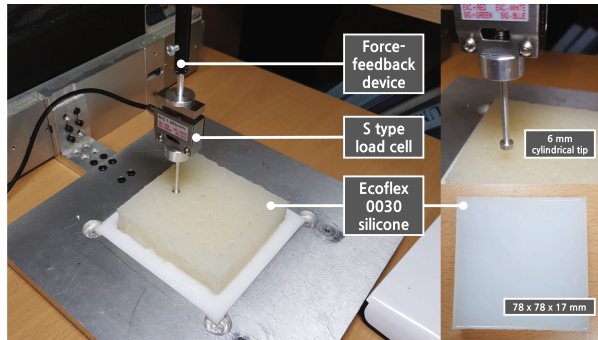
Fig. 1. Data acquisition setup.

2   Data Acquisition

In this section, we define our setup for collecting position and force response data of a viscoelastic deformable object. We fabricate one homogeneous deformable object by mixing Smooth-On-Ecoflex 0030 part A and B with Smooth-On-Silicone thinner in the ratio of 1:1:0. In the setup, a S-type load cell (DBCM-2 Kg- Bongshin) is attached to the tip of a force feedback device (PHANToM Premium 1.5 HF, 3D Systems, Inc.) as shown in Fig. 1. The position data is collected by the sensors of the force feedback device, and the response force data

is measured by the load cell, which is further connected to a data acquisition card (DAQ PCI-6220, National Instrument, Inc.). Sampling rates of both the device and the load cell are 2 kHz.

We use an automated approach for data acquisition, and collect the discrete-time interaction data for many pushing interactions at one point of the silicone (away from the boundary points as shown in the Fig. 1). In the automated app-roach, tip of the device might be controlled in two ways: position or force con-trolled. In this paper, a force controlled approach is adopted. A force control signal is commanded to the tip of the force feedback device. In response to this control signal, the position and response force signals are measured from the force feedback device and the load cell, respectively.

We collect the data using two types of force control signals: ramp and creep. A ramp control signal, as the name suggests, linearly increases with a certain slope S_1 (N/s) till it reaches a target force level F, then it decreases linearly with another slope S_2 (N/s) and drops down to zero. The rising slope S_1 randomly picks values from a set $A = \{1/10,2/10,3/10,4/10,5/10,6/10,7/10,8/10,9/10,10/10, 10/9,10/8,10/7,10/6,10/5,10/4,10/3,10/2,10/1\}$. And, the falling slope S_2 also picks the value from the same set with a negative sign. The target force level F is an integer chosen from 3 to 10 N. We collect the data for more than 100 such ramp control signals. Another force control signal takes a constant target value C for a certain time T, and zero for rest of the time. This kind of signal is used for a creep test of a viscoelastic object, thus we name this control signal a creep control sig-nal. The constant C takes the values similar to the target force level F in the ramp signal, and T takes integer values from 2 to 5 s. The creep control signal attains its constant target value in 0.1 s. We collect the position and force response data for 20 such creep control signals. In Fig. 2a and b, we show the measured position and response forces for a typical ramp and creep control signal, respectively. Here onwards, the data measured by both control signals are referred to as the ramp and creep data.

(a)   (b)
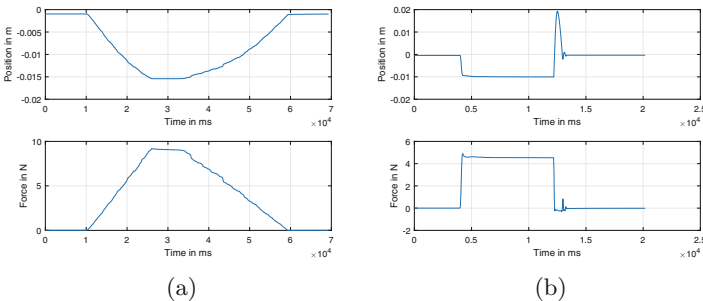
Fig. 2. Measured position and response force signals for a typical (a) ramp and (b) creep force signals.

3   Random Forest Regression Modeling

Having collected the data for a silicone object during a pushing interaction, we aim for finding a non-parametric input-output relationship between the position and response force. For the purpose, we employ a well known non-parametric machine learning technique: random forests [1]. Here we use the random forest for regression, not for classification. A random forest consists of many decision trees, and the results of the trees are averaged to find the final outcome for a regression problem. Random forest is known to be free from over-fitting of the data, and is capable of handling a large number of input attributes (both numerical and categorical). In addition, it has many other advantages like handling of missing values and outliers.

In literature, the viscoelastic behavior is mathematically represented by a spring and a damper element. Thus, the response force is a function of both position and velocity. In [3,6], both position and velocity values are used in the input feature vector for training the RBFs. Here in this work, we use the current and past two position samples for input features (sampling rate $= 2\,\text{kHz}$, thus past 1 ms position information), and the response force for output. In other words, instead of using direct velocity information in the feature vector, we consider past 1 ms position information for modeling damping behavior of the viscoelastic material. If $P_z[n]$ be the nth position sample along Z axis, the nth input feature vector is defined as

$$I[n] = \{P_z[n], P_z[n-1], P_z[n-2]\} \tag{1}$$

If the measured force along Z axis is denoted as F_z, then the random forest is trained on $(I[n], F_z[n])$ pair.

As mentioned in the previous section, we have collected two types of data: ramp and creep. A ramp type of data has been used for training the forest. Ramp data consists of more than 100 discrete-time interactions (position/force). We generate the input feature vector for each such interaction, and stack them together. In this way, we get the overall input/output feature vector of length more than six millions. For training the random forest, we randomly pick only N number of instances from the overall feature vector. This random sampling ensures that the training data has samples from different kinds of ramp type interactions (different slopes, and different amplitudes), so the trained model should be able to generalize the results on unseen signals. We train the random forest (100 decision trees) with different values of N: 2,000, 5,000, 10,000, 20,000, 30,000, 40,000, 50,000 and 100,000 (i.e, at most 1% of the overall feature vector). To observe the effect of training size N on the modeling, we test the trained random forest model on one typical ramp interaction, and compute the sum of squared error (SSE) between the predicted and the measured response. In Fig. 4a, the SSE is plotted against the training size N. As expectedly, the SSE decreases as the N increases. However, the modeling time and the size of the trained model also get increased with a more number of training samples. In addition, the size of the trained model has an inverse relationship with the
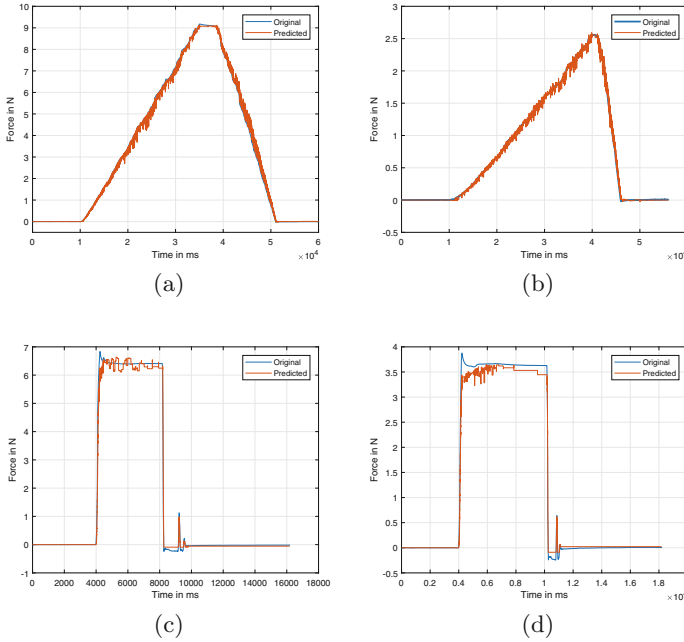
Fig. 3. Force responses predicted by random forest modeling with 20,000 training samples: (a)–(b) and (c)–(d) are for ramp and creep data, respectively. Left column: high range of force; Right column: low range of force.
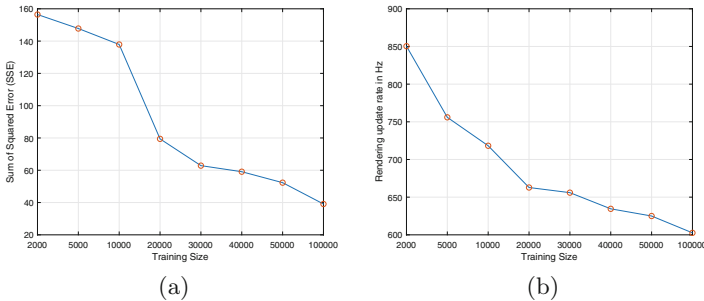
Fig. 4. Measured position and response force signals for a typical (a) ramp and (b) creep controlled force signals.

haptic rendering update rate (explained in the next section). Thus, there is a trade-off between the modeling accuracy and the update rate.

Next, we check the performance of the trained random forest model. Note that the model is trained on randomly chosen samples of the ramp signals, not on a complete one ramp kind of interaction. Thus, firstly we check how accurately the model reproduces ramp interactions. Figure 3 shows the response forces predicted by the model trained on 20,000 training samples. We observe

that the model reproduces all the ramp interactions with a good accuracy as shown in Fig. 3a and b, irrespective of slopes (S_1 and S_2) and target force (F). However, the predicted responses has some noise, but that can easily be filtered out. The model also predicts creep interactions (unseen data) quite accurately as shown in Fig. 3c and d, irrespective of the values of C and T. Thus, our random forest based modeling provides promising results.

4   Rendering

Next, we employ the trained forest model for haptic rendering a virtual environment. When interacting with the virtual environment (pushing interaction), we get a resulting force computed by the trained model. Figure 4b plots the force update rate against the training size of the model. The update rate shows a decreasing trend as the training size increases, showing a trade-off between the modeling accuracy and the update rate. However, in this paper, we have not evaluated the rendering performance by a subjective experiment, but by our own experience, the model trained on 20,000 samples provides smooth and stable interaction forces.

5   Conclusion

In this paper, we have provided preliminary results of random forest based modeling and rendering of the viscoelasticity of a deformable object. The results of our approach are very promising, both for modeling and rendering. This approach is capable of handling large datasets as we need at most 1% of the overall feature vector for training the random forest. In this paper, we have tested the approach only on one object. In future, we will test the approach on different deformable objects. Extending this approach to inhomogeneous objects is also in our pipeline. We would also like to include more past position information for modeling the object, and check how the modeling and rendering performances are affected by this.

References

1. Breiman, L.: Machine Learning, Chap. 1, pp. 5–32. Springer (2001)
2. Fong, P.: Sensing, acquisition, and interactive playback of data-based models for elastic deformable objects. Int. J. Robot. Res. **28**(5), 630–655 (2009)
3. Hover, R., Kósa, G., Szekly, G., Harders, M.: Data-driven haptic rendering–from viscous fluids to visco-elastic solids. IEEE Trans. Haptics **2**(1), 15–27 (2009)
4. Sianov, A., Harders, M.: Data-driven haptics: addressing in homogeneities and computational formulation. In: World Haptics Conference (WHC), pp. 301–306. IEEE (2013)
5. Sianov, A., Harders, M.: Exploring feature-based learning for data-driven haptic rendering. IEEE Trans. Haptics **1**, 1–1 (2018)
6. Yim, S., Jeon, S., Choi, S.: Data-driven haptic modeling and rendering of viscoelastic and frictional responses of deformable objects. IEEE Trans. Haptics **9**(4), 548–559 (2016)

A Teleoperation System for Reproducing Tactile Perception Using Frequency Channel Segregation

Po-Hung Lin and Shana Smith[(✉)]

Department of Mechanical Engineering, National Taiwan University, Taipei,
Taiwan, R.O.C.
{r05522606,ssmith}@ntu.edu.tw

Abstract. Nowadays, haptic feedback technology has been applied to many applications to help users acquiring more information concerning surrounding environments. In this research, a real-time teleoperation system was developed to bring vibrotactile sensation concerning object surface texture from a remote location to the local users. A force sensor and a PVDF sensor were used to design a data recording device, which was attached to a remote slave robot arm, for recording physical surface texture information. Based on the different sensitivity frequency ranges of the mechanoreceptors in human glabrous skin, a novel tactile rendering device was designed to trigger frequency-channel-segregated vibrotactile stimuli in the master's side. Two bending piezoelectric actuators were used to trigger different stimulation intensities with different frequency ranges. To examine the efficacy of the teleoperation system, a tactile discrimination test was conducted. Users were asked to match the simulated surface textures with physical surface textures. The correctness of the discrimination test was about 87.5%. The results also showed that the developed system can produce realistic remote surface textures in real time.

Keywords: Vibrotactile feedback · Teleoperation ·
Surface texture reproduction · Frequency channel segregation ·
Haptics feedback · Piezoelectric actuators

1 Introduction

1.1 Background

Haptic sensation is an important information for humans to explore external environment. Haptic feedback is not only important in the physical world but also in a virtual world. Rendering realistic haptic sensation can increase the realism and immersion of a virtual environment. In teleoperation applications, haptic feedback technology can help reduce task errors and increase work efficiency.

In general, haptic feedback can be categorized into two categories: kinesthetic feedback and tactile feedback. Kinesthetic feedback is related to human limb position, movement and orientation in space. Tactile feedback is related to skin deformation, pressure, thermo-differences and mechanical vibration sensation. Vibrotactile feedback

is a technology to create tactile sensations by stimulating specific mechanoreceptors in human skin using vibration actuators [1–3]. In this research, vibrotactile feedback was used to render realistic surface texture information from a remote location to the local users.

1.2 Motivation and Purpose

Although there has been a lot of research concerning vibrotactile feedback applications, most vibrotactile feedback devices can only provide meaningless or monotone tactile stimulus. Users can only receive a sense of touch, not detailed object texture information. Thus, methods for rendering realistic and meaningful tactile sensations become important for acquiring more object information.

There are several challenges in providing realistic texture information to users. First, methods to record detailed surface texture information are difficult because surface texture information is often complex and with broad frequency bandwidth. Second, methods to trigger an actuator to render the same tactile sensation is another issue because there is a complicated relation between the physical surface texture information and the mechanical behavior of the actuator. Third, in human glabrous skin, different mechanoreceptors have different frequency sensitive ranges. In this study, a teleoperation system was developed, using frequency channel segregation, to assist local users to explore remote objects.

2 System Architecture

The system contained two parts, the master side and the slave side, as shown in Fig. 1. The master side included a graphical user interface, a vibrotactile feedback rendering device and a Leap Motion hand tracking device. Two piezoelectric benders were used to design a rendering device to render different frequencies for remote texture information on users' fingers. The Leap Motion was a remote motion sensor for tracking human hand motions.
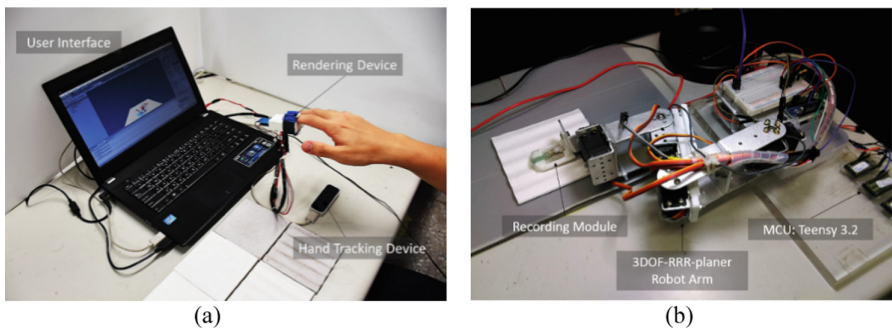
Fig. 1. Teleoperation system: (a) master side and (b) slave side sub-systems
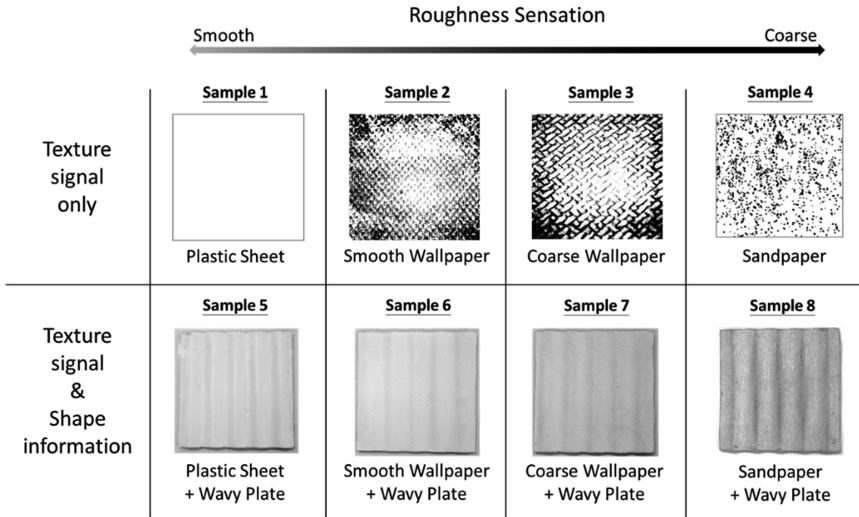
Fig. 2. Test samples

The hand motion information from the master side was transformed into quantitative data for remote slave robot arm control. The slave side included a RRR-planer robot arm and a texture recording module. The RRR-planer robot arm on the slave side was used for exploring remote physical object surface texture data. A PVDF film sensor and one force sensor were assembled as a recording module, attached to the robot arm, for collecting texture information. The motion of the remote robot arm was synchronized with and controlled by the local users' hand motions.

3   Results and Conclusions

This study developed a vibrotactile feedback teleoperation system using frequency channel segregation to enable users to identify different surface textures in remote areas. Eight test samples, as shown in Fig. 2, were used to test the effectiveness of the system. The user test results showed that subjects can clearly distinguish different surface textures. For high-frequency surface textures, the correct rate is about 90%. For low-frequency surface textures, the correct rate is about 75%. In the future, this technology could be applied to more human-machine interactions, such as teleoperated surgery systems and space exploration.

Ethical Approval. All procedures performed in studies involving human participants were in accordance with the ethical standards of the institutional and/or national research committee and with the 1964 Helsinki declaration and its later amendments or comparable ethical standards.

Informed Consent. Informed consent was obtained from all individual participants included in the study.

References

1. Choi, S., Kuchenbecker, K.J.: Vibrotactile display: perception, technology, and applications. Proc. IEEE **101**(9), 2093–2104 (2013)
2. Goldstein, E.B.: Sensation and Perception, 10th edn. Cengage Learning, Boston (2017)
3. Tan, H.Z., Durlach, N.I., Reed, C.M., Rabinowitz, W.M.: Information transmission with a multifinger tactual display. Percept. Psychophysics **61**(6), 993–1008 (1999)

Signal Generation for Vibrotactile Display by Generative Adversarial Network

Shotaro Agatsuma[1(✉)], Junya Kurogi[2], Satoshi Saga[2], Simona Vasilache[1], and Shin Takahashi[1]

[1] University of Tsukuba, 1-1-1 Tennodai, Tsukuba, Ibaraki 305-8577, Japan
`agatsuma@iplab.cs.tsukuba.ac.jp`, {`simona,shin`}`@cs.tsukuba.ac.jp`
[2] Kumamoto University, 2-39-1 Kurokami, Chuo-ku,
Kumamoto-shi, Kumamoto 860-8555, Japan
{`kurogi,saga`}`@saga-lab.org`

Abstract. Various methods have been proposed for collecting vibrotactile information. However, the collection procedure requires manual scanning of texture, collection of vast information may be difficult. Owing to the fast progress of machine learning technologies, even with little information, there is a possibility to generate further virtual data from existing collected data by using Generative Advisory Network (GAN). In this paper, we proposed a generation model of vibrotactile information by Deep Convolutional GAN (DCGAN) from the collected acceleration data. We generated various vibrotactile information by using the proposed DCGAN, and compared the tactile stimulation based on the generated data with the actual texture.

Keywords: Vibrotactile information · Acceleration · DCGAN

1 Introduction

To collect many vibrotactile information, several methods have been proposed. However, the collection procedure requires manual scanning of texture depending on the condition of the touch, collection of vast information may be difficult. Owing to fast progress of machine learning technologies, even with smaller information, there is a possibility to generate further virtual data from existing collected data by using Generative Advisory Network (GAN) [1]. If such generation method is realized, it may be possible to reduce the collecting conditions and the collection cost of vibrotactile data In this paper, as a first step for realizing the proposed method, we generated vibrotactile information by using Deep Convolutional GAN [2]. In addition, we held an experiment to compare the similarity of generated virtual stimulation with actual texture.

2 Systems

In this section, we described the GAN, which is used for the generation of virtual stimulation, and our vibrotactile display, which is used to display vibrotactile information to the user during the experiments.

GAN is one of the many existing machine learning method, which is mainly used for virtual image generation. It is composed of two models: generator and discriminator. The generator generates data from the learned result, whereas the discriminator evaluates the data generated by generator. In this paper, we used DCGAN. Our generator and discriminator have six convolution layers. The input data for the generator are random vectors; the output of the generator is 3-axis vibration data. The input data of the discriminator is the 3-axis vibration data. whereas the output data is the probability of whether input data is generated data or not.

By employing the generated data, we held an experiment to evaluate the similarity of the virtual stimulus. We used the display method proposed by Saga et al. [3]. The display employs the tension of the thread to generate shearing force to the user's fingertip. Using this shearing force the display reproduce the texture feelings on a flat touchscreen.

3   Experiment

We held an experiment to evaluate the reality of tactile stimulation using the generated virtual information. By comparing the stimulation between the virtual information and the actual one, the participants evaluated the rate of reality between 1 and 5. We explained the informed consent (based on ethical guidelines of the University of Tsukuba) to all participants and obtained their consent.
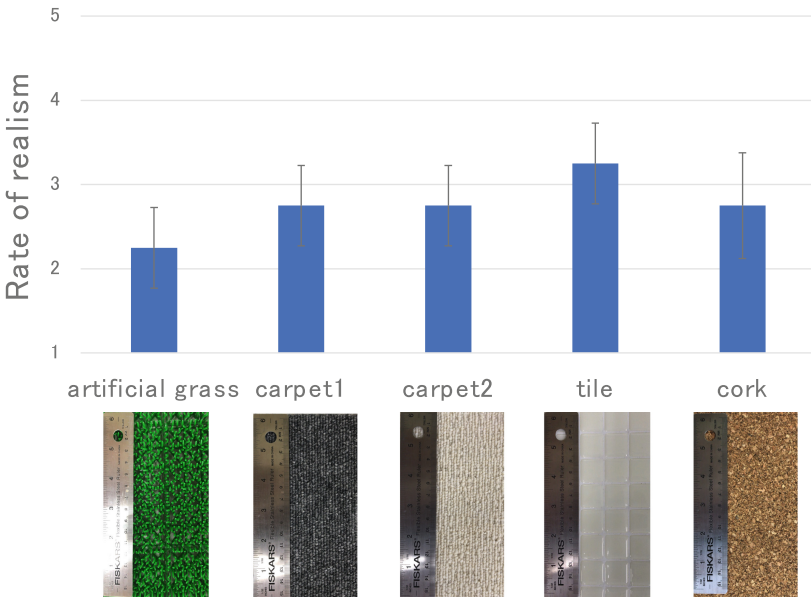
Fig. 1. Experiment result and textures. The bar graph shows the average of the obtained rates. The black line on the bar graph shows the range of the obtained rates.

One participant (male, 22 years old) wore an accelerometer on his finger and collected acceleration data by tracing five types of textures with the finger. By using the collected vibrotactile information, the generator learned the model, and generated the virtual vibrotactile information using DCGAN model. In this experiment, two dimensional vibrotactile stimulation was generated during the user's free movement on the touchscreen. The virtual tactile stimulation and the actual one were given to four participants (male, 20s), and they were asked to evaluate the rate of reality, i.e. how much the virtual stimulation reproduces the actual texture, using a 5-point rating (5 being the maximum).

Figure 1 shows the textures used in this experimental and the experimental results of rating. The tile texture obtained the highest rate. On the other hand, the artificial grass obtained the lowest rate. In the case of touching actual tile texture, the participants induced stick-slip movement on the flat surface. When collecting acceleration from tile, the participant also induced stick-slip movement. Thus the difference of sticky region and un-sticky region is clear compared to other textures. From this result, it was found that such clear difference between regions induced higher rate of reality compared to harsh and random textures. It is assumed that our DCGAN model learned this feature and generated tile vibrations with higher reality.

4   Conclusion

In this paper, we generated the virtual vibrotactile information using DCGAN. We held a reality rating experiment using virtual information and actual information, and evaluated how much realistic information could be generated with the virtual one. Based on the result of the experiment, it was found that the proposed method can present vibration with higher reality when the method reproduces flat surface texture. That is because our DCGAN model can learn stick-slip movement on the flat surface. In the future, we improve the DCGAN to generate more realistic information.

References

1. Goodfellow, I., Pouget-Abadie, J., Mirza, M., Xu, B., Warde-Farley, D., Ozair, S., Courville, A., Bengio, Y.: Generative adversarial nets. In: Advances in Neural Information Processing Systems, pp. 2672–2680 (2014)
2. Radford, A., Metz, L., Chintala, S.: Unsupervised representation learning with deep convolutional generative adversarial networks. CoRR, vol. abs/1511.06434 (2015)
3. Saga, S., Deguchi, K.: Lateral-force-based 2.5-dimensional tactile display for touch screen. In: Haptics Symposium (HAPTICS), 2012 IEEE, pp. 15–22. IEEE (2012)

Hands-On Demonstration
of Heterogeneous Haptic Texturing
# of Mesh Models Based on Image Textures

Arsen Abdulali(✉) , Waseem Hassan , Baek Seung Jin, and Seokhee Jeon

Department of Computer Science and Engineering, Kyung Hee University,
Yongin-si 446-701, Republic of Korea
{abdulali,waseem.h,jksdgh78,jeon}@khu.ac.kr

Abstract. In this article, we introduce a framework for heterogeneous assignment of multiple haptic textures to mesh objects based on image textures. The framework consists of two applications, i.e., texture assignment and rendering programs. A user-friendly interface of the framework allows to assign and render textured mesh models in four steps. First, the user provides an image texture file to the algorithm that automatically selects perceptually closest haptic texture from the library. Then, the user is offered to texture object faces by stroking over an object surface with a virtual brush. Several haptic textures can be assigned to different object surfaces of a single mesh model. The haptic information for each face is embedded to mesh object and stored in a generic *.ply file. Finally, a textured mesh object is loaded by rendering application.

Keywords: Haptic texture assignment · Rendering

1 Introduction

Recent haptic texture rendering algorithms provide a highly realistic vibrotactile feedback. These algorithms could potentially drive the research in virtual reality to a new level by allowing users to interact with a virtual object and feel surface textures. However, a shape of objects in a virtual world is usually changed during simulation having several heterogeneously distributed textures. For example, a human avatar in a computer game usually has distinct textures for skin, cloth, and shoes. In such cases, it becomes challenging to assign a haptic texture model to a specific dynamically transformed surface of a three-dimensional mesh object.

Current approaches render a haptic texture in a two-dimensional canvas of a touch screen of a tablet [2,4] or assign a single haptic texture to a complete mesh model [3]. Culbertson et al. rendered isotropic haptic textures on the tablet where the vibrotactile signal is interactively synthesized with respect to contact force and a movement velocity [4]. This idea was further extended in [2] to rendering anisotropic haptic texture by decomposing movement velocity into two-dimensional velocity vector. In [3], the authors developed a rendering framework

with one hundred haptic textures, where an isotropic haptic texture model can be assigned to a single mesh object.

In this paper, we developed a framework that allows VR designers to manually texture a mesh object with multiple haptic texture models and render it in a virtual environment. In order to alleviate the need of modeling haptic textures, we applied an automatic haptic texture assignment algorithm [5], which selects perceptually closest haptic texture model from the library based on a given image texture. Our framework consists of two software applications, i.e., object texturing and rendering programs. The framework is user-friendly and requires only four steps, which are briefly summarized as follows:

- A user provides an image texture file and the algorithm selects perceptually closest sample from the library.
- A user applies selected haptic texture to faces of a mesh object using a computer mouse or touchscreen.
- The textured mesh model is saved into "*.ply" file where haptic texture models are assigned to object faces.
- A textured mesh object is loaded by the rendering software allowing a user to explore virtual textures.

2   Object Texturing Application

The application for the object texturing consists of texturing interface, i.e., a virtual scene with a mesh model and navigation panel for basic object manipulations, such as mesh model loading, object rotation, scaling and image texture loading (see Fig. 1). In order to texture a mesh model, the user should provide a path to the "*.ply" file and image texture by pressing corresponding "OPEN" buttons. Once a user selects an image texture, the automatic assignment algorithm is invoked.

Automatic assignment algorithm [5] computes a set of distinct features from the given image texture. The authors established a haptic texture library of 84 samples in the form of three-dimensional perceptual space. In order to retrieve a perceptually closest sample from the library, the perceptual space was subdivided into sixteen groups of textures using a clustering algorithm. Support Vector Machine (SVM) was used to map a feature vector of an image to one out of sixteen perceptual groups. Once a group with perceptually closest samples is determined, the algorithm selects the most similar sample within the group based on Binarized Statistical Image Features (BSIF) features using chi-squares distances. The detailed information is provided in [5].

The user can start manual texturing using a virtual brash when a mesh model is successfully loaded and perceptually closest haptic model is selected. In order to provide visual feedback, surfaces with assigned haptic models are textured by the sample selected from the library. In rendering, the original image texture can be used instead. When the texturing process is over, the user presses the "Save PLY" button and specifies a path to a resultant "*.ply" file.
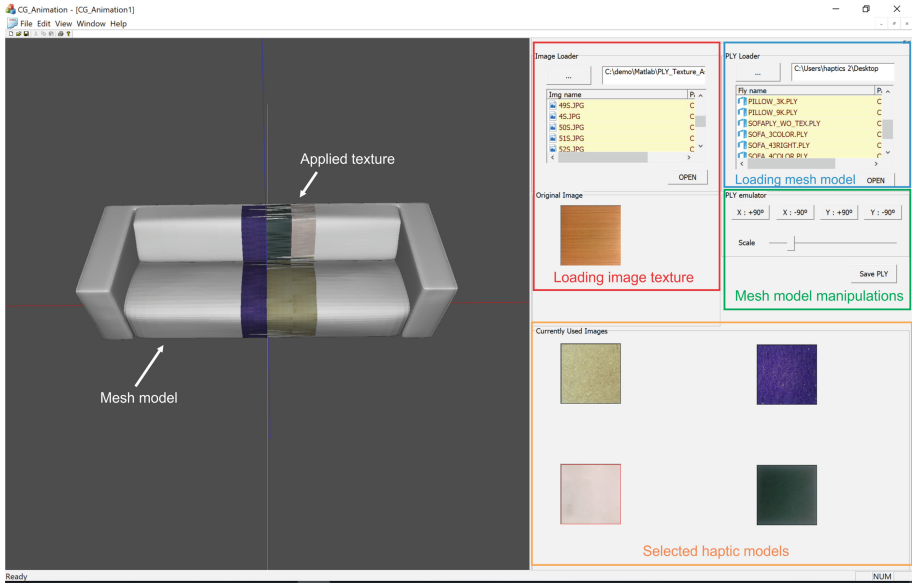
Fig. 1. Graphical user interface of the object texturing application

3   Rendering Application

In order to render the mesh model, the user should start the second application and provide a path to the textured "*.ply" file. The mesh model appears on the scene (see Fig. 2), and the user can touch the object using end-effector of a haptic device. Upon contact, a collision detection algorithm returns the id of the face and the id of the corresponding haptic texture model is retrieved.

In order to render haptic textures, we utilized a Radial Basis Functions Network (RBFN) based stochastic model, which we previously proposed in [1]. In this work, we focus on rendering isotropic haptic textures. Therefore RBFN models were trained for two-dimensional input, i.e., normal force and velocity magnitude. During rendering, a selected RBFN model along with two contact inputs (normal force and velocity magnitude) are fed into a runtime computing library, which we demonstrated in [2]. The computing library estimates a vibrotactile signal and applies to a vibrotactile actuator (Haptuator MM3C; Tactile Labs Inc., Montreal, Canada) via data acquisition device (NI USB-6251; National Instruments, Austin, Texas, USA).

4   Demonstration Protocol

The demonstration consists of two steps. First, a demonstration attendee sits in front of the tablet-PC running our texturing application. The user can select one or several image textures and apply corresponding haptic texture models
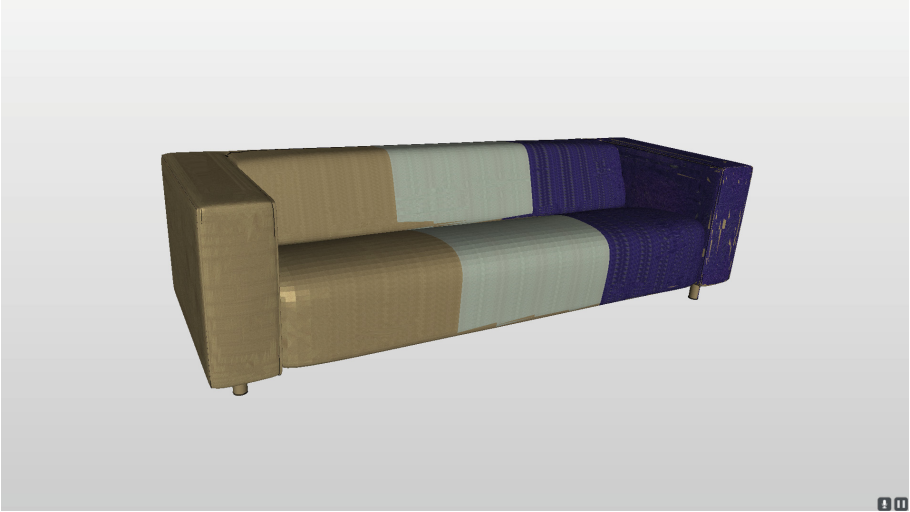
Fig. 2. Graphical user interface of the rendering application

to the mesh model. The image textures can either be in the form of a photo taken by the user or some texture image form online datasets. When the user finishes object texturing, the ".ply" file is saved and transferred to the rendering PC through the network. Second, the attendee moves to the rendering PC and explores a virtual mesh model. After the demonstration, attendees will be offered to volunteer in a short survey.

Note that perceptual characteristics of the data-driven model were evaluated in [1] and were felt realistic by Asia Haptics 2016 conference attendees [2]. On the other hand, the accuracy of haptic texture assignment algorithm was rated 71.4% in [5]. In this work, we developed a manual haptic texturing concept for VR and computer games designers. Thus we aim to get feedback regarding user experience for proposed texturing and rendering interfaces.

5   Conclusion

In this article, we developed a framework to demonstrate the concept of haptic texturing. Our framework consists of two applications. The first program is a graphical user interface that allows a user to apply a haptic texture to a mesh model and save it into a generic "*.ply" file. The second application renders a haptically textured mesh object.

References

1. Abdulali, A., Jeon, S.: Data-driven modeling of anisotropic haptic textures: data segmentation and interpolation. In: International Conference on Human Haptic Sensing and Touch Enabled Computer Applications, pp. 228–239. Springer (2016)
2. Abdulali, A., Jeon, S.: Data-driven rendering of anisotropic haptic textures. In: Proceedings of the Asia Haptics 2016 Conference, December 2016
3. Culbertson, H., Delgado, J.J.L., Kuchenbecker, K.J.: One hundred data-driven haptic texture models and open-source methods for rendering on 3D objects. In: 2014 IEEE Haptics Symposium (HAPTICS), pp. 319–325. IEEE (2014)
4. Culbertson, H., Romano, J.M., Castillo, P., Mintz, M., Kuchenbecker, K.J.: Refined methods for creating realistic haptic virtual textures from tool-mediated contact acceleration data. In: Haptics Symposium (HAPTICS), 2012 IEEE, pp. 385–391. IEEE (2012)
5. Hassan, W., Abdulali, A., Abdullah, M., Ahn, S.C., Jeon, S.: Towards universal haptic library: library-based haptic texture assignment using image texture and perceptual space. IEEE Trans. Haptics **11**, 291–303 (2017)

Painting Skill Transfer Through Haptic Channel

Ahsan Raza$^{(\boxtimes)}$, Muhammad Abdullah, Waseem Hassan, Arsen Abdulali,
Aishwari Talhan, and Seokhee Jeon

Department of Computer Science and Engineering, Kyung Hee University, 1732,
Deogyrong-daero, Giheung-gu, Yongin-si, Gyeonggi-do 17104, Republic of Korea
{ahsanraza,abdullah,waseem.h,abdulali,aishwari99,jeon}@khu.ac.kr

Abstract. In this paper, we focused on designing a system that can
guide and train a user in painting an art work. Initially, we aim to develop
a system which can guide a user with basic strokes of Korean language
calligraphy. The proposed system is implemented in a sequence of three
steps. Firstly, we collected the data from the surfaces of the canvas and
different orientations of a painting brush. Then based on the data, a
relationship is established among the collected parameters by building
a machine learning model. Finally, actuators attached with the handle
of the brush provides the vibrotactile and force feedback based on the
built model. The actuator guides the user in order to paint the required
object.

Keywords: Haptic painting · Painting skill · Haptic guidance ·
Deep learning · Haptic rendering

1 Introduction

Every art has a unique way that forces our senses to perceive the world in
a distinct manner. Painting is among those arts that makes human beings to
perceive the world in an exclusive and thoughtful way. This skill can be mastered
by acquiring the native techniques and practices under the guidance of an expert.
During the course of a painting, some parameters such as the force of a stroke and
brush orientation are considered important in order to produce elegant artwork.
However, in the modern world this form of art is on its decline due to lack of
experts and interest. Therefore, the need of the hour is to device modern methods
to preserve such art. One such method can be to use technology to preserve the
knowledge and skills of expert painters and use that preserved knowledge to
teach new students [2,3].

   As the number of experts is ever declining, we need to design a system which
can guide a naive user to achieve expert level painting skills. In order to design
such a system, we need to establish a relationship between all the subtle parame-
ters of painting such as force, acceleration, brush orientation etc., when a master
creates a painting. Such system allows users with poor painting skills to be guided

through the process of learning art in the absence of an expert. However, the calculation of the required parameters should be done precisely so the system can guide the user in a similar way as an expert guides. Thus, a framework consisting of data collection, modeling and rendering is needed in order to build the required system.

(a) Tracking system   (b) Demonstration scenario
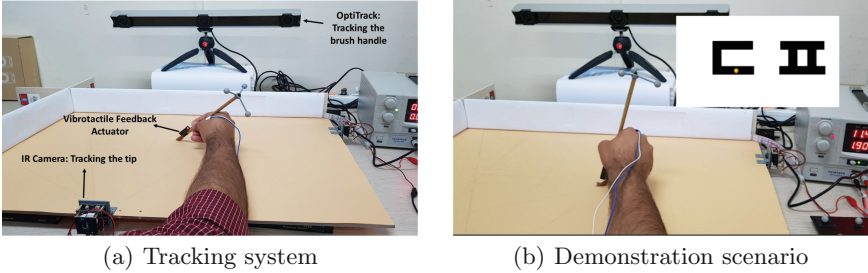
Fig. 1. Illustration of the overall system

In order to achieve a realistic skill transfer system, the collected data should cater for the all the subtle nuances of painting. This realism is dependant on various parameters, i.e., the brush tip position, brush handle orientation, brush stroking velocity, surface texture of the canvas, and friction of the canvas. The brush tip, handle, and stroking velocity are tracked in real time. All these data are recorded during the data collection phase.

A sophisticated machine learning model is created from these data using deep learning. This model is intrinsically based on the intricate relationships between the collected data parameters. Therefore, it can be assumed that this model has the ability to preserve the finer details of the painting skill, as a result of which the realism of the model enhances significantly.

The last step in this system is rendering the haptic response. Rendering is a two step process in this system. First, a vibrotactile feedback of the surface profile is rendered by reproducing the tool-surface-interaction vibrations using the system proposed in [1]. Second, a force and torque feedback, for keeping the naive user on the correct track, is provided by using an asymmetric sine wave.

The main contributions of this work are listed as follow:

– Real time tip tracking using two infrared cameras and OptiTrack V120.
– Using deep learning to create a unified and realistic model that caters for the various parameters involved during painting.
– Haptic guidance using force feedback generated by using an asymmetric sine wave.
– A prototype paint brush equipped with various sensors for haptic guidance for painting skill transfer.

2   Demonstration

The purpose of this demonstration is to provide directions to the user to paint or draw a specific object. In the current scenario, the user will be learning basic strokes of Korean language calligraphy. The user will select a specific alphabet from the list of alphabets, and the system will guide and help the user to draw the alphabet aesthetically correctly. The haptic actuator can guide the user to keep track of a specific pattern to paint the required object. If the user deviates from the path, the actuator provides force feedback which keeps the user on the directed path. An illustration of the equipment (Fig. 1(a)) and a reference example (Fig. 1(b)) is shown in Fig. 1.

References

1. Abdulali, A., Jeon, S.: Data-driven rendering of anisotropic haptic textures. In: International AsiaHaptics Conference, pp. 401–407. Springer, Heidelberg (2016)
2. Baxter, B., Scheib, V., Lin, M.C., Manocha, D.: Dab: interactive haptic painting with 3D virtual brushes. In: Proceedings of the 28th Annual Conference on Computer Graphics and Interactive Techniques, pp. 461–468. ACM (2001)
3. Vandoren, P., Van Laerhoven, T., Claesen, L., Taelman, J., Raymaekers, C., Van Reeth, F.: Intupaint: bridging the gap between physical and digital painting. IEEE (2008)

Data-Driven Multi-modal Haptic Rendering Combining Force, Tactile, and Thermal Feedback

Seongwon Cho$^{(\boxtimes)}$, Hyejin Choi, Sunghwan Shin , and Seungmoon Choi

Pohang University of Science and Technology,
Pohang, Gyeongbuk 37673, South Korea
{kardy04,hyejin1208,scaut11,choism}@postech.ac.kr
http://hvr.postech.ac.kr

Abstract. We introduce a data-driven multi-modal haptic rendering system which simultaneously presents force, tactile, and thermal feedback. To handle force, tactile, and thermal feedback together, a vibration actuator and a peltier module are attached to a force-feedback device. Several haptic properties of an object—shape, texture, friction, and viscoelasticity—are considered as components of force rendering. About tactile feedback, we combine contact transient and texture vibration when the user contacts and explores a surface. Thermal sensation between skin and an object rendered by considering both heat flux and the initial temperatures of the object and skin. Rendering models for all the modalities are collected from real interaction and modeled in a data-driven manner. We expect that our multi-modal rendering system improves realism of haptic sensation in the virtual environment.

Keywords: Multi-modal rendering · Data-driven model ·
Haptic feedback · Rendering

1 Introduction

When people touch an object, haptic properties of the object such as shape, texture, and temperature are delivered to them. In haptics research, it is an important task to provide assorted types of haptic information while interacting with virtual objects because people can discriminate and identify objects based on those haptic properties. To this end, many researchers have developed haptic modeling and rendering methods to provide realistic and immersive haptic feedback. Data-driven approach is one of the most brilliant ways to generate an accurate model based on collected data from real situations. Data-driven modeling and rendering can be applied to force, tactile, and thermal rendering [3, 22]. However, to our knowledge, there are not many studies integrating force, tactile, and thermal feedback together. Therefore, we develop a multi-modal haptic rendering system combining force, tactile, and thermal feedback with data-driven approaches of our previous works.

2   Multi-modal Rendering

2.1   System Overview

We developed a multi-modal haptic rendering system to provide realistic haptic sensations by unifying force, tactile, and thermal feedback. Figure 1 shows an overview of our multi-modal haptic rendering system.
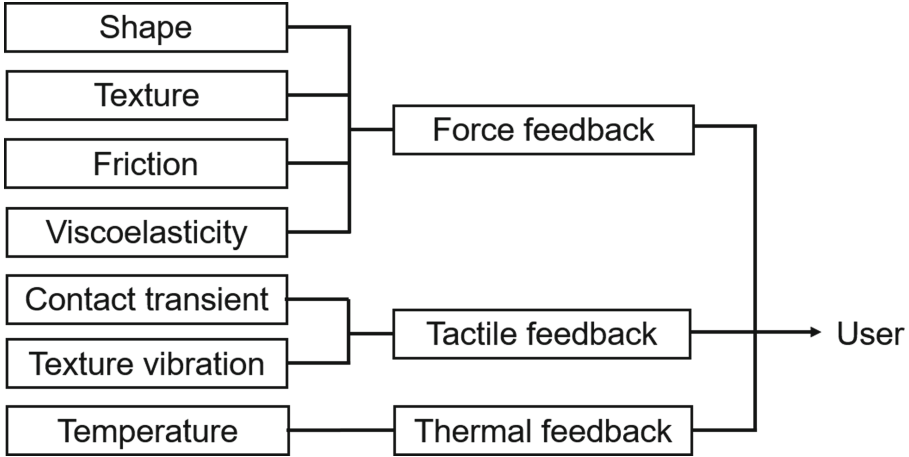
Fig. 1. System overview of our multi-modal rendering system.

2.2   Force Feedback

Shape. To reconstruct a mesh of a real object in virtual reality, the shape modeling system of Yim and Choi is used, which considers the surface deformation of the object [25]. When a user taps on the surface of an object to collect sample points, the system detects tapping and compensates for an error occurring due to surface deformation of the object. As a result of the modeling system, the base shape of a real object is reconstructed in a virtual environment.

Texture. Haptic texture is an indispensable property of haptic perception, which provides fundamental haptic information on the object. Most of the early haptic texture researches used the geometry profile of a textured surface to compute the response force of a force-feedback device [2, 10, 15, 16]. The great advantage of rendering textured surface using force feedback is that users can feel convincing roughness sensations of texture. Previous researches on haptic texture have demonstrated that we can control the user's perceived roughness and deliver the sensation of rough textures by varying the lateral force at the surface or the penetration depth or both of them. However, haptic texture rendering using force feedback became unpopular because we had difficulties in capturing the geometry of textured surface with a high resolution. To solve this problem,

we adopt a geometry-based model using photometric stereo algorithm [23], which is one of the most accurate algorithms for 3D surface reconstruction. The algorithm can capture the geometry with a resolution about $10\,\mu$m, which is ten times better than previous image-based methods. After we obtain the height map of the surface by photometric stereo algorithm, it is mapped onto the base mesh model of a virtual object. When the user interacts with a textured object, the texture's response can be calculated using the height map.

Friction. Friction is also one of the keys for delivering realistic haptic sensations of an object since it is highly correlated to the slipperiness and stickiness perception of a surface. Out of many approximated friction models, we adopt the Dahl model [6] because it can accurately imitate the behaviors of various real frictional responses with reasonable complexity in spite of its relative simple equation. Also, this model has been frequently used in haptics research to render friction. To reduce the complexity of calculation, we adopt a discrete time representation of Dahl model [14] as follows:

$$f_D(t+1) = f_C(t)sgn(v(t)) + (f_D(t) - f_C(t)sgn(v(t)))e^{-\frac{K}{f_C(t)}|x(t)-x_0|} \tag{1}$$

where f_D is the frictional force, x is the tangential displacement, v is the tangential velocity, K is the stiffness coefficient, and x_0 is the initial displacement. We use collected data by stroking the real surfaces with stylus in [23] for parameter identification of the Dahl model. The computed frictional force is added to the interaction force with a virtual object.

Viscoelasticity. Jeon et al. showed that Hunt-Crossley model can be effective to modulate stiffness for a haptic AR system [13]. We also use the Hunt-Crossley model to render the viscoelasticity of an object [12] owing to its balanced performance between modeling accuracy and the ease of parameter identification. The Hunt-Crossley model is given by

$$f(t) = Kx^n(t) + Bx^n(t)\dot{x}(t), \tag{2}$$

where K is the stiffness parameter, B is the damping parameters of the object, and $x(t)$ is the normal displacement. This model can capture the deformation behavior of object for haptics. Having collected data in [23] by pushing the target material downward, we used the data for parameter identification of the Hunt-Crossley model. Computed viscoelasticity force is added to the interaction force with a virtual object.

2.3   Tactile Feedback

Contact Transient. Rendering transient vibrations, which occur when a user taps on an object, is essential to support realistic re-creation of stiff objects in virtual environments. Wellman and Howe studied vibrotactile feedback in

virtual environments and suggested a simple exponentially damped sinusoidal model [24]. Okamura et al. also demonstrated the effect of vibration feedback using the decaying sinusoid models [18]. We add contact transient vibrations using the decaying sinusoidal model to enhance the realism of virtual materials at contact.

Texture Sensation. Another effective approach for haptic texture rendering is to use vibration feedback. Because of its effectiveness to deliver roughness sensation, it also has many associated studies [1]. According to the duplex theory of tactile texture perception, texture perception is mediated by vibrational cues for fine texture and by spatial cues for coarse texture [7–9, 11, 19, 20]. Therefore, along with the geometry model generating spatial cues, we use a vibrotactile feedback for haptic texture rendering to deliver the texture sensations caused by very fine irregularities on the surface. Among many studies for haptic texture utilizing vibrational cues we choose to use the method based on linear predictive coding (LPC) [21], one of the most successful and widely used algorithms for haptic texture rendering [4,5,20]. We first collect contact vibration data from real materials. Then, we construct a LPC model that generates spectrally-identical signal to the collected data. When a user strokes on a textured surface, we use the constructed LPC model to synthesize an appropriate vibration. The synthesized signal is rendered using a voice-coil actuator because it supports the rendering of high-amplitude and wide-band signals.

2.4   Thermal Feedback

Coldness/warmness is one of the prominent psychophysical dimensions that compose tactile textures [17]. For this reason, thermal rendering is inevitable for the highly realistic re-creation of real objects in a virtual environment. We adopt a data-driven thermal rendering framework that considers both the heat flux and initial temperature of hand and object [3]. We collect the heat flux and hand temperature data while a user touches an object under various initial temperature conditions. A thermal response is synthesized to render heat flux to a user by interpolating the collected data.

3   Conclusion

In this research, we develop a data-driven multi-modal haptic rendering system that covers force, tactile, and thermal feedback. Integrated hardware is designed to deliver force, tactile, and thermal feedback together to improve the realism of virtual reality experiences.

References

1. Andrews, S., Lang, J.: Interactive scanning of haptic textures and surface compliance. In: Proceedings of 3DIM, pp. 99–106. IEEE (2007)
2. Basdogan, C., Ho, C., Srinivasan, M.A.: A raybased haptic rendering technique for displaying shape and texture of 3D objects in virtual environments. In: ASME Winter Annual Meeting, vol. 61, pp. 77–84 (1997)
3. Choi, H., Cho, S., Shin, S., Lee, H., Choi, S.: Data-driven thermal rendering: an initial study. In: Proceedings of the IEEE Haptics Symposium, pp. 344–350 (2018)
4. Culbertson, H., Lopez Delgado, J., Kuchenbecker, K.: One hundred data-driven haptic texture models and open-source methods for rendering on 3D objects. In: Proceedings of IEEE HAPTICS, pp. 319–325, February 2014. https://doi.org/10.1109/HAPTICS.2014.6775475
5. Culbertson, H., Unwin, J., Goodman, B., Kuchenbecker, K.: Generating haptic texture models from unconstrained tool-surface interactions. In: Proceedings of IEEE WHC, pp. 295–300, April 2013. https://doi.org/10.1109/WHC.2013.6548424
6. Dahl, P.R.: Solid friction damping of mechanical vibrations. AIAA J. **14**(12), 1675–1682 (1976)
7. Fritz, J.P., Barner, K.E.: Stochastic models for haptic texture. In: Proceedings of SPIE, pp. 34–44. International Society for Optics and Photonics (1996)
8. Guruswamy, V., Lane, J., Lee, W.: Modelling of haptic vibration textures with infinite-impulse-response filter. In: Proceedings of IEEE HAVE, pp. 105–110 (2009)
9. Guruswamy, V.L., Lang, J., Lee, W.S.: IIR filter models of haptic vibration textures. IEEE Trans. Instrum. Meas. **60**(1), 93–103 (2011)
10. Hayward, V., Yi, D.: Change of height: an approach to the haptic display of shape and texture without surface normal. In: Experimental Robotics VIII, pp. 570–579 (2003)
11. Hollins, M., Bensmaïa, S., Risner, R.: The duplex theory of tactile texture perception. In: Proceedings of the 14th Annual Meeting of the International Society for Psychophysics, pp. 115–121 (1998)
12. Hunt, K., Crossley, F.: Coefficient of restitution interpreted as damping in vibroimpact. J. Appl. Mech. **42**(2), 440–445 (1975)
13. Joen, S., Choi, S.: Stiffness modulation for haptic augmented reality: extension to 3D interaction. In: Proceedings of the IEEE Haptics Symposium, pp. 273–280 (2010)
14. Mahvash, M., Okamura, A.M.: Friction compensation for a force-feedback telerobotic system. In: Proceedings of IEEE ICRA, pp. 3268–3273 (2006)
15. Massie, T.H.: Initial haptic explorations with the phantom: virtual touch through point interaction. Ph.D. thesis, Massachusetts Institute of Technology (1996)
16. Minsky, M.D.R.: Computational haptics: the sandpaper system for synthesizing texture for a force-feedback display. Ph.D. thesis, Massachusetts Institute of Technology (1995)
17. Okamoto, S., Nagano, H., Yamada, Y.: Psychophysical dimensions of tactile perception of textures. IEEE Trans. Haptics **6**(1), 81–93 (2013)
18. Okamura, A., Cutkosky, M., Dennerlein, J.: Reality-based models for vibration feedback in virtual environments. IEEE/ASME Trans. Mechatron. **6**(3), 245–252 (2001). https://doi.org/10.1109/3516.951362
19. Pai, D.K., Rizun, P.: The WHaT: a wireless haptic texture sensor. In: Proceedings of HAPTICS, pp. 3–9. IEEE (2003)

20. Romano, J., Kuchenbecker, K.: Creating realistic virtual textures from contact acceleration data. IEEE Trans. Haptics **5**(2), 109–119 (2012). https://doi.org/10.1109/TOH.2011.38

21. Romano, J., Yoshioka, T., Kuchenbecker, K.: Automatic filter design for synthesis of haptic textures from recorded acceleration data. In: Proceedings of IEEE ICRA, pp. 1815–1821, May 2010. https://doi.org/10.1109/ROBOT.2010.5509853

22. Shin, S., Choi, S.: Hybrid haptic texture rendering using kinesthetic and vibrotactile feedback. In: International AsiaHaptics Conference, pp. 75–81 (2016)

23. Shin, S., Choi, S.: Geometry-based haptic texture modeling and rendering using photometric stereo. In: Proceedings of IEEE HAPTICS (2018)

24. Wellman, P., Howe, R.D.: Towords realistic vibrotactile display in virtual environments. In: Proceedings of the ASME Dynamic Systems and Control Division, pp. 713–718 (1995)

25. Yim, S., Choi, S.: Shape modeling of soft real objects using force-feedback haptic interface. In: Proceedings of IEEE HAPTICS, pp. 479–484 (2012)

Haptic Technology

Development of a Teleoperation Precision Grasping System with a Haptic Feedback Sensation on the User's Fingertip

Aiman Omer[1(✉)], Jamal Hamdi[2], and Atsuo Takanishi[3]

[1] Waseda University, Tokyo, Japan
a.omer@kurenai.waseda.jp
[2] Department of Medicine and Surgery, Umm Al-Qura University,
Makkah, Saudi Arabia
jthamdi@uqu.edu.sa
[3] Department of Modern Mechanical Engineering, Waseda University,
Tokyo, Japan
contact@takanishi.mech.waseda.ac.jp

Abstract. Tactile feedback sensation is an important factor in the surgical and medical application. A simple gripper is developed to perform precision grasping using teleoperation technology. The system provides the user with the tactile feedback sensation through a haptic device that applies forces on the user's fingertip based on the measured force at the gripper's fingertip.

Keywords: Precision grasping · Haptic feedback sensation · Teleoperation

1 Introduction

New surgical methods and techniques, such as laparoscopic surgery and Robotic surgery, are been developed to improve the surgical operation in terms of efficacy and recovery time reduction. However, there are some limitations such as the absence of tactile feedback sensation, which is an important factor in surgical operations [1]. To improve the performance of the laparoscopic surgery, a group of researchers developed a technique called Hand-Assistive Laparoscopic Surgery (HALS). In the HALS technique, the surgeon inserts his/her hand inside the patient body to gain access to the organ and receive tactile sensation feedback. It can help the surgeon to improve his/her Eye/Hand coordination by touching the organs as well as removing some tissue or organ parts in some operations [2, 3].

HALS technique has some limitations and disadvantages such as fatigue cased by keeping the same arm posture for a long time during the operation, and the risk of injuring the patient. Therefore, we proposed the idea of using a robotic hand instead of the surgeon's hand to perform HALS operation. There is some research work made to develop robotics technology that can be used for grasping during a surgical operation [4]. The robotic gripper could simulate a grasping motion of 2 fingers (Thumb and Index finger). Some research group had developed a robot hand for surgical applications that are made of 3 fingers [5].

The human's hand can perform four type of grasping motion; power grasp, precision grasp, excluding, and extending. Precision grasping could be one of the methods to define the condition of a tissue or an organ inside the human body. The surgeon could identify certain diagnosis such as cancer using precision grasping. Therefore, we focused on the precision grasping, at the current stage of our research, as one of the grasping motion used for medical application [6]. Developing a robotic gripper that can perform precision grasping for surgical applications could be a useful innovation.

In this research we have made a first prototype of the system that we are planning to achieve in the long term. We have developed a simple 2 DOF gripper that can be controlled using the Index finger. The gripper can simulate precision grasping using thumb and index fingers. The gripper is equipped with a force sensor that can measure the grasping force. The measured forces are transferred to the user's fingertip through a haptic device that can apply applied and shear forces along the 3 axes.

2   System Overview

The system overview is presented in Fig. 1. In the system the input interface measures the index finger movement in the user's hand. The motion data is used to control a 2 DoF gripper. The gripper is equipped with a 3 axes force sensor that measures the applied force on the gripper fingertip. The amount of measured force is transmitted to the user's fingertip through a haptic device.
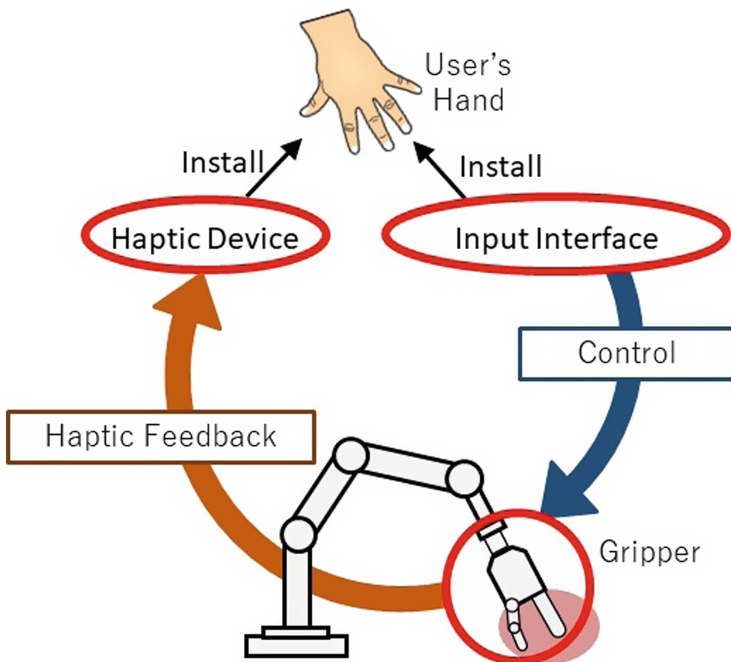
Fig. 1.   The system overview

3 Hardware Design

The hardware of the system is consist of 3 parts; the gripper, the input interface, and the haptic feedback device. The gripper is made of a 2 DoF finger (Fig. 2) that is based on NAIST OpenHand M2S design [7]. The input interface is made of exoskeletons that have 2 encoders, which is attached to the user's index finger (Fig. 3). The third part is the haptic feedback device that can apply forces along 3 axes on the user's fingertip (Fig. 4).
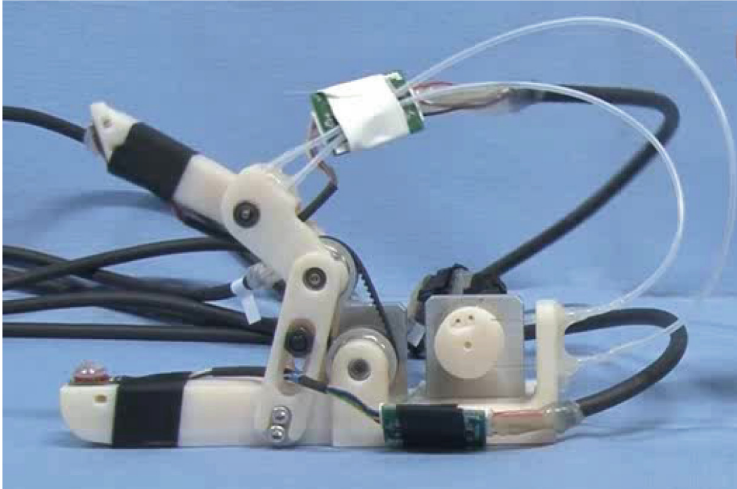
Fig. 2. The 2 DoF gripper that is equipped with a 3 axes force sensor.
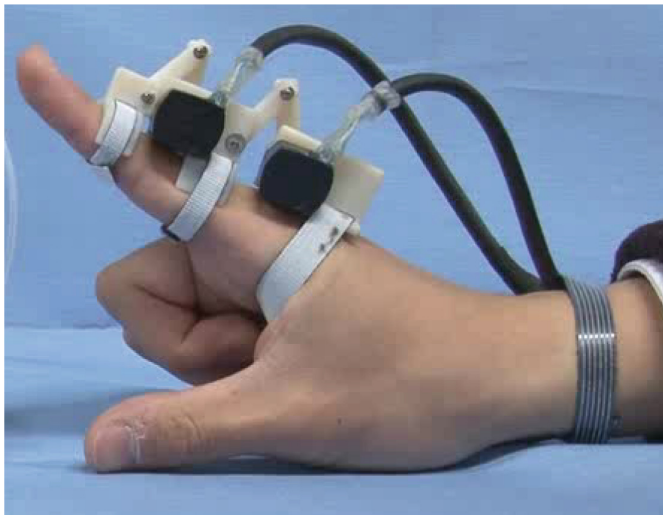
Fig. 3. The input interface attached to the user's index finger.

Fig. 4. The haptic device attached to the user's fingertip.

4   Control

The gripper is controlled by moving the index finger. Each encoder measures the orientation angle of the MCP and PIP joint. The measured orientation data is used to control the actuators in the gripper in the same order.

The force sensor on the gripper fingertip measures forces along 3 axes. The amount of the measured forces is sent by signals to the haptic feedback device. The device is made of a plate that moves along 3 axes. Based on the measured forces the plate will apply forces (normal and shear forces) into the user's fingertip.

5   Experiments

We have tested the system to grasp 3 types of objects; solid block, soft material, and a piece of cloth. The user was able to grasp the object and to some extent was able to recognize the softness of the object holding (Fig. 5). The initial tests showed that the system is able to perform as expected; however, it still needs some improvement in order to have better performance.
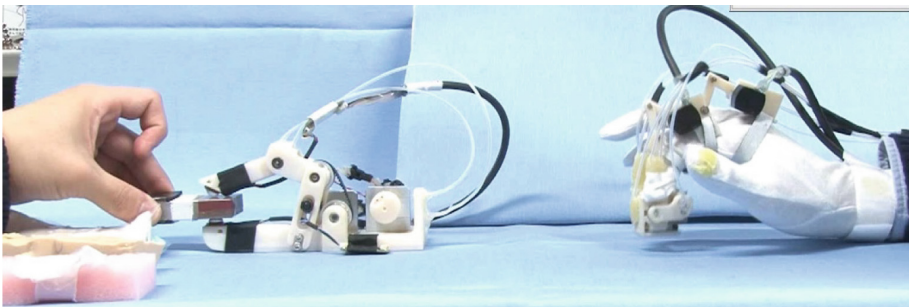
Fig. 5. Experiment test of the system. (Note: *All the experiments were conducted in accordance with the ethical rule, and were approved by the Ethical Committee at Waseda University.*)

6   Conclusion

We were able to develop a gripper with a haptic feedback system. The system was tested by some students to check the ability of the system to transmit the softness sensation into the user's fingertip. The system was able to function and users were able to identify the softness of the object that the gripper was holding.

7   Future Work

The system will be developed to have a robotic hand instead of the simple gripper. The system is going to be developed in order to be used for medical and surgical application.

References

1. Sokhanvar, S., Dargahi, J., Najarian, S., Arbatani, S.: Tactile Sensing and Displays: Haptic Feedback for Minimally Invasive Surgery and Robotics. Wiley, Hoboken (2013)
2. Kaban, G.K., Czerniach, D.R., Litwin, D.E.M.: Controversies in laparoscopic surgery: hand-assisted laparoscopic surgery, pp: 101–109. Springer (2006)
3. Meijer, D.W., Bannenberg, J.J.G., Jakimowicz, J.J.: Hand-assisted laparoscopic surgery: an overview. In: Surgical Endoscopy, pp: 891–895 (2000)
4. Yoshida, K., et al.: Development of five-finger robotic hand using master-slave control for hand-assisted laparoscopic surgery. In: Proceeding of the 38th Annual International Conference of the Engineering in Medicine and Biology Society (EMBC) (2016)
5. Takayama, T., Omata, T., Futami, T., Akamatsu, H., Ohya, T., Kojima, K., Takase, K., Tanaka, N.: Detachable-fingered hands for manipulation of large internal organs in laparoscopic surgery. In: Proceedings of 2007 IEEE International Conference on Robotics and Automation, Roma, Italy, pp. 244–299 (2007)
6. Spiers, A., Baillie, S., Pipe, T., Persad, R.: Experimentally driven design of a palpating gripper with minimally invasive surgery considerations. In: Proceeding of IEEE Haptics Symposium, pp. 261–266 (2012)
7. Robohub website. https://robohub.org/naist-openhand-m2s-released/. Accessed 16 Feb 2017

Skin Vibration-Based Tactile Tele-Sharing

Tomohiro Fukuda[(✉)] and Yoshihiro Tanaka

Nagoya Institute of Technology, Gokiso-cho, Showa-ku, Nagoya, Japan
`t.fukuda.184@nitech.jp`, `tanaka.yoshihiro@nitech.ac.jp`

Abstract. This paper presents the sharing of tactile experiences between distant locations. A wearable sensor using a PVDF (polyvinylidene difluoride) film was used to detect the skin vibration on the finger, and the audio channel of computers was used to transmit the vibration information bidirectionally. We developed a prototype module having functions of inputting the sensor output as an audio signal and of driving a vibrator according to the audio signal. It was confirmed that the tactile information during various tasks could be transmitted via the Internet by using conventional videophone software.

Keywords: Tele-sharing · Skin-propagated vibration · Audio channel

1 Introduction

Tactile information is essential for interpersonal communication as well as visual and auditory information. Whereas technologies of recording, playing, and transmitting visual and auditory information have been well matured, those for tactile information are now developing. If tactile information could be shared, it is effective in various situations such as texture designs and skill training. There are some works that aimed at the sharing of tactile experiences. For instance, Matsuzono et al. proposed HaptI/O that enables to share vibration measured by an accelerometer embedded in a small box via the Internet [1]. It can share the tactile information mediated by the box device; however, it cannot share the information during natural touch with the bare finger.

We aim to achieve bidirectional transmission of tactile information during natural touch. We focused on skin-propagated vibration and used a wearable sensor using a PVDF (polyvinylidene difluoride) film developed by Tanaka et al. [2]. The sensor does not interfere with natural touch by the bare finger. Thus, it is advantageous to obtain the tactile information during various kinds of sensory-motor tasks such as haptic exploration, object manipulation, and tool use. In this paper, we attempted to use the audio channel of a computer to transmit acquired skin vibration information. It allows using conventional videophone software to transmit tactile information with video image via the Internet. There are some studies that utilized the audio channel to transmit tactile information and showed its effectiveness (e.g., [3] and [4]). We developed a prototype of a module to transmit skin vibration information as the audio signal.

2   Prototype Module

Figure 1 shows the photograph and the schematic diagram of the module. The wearable sensor is connected to a voltage follower to convert its output impedance, and then, the signal is filtered by a high-pass filter (cut-off frequency of 15.9 Hz) to cut an undesired DC component. The signal is finally amplified by an instrumentation amplifier and input to a USB audio interface (Sound Blaster PLAY!3, Creative Technology Ltd.). The skin vibration of the communication partner is output from the audio interface and amplified by a D-class amplifier to drive a vibrator. In this way, this module allows transmitting the skin vibration information as the audio signal bidirectionally by using conventional videophone software (e.g., Skype and Google Hangouts).
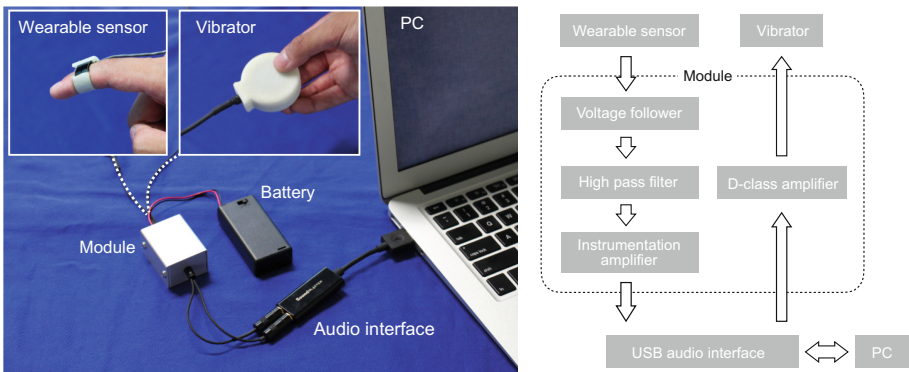
Fig. 1. Photograph and schematic diagram of prototype module for tactile tele-sharing.

3   Results and Discussion

It was confirmed that the prototype modules could bidirectionally transmit the skin vibration during various tasks via the Internet. Figure 2 is screenshots during the tactile tele-sharing by Skype in haptic exploration and a screwing task. There was no substantial delay between the video and the tactile presentation, and it might be owing to video-audio synchrony of the videophone software. In the current setup, the audio channel was occupied by the tactile information, and we used another account of the videophone software on an additional computer or a smartphone to share the auditory information. Here, the location of the measurement of the skin vibration is different from the interaction site (finger pad). The previous study showed that inserting the inverse of the typical transfer function from the finger pad to the measuring location brought more convincing texture presentation [5]; thus, we will add an equalizer circuit in the module to enhance the quality of the tactile presentation. Moreover, although the use of

only vibration information can bring the simplicity of the entire setup, we will discuss the necessity to introduce transmitting kinesthetic information together for more effective tele-sharing.
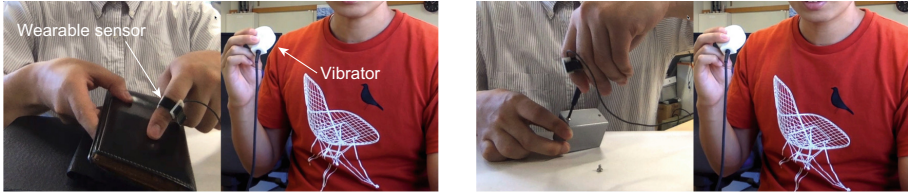
Fig. 2. Screenshots during the tactile tele-sharing by Skype in haptic exploration (left panel) and a screwing task (right panel).

Ethical Approval. The procedure performed in the study involving human participants were in accordance with the 1964 Helsinki declaration and its later amendments or comparable ethical standards.

Informed Consent. Informed consent was obtained from all individual participants included in the study.

References

1. Matsuzono, S., Nakamura, H., Kato, D., Peiris, R., Minamizawa, K.: HaptI/O: physical I/O node over the Internet. In: Prattichizzo, D., et al. (eds.) Haptics: Science, Technology, and Applications, EuroHaptics 2018. LNCS, vol. 10894, pp. 99–110. Springer, Cham (2018)
2. Tanaka, Y., Nguyen, D.P., Fukuda, T., Sano, A.: Wearable skin vibration sensor using a PVDF film. In: Proceedings of IEEE World Haptics Conference, pp. 146–151 (2015)
3. Minamizawa, K., Kakehi, Y., Nakatani, M., Mihara, S., Tachi, S.: TECHTILE Toolkit: a prototyping tool for designing haptic media. In: Proceedings of ACM SIGGRAPH 2012 Emerging Technologies (2012). Article no. 22
4. Israr, A., Zhao, S., McIntosh, K., Schwemler, Z., Fritz, A., Mars, J., Bedford, J., Frisson, C., Huerta, I., Kosek, M., Koniaris, B., Mitchell, K.: Stereohaptics: a haptic interaction toolkit for tangible virtual experiences. In: Proceedings of ACM SIGGRAPH 2016 Studio (2016). Article no. 13
5. Takekawa, Y., Hasegawa, T., Tanaka, Y., Minamizawa, K., Sano, A.: Tactile display based on skin-propagated vibration. In: Hasegawa, S., et al. (eds.) Haptic Interaction, AsiaHaptics 2016. LNEE, vol. 432, pp. 121–123. Springer, Singapore (2016)

Remotely Displaying Cooling Sensation Using Ultrasound Mist Beam

Mitsuru Nakajima[1(✉)], Keisuke Hasegawa[2(✉)],
Yasutoshi Makino[1(✉)], and Hiroyuki Shinoda[1(✉)]

[1] Graduate School of Frontier Science, The University of Tokyo,
5-1-5 Kashiwanoha, Kashiwa-shi, Chiba 277-8561, Japan
nakajima@hapis.k.u-tokyo.ac.jp, {Yasutoshi_Makino,
Hiroyuki_Shinoda}@k.u-tokyo.ac.jp
[2] Graduate School of Information Science and Technology, The University
of Tokyo, 7-3-1 Hongo, Bunkyo-ku, Tokyo 113-8656, Japan
Keisuke_Hasegawa@k.u-tokyo.ac.jp

Abstract. This study describes a midair haptic display that provides a cooling sensation using ultrasound-driven cold air flow cooled by mist vaporization. Non-contact thermal display using ultrasound-driven cold air flow has been reported, but the system uses dry ice as the cold-air source, which limits the range of practical applications. In this study, we propose a method using mist vaporization instead of dry ice to extend the application. Using this system, we demonstrate transporting cold air to a localized spot on a user's skin.

Keywords: Cooling sensation · Ultrasound beam · Acoustic air flow · Bessel beam · Mist

1 Introduction

In recent years, while many methods present mechanical tactile stimuli and render mechanical interactions between human bodies and objects, it is widely known that thermal sensation enriches haptic experiences [1, 2]. A number of researches have focused on thermal sensation, and the majority of them are contact-type devices using thermoelectrical heat pumps of Peltier elements [3, 4].

Noncontact thermal displays are still few but have already been proposed. Strong light irradiation realizes remote heating [5], and remote cooling is achieved by transporting cold air to a skin surface using acoustic stream [6]. The latter system contains an ultrasound phased array that generates an electronically steerable ultrasound beam, which results in a steerable narrow air flow. The ultrasonic beam can be narrowed down to a comparable size to the ultrasound wavelength, 8.5 mm in our setup. The narrow beam could successfully transport a cold air mass and generate a localized cold spot on a skin away from the device. However, since dry ice was used as the cold-air source, preparation of the dry ice is a problem, which limits the range of practical applications (Fig. 1).

In this paper, we propose an effective cooling method by using mist vaporization to extend the application.
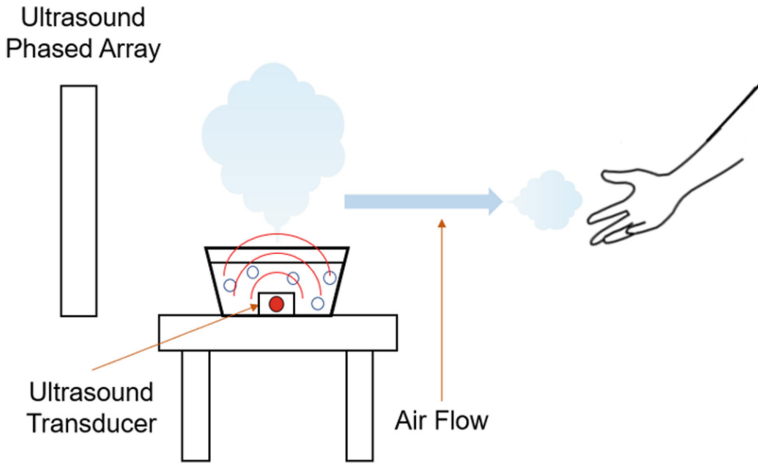
Fig. 1. System overview

2   Prototype

We show the overall system in Fig. 2. This system is composed of 40 kHz ultrasound phased arrays, ultrasound transducer for generating mist (IM1-24/LW SEIKO GIKEN INC), and water tank. The ultrasound phased array is set up so that it can radiate ultrasound in the horizontal direction toward a water tank. The ultrasound transducer generates 400 ml mist per hour. The center particle diameter of the generated mist is as small as 4 ~ 5 μm. The ultrasound transducer is set up in water tank which stored 2 l of water. The transducer produces rich mist as the lower right of Fig. 2. A part of the mist is transported by the air flow generated from the ultrasound phased array.
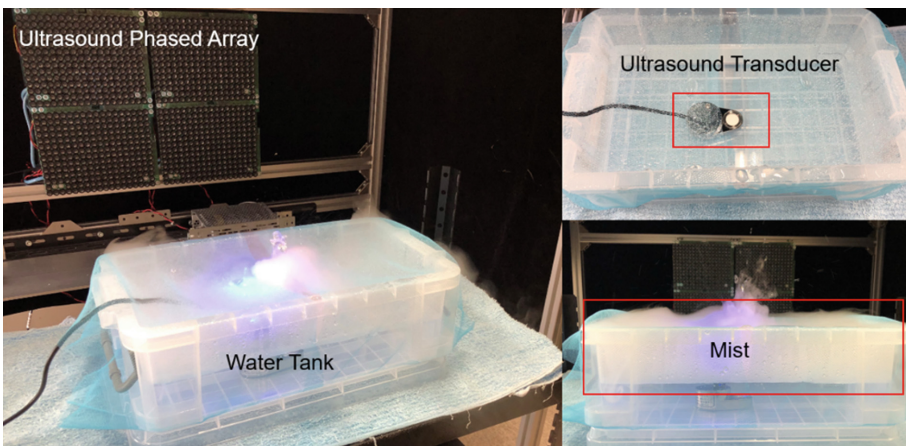
Fig. 2. Proposed system

2.1 Generation of Airflow Driven by Ultrasound Beam

The air flow driven by ultrasound is known as acoustic streaming [7]. With single-frequency sinusoidal sound sources, the driving force per unit mass exerted by the air is known to be proportional to the acoustic power [8]. Therefore, a straight sound beam entails a straight air flow parallel to the beam. As an example of such a straight beam, a Bessel beam was generated in an electronically steerable manner, by means of ultrasound transducer phased arrays [9].

2.2 Skin Surface Temperature Change

The system could effectively cool the skin surface. From the observation by thermography, the surface temperature dropped by $3.5 \sim 3.8°$ in 50 s. It was unexpected the temperature drop was larger than the dry ice case in the previous study, and it actually felt cooler for the authors. Since the heat of water vaporization is as large as 2442 kJ/kg, efficient vaporization in ultrasound beam can effectively cool the skin surface. The conference participants experience the cool sensation using this system.

References

1. Yang, G.G., Kyung, K., Srinivasan, M.A., Kwon, D.: Quantitative tactile device with pin-array type tactile feedback ans and thermal feedback. In: Proc. IEEE ICRA 2006, pp. 3917–3922 (2006)
2. Wettach, R., Behrens, C., Danielsson, A., Ness, T.: A thermal information display for mobile application. In: Proceedings in MobileHCI 2007, pp. 182–185 (2007)
3. Sato, K., Maeno, T.: Presentation of rapid temperature change using spatially divided hot and cold stimuli. J. Robot. Mechatron. **25**(3), 497–505 (2013)
4. Sato, K.: Augmentation of thermal sensation on finger pad using stimuli for finger side. In: EuroHaptics2016, pp. 371–379 (2016)
5. Saga, S.: Thermal-radiation-based haptic display: basic concept. In: Proceedings of IEEE World Haptics 2015, WIP-28, June 2015
6. Nakajima, M., Hasegawa, K., Makino, Y., Shinoda, H.: Remotely displaying cooling sensation via ultrasound-driven air flow. In: IEEE Haptics Symposium 2018, Oral Session 7B (Technical papers), 25–28 March, San Francisco, California, USA, pp. 340–343 (2018)
7. Hamilton, M.F., Blackstock, D.T.: Nonlinear Acoustics. Academic Press, San Diego (1998)
8. Nomura, S., Murakami, K., Sasaki, Y.: Streaming induced by ultrasonic vibration in a water vessel induced by ultrasonic vibration in a water vessel. Jpn. J. Appl. Phys. **39**(6A), 3636–3640 (2000). Part no. 1
9. Hasegawa, K., Qiu, L., Noda, A., Inoue, S., Shinoda, H.: Electronically steerable ultrasound-driven long narrow air stream steerable ultrasound-driven long narrow air stream. Appl. Phys. Lett. **111**(7), 064104 (2017)

Interactive Virtual Fixture Generation
for Shared Teleoperation
in Unstructured Environments

Vitalii Pruks[(✉)] and Jee-Hwan Ryu

Department of Mechanical Engineering, KOREATECH,
1600, Chungjeol-ro, Byeongcheon-myeon, Dongnam-gu, Cheonan-si,
Chungcheongnam-do 31253, Republic of Korea
{vprooks,jhryu}@koreatech.ac.kr
http://robot.kut.ac.kr

Abstract. We present a method of virtual fixture generation for shared teleoperation. The method is based on an interactive selection of 2d image features obtained from a 3d camera. The preferred features are then automatically transformed into several possible 3d geometries which the human operator chooses to define the virtual fixture. The generated virtual fixtures are utilized in the teleoperator's control system to render haptic assistance on the master device. The proposed method is intuitive, easy to use, and applies to unstructured environments. The proposed method is implemented as a graphical user interface that enables virtual fixture-based control of a robotic manipulator located at a remote site.

Keywords: Virtual fixture · Shared teleoperation ·
Unstructured environment · Virtual fixture generation ·
Computer vision

1   Introduction

Virtual fixtures have proven their effectiveness in teleoperation since their first introduction in [4,5]. As shown in [1], virtual fixtures have drawn much attention from researchers and resulted in a significant amount of works. However, the usage of virtual fixtures becomes less practical due to a necessity of their generation which requires implementation of the task-specific computer vision and control algorithms. Thus, virtual fixtures, in general, could not be applied to unstructured environments.

The initial solutions to the problem of the virtual fixture generation have been introduced in [3,6]. A more generic approach describing interactive virtual fixture generation is presented in [2].
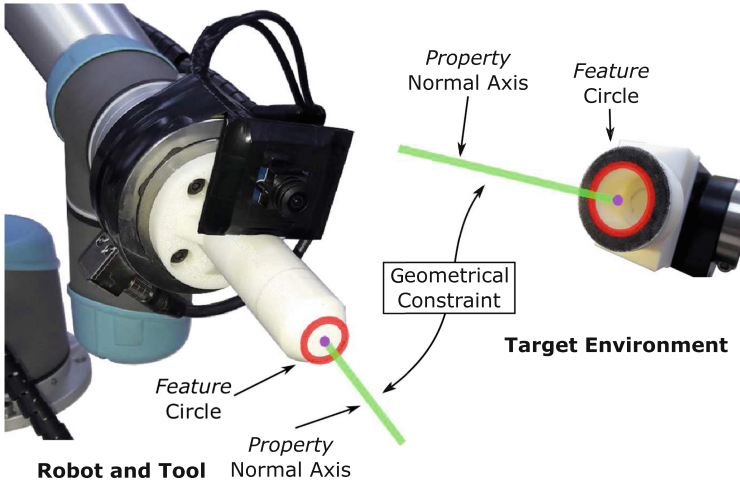
Fig. 1. The proposed concept of virtual fixture generation. First, the human operator selects a feature of the tool; the corresponding depth data is used to compute the normal axis to the chosen feature. Then the human operator selects a feature at the target environment and generates a normal axis property of the selected feature. Finally, the human decides the geometrical constraint that forces the two normal axes to align with each other. The evaluated result of the constraint acts as a virtual guidance force.

This work presents a graphical user interface to generate virtual fixtures which are used to assist the human operator in the execution of teleoperation tasks. The user interface enables constructing the virtual fixtures interactively, which, opposed to automatic virtual fixture generation methods, allows the human operator to choose one of the several possible virtual fixtures that can be associated with the same target in the remote environment. The proposed method applies to unstructured environments because it does not rely on prior knowledge about the environment.

2   Interactive Virtual Fixture Generation

In general, virtual fixtures modify the forces or velocities rendered on the haptic display based on the relative pose of two geometries, one associated with the robot's tool, and the other - with the target environment. So, generating a virtual fixture requires creating two geometrical objects in the virtual environment representing the current state of the robot and the environment and choosing an appropriate constraint between the two geometries.

The primary challenge of virtual fixture generation is the association of the geometries with the remote environments. The representations of geometries are shapes that have 6 degrees of freedom, and their poses should be set correctly in the virtual environment. Doing such operations without any assistance from the computer can be challenging. We propose a solution to the problem that

combines the capability of the computer to do accurate computations on the sensory data with the capability of the human to make correct decisions about the situation at the remote site. This is possible by letting the human operator define virtual fixtures through interaction simply with a 2d image obtained from a camera located at the robot's base.

The proposed method consists of the steps visualized in Fig. 1. First, the human operator selects a feature on the robot's tool. Then, the feature's pixels are automatically mapped to the corresponding 3d points which enable computing the center of the circle and a normal to the plane where the circle belongs. The obtained normal axis becomes the tool's normal axis geometry. Then, the human operator examines the target environment and defines a normal axis property of the hole the same way as has been done for the robot's tool. Finally, given the two geometries, the human operator chooses an appropriate constraint, for example, the alignment of the two normal axes. The system estimates the constraint given the spatial poses of the geometries and produces the necessary guidance force. Please note that the tool geometry's pose is updated automatically when the robot moves. The procedure does not require precise actions from the human operator and thus is fast to execute.

3   Experimental Setup

The method of virtual fixture generation is embodied in a graphical user interface. It receives color camera images from the Kinect sensor located at the robot's base and computes a variety of features in the background: edges, line segments, and ellipses. The human operator moves the computer mouse over the image and selects an appropriate feature. If several different features pass through the same mouse cursor position, the human operator can select the necessary one from a pop-up menu that appears on mouse click. The user interface lists all the possible geometries that can be associated with the selected feature viz. Center point, normal axis, plane, and cylinder. Once several geometries are computed, the user selects two of them and chooses a geometrical constraint. The user interface registers the geometrical constraint as a virtual fixture in the teleoperator's control system which evaluates the guidance forces and torques and renders them at the master device.

We consider only a single example of teleoperated peg-in-hole task. The shared teleoperation setup consists of a UR5 robotic manipulator with the tool of a cylindrical shape attached to the robot's end-effector. The F/T-sensor connected to the tool measures force and torque of the contact with the environment. A manipulation target is an object with a cylindrical hole. The haptic display is Phantom Premium 3.0 6DoF, and it renders measured forces and torques together with virtual guidance forces and torques. The proposed user interface is located at the master device, and displays view of the remote environment through the Kinect sensor installed at the robot's base.

References

1. Bowyer, S.A., Davies, B.L., Rodriguez, Y., Baena, F.: Active constraints/virtual fixtures: a survey. IEEE Trans. Robot. **30**(1), 138–157 (2014). https://doi.org/10.1109/TRO.2013.2283410
2. Pruks, V., Farkhatdinov, I., Ryu, J.H.: Preliminary study on real-time interactive virtual fixture generation method for shared teleoperation in unstructured environments. In: Prattichizzo, D., Shinoda, H., Tan, H.Z., Ruffaldi, E., Frisoli, A. (eds.) Haptics: Science, Technology, and Applications, pp. 648–659. Springer, Cham (2018)
3. Quintero, C.P., Dehghan, M., Ramirez, O., Ang, M.H., Jagersand, M.: Flexible Virtual Fixture Interface for Path Specification in Tele-Manipulation, pp. 5363–5368 (2017)
4. Rosenberg, L.: Virtual fixtures: perceptual tools for telerobotic manipulation. In: Proceedings of IEEE Virtual Reality Annual International Symposium, pp. 76–82. IEEE (1993)
5. Rosenberg, L.B.: The Use of Virtual Fixtures as Perceptual Overlays to Enhance Operator Performance in Remote Environments (1992)
6. Selvaggio, M., Member, S., Notomista, G., Member, S., Chen, F., Gao, B., Trapani, F., Caldwell, D.: Enhancing bilateral teleoperation using camera-based online virtual fixtures generation. In: IEEE/RSJ International Conference on Intelligent Robots and Systems (IROS), pp. 1483–1488. IEEE, October 2016

Circular Lateral Modulation in Airborne Ultrasound Tactile Display

Ryoko Takahashi[(✉)], Saya Mizutani, Keisuke Hasegawa, Masahiro Fujiwara, and Hiroyuki Shinoda

The University of Tokyo, Tokyo, Japan
{takahashi,mizutani}@hapis.k.u-tokyo.ac.jp,
{Keisuke_Hasegawa,Masahiro_Fujiwara}@ipc.i.u-tokyo.ac.jp,
Hiroyuki_Shinoda@k.u-tokyo.ac.jp

Abstract. Airborne Ultrasound Tactile Display (AUTD) can present tactile stimulus on the skin, but the generated pressure is too small in many cases to be perceived on the hairy part. In a previous paper, we proposed a lateral modulation (LM) method where the ultrasound focus was reciprocated along the skin surface instead of amplitude modulation (AM). LM provided clear vibrotactile stimuli even on the hairy skin. In this research, we examine a new modulation named LMc where the ultrasound focus follows a circumference on the skin. In this method, the frequency of the pressure received by each skin receptor is constant regardless of the position. The conference participants experience the difference among AM, LM, and LMc.

Keywords: Midair haptics · Haptic display

1   Introduction

Airborne Ultrasound Tactile Display (AUTD) [1,2] is an ultrasound transducer array that generates acoustic radiation pressure by controlling the phase shift and amplitude of the transducers and present tactile stimulus. With this device, the users don't need to attach any device to their body, so it has the possibility to realize tactile presentation on any position of the body. One problem of such AUTD is that the stimulation is weak. Since the static pressure by a typical AUTD does not have sufficient strength to be perceived by humans, Amplitude Modulation (AM) that modulates the amplitude of the ultrasound pressure with a waveform has been used for presentation of tactile stimuli. However, the pressure that can be presented with AM is still too small to be perceived on the hairy skin in many cases. The authors proposed Lateral Modulation (LM) that moves a stimulus presentation point at a high speed on a line segment, and shows that objectively and subjectively strong tactile stimuli can be presented in the range of 50 to 200 Hz [3] Furthermore, it has been shown that the perception intensity increases with focal movement in tactile presentation of a larger spatial pattern [4]. In LM, the frequency of the pressure received by the skin varies

depending on the position on the skin. For example, at the stimulation center point, the frequency of the pressure is twice the frequency at the edge of the stimulation area. In this research, we propose a new lateral modulation method LMc in which the frequency of the pressure applied to the skin is constant at any position within the stimulation area.

2 Method

In this paper, we propose a new modulation method where the ultrasound focus position is moved along a circumference on a skin. The outline of the method is shown on the left in Fig. 1. We call this method LMc. In AM, the output of the ultrasound power varies with time. In LMc, the power is constant, so the maximum output of the device can always be used. The average of the pressure given to the stimulation range is about twice as that of AM. In LMc, the frequency of the pressure received at a certain point in the stimulus presenting area is constant, and it is equal to the frequency of ultrasound focal movement.
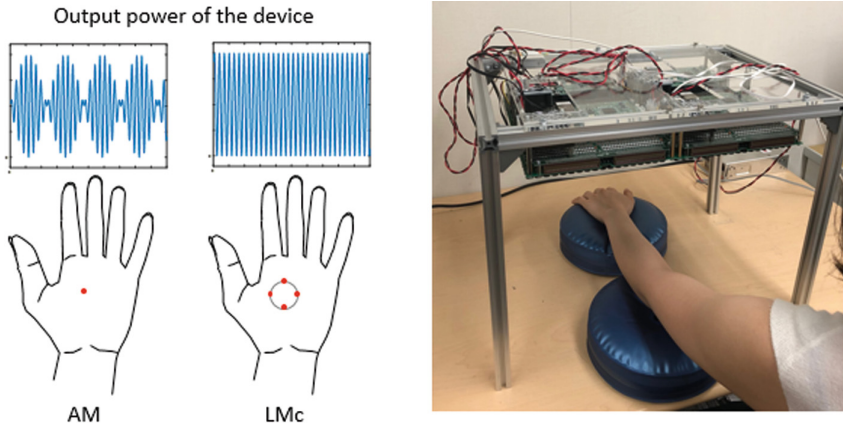
Fig. 1. Left: the ultrasound focal position and the temporal change of the device output in AM and LMc. Right: the appearance of the system.

3 Implementation

In the demonstration, we use a workspace with 4 AUTDs. The right of Fig. 1 shows the appearance of the system. AUTD has transducers resonating at 40 kHz, and it presents a pressure spot of about 8.5 mm in diameter. The focal position moves on a circumference with a radius of 5 mm, at a refresh rate of 1 kHz. When the users put their arm under the device, they can compare the AM, LM and LMc stimuli with the equal maximum output, and confirm that a clear vibrotactile stimulus can be felt by LMc. The experiment was approved by the Ethical Committee in the University of Tokyo. Informed consent was obtained from all individual participants included in the study.

4   Conclusion

In this paper, we showed a new modulation method of midair ultrasound focus LMc, which provides clear vibrotactile stimuli on the skin. The presentation of haptic stimuli on the hairy skin can be enabled by this method. In future, full-body haptic systems by ultrasound can be realized with this method. Unlike in the case of LM, the frequency of the pressure received at a certain point of the skin is constant regardless of the position in this LMc.

References

1. Iwamoto, T., Tatezono, M., Shinoda, H.: Non-contact method for producing tactile sensation using airborne ultrasound. In: Proceedings of EuroHaptics 2008, pp. 504–513 (2008)
2. Hoshi, T., Takayuki, M., et al.: Noncontact tactile display based on radiation pressure of airborne ultrasound. IEEE Trans. Haptics **3**(3), 155–165 (2010)
3. Takahashi, R., Hasegawa, K., Shinoda, H.: Lateral modulation of midair ultrasound focus for intensified vibrotactile stimuli. In: Proceedings of EuroHaptics 2018, pp. 276–288. Springer, Cham (2018)
4. Frier, W., Ablart, D., et al.: Using spatiotemporal modulation to draw tactile patterns in mid-air. In: Proceedings of EuroHaptics 2018, pp. 270–281. Springer, Cham (2018)

Analysis and Design of Surgical Instruments for the Development of a Shoulder Joint Arthroscopic Surgery Simulator

Tae-Keun Kim[1], Geon Won[1], Jong-bum Park[1], Saehan Kim[1],
Byung-jin Jung[1], Jung-Hoon Hwang[1(✉)], Jaeuk Ahn[2], Minju Song[2],
and Chang Nho Cho[3]

[1] KETI (Korea Electronics Technology Institute), Bucheon-si, Korea
{taekeunkiml7,hwangjh}@keti.re.kr
[2] Naviworks, Anyang-si, Korea
[3] KERI (Korea Electrotechnology Research Institute), Changwon-si, Korea

Abstract. Arthroscopic surgery is a minimally invasive surgery which provides a number of benefits, such as faster recovery and minimal incision. However, due to the limited field of view caused by the use of an arthroscope and the difficulties associated with maneuvering surgical instruments through a narrow portal, a highly skilled surgeon is often required. To cope with this, various surgical training simulators have been developed. This study proposes novel designs for the surgical instruments to be used for a shoulder joint arthroscopic surgery simulator. In-depth analysis on the surgical instruments used in the shoulder joint arthroscopic surgery training has been conducted, and novel surgical instruments for a training simulator is developed. The developed surgical instrument is equipped with sensors and actuators to deliver haptic sensation to the users.

Keywords: Haptic device · Arthroscopic surgery · Surgery simulator ·
Surgical instrument · Haptic simulator

1 Introduction

Due to the increases in life expectancy and outdoor activities, an increased number of population are suffering from the rotator cuff tear of shoulder joints. Often, arthroscopic surgery, which ensures minimal damages to the tissue and muscle and faster recovery, is performed to treat the rotator cuff tear [1–3]. However, arthroscopy is conducted using an arthroscope and thus, the motion of the surgeon and the resulting movement of the surgical instruments are inverted. Furthermore, the surgical instruments are inserted through the cannula installed at the shoulder joint. Thus, a highly skilled surgeon is often required for an arthroscopic surgery.

Along with the recent advancements in virtual reality, many studies have been conducted on the development of surgical simulators based on virtual reality and haptic devices. ARTHRO Mentor (Simbionix, USA) is considered as one of the most advanced surgical simulator [4]. The simulator allows the user to learn the key aspect

of the surgical procedures through various anatomical models, 3D images and haptic sensations. Another virtual reality-based surgical simulator for a knee surgery has been developed by Zhang [5] and Lu [6]. These studies also investigated the control system, tissue deformation simulation and collision detection for the training simulator. Park [7] combined a haptic device with a shoulder model for the shoulder joint arthroplasty training system. In this study, the force and motion data recorded from actual arthroscopic surgeries are used to develop an accurate simulation model, along with the optimized range of motion and haptic sensation.

In this study, based on Park's study [7], various surgical instruments for the shoulder joint arthroscopic surgery haptic simulator have been developed. First, the developed shoulder joint arthroscopic surgery simulator and the structure of the haptic device will be introduced. Then, the analysis on the surgical instruments used for arthroscopy and the developed surgical instruments for haptic devices are presented.

2 Development of Surgical Instruments for Shoulder Joint Arthroscopic Surgery Simulator

2.1 Shoulder Joint Arthroscopic Surgery Simulator

The developed shoulder joint arthroscopic surgery simulator consists of one shoulder model and two haptic devices (Fig. 1). Each haptic device has six degrees of freedom (DOF), of which four are active joints and two are passive joints. Joint 1–3 are actuated through wire-tendon mechanism whereas joint 4 is directly actuated. An encoder is attached to each joint, and various surgical tools can be installed at the end-effector.
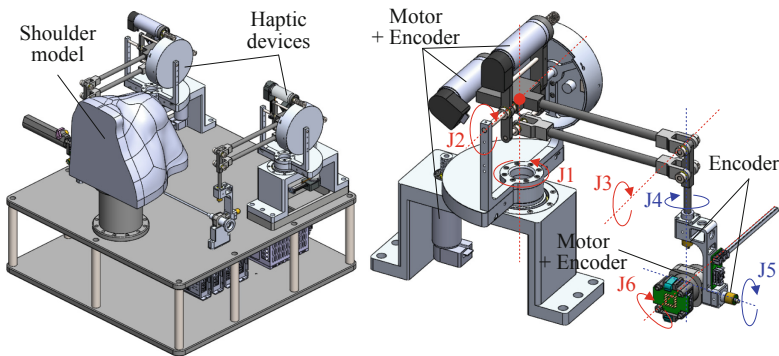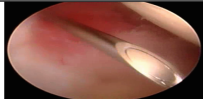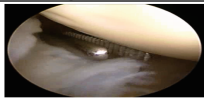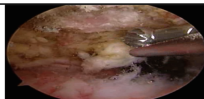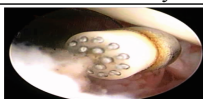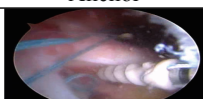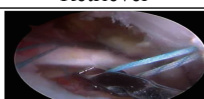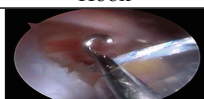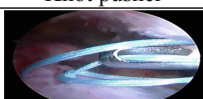
Fig. 1. Design of arthroscopic surgery training simulator for shoulder joint and haptic device

2.2 Analysis of Surgical Instruments for Shoulder Joint Arthroscopic Surgery

The typical surgical instruments used for the shoulder joint arthroscopy are listed in Table 1. A needle is used to make a small incision, and a straight hemostat and a

cannula are used to enlarge the incision and create the portal. To examine the surgery area, various probes can be inserted to the portal, and muscles and tissues can be removed using a scissor. A Shaver and a burr are also used to remove undesired tissues, while electrocautery is used to achieve hemostasis. Once the procedure is complete, the tissue can be sutured by an anchor with a thread. During the suturing, the thread is maneuvered by a retriever and a hook. To create a knot, a knot pusher can be used.

Table 1. Typical surgical instruments for shoulder joint arthroscopy.
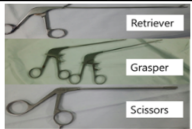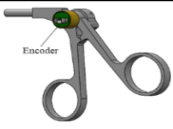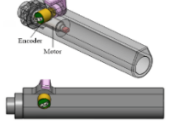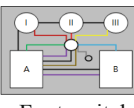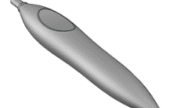
Needle	Straight hemostat	Cannula	Probe
Scissor	Shaver	Burr	Electrocautery
Anchor	Retriever	Hook	Knot pusher

2.3   Design of Surgical Instruments

In this study, a shaver, electrocautery and a scissor, which are the most widely used surgical instruments for arthroscopy, are selected as the target instruments for the haptic surgical simulator. As shown in Table 2, for scissor-type instruments, encoders are installed to detect the instrument movements while dip switches are used to select between the retriever, grasper or scissor. On the other hand, for a shaver, an encoder is used to detect its pneumatic control, and the encoder data is also utilized to control a motor to simulate the vibration. As for the electrocautery, it can be activated using a foot switch.

The developed surgical instruments can be attached to the haptic device through the torsion spring-based lock mechanism and magnets. Pogo pins are used to deliver the control and sensor signals, and Fig. 3 depicts the developed haptic device and surgical instruments (Fig. 2).

Table 2. Sensors and actuators for surgical instruments.

Needle	Surgical equipment	Sensor and actuator		Design
Scissor type		Scissor action : Encoder	Tool selection : Dip switch	
Shaver		Pneumatic control : Encoder	Vibration effect : Vibration motor	
Electro-cautery & foot switch		On/off control : Foot switch		
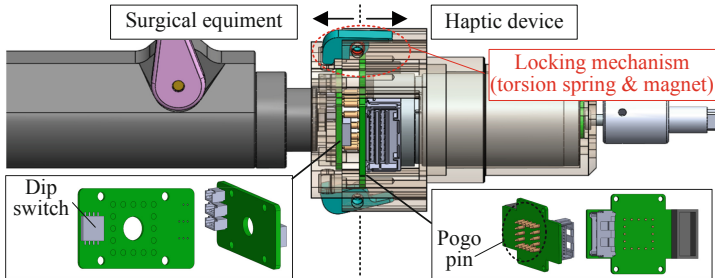
Fig. 2. Design of arthroscopic surgery training simulator for shoulder joint and haptic device

(a)   (b)   (c)   (d)
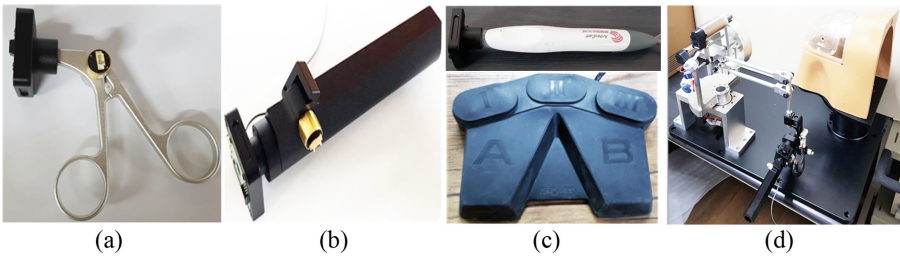
Fig. 3. A figure caption is always placed below the illustration. Short captions are centered, while long ones are justified. The macro button chooses the correct format automatically.

3   Conclusion

In this study, surgical instruments with haptic capability have been developed for the shoulder joint arthroscopic surgical simulator. Surgical instruments required for arthroscopy are analyzed, and using various sensors and actuators, surgical instruments which can be used for haptic devices have been developed.

As the future study, a repositionable shoulder model will be developed to simulate a surgical procedure with various patient postures, and the feasibility of the developed haptic devices and surgical instruments will be further investigated.

References

1. Gartsman, G.M., Brinker, M.R., Khan, M.: Early effectiveness of arthroscopic repair for full-thickness tears of the rotator cuff: an outcome analysis. J. Bone Joint Surg. Am. **80**(1), 33–40 (1998)
2. Hersch, J.C., Sgaglione, N.A.: Arthroscopically assisted mini open rotator cuff repairs. Functional outcome at 2- to 7-year follow-up. Am. J. Sports Med. **28**, 301–311 (2000)
3. Warner, J.J., Tétreault, P., Lehtinen, J., Zurakowski, D.: Arthroscopic versus mini-open rotator cuff repair: a cohort comparison study. Arthroscopy **21**(3), 328–332 (2005)
4. Simbionix Homepage. http://www.simbionix.com
5. Zhang, G., Zhao, S., Xu, Y.: A virtual reality based arthroscopic surgery simulator. In: International Conference on Robotics, Intelligent Systems and Signal Processing, pp. 272–277, China (2003)
6. Lu, J., Chen, J., Çakmak, H., Maass, H., Kühnapfel, U., Bretthauer, G.: A knee arthroscopy simulator for partial meniscectomy training. In: Asian Control Conference, pp. 763–767, Hong Kong (2009)
7. Park, J.-B., Kim, T.-K., Won, G., Jung, B., Hwang, J.-H.: Analysis of surgical motion, force, and workspace for the haptic interface design in the shoulder arthroscopy simulator. In: International Conference on Green and Human Information Technology, Thailand (2018)

An Attempt of Displaying Softness Feeling Using Multi-electrodes-based Electrostatic Tactile Display

Hirobumi Tomita[1(✉)], Satoshi Saga[2], Hiroyuki Kajimoto[3], Simona Vasilache[1], and Shin Takahashi[1]

[1] University of Tsukuba, 1-1-1 Tennodai, Tsukuba, Ibaraki, Japan
{tomita,Simona}@iplab.cs.tsukuba.ac.jp, shin@cs.tsukuba.ac.jp
[2] Kumamoto University, 2-39-1, Kurokami, Chuo-ku, Kumamoto, Japan
saga@saga-lab.org
[3] The University of Electro-Communications, 1-5-1 Choufugaoka, Choufu, Tokyo 182-8585, Japan
kajimoto@kaji-lab.jp

Abstract. Touch screens used as interfaces rarely give tactile feedback to users. We developed a electrostatic-force-based tactile display, however, it cannot express softness feelings on the screen. In this research, we attempted to display softness feeling by using multi-electrodes and a pressure sensor. When using our system, we observed that the user can feel change of the display area on the fingertip when his pressure toward the surface is changed.

Keywords: Haptic display · Electrostatic force · Multi-electrodes

1 Introduction

Touch screens used as interfaces rarely give tactile feedback to users. There are a lot of researches that have employed vibrations to display tactile sensation. Recently, electrostatic-force-based tactile display have been developed [1]. However, this display device cannot express softness feelings on the screen. Several researches revealed that the change of contact area on a fingertip induces softness feelings to the user. Thus we consider the feasibility of the method with the electrostatic force display.

In this paper, we proposed displaying softness feeling with our display and attempted to use the system.

2 Method of Displaying Softness and Prototype

Fujita, et al. and Bicchi, et al. investigated whether the finger feels soft by changing the contact area of the fingertip [2,3]. When an user is pressed on a

tactile display, he/she feels softness in case the contact area is widened, otherwise he/she feels hardness in case the contact area does not change. We assumed that softness expression can be displayed by changing the presentation area to be widened with the electrostatic force display. We created multi-electrodes to change the presentation area, and developed an area-controllable electrostatic force display (Fig. 1).
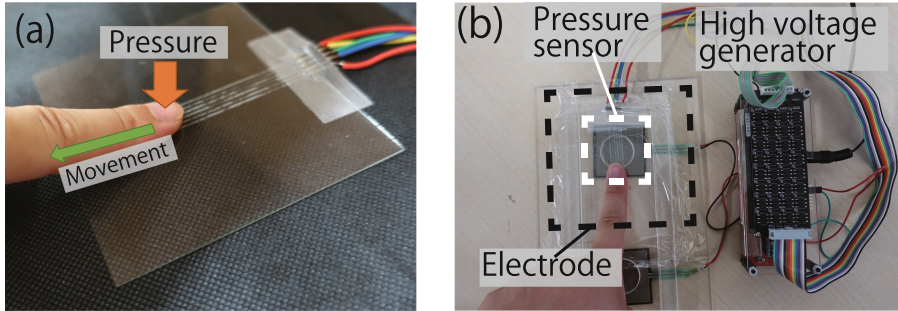
Fig. 1. (a) The user rubbed back and forth on the multi-electrodes, which is generated by dividing one ITO electrode into five lines. (b) Overview of the system. It consists of electrodes, pressure sensor, and high-voltage generator.

Our electrostatic tactile display features of a high voltage generator, a pressure sensor, multi-electrodes and an insulator. The a high voltage generator includes an mbed LPC1768 microcontroller, which controls maximum 600 V of output voltage and maximum 16 channels of multiple switching outputs by modifying its firmware. The various types of waveforms can be output to the electrode surface for displaying various types of electrostatic tactile feedback. An insulator is placed on the electrode. Multi-electrodes is created by dividing one ITO electrode into five lines. The pressure sensor is installed under the multi-electrodes to measure the user's pressure.

We conducted a preliminary experiment to evaluate whether softness feeling can be displayed to the user by our proposed method. Initially, the experimenter explained the informed consent based on ethical guidelines of University of Tsukuba, and their consent is obtained. We asked him/her whether the change of the tactile sensation is felt, and whether the softness feeling is felt on the tactile display. We collected the following answer from several participants, "I felt the change of the tactile sensation, however, I hardly felt the softness ever". Thus, we considered that our proposed method can make user feel some kind of changes of the display area on the fingertip skin surface, however, cannot make the user perceive the softness feeling. We plan to perform other displaying methods by using different layout of multi-electrode to generate softness feelings.

3   Conclusion

In this paper, we attempted to display softness feeling using electrostatic force display. We focused on the fact changing the contact area on the fingertip induce softness feeling to the user. The changing presentation area is implemented by using multi-electrodes. We produced a prototype system and a preliminary experiment. The results showed that the users can feel change of the display area but it is difficult for them to perceive the tactile sensation as softness feeling with the proposed method. We plan to perform other displaying methods by using different layout of multi-electrodes.

References

1. Bau, O., Poupyrev, I., Israr, A., Harrison, C.: TeslaTouch: electrovibration for touch surfaces. In: Proceedings of the 23rd Annual ACM Symposium on User Interface Software and Technology, UIST 2010, pp. 283–292. ACM, New York (2010). https://doi.org/10.1145/1866029.1866074
2. Bicchi, A., Scilingo, E.P., De Rossi, D.: Haptic discrimination of softness in teleoperation: the role of the contact area spread rate. IEEE Trans. Robot. Autom. **16**(5), 496–504 (2000)
3. Fujita, K., Ohmori, H.: A new softness display interface by dynamic fingertip contact area control. In: 5th World Multiconference on Systemics, Cybernetics and Informatics, pp. 78–82 (2001)

Tactile Transfer Glove Using Vibration Motor

Sang Hun Jung[1,2] and Bummo Ahn[1,3(✉)]

[1] Robotics R&D Group, Korea Institute of Industrial Technology, Ansan,
Republic of Korea
bmahn@kitech.re.kr
[2] Department of Mechanical Engineering, Incheon National University, Incheon,
Republic of Korea
[3] Robotics and Virtual Engineering, University of Science and Technology,
Ansan, Republic of Korea

Abstract. Virtual reality environment gives a variety of realistic experience to users. To provide realistic information to the users in virtual reality, several devices are necessary. The visual and auditory information is transferred by VR goggle. The tactile information can be provided by tactile transfer device. In this research, we, therefore, suggest tactile transfer gloves that can be used with VR goggle. The glove is consisted of flex sensor, vibration motor, fabric glove, and electrical circuit. The resistance sensor, which changes with the degree of flexion, controls intension and frequency of the vibration motor. Consequently the glove give tactile feedback to users by regulating intension and frequency of motor depending on degree of flexion of finger. The developed tactile transfer glove can be used to provide realistic information for users in virtual reality environment.

Keywords: Virtual reality · Tactile transfer glove · Vibration feedback · Flex sensor · Finger bending motion

1 Introduction

Virtual reality (VR) is an interface that can interact between people and computer. The VR environment is a computer generated imaginary space that can give realistic experiences to users. As VR becomes more and more popular, people increasingly want to get more realistic sensation in the virtual reality environment. However, in order to realistically recognize these virtual reality environments, users have to sense visual, auditory, and tactile information. The Oculus Rift (Oculus VR Inc., California, USA) and HTC Vive (HTC Inc., Xinbei, China) transfer visual and auditory information to users. Through the VR goggles, however, the users cannot get any tactile information of virtual objects. Therefore, several research groups have tried to develop tactile feedback devices to address the limitation that cannot transfer tactile feedback with only VR goggle. Some developed devices such as Apollo Developer/Professional (Manus-VR, Eindhoven, Netherlands) and Glove One (NeuroDigital Technologies, Almeria, Spain) can provide vibration feedback to users. Furthermore, Dexmo (Dexta Robotics Inc., Shenzhen, China) [1], AxonVR (HaptX Inc., Seattle, USA), Wolverine (Stanford Univ. SHAPE Lab, Stanford, USA) [2] and many fingertip devices [3–5] transfer force

feedback to users. However, these developed devices need to combine motion tracking system in order to measure finger motions in virtual reality environment.

In this research, we, therefore, suggest tactile feedback transfer method using analyzing user's finger motion without motion tracking devices. In addition, we developed tactile feedback glove to validate the suggested method.

2   Materials and Methods

The suggested feedback glove is composed of a custom-made fabric glove, flex sensor (Sparkfun co., Boulder, USA), coin-shaped vibration motor (Neotics Inc., Go-yang, Republic of Korea), Arduino UNO (IDII co., Ivrea, Italy) and Keyes L298 N DC motor driver (LK embedded co., Seoul, Republic of Korea). The proposed glove has two pockets at the thumb, index finger, and middle finger respectively. The pockets are located at the surface of finger and the fingerprint. To analyze the motion of finger, a bend sensor is inserted in the pocket on the surface of the finger. The bend sensor has characteristic that its resistance value changes depending on bending of sensor. In addition, the measured value is converted to a number between 0 and 254 in order to PWM control of vibration motor. To transfer tactile information, the vibration motor is inserted in the pocket of the fingerprint. As a result, the inserted motor can transfer vibration feedback to the fingerprint.
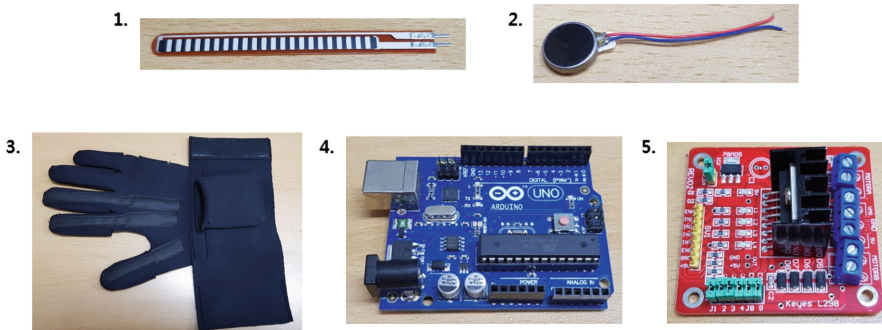
Fig. 1. The materials: 1. flex sensor, 2. coin-shaped vibration motor, 3. fabric glove, 4. Arduino UNO, and 5. motor driver

3   Discussion

Arduino UNO applies 5 V to circuit and takes analog input as the voltage value from 0 V to 5 V. The value are printed on serial monitor of Arduino. Because used flex sensor changes resistance value of circuit compared to bending, the applied voltage is converted and read as voltage value from 0 V to 5 V. The flex sensor is located in

glove and changes resistance depending on a bending of the finger. Consequently Fig. 2 shows that the difference in resistance compared to flexion of finger. Based on the graph, the resistance value increases depending on a degree of the arching of bend sensor. Because the bend sensor is located on the finger, the increased resistance value means the bended finger. To control intension and frequency of the motor, the resistance value is converted to a number from 0 to 254. The intension and frequency of motor consequently change based on a degree of the flexion of finger. In this experiment, when the finger is straight, the motor gives no feedback to users. On the other hand, when the finger is bended, the intension of motor increases and the frequency of motor shortens gradually compared to flexion of finger. Finally, the motor transfer max intension and continuous vibration in order to notify of contacting the virtual objects.
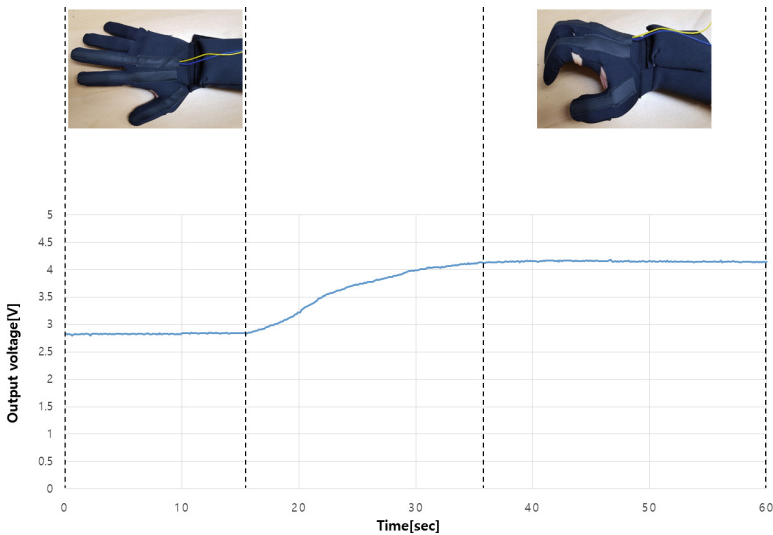
Fig. 2. The change of resistance value compared to flexion of finger

4 Result and Future Work

In this research, we proposed tactile transfer glove. To sense objects in virtual reality environment, the glove is necessary. The users can get vibration feedback through the glove when the finger touch virtual object. However, the glove has two limitations yet. We, therefore, plan to address these limitations in future research. First, the feeling virtual object is hard with only vibration motor. When people grasp the objects in real environment, a reaction force which proportionately increases compared to pressing intension is transferred into the fingerprint. To recognize more realistic tactile feedback in virtual environment, the reaction force on the fingerprint is necessary when the users grasp the virtual object. However, the materializing the force feedback is hard with only vibration motor. To give more realistic feedback, therefore, we will plan to develop fingertip haptic device that can transfer the force feedback on the fingerprint

using servo motor [6]. Second, the finger continuously can move after touching the virtual objects. When the users grasp the rigid objects in real environment, the finger cannot pass through the objects although the users apply more force. To transfer more realistic tactile feedback, the fingers don't have to pass through virtual objects. However, while the above-mentioned fingertip device can transfer sensation of touching virtual objects, the finger can pass through the virtual objects. We, therefore, will research a method which stop the finger after touching virtual objects.

References

1. Gu, X., Zhang, Y., Sun, W., Bian, Y., Zhou, D., Kristensson, P.O.: Dexmo: an inexpensive and lightweight mechanical exoskeleton for motion capture and force feedback in VR. In: CHI 2016 Proceedings of the 2016 CHI Conference on Human Factors in Computing Systems (2016)
2. Choi, I., Hawkes, E.W., Christensen, D.L., Ploch, C.J., Follmer, S.: Wolverine: a wearable haptic interface for grasping in virtual reality. In: Proceedings of RSJ International Conference on Intelligent Robots and Systems (IROS) (2016)
3. Leonardis, D., Solazzi, M., Bortone, I., Frisoli, A.: A 3-RSR haptic wearable device for rendering fingertip contact forces. Proc. IEEE Trans. Haptics **10**(3), 305–316 (2017)
4. Gabardi, M., Solazzi, M., Leonardis, D., Frisoli, A.: A new wearable fingertip haptic interface for the rendering of virtual shapes and surface features. In: Proceedings of IEEE Haptics Symposium (HAPTICS) (2016)
5. Pierce, R.M., Fedalei, E.A., Kuchenbecker, K.J.: A wearable device for controlling a robot gripper with fingertip contact, pressure, vibrotactile, and grip force feedback. In: Proceedings of IEEE Haptics Symposium (HAPTICS) (2014)
6. Scheggi, S., Meli, L., Pacchierotti, C., Prattichizzo, D.: Touch the virtual reality: using the Leap Motion controller for hand tracking and wearable tactile devices for immersive haptic rendering. In: Proceedings of ACM Special Interest Group on Computer Graphics and Interactive Techniques Conference, SIGGRAPH (2015)

A Large-Scale Fabric-Based Tactile Sensor Using Electrical Resistance Tomography

Hyosang Lee[1] , Kyungseo Park[2] , Jung Kim[2] ,
and Katherine J. Kuchenbecker[1(✉)]

[1] Max Planck Institute for Intelligent Systems,
Heisenbergstr. 3, Stuttgart 70569, Germany
{hslee,kjk}@is.mpg.de
[2] Korea Advanced Institute of Science and Technology,
Daehak-ro 291, Daejeon 34141, South Korea
{bbq2686,jungkim}@kaist.ac.kr

Abstract. Large-scale tactile sensing is important for household robots and human-robot interaction because contacts can occur all over a robot's body surface. This paper presents a new fabric-based tactile sensor that is straightforward to manufacture and can cover a large area. The tactile sensor is made of conductive and non-conductive fabric layers, and the electrodes are stitched with conductive thread, so the resulting device is flexible and stretchable. The sensor utilizes internal array electrodes and a reconstruction method called electrical resistance tomography (ERT) to achieve a high spatial resolution with a small number of electrodes. The developed sensor shows that only 16 electrodes can accurately estimate single and multiple contacts over a square that measures 20 cm by 20 cm.

Keywords: Fabric-based tactile sensor · Electrical resistance tomography · Large-scale tactile sensing

1 Introduction

Robots working in unstructured environments and alongside people need to be able to sense contact information from both intentional and unintentional interactions [1]. Because physical contacts can occur all over a robot's body, tactile sensors need to be able to measure contact information from all exposed parts of a robot, not just the fingertips. Depending on the contact location, existing tactile sensors tend to compromise sensing performance as well as practical requirements such as mechanical compliance, manufacturability, and reliability [2]. Electrical resistance tomography (ERT) was introduced as a new way to achieve mechanical compliance and manufacturability in tactile sensors. The ERT method is an imaging technique that estimates the internal conductivity distribution of a conductive medium using only a small number of electrodes [3]. This reconstruction approach enables the fabrication of soft

---

H. Lee and K. Park—These authors contributed equally to this work.

tactile sensors that can cover large flat and/or curved surfaces with low fabrication cost [4, 5]. ERT electrodes are typically placed only around the edges of the sensing surface, which can be made of conductive rubbers [5, 6], conductive fabrics [7, 8], or ionic liquids [9]. Regardless of the chosen material, sensors of this type tend to have relatively poor spatial resolution near the center of the sensing surface.

This demonstration presents a tactile sensor made of fabric layers that have different levels of conductivity. A double layer of conductive fabrics serves as the pressure-sensitive conductive medium. Conductive thread traces are sewn onto a non-conductive fabric layer and then into the conductive fabric to form an array of point electrodes. Compared to the conventional ERT-based tactile sensors, the presented sensor has four of its sixteen electrodes placed inside of the sensing region to improve spatial resolution. Electrical currents are injected between different electrode pairs, and the resulting voltage potentials are measured at other pairs through the conductive thread traces. As a result, single and multiple contacts can be estimated.

2   Details of the Fabric-Based Tactile Sensor

As shown in Fig. 1(a), a fabric sheet with low conductivity is connected to the conductive thread electrodes. The developed sensor utilized 16 electrodes distributed in a regular 4-by-4 grid over a square measuring 20 cm by 20 cm. Highly conductive fabric patches adhered on a non-conductive fabric sheet are placed over the low-conductivity fabric. When surface normal forces are applied on the outside of the non-conductive fabric, one or more highly conductive fabric patches contact the low-conductivity fabric sheet and therefore increase the combined conductivity of the double layer in the region of the contact. This conductivity change is estimated using electrical resistance tomography, as described above.
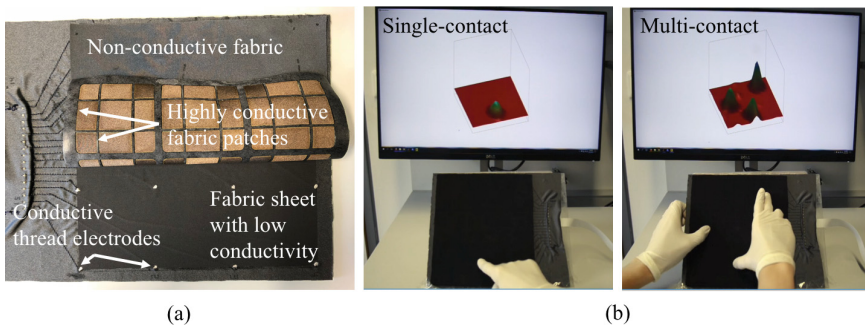
Fig. 1. (a) The internal construction of the fabric-based tactile sensor. (b) Single-contact and multi-contact demonstrations using the tactile sensor.

Figure 1(b) shows a sample physical interaction with the sensor and the corresponding tactile contact reconstruction for single and multiple contact cases. Although it has only 16 electrodes, the developed tactile sensor can reconstruct the tested contact locations and amplitudes with good apparent accuracy.

References

1. Dahiya, R.S., Metta, G., Valle, M., Sandini, G.: Tactile sensing: from humans to humanoids. IEEE Trans. Robot. **26**(1), 1–20 (2010)
2. Lumelsky, V.J., Cheung, E.: Real-time collision avoidance in teleoperated whole-sensitive robot arm manipulators. IEEE Trans. Syst. Man Cybern. **23**(1), 194–203 (1993)
3. Holder, D.S.: Electrical Impedance Tomography: Methods, History and Applications. CRC Press, Boca Raton (2004)
4. Kato, Y., Mukai, T., Hayakawa, T., Shibata, T.: Tactile sensor without wire and sensing element in the tactile region based on EIT method. In: IEEE Sensors, pp. 792–795 (2007)
5. Lee, H., Kwon, D., Cho, H., Park, I., Kim, J.: Soft nanocomposite based multi-point, multi-directional strain mapping sensor using anisotropic electrical impedance tomography. Sci. Rep. **7**, 39837 (2017)
6. Shimojo, M., Namiki, A., Ishikawa, M., Makino, R., Mabuchi, K.: A tactile sensor sheet using pressure conductive rubber with electrical-wires stitched method. IEEE Sens. J. **4**(5), 589–596 (2004)
7. Visentin, F., Fiorini, P., Suzuki, K.: A deformable smart skin for continuous sensing based on electrical impedance tomography. Sensors **16**(11), 1928 (2016)
8. Yao, A., Soleimani, M.: A pressure mapping imaging device based on electrical impedance tomography of conductive fabrics. Sensor Rev. **32**(4), 310–317 (2012)
9. Chossat, J.-B., Shin, H.-S., Park, Y.-L., Duchaine, V.: Soft tactile skin using an embedded ionic liquid and tomographic imaging. J. Mech. Robot. **7**(2), 021008 (2015)

Haptic Eye: A Contactless Material Classification System

Tamas Aujeszky, Georgios Korres[✉], and Mohamad Eid

Department of Engineering, Applied Interactive Multimedia Laboratory (AIMLab),
New York University Abu Dhabi, Abu Dhabi, UAE
{tamas.aujeszky,george.korres,mohamad.eid}@nyu.edu,
http://wp.nyu.edu/aimlab

Abstract. In this paper we demonstrate a system capable of classifying different types of materials in a contactless fashion by using active infrared thermography and machine learning algorithms. A laser diode heats the materials and the infrared camera records the thermal dissipation signature of each material. These data are then fed to machine learning algorithms to classify the materials. This system can potentially be used in teleoperation applications for robots that operate in unknown scenes.

1 Introduction

Infrared thermography has been used for decades for nondestructive testing and evaluation purposes, and recently it has started to emerge as a contactless material characterization tool that is suitable for performing thermal modeling of real-life objects [2]. The Haptic Eye prototype demonstrated material classification by subjecting samples to thermal excitation and capturing the thermal footage of their cooldown process, then applying a set of machine learning classifiers on a number of extracted features [1]. Our latest approach uses convolutional neural networks for classification between samples and regression to thermal properties.

2 Demonstration Setup

The setup of the demonstration is shown in Fig. 1. The following components are comprising the Haptic Eye demonstration: A laser source for stimulating the material by slightly changing its temperature on a specified spot, an infrared camera that is capable of capturing the thermal signature of the laser stimulation, a rotating base that rotates the Haptic Eye to target different sample materials, and a control board that controls the whole demonstration setup. For the data acquisition, the further processing and the final classification of the sample materials, an ordinary laptop is used. Figure 2 is showing the center temperature dissipation of the laser stimulation from three different materials of an experimental session.

In this demonstration, the Haptic Eye uses the laser diode to stimulate the first material for about 10 s, then the infrared camera records the thermal dissipation and proceeds to the next material. When data from all materials is acquired, it classifies them accordingly. A Graphical User Interface (GUI) is developed to present in detail the entire acquisition and classification processes in real time. A link to the video demonstration is available at the following URL: https://www.youtube.com/watch?v=828SEeedqbo.
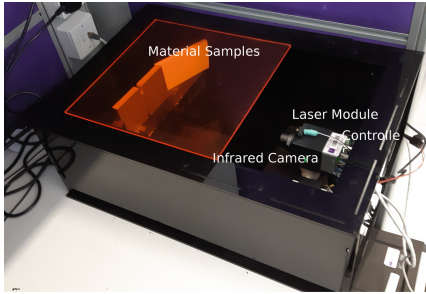
Fig. 1. The Haptic Eye system setup
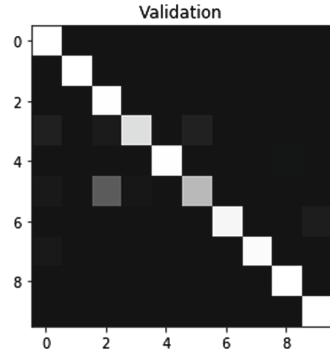
Fig. 2. Confusion matrix for 10 material samples

3 Conclusion

In this paper we present a system which is capable of classifying different materials in a contactless fashion by utilizing infrared thermography and convolutional neural networks. Haptic Eye is a very promising system which could potentially be used for accurate teleoperation procedures where a deep knowledge of the unknown environment is needed. In our future work, we will try to develop more robust classification and/or regression methods for material characterization. Furthermore, we will develop the hardware to reduce the form factor of the system in order to be used as a sensor on a tele-operated robotic platform.[1]

References

1. Aujeszky, T., Korres, G., Eid, M.: Thermography-based material classification using machine learning. In: 2017 IEEE International Symposium on Haptic, Audio and Visual Environments and Games (HAVE), pp. 1–6. IEEE (2017)
2. Aujeszky, T., Korres, G., Eid, M.: Measurement-based thermal modeling using laser thermography. IEEE Trans. Instrum. Meas. **67**(6), 1359–1369 (2018)

---

[1] Concrete, PE block, acrylic, coal, marble, sorbothane, LPL, HPL, steel and silicone.

"HaptiComm", a Haptic Communicator Device for Deafblind Communication

Basil Duvernoy[1(✉)], Sven Topp[2(✉)], and Vincent Hayward[3(✉)]

[1] Institut des Systèmes Intelligents et de Robotique, UPMC, Paris, France
duvernoy@isir.upmc.fr
[2] School of Psychology, University of Sydney, Sydney, Australia
s.topp@hapticomm.tech
[3] Institute of Philosophy, School of Advanced Study,
University of London, London, UK
hayward@cim.mcgill.ca

Abstract. When people are deaf and blind, daily life is made difficult owing to the lack of linguistic communication that is normally mediated by sight and hearing. The project described herein aims at helping deafblind individual overcome this communication barrier. We describe a tactile communication apparatus that is capable of rich and efficient reproduction of the tactile signs employed by several tactile deafblind languages.

Keywords: Haptic device · Deafblind · Communication · Tactile · Actuators

1 Introduction

With a view to facilitate communication with people who are deafblind, a most urgent need is to make linguistic interaction possible without the help of others. Here, we describe the prototype of a tactile communication device for the deafblind community that is motivated by the latest discoveries regarding "early touch" on Jörntell et al. (2014), Shao et al. (2016); while following a minimalist design approach for robustness, ease of replication, and low cost.

2 Deafblindness

Deafblindness is a disability where the combined loss of vision and hearing impact one's ability to communicate freely. In Western countries, the incidence of Deafblindness is surprisingly high. Broad criteria identifying significant repercussion of dual sensory loss put the incidence of Deafblindness to one person in 250. Stricter criteria put this number at 1:1000. However, in countries like Canada and Australia, it is estimated that indigenous populations, and those with limited medical access, have an even higher incidence of Deafblindness.

2.1 Inclusion and Communication

Deafblind individuals face many challenges, including orientation, inclusion in society, and even access to ordinary communication and transport options. Frequently, these challenges result in isolation and risk of mental health sequelae.

This disability also implies to develop other technics of communication than the mainstream ones which use mainly vision and audition. The deafblind languages are not as known as, for instance, the visual sign language implying a lack of technological support for the deafblind community. It exists technological aids, such as braille tablets, but such medias are inconvenient for most deafblind individuals.

Moreover, tactile signers cannot interpret speech to more than one deafblind individual at a time and for sessions that can last no longer than 45 min, reducing the possibilities to communicate with the world.

2.2 Languages

Due to the variety of possible manner to acquire deafblindness and the large number of country, the deafblind technics could be particularly different.

One type of these technics, which is the one the HaptiComm focus on, is called deafblind tactile fingerspelling technics. By touching the sensitive inside region of the hand to communicate, the locutor signs tactile symbols which correspond to letters, words and ideas. These symbols are based mostly on brief finger tapping and swiping as shown in Fig. 1.

Fig. 1. The Australian deafblind tactile fingerspelling.

Furthermore, the expressiveness of these languages is like that of speech. There is prosody, emphasis, and other forms of modulation similar to speech that operate at the lexical, grammatical and semantic levels, in addition to non-lexical short-hand symbols, smileys, geometric figures, directional cues and so-on.

The technology that we develop can address these forms of modulation.

3 Haptic Display

HaptiComm recognises that haptics naturally supports linguistic communication within the deafblind community. It is a hardware and software platform that is highly flexible in its design, is inexpensive, and easy to reproduce. Predominantly 3D printed and able to be customised, the HaptiComm platform supports a broad range of applications when coupled to speech recognition, text messaging, or optical character recognition inter alia. The device is shown in Fig. 2.

3.1   Overview

The HaptiComm hardware operate from first principles with an array of up to 32 strategically placed actuators facing the receiver's hand. These actuators Duvernoy et al. (2018) are very simple, yet efficiently cater to the two required modes of mechanical interaction, namely, tapping and swiping on the skin, and have large dynamic and frequency ranges. It implies they can tap loci in the volar region of the hand, dissipating an impact energy similar to that of a real tapping finger. Each actuator can also apply a gentle bias force on the skin and vibrate it within the full vibro-tactile frequency range. These operations can be repeated many times per second and per actuator to reproduce with fidelity the sensation of fingers tapping and sliding over the volar region of the hand. Since elemental signals, including tap, place-and-hold and slides, form the basis of the natural codes—and of languages based on them—such as "English Deafblind Manual", Australian "Deafblind Tactile Fingerspelling", Italian "Malossi", German "Lorm", reduced forms of Japanese "Finger Braille", and others, the HaptiComm hardware has a broad applicability because the learning curve for its use is short.
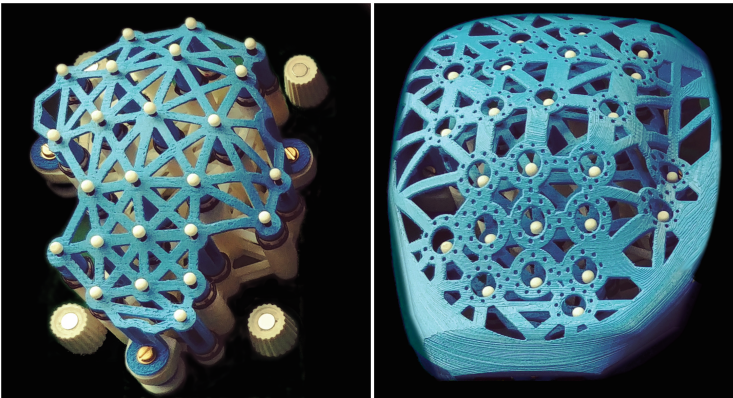
Fig. 2. Overview of the tactile communicator

3.2   Interface Design

The interface has an outer shell that fits the shape of the palm of the hand at rest. This shell has few contact with the skin for the evacuation of the sweat and heat. To avoid interference between actuators, the structure holding the actuators is mechanically decoupled from the shell.

3.3 Software and Tactile Motions

The software extracts sentences from speech and translate them into tactile symbols. Creating the sensation of a human hand tapping and swiping is important for the intelligibility of the spelling. The 24 actuators are strategically placed so that the stimulation regions optimally approximate with the hand regions used during spelling. Swiping sensations are created by producing apparent movement from a carrier signal (Békésy (1959), Sherrick Jr. (1964), Sherrick and Rogers (1966)). Using optimised WAV files in order to create the signals used by the actuator to recreate the symbols, a proper modulation of amplitude and timing provides the sensation of continuous sliding movements.

4 Summary

We created a device of minimal complexity that is easily replicated and low cost. Yet it is capable of a great range of expressiveness thank to the care that was put in its mechanical organization, the distribution of actuators to take advantage of the non-local property of early haptic processing, and the design of actuators that have time constants that are compatible with the basic physics of tactile interaction with the hand.

References

Békésy, G.V.: Similarities between hearing and skin sensations. Psychol. Rev. **66**(1), 1–22 (1959)

Sherrick Jr., C.E.: Effects of double simultaneous stimulation of the skin. Am. J. Psychol. **77**(1), 42–53 (1964)

Duvernoy, B., Farkhatdinov, I., Topp, S., Hayward, V.: Electromagnetic Actuator for Tactile Communication, pp. 1–10 (2018)

Jörntell, H., Bengtsson, F., Geborek, P., Spanne, A., Terekhov, A.V., Hayward, V.: Segregation of tactile input features in neurons of the cuneate nucleus. Neuron **83**(6), 1444–1452 (2014)

Shao, Y., Hayward, V., Visell, Y.: Spatial patterns of cutaneous vibration during whole-hand haptic interactions. Proc. Nat. Acad. Sci. **113**(15), 4188–4193 (2016)

Sherrick, C.E., Rogers, R.: Apparent haptic movement. Percept. Psychophys. **1**(3), 175–180 (1966)

Real-Time Mapping of Sensed Textures into Vibrotactile Signals for Sensory Substitution

Jaeyoung Park[✉], Woo-seong Choi, and Keehoon Kim

Korea Institute of Science and Technology, Seoul, Korea
{jypcubic,dswwfg,khk}@kist.re.kr

Abstract. This paper presents a method to transform a surface texture sample sensed with a force-torque sensor into a vibrotactile stimulus in real time, as a technique to let a hand amputee feel the surface of objects. We built a convolution neural network with the contact force for real-time texture classification and haptic rendering. The neural network was constructed from the contact force between the force-torque sensor and sliding physical texture samples with three wavelengths. Once the classifier is constructed and if the force-torque sensor moves over a texture, the classified texture is mapped to a sinusoidal source signal generated with a DAQ board. We mapped the textures with the wavelengths of 3.14, 6.28, and 9.42 mm into sinusoids with the frequency of 150, 100 and 50 Hz. Then, the source signal is amplified and drives a piezoelectric actuator installed on a user's forearm, to provide a vibrotactile stimulus corresponding to the sensed texture.

Keywords: Texture classification · Convolutional neural network · Lateral sliding

1 Introduction

One of the grand goals for biomedical engineers is to develop a prosthetic hand which can provide the functionality and the sensation as good as the amputee's real hand. Most of the current prosthetic hands use surface electromyogram (EMG) signals from muscles on the forearm to accurately detect the amputee's intention and to enable him/her to make dexterous hand motion. However, lacking sensory feedback about proprioceptive information significantly impedes the usage of the prosthetic hand and often leads the amputee to discontinue the usage of the prosthesis [1–3]. Therefore, various methods have been proposed to provide an amputee's prosthetic limbs with tactile feedback [4–6]. However, there are only a few commercially available myoelectric (EMG-controlled) prosthetic hands providing a user with sensory feedback [3]. Especially, it is hard to find previous efforts to provide the user with fine surface information e.g. textures, of an object, sensed with the prosthetic hand with cutaneous feedback [6].

This paper describes a system converting textures sensed with a force-torque sensor into vibrotactile signals for sensory substitution, in real time. The sensed texture samples are classified with a neural network algorithm and mapped to a vibratory signal.

The technique described in this paper can be used for a prosthetic hand, and if the finger slides over a textured surface, a vibratory signal corresponding to the texture is given to an amputee, substituting the cutaneous information with the vibratory signal.

2 Construction of Texture Classifier and Mapping Textures into Vibrotactile Stimuli

In this section, we describe the method to classify physical surface texture samples. The contact force data is measured and processed with a convolution neural network algorithm, which is used to identify input texture for haptic rendering of the texture into vibrotactile stimuli.

2.1 Texture Sample Training Setup

We built a surface texture training setup that can control the two components, the magnitude of force and velocity during sliding over a texture (Fig. 1 (a)). In the system, a deformable hemispheric 3-axis force sensor (Optoforce OMD-20-SE-40 N, $17 \times 25 \times 25$ mm, Onrobot.Inc) measures the contact force with the surface texture.
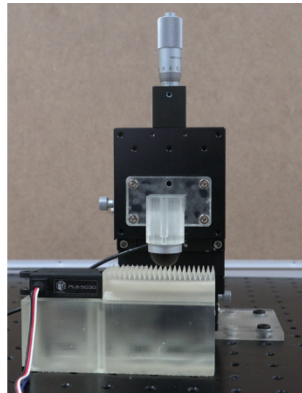
(a) Texture sample training setup. A physical surface texture sample slides over a linear stage and a force-torque sensor records the contact force data.

$\lambda = 3.14$ mm $\lambda = 6.28$ mm $\lambda = 9.42$ mm
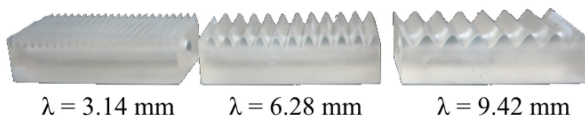
(b) Three physical surface texture samples used for the training with the wave length λ.

Fig. 1. Texture sample training setup and the physical surface texture samples.

The sensitivity of force measurement is 2.5 mN, and the data sample rate is 1000 Hz. A manual XYZ translational stage controls the magnitude of the contact force by adjusting a high-precision micrometer head. The linear stage is fixed on an aluminum alloy breadboard to minimize possible vibration due to the contact between the force sensor and the texture sample.

According to a study by Fishel and Loeb, the magnitude of force and velocity are the most definitive parameters of sliding motion during texture exploration [7]. We used three surface texture samples to acquire the data for texture learning with a neural network algorithm. The texture samples have three wavelengths (3.14, 6.28, and 9.42 mm) and a uniform peak-to-peak amplitude of 5 mm (Fig. 1(b)). A linear motor (PLS-5030, PoteNit. Inc.) moves the texture sample during the learning to create a lateral sliding movement. The linear motor moves with the maximum speed of 14 mm/s and is controlled with a UART communication.

2.2 Surface Texture Classification with CNN

We used a convolution neural network (CNN) algorithm to build a classifier of input texture sensed with a force sensor. The contact force data for the three texture samples were obtained from the lateral sliding movement of the textures. During the measurement, the height of the force sensor was fixed by adjusting the height of the linear stage. The velocity of the lateral sliding movement was fixed at 14 mm/s.

The force data were collected ten times for each texture sample. We measured the force sensor data by sliding surface texture samples and passed it to a low pass filter with the cut-off frequency of 15 Hz, which was input to the CNN. 70% of the measured force data was used as a training set, and 30% of the data was used as a test set to verify the performance of the trained CNN. Figure 2 shows the structure of the neural network consisting of total four layers. The input layer is an eight by eight image consisting comprised of preprocessed force sensor data. Each pixel on the image represents the magnitude of the acquired force data. The second is a convolution layer consisting of 32 filters in three by three size, where a rectified linear unit (ReLU) was used as an activation function. The third layer is another convolution layer comprised of 64 filters in three by three size with a ReLU as an activation function, as is for the second layer. The last layer consists of a fully-connected layer. Considering that the size of the image
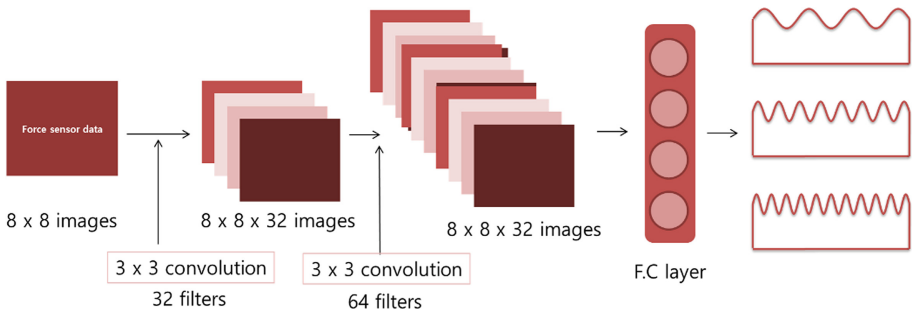
Fig. 2. Configuration of convolutional neural network used to build a texture classifier.

in the input layer is small, we did not use the max pooling layer, which is generally used for a CNN. We used the Tensorflow (Google Inc., U.S.A.) to construct a CNN, which is a most commonly used machine learning library.

2.3 Mapping Sensed Textures into Vibrotactile Stimuli

Figure 3 shows the overall structure of our system mapping sensed texture into a vibratory signal, in real time. Once the texture classifier is constructed, the force signal data from input texture is classified as learned instantly. Then, the classified texture is converted to a vibratory signal with a corresponding frequency, considering that a uniform force profile is generated from a specific texture when the contact force and the lateral sliding velocity are constant. We mapped the textures with the wavelengths of 3.14, 6.18, and 9.42 mm into vibrations with the frequency of 50, 100 and 150 Hz, respectively. Once the texture is classified, a sinusoidal source signal with the corresponding frequency is generated with a DAQ board (Model 826, Sensoray Co., Inc, U.S.A) and sent to a custom-built piezo amplifier. Then, an insulated piezoelectric actuator (a 9-mm ceramic disk mounted concentrically on a 12-mm metal disk; Murata, Inc., Japan) is driven to provide the user the texture sensed by the force sensor. Assuming the use of our proposed technique for a hand/finger amputee, we install the piezoelectric actuator on the surface of a user's forearm.
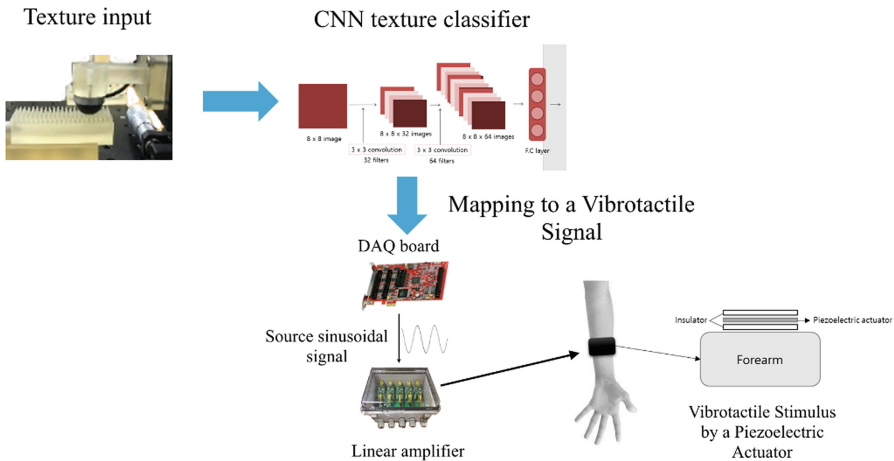
Fig. 3. Overall structure of the system mapping sensed textures into vibratory signals.

3 Conclusion

This paper proposes a system that classifies a real surface texture sample and converts into a vibratory signal in real time. This system can be used for a prosthetic hand that lets an amputee feel texture with a vibratory signal. We are planning to conduct sets of human subject experiments testing the participants' ability to discriminate between

different texture stimuli given only vibratory texture information. Also, we will examine the validity of our proposed method for an object grasp task with a robotic/prosthetic hand driven with EMG signal. Also, we will examine the validity of our proposed method for an object grasp task with a prosthetic hand with surface textures having shorter wavelengths than the ones used in the present paper.

References

1. Wright, T.W., Hagen, A.D., Wood, M.B.: Prosthetic usage in major upper extremity amputations. J. Hand Surg. **20**(4), 619–622 (1995)
2. Lundborg, G., Rosen, B.: Sensory substitution in prosthesis. Hand Clin. **17**(3), 481–488 (2001)
3. Schofield, J.S., Evans, K.R., Carey, J.P., Herbert, J.S.: Applications of sensory feedback in motorized upper extremity prosthesis: a review. Expert Rev. Med. Devices **11**(5), 499–511 (2014)
4. Kim, K., Colgate, J.E., Santos-Munne, J.J., Makhlin, A., Peshkin, M.A.: On the design of miniature haptic devices for upper extremity prosthetics. IEEE Trans. Mechatron. **15**(1), 27–39 (2010)
5. Kim, K., Colgate, J.E.: Haptic feedback enhances grip force control of sEMG-controlled prosthetic hands in targeted reinnervation amputees. IEEE Trans. Neural Syst. Rehabil. Eng. **20**(6), 798–805 (2012)
6. Antfolk, C., D'Alonzo, M., Rosén, B., Lundborg, G., Sebelius, F., Cipriani, C.: Sensory feedback in upper limb prosthetics. Expert Rev. Med. Devices **10**(1), 45–54 (2013)
7. Fishel, J.A., Loeb, G.E.: Bayesian exploration for intelligent identification of textures. Front. Neurorobotics **6**, 1–4 (2012)

Novel Devices

Hapto-Band: Wristband Haptic Device Conveying Information

Makiko Azuma$^{(\boxtimes)}$, Takuya Handa , Toshihiro Shimizu,
and Satoru Kondo

NHK (Japan Broadcasting Corporation),
1-10-11 Kinuta, Setagaya-ku, Tokyo, Japan
azuma.m-ia@nhk.or.jp

Abstract. We have developed a wristband haptic device called Hapto-band to intuitively convey various pieces of information such as ball direction and player actions in sports. Hapto-band has the advantage that it keeps both hands free and puts less burden on the user's body even when enjoying content for a long time. This device has four vibration actuators that are controlled wirelessly. When the user wears Hapto-band on the wrist, the four vibration actuators are in contact with four positions of the wrist, and various pieces of information can be conveyed by changing the vibration position and the vibration type. In this study, we developed a demonstration system to communicate information about player actions, such as serving/receiving, and the trajectory of the ball in volleyball games to the user via tactile sense by using Hapto-band, and we conducted an experiment to evaluate the effectiveness of using this device to convey player actions in sports.

Keywords: Haptic · Vibration · Universal design · Wearable

1 Introduction

We aim to intuitively convey changes and movements in videos, such as the ball direction and player actions in sports, via tactile sense. The cubic haptic device we have developed up to now [1] presents vibration stimulus to the user's fingertips, which are highly sensitive tactile sense areas. This cubic device has a mechanism for independently vibrating each face of the cube to convey information by changing the face to be vibrated depending on the information type. In an evaluation experiment on this device, we found it was easy for participants to distinguish the vibrating face when they pressed their fingertips against the face. On the other hand, some visually impaired participants gave the opinion that it was tiring to always grasp the device when enjoying content for a long time. In prior studies where information was transmitted by vibration without grasping the device by hand, multiple vibration boxes were attached separately to the head to present the direction [2], however, this device used one vibration actuator in each box. In another study, vibration stimuli were presented synchronously with the content by controlling vibration devices attached to the user's whole body, as used in the "Synesthesia Suit" [3]. This system is large and is controlled by wire, so it takes time for the user to put it on.

In this study, we aimed to develop a wristband device that keeps both hands free and puts less burden on the user's body even when enjoying content for a long time. Therefore, we have developed a wristband haptic device called Hapto-band, which has multiple vibration actuators controlled wirelessly to transmit detailed information. The device presents a vibration stimulus to the user's wrist. We used a wristband device because it is relatively easy to wear and it is possible to use two coordinate systems by using both wrists to convey more information.

The Apple watch [4] is an example of a device that transmits information by presenting vibration stimuli to the wrist. Such a device transmits information by presenting several types of vibration stimuli, but one vibration stimulus is always presented from the same one place because the entire housing vibrates.

Hapto-band has specifications such that the vibration actuator is in contact with four positions of the wrist, and it is possible to transmit various kinds of information by changing the position of the vibration stimulus and the vibration type of each actuator.

We devised a demonstration system using Hapto-band to transmit player actions, such as serving and receiving, and the trajectory of the ball in volleyball games to the user via tactile sense and conducted an experiment to evaluate the effectiveness of the device.

2   Demonstration Systems with Hapto-Band

2.1   Hapto-Band Details

When the user wears Hapto-band, the four vibration actuators are in contact with four positions of the wrist. The band wrapped around the wrist is made of cloth. Velcro tape is attached to the underside of the band, and the position of each actuator can be adjusted according to the target stimulus position and the user's wrist thickness. Figure 1 shows an example case in which four actuators are in contact with four positions of the wrist (up, down, left, and right as seen from the user's side). A Haptic$^{\text{TM}}$ reactor (Alps Electric Co., Ltd.) [5], which vibrates when a sound signal is input and can give various feelings of touch, is used for the actuator. Also, to alleviate the discomfort caused by the actuator's edge pressing into the skin, a resin plate was bonded to the actuator so that the plate is sandwiched between the actuator and the skin. The actuator controller is in a resin box through which the band of cloth passes, and the box and actuators are worn on the wrist.

The device is controlled with a PC. The PC transmits two kinds of signal: one is for ON/OFF communication of the actuator and the other is a sound signal that is input to the actuator. To make it easy for the user to handle the device, communication between the actuators and the PC is performed wirelessly. A wireless microcomputer is used for ON/OFF communication. A MONOSTICK on the PC side and TWELITE on the device side (both are made by Mono Wireless Inc.) are used. To communicate sound signals, a Bluetooth-compatible transmitter on the PC side and a Bluetooth-compatible receiver on the device side are used. The controller box of the Hapto-band includes a control circuit with a wireless microcomputer (TWELITE), Bluetooth-compatible receiver for receiving the sound signal, and amplifier to amplify the sound signal.

A lithium polymer battery is also included in this box. Since the weight of the device is about 108 g, which is equivalent to that of an ordinary wristwatch, fatigue while wearing the device is considered to be mild.
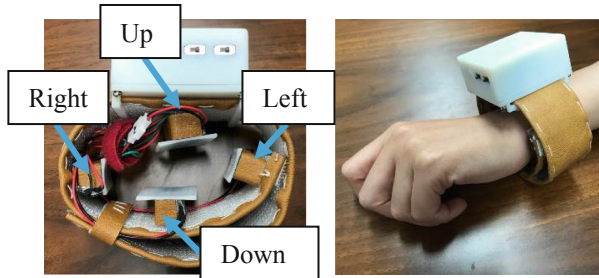
Fig. 1. Overview of Hapto-band

2.2   System Configuration

Figure 2 shows the outline of the system configuration when information is transmitted with Hapto-band.

First, a video of a ball game such as volleyball is input to the video analysis unit, the position of the ball is analyzed for each frame, and the vectors of velocity and acceleration are calculated. Based on these results, the playing side of the court and the type of event (serving, receiving, etc.) are judged, and the device control unit controls the haptic device to present the vibration stimulus corresponding to the judgment. For the video analysis unit, we will use object tracking technology developed by Takahashi et al. [6] and so on in future work. In this study, we developed the device control unit and the haptic device.
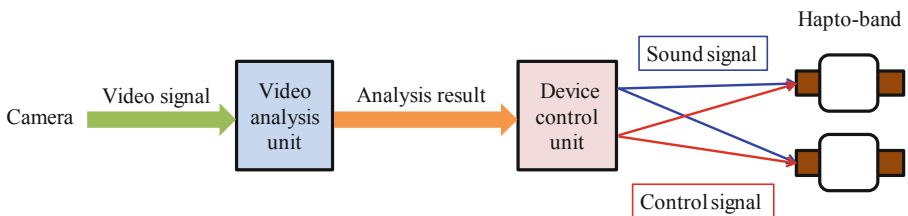
Fig. 2. System configuration overview

3   Evaluation Experiment

3.1   Method
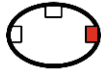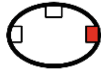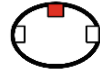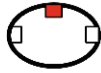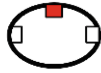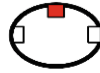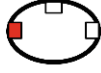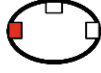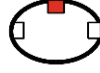
We conducted an experiment to evaluate the effectiveness of information transmission using Hapto-band.

The three participants were visually impaired, and each participant wore a Hapto-band on the left wrist. In this experiment, we assumed information transmission for volleyball games and presented vibration expressing four kinds of events: serving, receiving, "out", and "in". We aimed for intuitive expressions that are easy to understand; up to three of the four actuators (up, left, right as seen from the participant's side) were used for expressing each event.

In the experiment, the participants were asked what kind of event happened after a vibration was presented. The vibration is presented in accordance with the following three conditions. Condition 1 is the presentation position of the vibration and the type of the vibration (sound signal), which varies depending on the type of event, Condition 2 is only the presentation position of the vibration varies depending on the type of event and the type of vibration (sound signal) is always the same, and Condition 3 is only the type of vibration (sound signal) changes depending on the type of event and the presentation position of the vibration is always the same. Table 1 shows what kind of vibration stimulus was presented for each type of event. We presented the vibration 20 times (4 events × 5 times) under each of the three conditions, and the participants practiced several times before each experiment under each condition. Although the order of presenting the event was random for each condition, the order of events was the same for the participants.

After the experiment, we interviewed the participants about using Hapto-band.

Table 1. Stimulus presentation method

		Condition 1	Condition 2	Condition 3
Serving	Position			
	Sound	Pattern 1	Pattern 0	Pattern 1
Receiving	Position			
	Sound	Pattern 2	Pattern 0	Pattern 2
Out	Position			
	Sound	Pattern 3	Pattern 0	Pattern 3
In	Position			
	Sound	Pattern 4	Pattern 0	Pattern 4

Note that view of wrist is as seen from participant's side. Red actuator vibrates.

All procedures performed in studies involving human participants were in accordance with the ethical standards of the institutional committee and with the 1964 Helsinki declaration and its later amendments or comparable ethical standards. Informed consent was obtained from all individual participants included in the study.

3.2   Results

Figure 3 shows the results. Regarding the average correct answer rate, the same result was obtained for Condition 1, where both the position of the vibration presentation and the vibration (sound signal) were different, and Condition 3, where only the vibration (sound signal) was different, which is a high correct answer rate. On the other hand, the correct answer rate of Condition 2, where only the vibration presentation position was different, was lower than the correct answer rates of Condition 1 and 3.
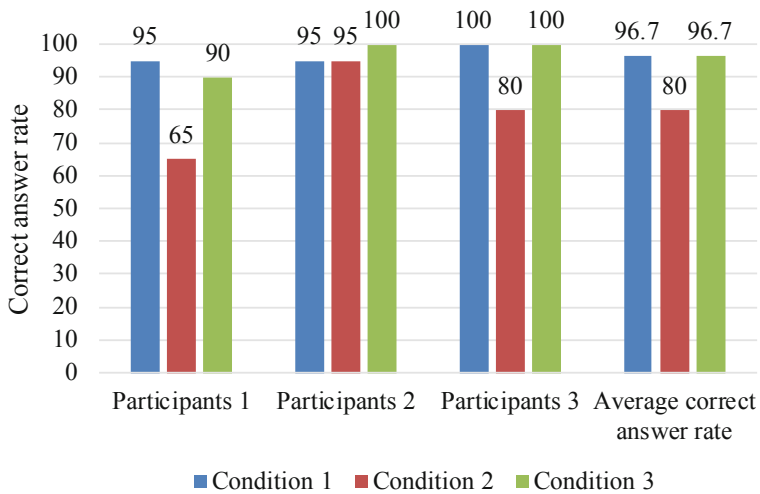
Fig. 3. Results (correct answer rate)

3.3   Discussion

In the interview after the experiment, all participants answered that Condition 1, where both the position of the vibration presentation and the vibration (sound signal) were different, is most easily understandable. There was also an opinion that the presentation positions in Condition 1 and 2 are intuitive expressions that are easy to understand. As the sound was generated by the vibration of the actuator in the experiment, there was an opinion that under Condition 1 and 3, where the sound signal was different depending on the event, it was easy to distinguish the event by listening to the sound in addition to the difference in vibration. However, all participants said it was difficult to distinguish the event by only the sound when people were around or in a noisy environment.

As expected, the correct answer rate and the interview result show that it is easiest for participants to understand under Condition 1, so this method is considered to be the most effective. The correct answer rate is as high as 96.7%, suggesting that Condition 1 is effective for information transmission using Hapto-band. On the other hand, there was an opinion that some sound signals used for vibration presentation were hard to detect.

Ideally, different sound signals that generate vibrations that are easy to detect should be prepared, and there should be a wide range of choice.

4   Conclusion

We have developed a wristband haptic device called Hapto-band, which has four vibration actuators in contact with four positions of the wrist (up, down, left, and right) to intuitively convey various pieces of information such as ball direction and player actions in sports. It was suggested that intuitive and easy-to-understand information transmission is possible by changing the presentation position of vibration and the vibration type depending on the event that occurred. For future work, we will consider the sound signal to use based on the opinions received and will conduct a comprehension evaluation experiment for the progress of a volleyball game using Hapto-band.

References

1. Azuma, M., Handa, T., Shimizu, T., Kondo, S.: Development of vibration cube to convey information by haptic stimuli. In: 25th International Display Workshop, pp. 128–130. ITE, Sendai (2017)
2. Ariza, O., Lange, M., Steinicke, F., Bruder, G.: Vibrotactile assistance for user guidance towards selection targets in VR and the cognitive resources involved. In: IEEE Symposium on 3DUI (2017)
3. Konishi, Y., Hanamitsu, N., Minamizawa, K., Sato, A., Mizuguchi, T.: Synesthesia suit: the full body immersive experience. In: Special Interest Group on Computer Graphics and Interactive Techniques Conference VR Village Proceedings, SIGGRAPH 2016, Anaheim, USA, p. 1 (2016)
4. https://www.apple.com/ca/accessibility/watch/
5. HAPTIC is registered as a trademark in Japan, China, and the European Union (JP4619342/JP5471286, CN4730821/CN4730822/CN4730823, CTM4399606) and is used in commerce as a trademark in the United States, being enforceable under common law. https://www.alps.com/prod/info/E/HTML/Haptic/
6. Takahashi, M., Ikeya, K., Kano, M., Okubo, H., Mishina, T.: Robust volleyball tracking system using multi-view cameras. In: Proceedings of 23rd International Conference on Pattern Recognition, WePT.9, pp. 2741–2746 (2016)

A Surface Texture Display for Flexible Virtual Objects

Lei Lu[1,2], Yuru Zhang[1,2], Xingwei Guo[1,2], and Dangxiao Wang[1,2(✉)]

[1] State Key Lab of Virtual Reality Technology and Systems,
Beihang University, Beijing 100191, China
`hapticwang@buaa.edu.cn`
[2] Beijing Advanced Innovation Center for Biomedical Engineering,
Beihang University, Beijing 100191, China

Abstract. This paper presents a tactile device for displaying surface texture of flexible virtual objects. The texture is simulated using electrovibration effect produced by a flexible film. The deformation of the film is controlled by a DC motor to generate desired softness according to applied finger force. A prototype of the device is developed and integrated with a virtual environment. We show the application of the display using an online shopping scenario.

Keywords: Tactile device · Electrovibration · Flexible object ·
Texture display · Softness display

1 Introduction

Tactile devices are utilized to provide user with tactile stimulus. Thus far, a wide range of tactile devices have been developed to simulate different tactile feedback. In recent years, tactile devices that can provide multimodal tactile feedback have gained increased interests [1–4]. A few devices presenting softness and texture have been developed. Bianchi used two motors to control the deformation and vibration of an elastic fabric for simulating softness and texture [5]. Nakamura combined a deformable pad with a rigid texture display based on electrovibration effect for simulating softness and texture [6].

In this paper, we present a new tactile device for displaying softness and texture. The texture is simulated using a flexible texture display and the deformation of the display is controlled by a DC motor to generate desired softness according to applied finger force. By controlling the deformation of the flexible electrostatic display, a large range of softness can be simulated as compared to the existing device using rigid texture display. We developed a prototype of the device and integrated it with a virtual environment to verify the function of the display.

2   System Design

Figure 1 shows the schematics of the tactile device. Texture sensation is simulated by FlexTouch, a flexible film described in [7] (Fig. 2). The flexible film is composed of three layers including a base layer, a conducting layer and an insulating layer. When the conducting layer is excited with a periodic voltage, an electrostatic force appears between the insulating layer and a sliding finger. The friction F_f increases with the electrostatic force F_e, which depends on the input voltage v, i.e.

$$F_f = \mu F_e(v) \tag{1}$$

where μ is the friction coefficient.
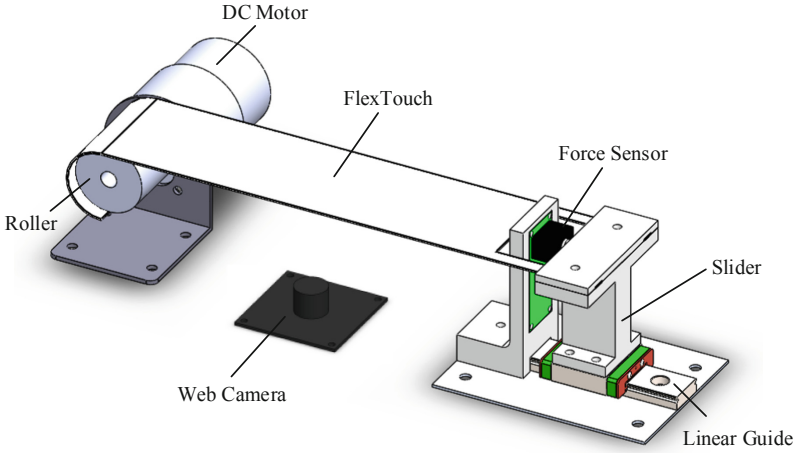
Fig. 1. Schematics of the tactile device

To simulate different textures, the input voltage is altered according to finger position which is detected using a web camera.

Softness sensation can be divided into kinesthetic softness and cutaneous softness [8]. The device presented in this paper generates only kinesthetic softness. The displayed stiffness is

$$k = \frac{F_n}{\Delta z} \tag{2}$$

where F_n is the normal force applied by the finger and Δz is the vertical displacement of the film. The desired stiffness is achieved by measuring the normal force and controlling the displacement accordingly.

PEN, $0.12mm$
Conductive layer, ITO, $180nm$
Insulator, resin, $5\mu m$

F_e

F_f

Motion direction

Tactile Stimulus

Control and display
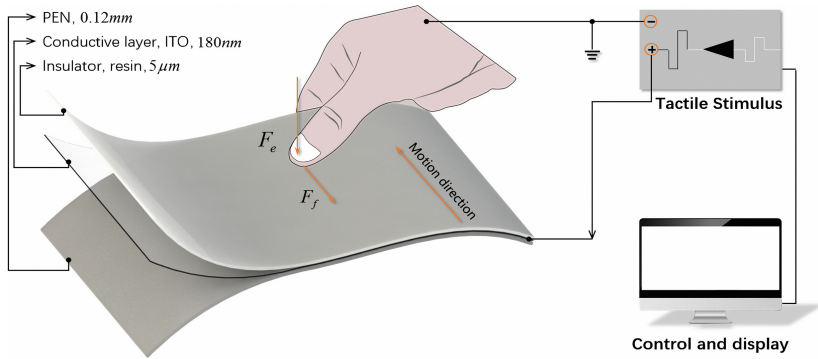
Fig. 2. Working principle of FlexTouch [7]

3 Prototyping

Figure 3 shows a prototype of the tactile device. The right end of the film is connected to a 3D-printed slider, which is mounted on a linear guide (MGW7C, HIWIN Technologies Corp., Taiwan). A one-dimensional force sensor (FSG015WNPB, Honeywell International Inc., USA) is placed against the slider. To support the force sensor, a 3D-printed bracket is adopted. A piece of fabric is connected between the left end of the film and the roller driven by a DC motor (Minibalance, China). The DC motor is equipped with a relative magnetic encoder. A web camera (with a resolution of 1280×720) is mounted on the base of the device beneath the film to detect finger position.

DC Motor

FlexTouch

Force Sensor

Roller

Slider

Linear Guide

Web Camera
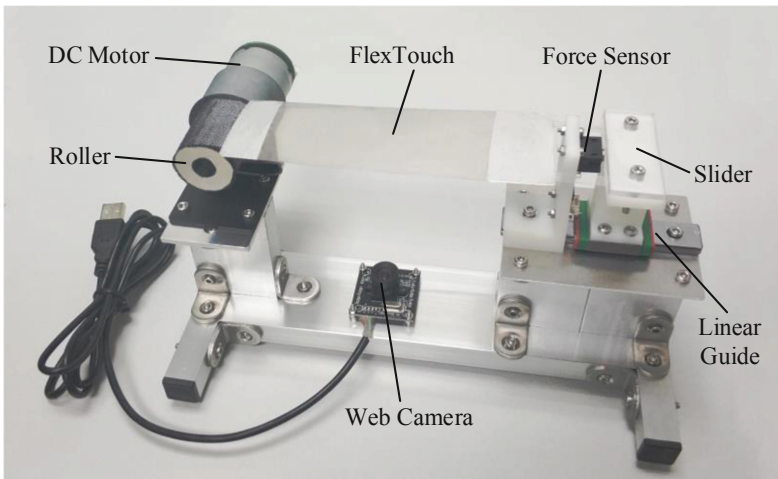
Fig. 3. Prototype of the tactile device

OpenCV computer vision library is used to develop the algorithm of finger position detection. The input voltage for the film is generated by a DSP platform and a custom designed amplification circuit. A microcontroller board (Arduino Mega 2560, Italy) is used to process the input data of the force sensor and control the motor position accordingly.

4   Example Application

An online shopping scenario shown in Fig. 4 is constructed utilizing Unity game engine. The user can control the virtual hand to explore surfaces of different flexible virtual objects in the scenario. Two kinds of gesture are supported in the exploring process, i.e., sliding finger horizontally to perceive texture and pressing finger vertically to perceive softness.
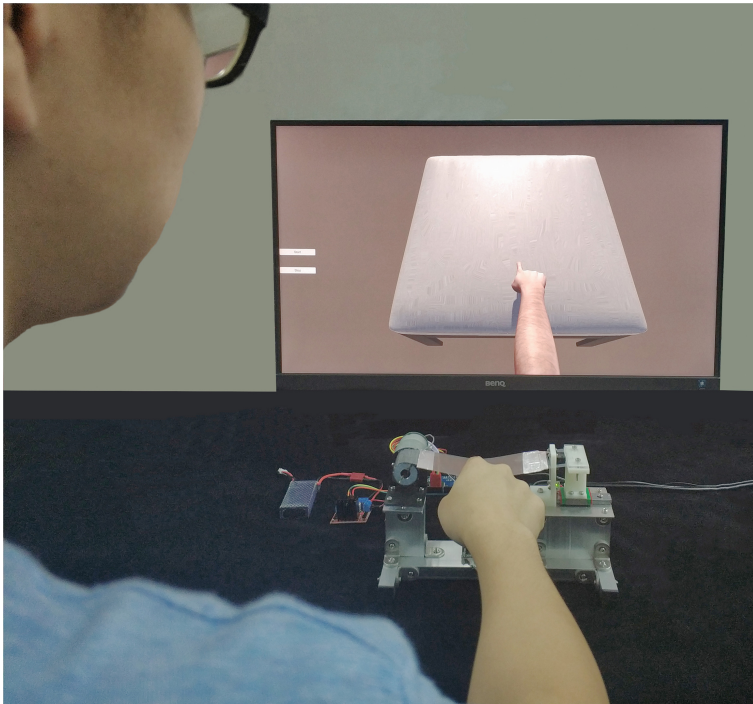
Fig. 4. Feel the texture and softness of an online product

5   Conclusion

We have presented a tactile device for displaying surface texture of flexible virtual objects. The device was implemented and integrated with a virtual environment. An online shopping scenario was demonstrated. The preliminary result shows that the device is able to simulate texture and softness of flexible virtual objects. The estimated displayed stiffness ranges from 0.1 N/mm to 2 N/mm. We expect this device can enhance users' experience in broad applications of virtual reality.

References

1. Nakamura, T., Yem, V., Kajimoto, H.: Hapbelt: haptic display for presenting vibrotactile and force sense using belt-winding mechanism. In: SIGGRAPH Asia 2017 Emerging Technologies, pp. 1–2 (2017)
2. Yem, V., Kajimoto, H.: A fingertip glove with motor rotational acceleration enables stiffness perception when grasping a virtual object. In: International Conference on Human Interface and the Management of Information, pp. 463–473 (2018)
3. Hashizume, S., Takazawa, K., Koike, A., Ochiai, Y.: Cross-field haptics: tactile device combined with magnetic and electrostatic fields for push-pull haptics. In: SIGGRAPH ASIA 2016 Emerging Technologies, p. 13 (2016)
4. Murakami, T., Person, T., Fernando, C.L., Minamizawa, K.: Altered touch: miniature haptic display with force, thermal and tactile feedback for augmented haptics. In: ACM SIGGRAPH 2017 Emerging Technologies, p. 2 (2017)
5. Bianchi, M., Poggiani, M., Serio, A., Bicchi, A.: A novel tactile display for softness and texture rendering in tele-operation tasks. In: World Haptics Conference, pp. 49–56 (2015)
6. Nakamura, T., Yamamoto, A.: Extension of an electrostatic visuo-haptic display to provide softness sensation. In: Haptic Symposium, pp. 78–83 (2016)
7. Guo, X., Zhang, Y., Wang, D., Jiao, J.: Absolute and discrimination thresholds of a flexible texture display. In: World Haptics Conference, pp. 269–274.(2017)
8. Tiest, W.M.B., Kappers, A.M.L.: Cues for haptic perception of compliance. IEEE Trans. Haptics **2**, 189–199 (2009)

Enhancing Haptic Experience in a Seat with Two-DoF Buttock Skin Stretch

Arata Horie[✉], Akito Nomura, Kenjiro Tadakuma, Masashi Konyo, Hikaru Nagano, and Satoshi Tadokoro

Graduate School of Information Sciences, Tohoku University,
6-6-01 Aramaki Aza Aoba, Aoba-ku, Sendai-shi, Miyagi 980-8579, Japan
{horie.arata,konyo}@rm.is.tohoku.ac.jp

Abstract. We propose a buttock skin stretch device that adopts a two-degree-of-freedom horizontal movement mechanism. We have confirmed that an acceleration sensation of self-motion can be induced by a buttock skin stretch device with one degree of freedom. In this paper, we propose a two-degree-of-freedom buttock skin deforming device that extends the direction of skin deformation, which was only in the left and right directions, to the forward and backward directions. We focused on the range of motion, position accuracy, and driving speed, and evaluated the performance of the device as a buttock skin-deforming device.

Keywords: Skin stretch device · Force perception ·
Self-motion perception · Buttock skin

1 Introduction

A method for presenting direction and shear force by shear deformation of the skin is known. Heretofore, methods for shear deforming the skin of the finger pads and arms have been proposed to present a sense of force to the fingertip and induce the posture of the arm [1–3].

We have proposed a method to shear deform the buttock skin with one degree of freedom [4]. This method differs from the conventional method of skin deformation in two points, namely that the buttocks are used as the target part of the skin deformation and the aim is to induce a sense of self-motion. By applying the method of skin shear deformation, acceleration sensation of self-motion is induced, which originally requires a large-scale motion platform [5] by using a compact and simple mechanism.

Although the proposed method has one degree of freedom, it could present the acceleration in the shoulder width direction, but not the acceleration in the forward and backward directions.

When riding on a moving vehicle, the forward and backward directions of a human are often the traveling direction. Therefore, presenting the acceleration in the forward and backward directions in humans is considered an important issue in reproducing the feeling of moving in the space by using a moving vehicle.

Fig. 1. Buttock skin stretch display placing on a chair

In this study, we propose a buttock skin stretch device that applies two-degree-of-freedom skin shear deformation to the buttocks and evaluate the performance of the device.

2   Two-Degree-of-Freedom Buttock Skin Stretch Device

2.1   Device Design

We developed a haptic device to shear deform the skin of the left and right buttocks with two degrees of freedom. We show the appearance of device we developed in Fig. 1. A user sits on the device and receives stimulus on the buttocks. Two sponge contactors are placed on the top of the device to deform part of the skin of the buttocks.

The mechanism inside the device is shown in Fig. 2. The two red parts are screws driven by different motors. Blue mounts can be independently slid by red screws. The green shaft and green plate are fixed, and the relative positions of the shafts are not changed and fixed at an angle of 90°. The blue mount and green shaft are connected by the linear bush, and the relative position between the mount and shaft is changed by sliding the shaft. When the two blue mounts move to the left and right while maintaining the distance, the green shaft and upper plate move to the left and right. When the distance between the two blue mounts changes, the slide of the linear bush moves the green shaft and upper plate back and forth.

2.2   Device Specifications

Distance of Movement. The range of movement in the left-right and forward-back directions was designed as 40 mm, which is considered to be a sufficiently
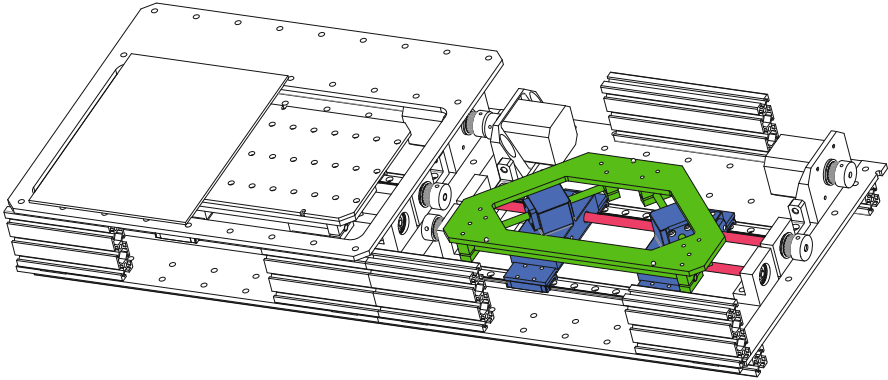
Fig. 2. The mechanism of two degree of freedom movement

large displacement to handle skin deformation while avoiding slippage. The movable range can be expanded by the size of the contactor and arrangement of parts supporting the buttocks.

Accuracy of Movement. The accuracy of the moving distance is determined by the driving method of the stepper motor (P-PMSA-U42D3, Shinano Kenshi). To drive the stepper motor at the maximum speed, we set the resolution to one step of $1.8°$. In that case, the moving distance of the contactor per step is $16\,\mu$m, which is considered to be sufficiently high in handling skin deformations

Speed of Movement. The speed depends on the frequency of the pulse generated by the microcontroller (Arm, Mbed) and the driving method of the stepper motor. A pulse frequency of $1\,$kHz and a step angle per pulse of the stepper motor of $1.8°$ confirm that the contactor moves at $16\,$mm/s. The frequency of the pulse in this device is set to $1\,$kHz. At a frequency higher than this, a stepout due to a high acceleration and excessive heat generation of the motor were confirmed.

3   Demonstration

The demonstration setup is shown in Fig. 3. In the demonstration, acceleration/deceleration, centrifugal force at the time of curving, and inclination of the roll and pitch angles of the car body are presented at the driving simulator.

The driving simulator was built with Unity (Unity Technologies) and calculates the acceleration of two directions and the angle of the car. It sends the information to the device and deform the buttock skin.
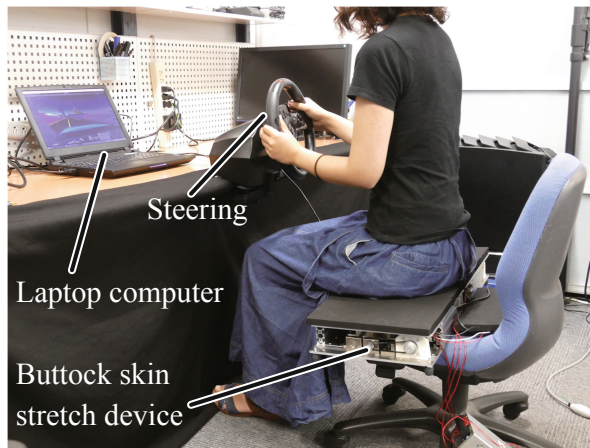
Fig. 3. Demonstration setup

4 Conclusion

We propose a buttock skin deforming device that adopts a two-degree-of-freedom horizontal movement mechanism. The device presented a skin deformation of 40 mm at the front-back and left-right directions. Its accuracy was 16 µm and speed was 16 mm/s. The proposed device was suggested to have sufficient performance to function as a skin-deforming device.

As a demonstration of the effectiveness of the device, we proposed a driving simu lator. The device can reproduce acceleration/deceleration, centrifugal force at the time of curving, and inclinations of the roll and pitch angles of the car body.

There was no participant involved subjective study.

References

1. Gleeson, B.T., Horschel, S.K., Provancher, W.R.: Perception of direction for applied tangential skin displacement: effects of speed, displacement, and repetition. IEEE Trans. Haptics **3**(3), 177–188 (2010)
2. Minamizawa, K., Fukamachi, S., Kajimoto, H., Kawakami, N., Tachi, S.: Gravity grabber: wearable haptic display to present virtual mass sensation. In: ACM SIG-GRAPH 2007 Emerging Technologies, p. 8. ACM (2007)
3. Chinello, F., Pacchierotti, C., Tsagarakis, N.G., Prattichizzo, D.: Design of a wearable skin stretch cutaneous device for the upper limb. In: 2016 IEEE Haptics Symposium (HAPTICS), pp. 14–20. IEEE (2016)

4. Horie, A., Nagano, H., Konyo, M., Tadokoro, S.: Buttock skin stretch: inducing shear force perception and acceleration illusion on self-motion perception. In: International Conference on Human Haptic Sensing and Touch Enabled Computer Applications, Springer, Heidelberg, pp. 135–147 (2018)
5. Tadokoro, S., Murao, Y., Hiller, M., Murata, R., Kohkawa, H., Matsushima, T.: A motion base with 6-DoF by parallel cable drive architecture. IEEE/ASME Trans. Mechatron. **7**(2), 115–123 (2002)

Stiffness Perception of Virtual Objects Using FOLDAWAY-Touch

Marco Salerno, Stefano Mintchev[✉], Alexandre Cherpillod,
Simone Scaduto, and Jamie Paik

Reconfigurable Robotics Laboratory, EPFL, Lausanne, Switzerland
stefano.mintchev@epfl.ch

Abstract. Haptic human interfaces are nowadays becoming more and more diffused also thanks to their combined use with Virtual Reality & Augmented Reality (VR & AR). Although many research platforms explore kinesthetic interaction with virtual objects, the only feedback available in widespread commercial devices is a rather simple vibration.

In this paper we introduce "FOLDWAY-Touch" a novel portable kinesthetic haptic interface whose technology can be easily integrated into hand-held devices. The key technological aspect is the miniaturization of the haptic mechanism achieved through the use of origami design and manufacturing principles. Another achievement of this paper is the use of FOLDAWAY-Touch in a virtual simulation to grasp objects with different levels of stiffness.

Keywords: Force feedback · Virtual reality · Origami

1 Introduction

Haptic human interfaces can be broadly categorized based on the type of feedback, either tactile or kinesthetic [1]. Most of the commercial haptic interfaces rely on tactile feedback generated by miniature vibration motors that elicits the mechanoreceptors in users' skin. While small and affordable, vibrotactile actuators are well suited for user-interface notifications, but fairly limited in conveying a sense of shape, force, or surface structure [2, 3]. For example, most of the commercial hand-held joysticks for VR (e.g. Oculus Touch, HTC Vive, and PlayStation Move) produce unrealistic vibrations to simulate the manipulation of objects. On the contrary, kinesthetic haptic interfaces can render forces that are perceived by users' muscles and joints. In virtual reality, high fidelity force feedback has been investigated through actuated gloves [4] and stationary robotic arms [5–9]. The latter are also available as commercial products for medical and recreational applications. However, while these products offer realistic force feedback, they are bulky and expensive. For expanding the potential market of kinesthetic haptics, major technological steps in miniaturization, portability and usability are necessary [10]. By addressing these challenges, kinesthetic haptic devices would become a viable solution for the integration of force feedback in handheld devices and in portable electronic apparels in use in our everyday life.

Within the Foldaway haptics project, we investigate new design and manufacturing solutions inspired by origami for haptics. The goal is to integrate force feedback for

users' fingers into devices with dimensions comparable to those of commercially available joysticks for VR.

Here we present "FOLDAWAY-Touch", a joystick capable of rendering a wide range of stiffness under the thumb of the user. The device can be held by the user in his hand and can be used in a VR simulation as illustrated in Fig. 1. In this paper we: (i) introduce "FOLDAWAY-Touch" joystick; and (ii) present a preliminary demonstration of FOLDAWAY-Touch for the manipulation of virtual objects.

Fig. 1. A user grasping a virtual object with FOLDAWAY-Touch portable joystick.

2   Materials and Methods

In this section we present an overview of FOLDAWAY-Touch main components, the accessory hardware employed for conducting tests in VR, and a description of the execution of the tests.

2.1   Hardware Description

FOLDAWAY-Touch joystick comprises the following main components: the handle, the Vive™ Tracker for localization, the haptic motorized parallel platform and cables for powering and sensory data transfer (see Fig. 2). The parallel platform, inspired by the Canfield joint [11], is placed under the thumb of the user. It replaces the classic gimbal mechanism found in commercial joysticks. In addition to pitch and roll rotations, with a range of motion of $\pm20°$, the mechanism can also be pressed like a button, with a range of motion of 35 mm. As illustrated in [11], the parallel platform is implemented with origami micromachining for ease of miniaturization and manufacturing.

The rotation of each of the three links at the base of the mechanism is tracked with a hall-effect sensor with an accuracy of 0.05°. Each link is also connected through bevel gears to a backdrivable DC motor (Maxon DCX08M DC motor with a planetary reduction stage of 1:32). The origami parallel platform, hall-effect sensors and motors are integrated inside the handle of the joystick. The electronics for the impedance control of the device works at a frequency of 1 kHz and allows to render different level of stiffness when the parallel platform is pressed by the thumb of the user. The electronics is connected to the joystick with a tether for data and power exchange. Experimental measurements showed that the haptic device can render stiffness in the range between 0.02 and 1.2 N/mm and can apply forces up to 2 N with an average power consumption of 1 W.
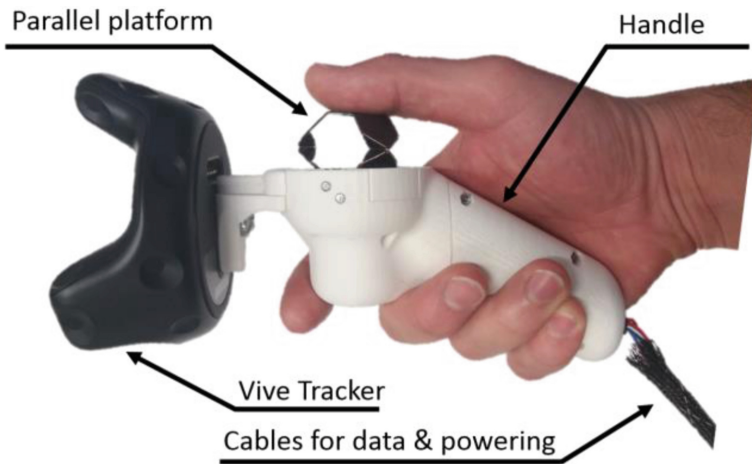
Fig. 2. FOLDAWAY-Touch haptic interface. The main components of the joystick are: the parallel platform implemented with origami micromachining, the Vive™ Tracker, the handle and the cables for data and powering. The hall-effect sensors to track the position of the parallel platform and the actuators for force rendering are integrated in the main body of the joystick. The electronic board for impedance control is connected via a tether.

2.2   Manipulation of Virtual Objects

The joystick is interfaced with the VR environment using the HTC Vive development kit (HTC, Taiwan) and software framework based on Unity (Unity, US, Ca). This setup allows to track and map the users' hand into the virtual word as illustrated in Fig. 1. The user can grasp virtual objects by pressing its thumb on the interface that reacts by applying a force to simulate the contact with objects and their stiffness (Fig. 1).

In our demonstration, the user is first invited to wear the VR equipment consisting in HTC Vive googles and holding the FOLDAWAY-Touch haptic interface in his right hand. Multiple spherical objects are placed on a table in VR environment and random spring constant, color and position are assigned to them (Fig. 3). The task to solve consists in:
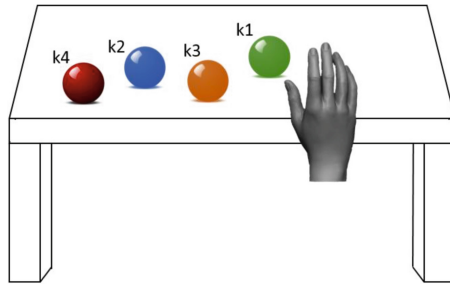
Fig. 3. Example of a task execution where the objects that the user has to classify are randomized in position, color and stiffness values.

- Grasping each object sequentially
- Ordering them according to increasing stiffness
- Execute 3 to 5 repetitions decreasing the stiffness difference between the objects

Task execution time and success rate are the data collected during the tests with users. From pilot tests we concluded that users can better discriminate between soft objects (average stiffness 0.3 N/mm) rather than between rigid ones (average stiffness 0.9 N/mm). The difficulties encountered in the discrimination of rigid objects is most probably caused by the limited range of motion of the device for high stiffness values due to motor saturation. High reduction motors in synergy with an admittance force rendering strategy would increase the maximum achievable displacement at peak force at the expense of a more complex sensing and control architecture.

3   Conclusions

Origami micromachining allows to develop ultra-portable and low-cost kinesthetic interfaces that can be integrated into portable devices. For example, FOLDAWAY-Touch leverage on origami design principles to replace the conventional gimbal found in joysticks with a 3 DoF force feedback interface. The force rendering capabilities have been exploited to make the interaction with virtual objects more realistic, enabling stiffness perception. Future versions of FOLDAWAY-Touch would require improvements to our current implementation. Although all mechatronic components are integrated inside the joystick, our device is still tethered for communication and power supply. Incorporating wireless communication and integrating a lithium polymer battery would enable fully untethered operation. With a 3.7 V 500 mAh li-po battery, the controller would run for at least one hour. Although the device can apply forces to the fingertips, other types of haptic feedback could be added to the device. For example, vibrotactile actuators to render contact with objects or texture, and Peltier elements to render heat/cold sensation. Finally, current implementation is composed of an origami mechanism with external sensors and actuators for control. An integrated solution where sensors and actuators are laminated inside origami mechanism [12] would allow to further reduce size and manufacturing costs.

Ethical Approval: All procedures performed in studies involving human participants were in accordance with the ethical standards of the institutional and/or national research committee and with the 1964 Helsinki declaration and its later amendments or comparable ethical standards.

Informed Consent: Informed consent was obtained from all individual participants included in the study.

References

1. Culbertson, H., Schorr, S.B., Okamura, A.M.: Haptics: the present and future of artificial touch sensations. Annu. Rev. Control Robot. Auton. Syst. **1**, 385–409 (2018)
2. Rekimoto, J.: Traxion: a tactile interaction device with virtual force sensation. In: Symposium on User Interface Software and Technology, pp. 427–431 (2013)
3. Kyung, K.U., Lee, J.Y.: Ubi-Pen: a haptic interface with texture and vibrotactile display. IEEE Comput. Graph. Appl. **29**(1), 56–64 (2009)
4. Bouzit, M., Popescu, G., Burdea, G., Boian, R.: The Rutgers Master II-ND force feedback glove. In: Proceedings - 10th Symposium on Haptic Interfaces for Virtual Environment and Teleoperator Systems, HAPTICS 2002, pp. 145–152 (2002)
5. Massie, T.H., Salisbury, J.K.: The PHANTOM haptic interface: a device for probing virtual objects. In: ASME Winter Annual Meeting, Symposium on Haptic Interfaces for Virtual Environment and Teleoperator Systems, vol. 55, pp. 1–6 (1994)
6. Novint Falcon, Novint Technologies Inc. http://www.novint.com/index.php/novintfalcon. Accessed 8 Jan 2018
7. Haption Virtuose 6D. https://www.haption.com/fr/products-fr.html. Accessed 8 Jan 2018
8. Omega. 3, Force Dimension. www.forcedimension.com/products. Accessed 8 Jan 2018
9. Van Der Linde, R., Lammertse, P., Frederiksen, E., Ruiter, B.: The HapticMaster, a new high-performance haptic interface. In: Proceedings of the EuroHaptic, Edinburgh, UK, pp. 1–5 (2002)
10. Benko, H., Holz, C., Sinclair, M., Ofek, E.: NormalTouch and TextureTouch. In: Proceedings of the 29th Annual Symposium on User Interface Software and Technology - UIST 2016, pp. 717–728 (2016)
11. Salerno, M., Zhang, K., Menciassi, A., Dai, J.S.: A novel 4-DOF origami grasper with an SMA-actuation system for minimally invasive surgery. IEEE Trans. Robot. **32**, 484–498 (2016)
12. Salerno, M., Firouzeh, A., Paik, J.: A low profile electromagnetic actuator design and model for an origami parallel platform. J. Mech. Robot. **9**, 41005–41011 (2017)

Using Wearable Haptics for Thermal Discrimination in Virtual Reality Scenarios

Guido Gioioso[1]([✉]), Maria Pozzi[1,2] [iD], Mirko Aurilio[2] [iD], Biagio Peccerillo[1] [iD], Giovanni Spagnoletti[1] [iD], and Domenico Prattichizzo[1,2] [iD]

[1] Department of Information Engineering and Mathematics, University of Siena, Siena, Italy
{gioioso,pozzi,peccerillo,spagnoletti,prattichizzo}@diism.unisi.it
[2] Advanced Robotics Department, Istituto Italiano di Tecnologia, Genoa, Italy
mirko.aurilio@iit.it
https://www.diism.unisi.it,
https://www.iit.it/research/lines/advanced-robotics

Abstract. Towards a more realistic feeling of interacting with virtual and remote objects, we developed a wearable cutaneous device for the proximal finger phalanx able to provide skin deformations and thermal cues on the user skin. A servomotor is used to move a belt applying a pressure on the user finger, while a Peltier cell renders thermal cues. In the proposed hands-on demonstration, a user wears such haptic ring and a VR headset, and interacts with a virtual environment. In the virtual scenario, objects with different temperatures are displayed and the user is asked to find the coldest or the hottest. During the interaction, the movements of the user hand are tracked by a Leap Motion sensor, while the haptic ring renders interaction forces and thermal cues, providing the user with the sensation of touching objects in the scene at different temperatures.

Keywords: Thermal feedback · Wearable haptics · Virtual Reality · Haptic ring

1 Introduction

The global wearable electronics market is forecast to grow at a compound annual growth rate (CAGR) of 23.30% during the period 2018–2022 [1]. Currently, off-the-shelf wearable devices provide limited haptic sensations, mainly focusing on vibro-tactile feedback. In this paper, we introduce a novel cutaneous device that can be worn on the proximal finger phalanx and is capable of providing skin deformations and thermal cues on the user skin. Such haptic ring proves effective in enhancing user experience during the interaction with virtual objects.

Thermal perception enriches human sense of touch with cues that help in discriminating the material composition of objects. Studying receptive fields,

location, and perceived temperature ranges of the skin receptors, called thermoreceptors, that mediate such stimuli, is fundamental for designing thermal displays [6]. One of the first tactile interfaces including thermal modules is a glove for teleoperation developed in 1993 [2]. Several thermal displays have been proposed since then [5]. Most of them embed Peltier devices to simulate different temperatures, and have been tested in psychophysical experiments where participants are asked to discriminate materials based on thermal cues [4].

There is an increasing interest in developing tactile displays for Virtual Reality and Augmented Reality environments [10]. In [7] a wearable interface providing force and thermal feedback to subject's finger has been realized. The device uses PWM-driven DC motors to generate haptic stimuli and a Peltier module placed in contact with the fingernail.

A non-wearable vibro-thermal interface has been instead developed in [8]. The system uses a set of thermal modules composed of couples of Peltier cells. One couple is used during heating phase and the other during cooling phase. This solution has been adopted in order to enable fast changes of temperature during the transition from heating to cooling phase and viceversa.

The device proposed in this paper embeds a servomotor that moves a belt applying a pressure on the user finger (similarly to [9]), and a Peltier cell that renders thermal cues (similarly to [3]). Its main advantage resides in having an on-board cooling system, that is controlled so to ensure both, good performance (comparable with human thermal perception) and stability of the device. As explained in Sect. 3, it can be used to enhance user experience during the interaction with a Virtual Reality scenario.

2   Haptic Ring

The proposed haptic ring weighs 21 g and is positioned on the proximal finger phalanx of the user, so to improve the capability of this device to be used together with unobtrusive hand tracking systems, such as the LeapMotion controller and the Kinect sensor. It is composed of a static upper body located on the nail of the finger, and a mobile end-effector that is in contact with the finger pad (Fig. 1). The upper body contains a small servomotor. A belt is attached to the motor pulley and connects the two parts. In this way, the platform is able to move towards or away from the finger. This motion allows to provide a variable pressure directly to the user's skin, thus recreating the sensation of making and breaking contact with virtual objects. The mobile platform can displace vertically up to 5 mm, and can deliver a normal force up to 5 N. Besides, it houses a $13 \times 13 \times 3.8$ mm Peltier cell[1] (Adaptive® Thermal Management, European Thermodynamics Limited) and its cooling system, represented by a $15 \times 15 \times 3$ mm fan[2] (Sunonwealth Electric Machine Industry Co., Ltd.).

---

[1] Peltier cell datasheet: docs-emea.rs-online.com/webdocs/144a/0900766b8144a996.pdf.
[2] Fan datasheet: www.sunon.com/pro2_page.php?pkid=8.
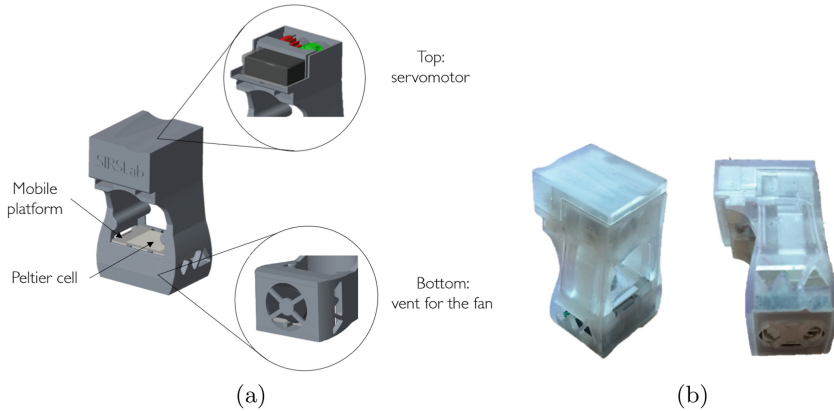
Fig. 1. Wearable haptic ring able to provide cutaneous force feedback and thermal cues: (a) 3D model, (b) real device.

The ring is connected to a wrist bracelet housing the controller and the driver for the Peltier cell. The communication with the controller is wireless, thanks to two XBee® RF modules (Digi International Inc.)[3].

3 Virtual Reality Game

As shown in Fig. 2, in the proposed demonstration a user wears an Oculus Rift (Oculus VR, LLC) and a haptic ring to interact with a virtual scenario implemented using the game engine Unity (Unity Technologies). User's hand movements are tracked by a Leap Motion sensor (mounted on the headset), while the haptic ring renders cutaneous force feedback and thermal cues, providing the user with the sensation of touching objects in the scene at different temperatures.

The virtual scenario reproduces a kitchen (Fig. 3). In the first part of the Virtual Reality experience, three bottles (Fig. 3a) are shown to the user, that is asked to choose the coldest. Then, three cups (Fig. 3c) are presented to the user, that is asked to choose the hottest. Once the choice is made, the game shows a green tick for correct answers and a red cross for wrong answers (Figs. 3b and d).

For the preliminary tests of the device, informed consent was obtained from all individual participants.

---

[3] XBee modules datasheet: www.sparkfun.com/datasheets/Wireless/Zigbee/XBee-Datasheet.pdf.
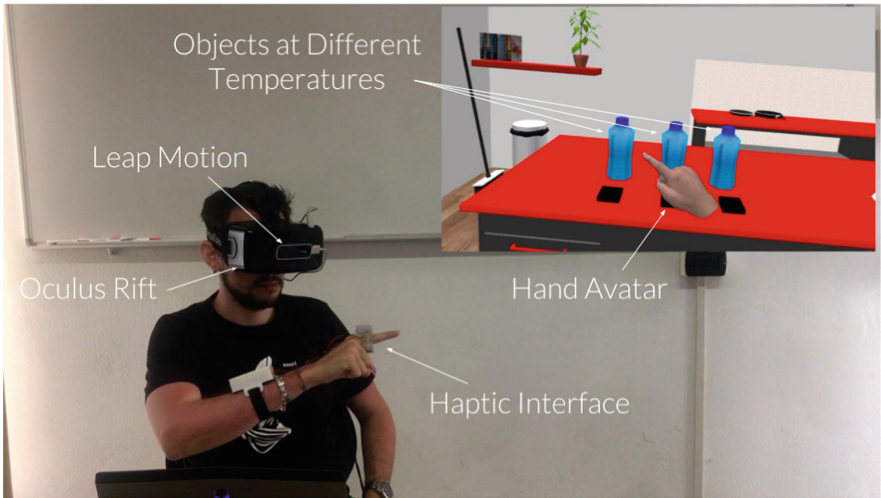
Fig. 2. Hands-on demonstration setup.

(a)

(b)

(c)

(d)
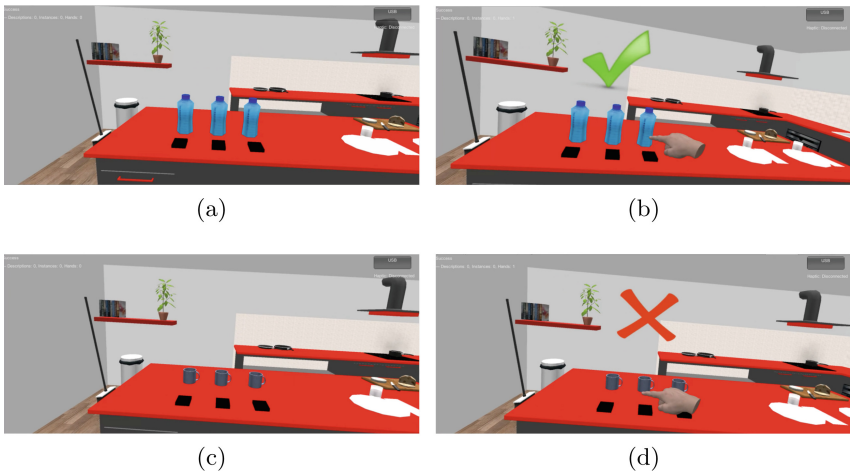
Fig. 3. Game in Virtual Reality. (a), (b) The user is asked to choose the coldest among three bottles. (c), (d) The user is asked to choose the hottest among three cups. The system displays a green tick if the answer is correct or a red cross if the answer is wrong.

References

1. Global wearable electronics market 2018–2022. https://www.researchandmarkets.com/research/qqb4tm/global_wearable?w=5. Accessed 1 Aug 2018
2. Caldwell, D.G., Gosney, C.: Enhanced tactile feedback (tele-taction) using a multifunctional sensory system. In: 1993 Proceedings IEEE International Conference on Robotics and Automation, vol. 1, pp. 955–960, May 1993
3. Gabardi, M., Leonardis, D., Solazzi, M., Frisoli, A.: Development of a miniaturized thermal module designed for integration in a wearable haptic device. In: 2018 IEEE Haptics Symposium (HAPTICS), pp. 100–105, March 2018
4. Ho, H.-N., Jones, L.A.: Contribution of thermal cues to material discrimination and localization. Percept. Psychophys. **68**(1), 118–128 (2006)
5. Jones, L.A., Ho, H.: Warm or cool, large or small? The challenge of thermal displays. IEEE Trans. Haptics **1**(1), 53–70 (2008)
6. Jones, L.: Thermal touch. In: Prescott, T., Ahissar, E., Izhikevich, E. (eds.) Scholarpedia of Touch, pp. 257–262. Atlantis Press, Paris (2016)
7. Murakami, T., Person, T., Fernando, C.L., Minamizawa, K.: Altered touch: miniature haptic display with force, thermal and tactile feedback for augmented haptics. In: ACM SIGGRAPH 2017 Emerging Technologies, p. 2. ACM (2017)
8. Nakatani, M., Sato, K., Sato, K., Kawana, Y., Takai, D., Minamizawa, K., Tachi, S.: A novel multimodal tactile module that can provide vibro-thermal feedback. In: International AsiaHaptics Conference, pp. 437–443. Springer (2016)
9. Pacchierotti, C., Salvietti, G., Hussain, I., Meli, L., Prattichizzo, D.: The hRing: a wearable haptic device to avoid occlusions in hand tracking. In: 2016 IEEE Haptics Symposium (HAPTICS), pp. 134–139, April 2016
10. Spagnoletti, G., Meli, L., Baldi, T.L., Gioioso, G., Pacchierotti, C., Prattichizzo, D.: Rendering of pressure and textures using wearable haptics in immersive VR environments. In: 2018 IEEE Conference on Virtual Reality and 3D User Interfaces (VR), vol. 00, pp. 691–692, March 2018

LinkGlide: A Wearable Haptic Display with Inverted Five-Bar Linkages for Delivering Multi-contact and Multi-modal Tactile Stimuli

Miguel Altamirano Cabrera[(✉)] and Dzmitry Tsetserukou[(✉)]

Skolkovo Institute of Science and Technology (Skoltech), Moscow 121205, Russia
miguel.cabrera@skoltech.ru, d.tsetserukou@skoltech.ru

Abstract. LinkGlide is a novel wearable palm-worn tactile display to deliver multicontact and multimodal stimuli at the user's palm. The array of inverted five-bar linkages generate three independent contact points to cover the whole palm area. The independent contact points allow to control different patterns in each of the points and provide multimodal tactile feedback, such as slippage, force vector, pressure, temperature, and vibration. With this novel haptic device, we can potentially achieve a highly immersive VR experience and make it more interactive.

Keywords: Haptic device · Multimodal stimuli ·
Multicontact stimuli · Virtual reality · Wearable display

1 Introduction

The large touch-sensitive area of the human palm plays a relevant role in the detection and handling of objects in daily life. An increasing number of VR/AR technologies are present nowadays in the market and are used for many different applications, e.g., simulators, and games. To achieve a highly immersive VR experience, it is needed to deliver multimodal stimuli at the user's palm, such as slippage, force vector, pressure, temperature, and vibration. The multicontact points allow to cover a bigger area of the palm and to provide stimuli in different positions at the same time.

A few wearable displays for VR reality that deliver the sensation of contact, gripping, gravity, and inertia to the single point of user's fingers have been proposed in [1,2]. In contrast to one single point, multicontact stimuli allow to cover a bigger area of, e.g., palm, and generate stimuli at different points simultaneously. Multicontact stimuli to present a surface undulation to the hand was proposed by [4], where the stimuli were provided only on the fingers of the users and not on the palm. The authors [6] introduced a wearable haptic interface to

---

The original version of this chapter was revised: The given name and surname of the first author were corrected. The correction to this chapter is available at https://doi.org/10.1007/978-981-13-3194-7_74
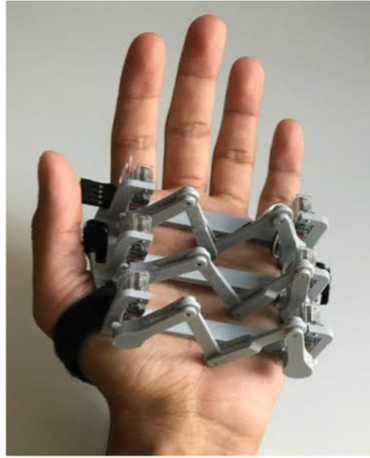
Fig. 1. A novel wearable haptic display *LinkGlide.*

provide torque feedback simulating the object weight sensation (single modality). To achieve a highly immersive experience in VR, the presented patterns should be similar to the experiencing the real object: contact state, size, weight, temperature, texture, stiffness, moving sensation. Up until now, there is not a wearable tactile display that provides multimodal and multicontact stimuli at the palm.

LinkGlide (see Fig. 1) is a novel palm-worn haptic display to provide multimodal and multicontact tactile stimuli at the palm of the user. *LinkGlide* consists of three 2-DoF LinkTouch devices [5] distributed in parallel planes to produce the sliding force and the contact state on the skin. Two servo motors of each LinkTouch device control the planar position between palm and linkage tip. Therefore, three dynamic contact points are created to deliver multimodal stimuli. The schematic and 3D CAD model are shown in Fig. 2(a) and (b), respectively.
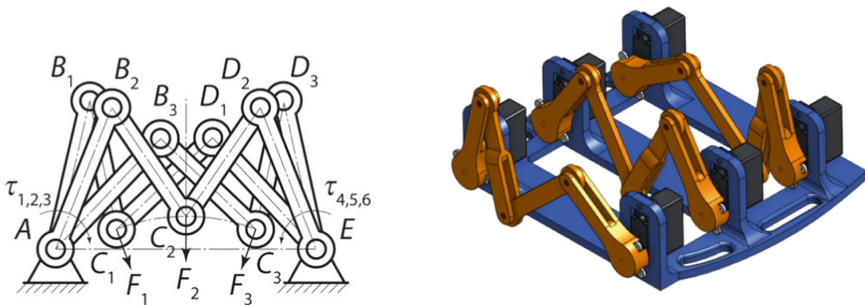
Fig. 2. (a) Schematic of *LinkGlide* robot; (b) 3D CAD model.

2 Design and Applications

The *LinkGlide* device provides the sense of touch at three different points in the palm of the user where multimodal stimuli are provided. The proposed device is based on LinkTouch technology [5]. The array of inverted five-bar linkages generates independent contact points covering the whole palm area. Each one of the contact points can be supplied by a vibration motor, a force sensor, and a Peltier element to provide independent multimodal stimuli. The independent control of the inverted five-bar linkages allows to generate different patterns at the user's palm and to move in different directions to simulate the detection and handling of objects, providing different force vector in each point. The current version consists of three LinkTouch devices, which can be modified according to the *LinkGlide* application.

The device has been provided with a TDK MPU-9250 Nine-axis (Gyro + Accelerometer + Compass) to calculate the movement and posture of the palm for integration in VR applications. The *LinkGlide* characteristics are listed in Table 1.

Table 1. Characteristics of LinkGlide.

Motors	Hitec HS-35HD
Weight	70 g
Material	PLA
Max. normal force at each contact point	4 N
Gyroscope	TDK MPU-9250 Nine-axis

LinkGlide can be used in the NurseSim [3] application (see Fig. 3) which was designed to teach nurses the proper posture to avoid musculoskeletal disorders.
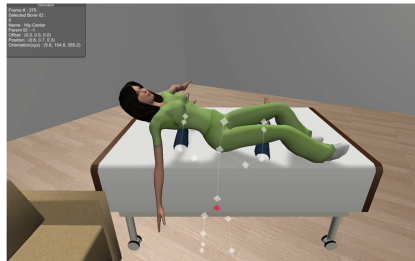
Fig. 3. NurseSim application.

The nurse trainee learns how to carry the patients who are disabled properly and safely using VR simulator. The training task in simulator includes appropriately lifting and gently transporting the patient up to the wheelchair or bed.

In order not to harm a virtual patient during the transportation, tactile feedback is necessary. The sensation of contact with the body, weight (by the cutaneous stimulus), slippage of the patient body, temperature, and texture of the clothes can be potentially presented by *LinkGlide*. When the person starts feeling the slippage of the patient in the hands, they fix the posture of arms to compensate the gravity action and avoid thus the drop of the patient.

The application BallFeel (see Fig. 4(a)) is designed to demonstrate how *LinkGlide* accurately presents the array of balls rolling on the palm. The position of each ball and its speed is presented by the independent unit of *LinkGlide*. RollFeel will demonstrate how to present the sensation of a solid cylinder rolling on the palm with haptic and visual feedback (see Fig. 4(a)). Figure 4(c) demonstrates application JumpFeel, where *LinkGlide* generates the feeling of bouncing a ball on the palm. The softness of the ball will be rendered by impedance control receiving the applied force from the touch sensor. The sensation of hand movement in VR is provided according to the posture and movement of the user's hand.
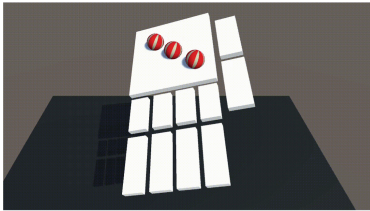
(a) Rolling of ball set on the hand.
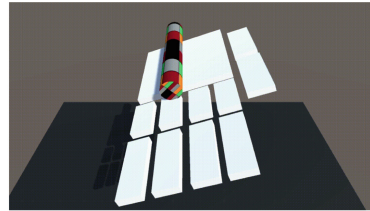
(b) Rolling of a cylinder in the hand.
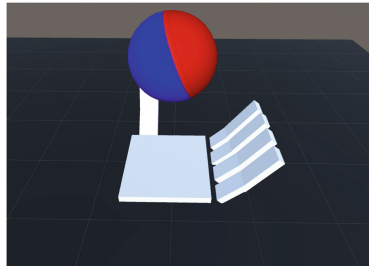
(c) Ball bouncing on the hand.

Fig. 4. The applications for the LinkGlide demonstration: (a) BallFeel; (b) RollFeel; (c) JumpFeel.

Other applications had been developed to demonstrate the multimodality of the device. CarFeel presents tactile sensation of moving car through palm (see Fig. 5) in different directions. During engine rev up or drifting, user will feel hot temperature generated by Peltier element. This will imitate the heat of engine and heat of tire friction. The vibration motors attached at the tip of linkages will

make user feel the engine roar. The very unique experience will be felt when car jumps over to another hand and user will have the continuous tactile sensation across both palms.
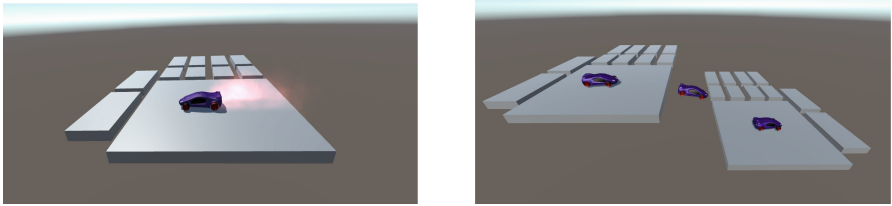
Fig. 5. The CarFeel application that generates the sensation of the car movement across palm.

The interaction with living creatures was taking into account in the development of the AnimalFeel application, where the motion of living creatures (e.g., animals, insects) can be reproduced by the haptic stimuli on the hand of the user. In Fig. 6, a spider walk is reproduced by the multicontact moving stimuli and by the vibration at the tips of the linkages.
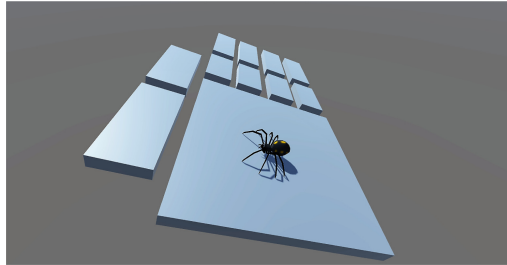
Fig. 6. The AnimalFeel application shows the interaction with spider crawling on the palm.

3   Conclusion

A novel wearable haptic device to provide multimodal (slippage, force vector, pressure, temperature, and vibration) and multicontact stimuli to the user's hand has been developed. Three sets of inverted five-bar linkages generate independent contact points. This haptic display can potentially achieve a highly immersive VR experience in medical simulators, navigation, and gaming with a new level of tactile fidelity.

References

1. Choi, I., Culbertson, H., Miller, M.R., Olwal, A., Follmer, S.: Grabity: a wearable haptic interface for simulating weight and grasping in virtual reality. In: Proceedings of the 30th Annual ACM Symposium on User Interface Software and Technology - UIST 2017, pp. 119–130 (2017). https://doi.org/10.1145/3126594.3126599, http://dl.acm.org/citation.cfm?doid=3126594.3126599

2. Choi, I., Hawkes, E.W., Christensen, D.L., Ploch, C.J., Follmer, S.: Wolverine: a wearable haptic interface for grasping in virtual reality. In: IEEE International Conference on Intelligent Robots and Systems, 2016 November, pp. 986–993 (2016). https://doi.org/10.1109/IROS.2016.7759169

3. Nakagawa, Y., Tsetserukou, D., Terashima, K.: Development of VR simulator for nurse training. In: AIP Conference Proceedings, vol. 29, pp. 29–39 (2014). https://doi.org/10.1063/1.4866615, http://aip.scitation.org/doi/abs/10.1063/1.4866615

4. Tanaka, Y., Goto, Y., Sano, A.: Haptic display of micro surface undulation based on discrete mechanical stimuli to whole fingers. Adv. Robot. **31**(4), 155–167 (2017). https://doi.org/10.1080/01691864.2016.1262790. https://www.tandfonline.com/doi/full/10.1080/01691864.2016.1262790

5. Tsetserukou, D., Hosokawa, S., Terashima, K.: Linktouch: a wearable haptic device with five-bar linkage mechanism for presentation of two-dof force feedback at the fingerpad. In: 2014 IEEE Haptics Symposium (HAPTICS), pp. 307–312, February 2014. https://doi.org/10.1109/HAPTICS.2014.6775473

6. Tsetserukou, D., Sato, K., Tachi, S.: ExoInterfaces: novel exoskeleton haptic interfaces for virtual reality, augmented sport and rehabilitation. In: Proceedings of the 1st Augmented Human International Conference, AH 2010, pp. 1:1–1:6. ACM, New York (2010). https://doi.org/10.1145/1785455.1785456, http://doi.acm.org/10.1145/1785455.1785456

Smart Bracelets to Represent Directions of Social Touch with Tactile Apparent Motion

Taku Hachisu[✉] and Kenji Suzuki

University of Tsukuba, Tsukuba, Ibaraki 3058573, Japan
hachisu@ai.iit.tsukuba.ac.jp, kenji@ieee.org

Abstract. We present a novel haptic interaction which represents a direction of social touch with a tactile apparent motion using a pair of smart bracelet devices. We define the direction as being from the hand actively touching to the hand passively touched. The device consists of a microcontroller, an acceleration sensor, an intra-body network module, and a vibrator. First, one device sends own acceleration data at the moment of physical contact with the other over wearers' hands (intra-body network). The other compares it to the own data, decides which one is actively touching or passively being touched, and sends the result to the partner device. Then, the devices drive the vibrators synchronizing the timing of the vibrations with each other according to our previously built model through the intra-body network. As a result, a tactile apparent motion is induced from the active to the passive. We aim that representing the direction provides awareness of the direction, which we expect to correct unilateral touch behavior.

Keywords: EnhancedTouch · Social touch · Tactile apparent motion · Vibrotactile feedback · Wearables

1 Introduction

Social touch is one of the most fundamental non-verbal communications. Midas touch effect, for example, has been demonstrated by Crusco and Wetzel [1], in which the ratio of the tip is increased by a server's touch to a customer. We are interested in quantifying and representing social touch in real time using wearable devices in order to investigate and facilitate the positive effect on social interaction in daily life. Thus far, we have developed a smart bracelet device, EnhancedTouch, which is capable of measuring when and who a user touches and illuminating according to a touch event [3].

This paper introduces a novel haptic interaction technique to represent a direction of touch with a tactile apparent motion (Fig. 1). We define the direction as being from one hand actively touching to the other passively being touched. The technique represents the direction with a tactile apparent motion [2], which is expected to provide awareness of the direction and to correct unilateral touch behavior.
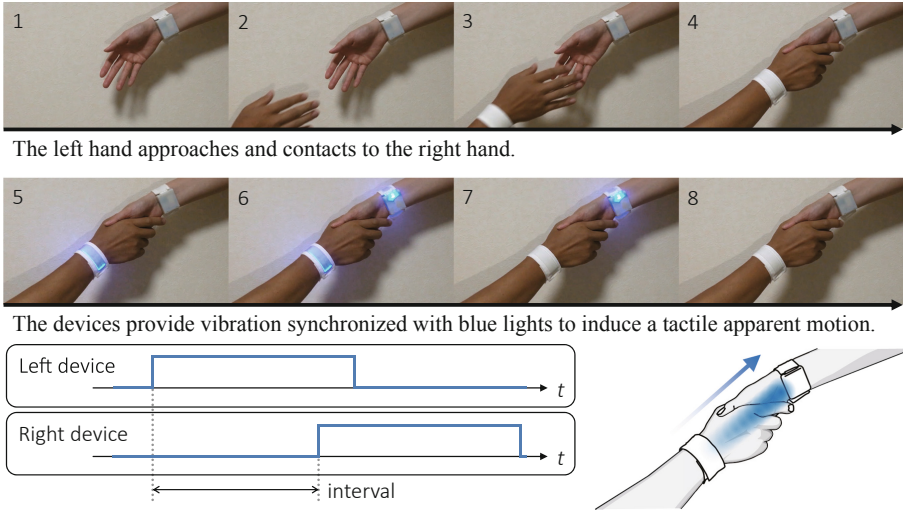
Fig. 1. Smart bracelets representing a direction of social touch (from the active to the passive) with a tactile apparent motion

2 Bracelet Device

We revised the EnhancedTouch device [3] to measure a direction and present a vibration. The revised device has an acceleration sensor and a vibrator. The device measures a touch event using intra-body network technology in which the device communicates with the partner device through electrical current following the hands when the two hand contact each other. In phase 4 of Fig. 1, the left device sends acceleration data at the moment of contact. The right device compares the received data with the own data. Because the own data is smaller, the right device identifies oneself as passive. Then, the right device sends a signal to tell the left device "you are active" through the intra-body network. Finally, the left device identifies oneself as active.

In phase 5–8 of Fig. 1, the devices provide vibrations with a specific interval to induce a tactile apparent motion from the active to the passive. The duration and interval of the vibrations are determined according to our previous study [2], that is, the duration is 240 ms while the interval is 120 ms. The devices communicate with each other through the intra-body network to synchronize the timing of the vibrations. The tactile apparent motion is repeatedly presented every one second until the end of the physical contact of the hands, that is, the disconnection of the network.

3   Conclusion

We introduced a novel haptic interaction which represents a direction of social touch with a tactile apparent motion using a pair of smart bracelet devices. In the future study, we will evaluate the method to measure the direction of touch by asking wearers the extent to which the measured directions match their subjective directions. Additionally, we plan to study the experience of the interaction using subjective and objective evaluations and to study the effect on social interaction.

There was no participate involved subjective study.

References

1. Crusco, A.H., Wetzel, C.G.: The midas touch: the effects of interpersonal touch on restaurant tipping. Pers. Soc. Psychol. Bull. **10**(4), 512–517 (1984)
2. Hachisu, T., Suzuki, K.: Tactile apparent motion through human-human physical touch. In: International Conference on Human Haptic Sensing and Touch Enabled Computer Applications, pp. 163–174. Springer, Cham (2018)
3. Suzuki, K., Hachisu, T., Iida, K.: Enhancedtouch: a smart bracelet for enhancing human-human physical touch. In: Proceedings of the 2016 CHI Conference on Human Factors in Computing Systems, CHI 2016, pp. 1282–1293. ACM, New York (2016). http://doi.acm.org/10.1145/2858036.2858439

Wearable Haptic Device that Presents the Haptics Sensation of the Finger Pad to the Forearm and Fingertip

Taha Moriyama$^{(\boxtimes)}$ and Hiroyuki Kajimoto$^{(\boxtimes)}$

University of Electro-Communications, 1-5-1 Choufugaoka, Chofu,
Tokyo 182-8585, Japan
{moriyama,kajimoto}@kaji-lab.jp

Abstract. Many methods have been proposed for presenting tactile sensations from objects in the virtual reality environment. In particular, many wearable tactile displays for the fingers, such as fingertip- mounted haptics display and glove-type haptics displays, have been developed. We developed a device that presents the haptic sensation of the fingertip to the fingers and to the forearm rather than only to the fingertip as a new haptic presentation method for virtual reality environment. The device adopts a vibrator on the fingertip to present positional and collisional information, and a five-bar linkage mechanism on the arm to present the strength and direction of force. Compared with fingertip-mounted haptic displays, combination of the two devices enables small size at the fingertip, yet direction of force can be expressed. Our preliminary test revealed that it is easily to associate the haptics sensation provided from the device to the forearm with their own fingertip.

Keywords: Virtual reality · Tactile displays · 5 bar-link mechanism · Vibration

1 Introduction

Many studies have attempted to present tactile information of the fingers in the virtual reality (VR) environment and many wearable tactile displays for the fingers, such as finger-type and glove type displays, have been proposed [1, 2]. However, the weight and size of the tactile displays typically hinder the free movement of the fingers, especially in the multi-fingers scenario. We have therefore proposed a method of presenting the haptic sensation of the fingertip, including the direction of force, to the forearm to address these issues.

When we manipulate an object, various kinds of tactile information are presented to the fingers. Among many sensory channels of the fingertips, one of the most important channels are those of the strength and direction of a force, which are indispensable information when manipulating object.

In our previous report, we developed a device using a five-bar link mechanism that presents information on the force, including the direction, perceived by the fingertip [3]. The top side of the forearm was found to be an appropriate part corresponding to

the index finger. Furthermore, by making the device correspond not only to the index finger but also to the thumb, it was possible to present a haptics sensation for the task of gripping and lifting object. We also conducted a user study, in which participants were asked to grip and lift an object in a VR environment. The result suggested that the use of the device can lead to an improvement in the realism. However, the comments from the users showed that training time was required to associate the haptic sensation provided from the device to the forearm with the haptics sensation of their fingertip.

To address this issue, we propose to attach small fingertip-mounted display using a vibrator, in combination with a five-bar linkage mechanism which presents the strength and direction of force to the forearm (Fig. 1). When touching an object in VR scene, haptics cue is given to the fingertip via vibrator for a short period of time. Then strength and directions of the force are given to the forearm.
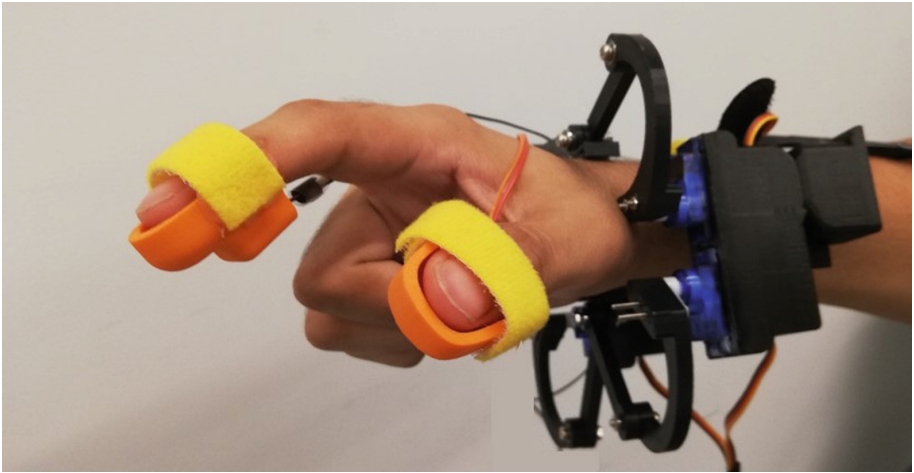
Fig. 1. Device design

2 System Design

The fingertip mounted device is made of acrylonitrile butadiene styrene injected by a three-dimensional printer. It embeds a small vibrator (13000 rpm) and it can be attached and detached using Velcro tape. The device for the forearm adopts a five-bar linkage mechanism, which, unlike the original structure, adopts an M-shaped structure. Tsetserukou proposed using this link mechanism for presenting the sensation of a force to the fingertip [4, 5] and to the palm. On the basis of this previous study, we have developed a device that can be worn on the forearm [3]. Two-degree-of-freedom (2DoF) movement can be achieved by controlling two servo motors. The parts that present the haptics sensation can move up and down (pressure sensation), left and right

(tangential friction sensation). The two devices are connected to a personal computer through a microcontroller (NXP mbed 1768). LeapMotion device was used for finger tracking (Figs. 2 and 3).
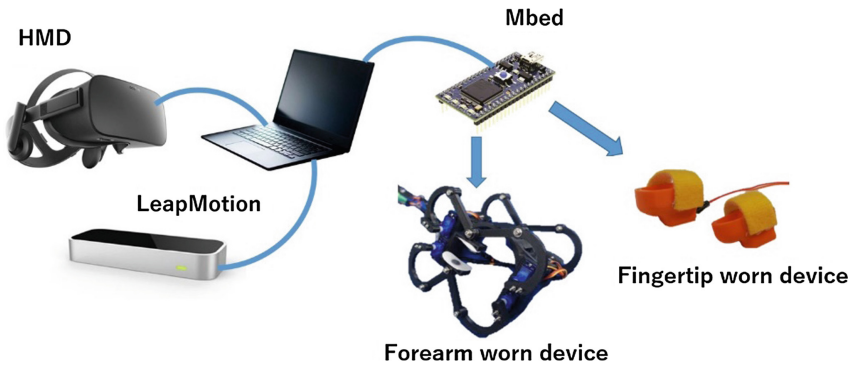
Fig. 2. System design
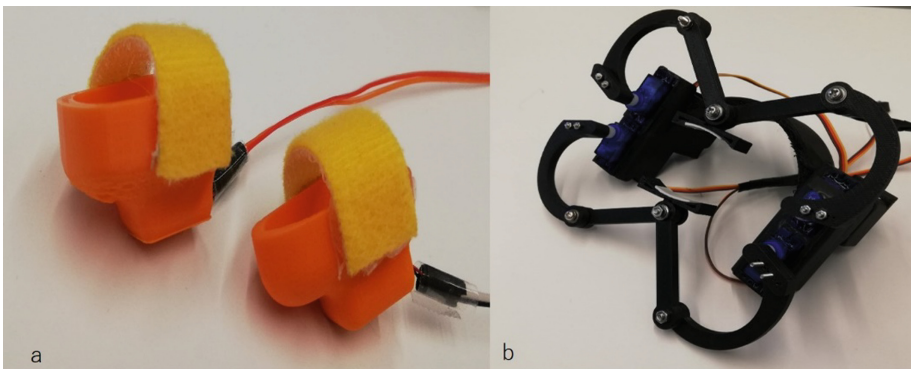
Fig. 3. Fingertip worn display (a); Forearm worn display (b)

3   User Experience

The following describes the user experience in our demonstration. Various objects were placed in VR space and users handled them using our developed devices. The presentation of vibration sensation to the finger is short time, and allows users to grasp which finger contacted and when the strength and directions of the force are expressed by the arm worn device. User can touch, grasp, and manipulate objects in VR scene, and tasks such as peg-in-hall is performed by the users (Fig. 4).
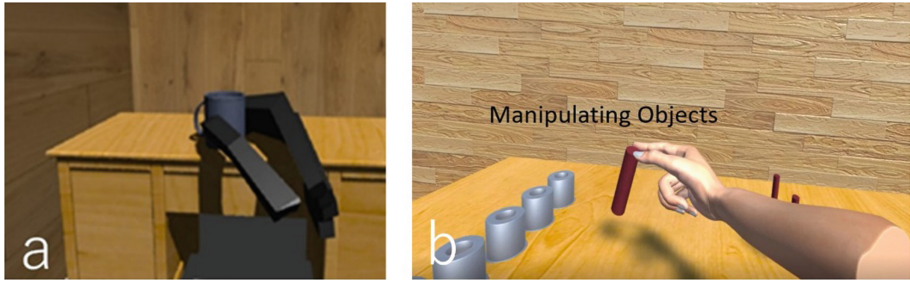
Fig. 4. Grasping a cup in VR environment (a); peg-in-hall application (b)

4   Conclusions and Future Work

We developed a device that presents the haptic sensation of the fingertip to the fingers and to the forearm rather than only to the fingertip. Specifically, we created a device that presents vibration sensation to the fingertips for the haptics cues to associate the haptics information provided to the forearm with the fingertips. Our preliminary test revealed that it is easily to associate the haptic sensation provided from the device to the forearm with their own fingertip.

Because the device on the forearm currently has only two DoFs, we could only present force to limited directions. We will improve the device by adding a third DoF to present various sensations.

The experiment was approved by ethical committee of the authors' institute.

References

1. Minamizawa, K., Kamuro, S., Fukamachi, S., Kawakami, N., Tachi, S.: GhostGlove: haptic existence of the virtual world. In: Proceedings of ACM SIGGRAPH 2008 New Tech Demos, p. 18 (2008)
2. Gabardi, M., Solazzi, M., Leonardis, D., Frisoli, A.: A new wearable fingertip haptic interface for the rendering of virtual shapes and surface features. In: Proceeding of Haptics Symposium 2016 (2016)
3. Moriyama, T.K., Nishi, A., Sakuragi, R., Nakamura, T., Kajimoto, H.: Development of a wearable haptic device that presents the haptics sensation to the forearm. In: Proceedings of Haptic Symposium 2018 (2018)
4. Tsetserukou, D., Hosokawa, S., Terashima, K.: LinkTouch: a wearable haptic device with five-bar linkage mechanism for presentation of two-DOF force feedback at the fingerpad. In: Proceedings of IEEE Haptic Symposium 2014, pp. 307–312 (2014)
5. Tsetserukou, D.: LinkGlide: a wearable haptic device with inverted five bar linkages for delivering multi-contact and multi-modal tactile stimuli. In: IEEE Haptics Symposium 2018 Work-in-Progress Session (2018)

The Thermal Feedback Influencer: Wearable Thermal Display for Enhancing the Experience of Music Listening

Yuri Ishikawa[1(✉)], Anzu Kawazoe[2], George Chernyshov[3], Shinya Fujii[4], and Masashi Nakatani[4,5]

[1] Faculty of Policy Management, Keio University, Tokyo, Japan
schneewittchenl24@keio.jp
[2] Media Arts and Technology, The University of California, Santa Barbara, Santa Barbara, USA
anzu@umail.ucsb.edu
[3] Graduate School of Media Design, Keio University, Tokyo, Japan
chernyshov@kmd.keio.ac.jp
[4] Faculty of Environment and Information Studies, Keio University, Tokyo, Japan
mn2598@sfc.keio.ac.jp
[5] JST PRESTO, Fujisawa, Japan

Abstract. This paper describes a new wearable thermal display, the Thermal Feedback Influencer, that can provide chilling stimuli to the skin in order to enhance emotional experiences of music listening. We developed a prototype device that can be attached to behind the ear. The device is designed to be small and lightweight enough to be worn comfortably. In this work, we describe basic concepts of this research, preliminary test results, details and evaluation of the developed prototype. We also summarize methods to provide thermal feedback with music and discuss the possible applications and future research plans.

Keywords: Thermal display · Musical interface · Wearable device · Frisson · Chill

1 Introduction

This paper presents our prototype capable of enhancing and inducing the sensation of frisson, an emotionally overwhelming experience, often combined with piloerection (also known as "goosebumps"). In this work, we concentrate on augmenting the music experience using thermal feedback and investigate the possibility of the frisson induction using this approach. Considering recent advances in interactive technologies, we focus on the development of devices that can enhance pleasure from listening to music. Previously, some studies use body sonic technology or vibrotactile feedback, and others use thermal feedback for increasing the pleasure of music listening.

For example, the Hapbeat [1] and Woojer [2] are wearable vibrotactile feedback devices, while the ThermOn [3] is the device that amplifies musical immersion using thermal feedback.

The changes in physiological and psychological evaluation are yet to be experimentally verified, especially when providing music and thermal haptic input at the same time. Therefore, in this study, we not only aim to develop a device that provides thermal feedback but also to clarify the influence of cold stimuli on physiological and psychological measures when listening to music [4]. In this paper, we present the first step of this study and explain how we developed the Thermal Feedback Influencer; we also describe possible applications, and future directions.

2   Developed Prototype

The Thermal Feedback Influencer is a wearable thermal display in ear-hook form-factor, which is small and light enough to wear comfortably. It can provide cold stimuli to the skin in synchrony with the music played to the listener. In this chapter, we describe the details of the developed device and how it provides the thermal feedback related to the music.

2.1   Hardware Development

For our prototype, we developed the ear-hook type device that is easy to put on and small enough to be supported by the ear (Fig. 1). The Peltier device is a basic heat pump, transferring heat from one side to another depending on the flow of the electric current. Considering the size, such device seems to be perfect for cold stimulation.
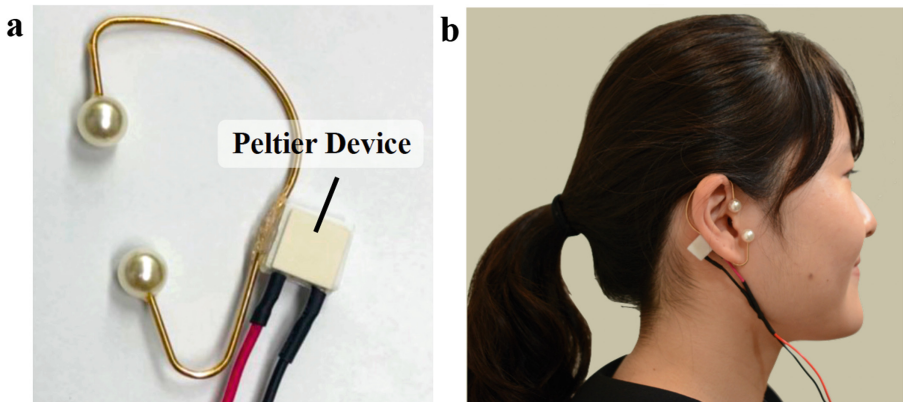
Fig. 1. Our developed thermal haptic display

For the device placement and stimuli application, we chose the area near the mastoid behind the ear. According to previous studies, it was reported that the sensation of frisson or goosebumps as a response to music listening is more likely to manifest itself on the head [5]. In addition, it is well known that the face area is the lowest sensitivity threshold [6]. Considering the above as well as the user comfort, we picked the area near the mastoid bone as the most suitable for our use case in terms of wearable comfortability and the ease of temperature presentation. Another consideration is the similar to ear-hook earphones form-factor of the device, designed to be compatible with existing earphones or headphones, that are comfortable to be worn even for prolonged periods of time. A 10×10 mm^2 Peltier device (TEC1-00712T125, Kaito Denshi) was attached to the ear hook made of copper wire so that colder surface of the Peltier device remains in contact with the mastoid. In addition, we designed a hooking cover for the reverse or the hot side of the Peltier element, in order to isolate it from the skin. We used an Arduino Nano to control the electric current using a PWM-driven SMPS module.

2.2   Software Development

In terms of the software development, it is important to consider the onset time of the cold stimuli and ensure it corresponds to the musical piece. Previous studies suggest that music has at least four acoustic features contributing to the sensation of frisson: (i) sound volume, (ii) pitch, (iii) roughness, and (iv) unexpected development of music [7]. In a previous study that analyzed the acoustic features of 190 songs, it was found that the sensation of goosebumps depends on the magnitude of the increase in the sound volume [8]. From the four outlined features contributing to the sensation of frisson, the sound volume is relatively easy to use for the feedback onset timing. As this device aims to enhance pleasurable experience in daily music listening, the software algorithm must be applicable to various types of music. Thus, considering the previous studies, we use a sound volume threshold trigger to activate the thermal feedback.

3   Hardware Evaluation

The thermal characteristics of the developed prototype device were evaluated using a compact thermal camera (FLIR C2, FLIR.) and a thermometer. During the evaluation, the room temperature was kept at 27 °C.

Thermography. We used thermal imaging to evaluate the changes in heat distribution around the ear (Fig. 2a). After the 1-s application of current to the Peltier device, the temperature reached the minimum at the 3.0 s and gradually increased afterwards (Fig. 2b).
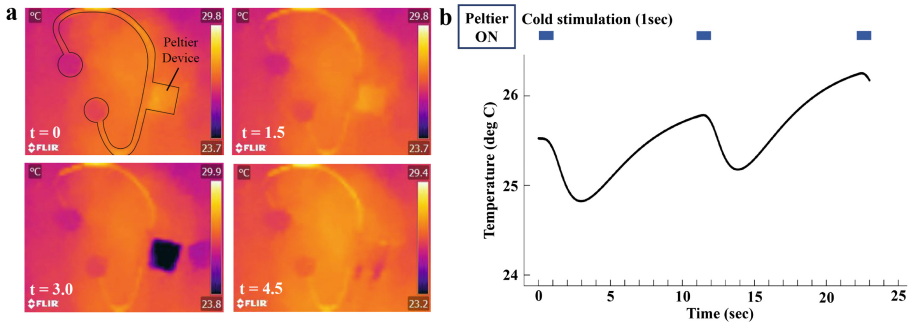
Fig. 2. Thermography (a) and temperature profile (b) of the developed device

Temporal Profile of Temperature in Thermal Feedback Device. The temperature of the surface in contact with skin was measured using the PowerLab 16/35 DAQ unit (PL35/16, AD Instruments) and the thermometer (ML309 Thermistor pod, MLT422/A Skin Temperature Probe, AD Instruments). On the Fig. 2(b) one can see the temperature corresponding to 3 consecutive 1 s-long applications of current in about 10 s intervals.

We confirmed the surface temperature of the Peltier device decreases by 0.7 after 3.0 s of cold stimuli, then rises by about 1.0 °C for the next 7.0 s. When a current was inputted to the Peltier device, the temperature falls and rises repeatedly, and the surface temperature continued to rise by about 0.3 °C per 10 s.

4   Discussion and Future Works

In this study, we developed a prototype device of thermal display for enhancing the emotional experience of music listening.

The experiment of thermal characteristics of the developed device showed that the temperature of the Peltier device decreases after 3.0 s of cold stimuli. Therefore, considering that the timing of cold stimuli has a time lag of about 3.0 s, we are trying to improve the software.

Moreover, modern Peltier devices have the efficiency rating of 60–70%, which results in the remaining 30–40% of energy being emitted as heat. Which results in gradual temperature increase of the element after continuous usage. Since the current prototype does not have any heat dissipation mechanisms, it tends to warm up, which eventually results in inability to provide cold feedback.

However, the baseline temperature increase is not significant if the onsets are short and spread out through the whole music piece. Providing the thermal feedback only a few times during one track seems to be a reasonable compromise. In future study, we plan to add heat dissipation element to the device, using a heat sink or liquid cooling.
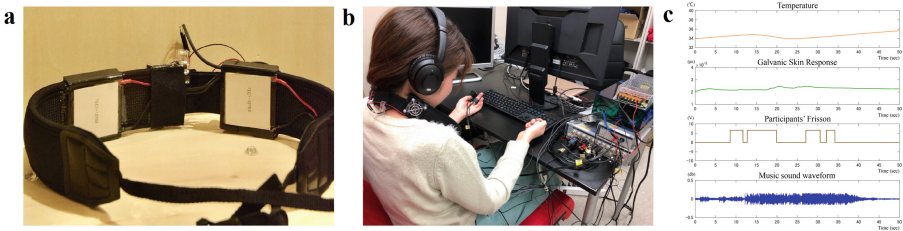
Fig. 3. First prototype device (a), experimental setup (b) and physiological evaluation when listening to music (c)

In the experiment, we used "Post War Dream (Pink Floyd)" that is likely to induce goosebumps and frisson according to the previous study of Panksepp (1995) [5].

This experiment used our first prototype device. For our first prototype, we also developed the neckless type device (Fig. 3a). for the device placement and stimuli application we chose the area near the back of the neck. A 30×30 mm^2 Peltier device (TEC1-12703, Kaito Denshi) was attached to the shoulder strap so that colder surface of the Peltier device remains in contact with the back of the neck (Fig. 3b).

In this pilot study, we picked 3 timings corresponding to certain acoustic features (magnitude of sound and unexpected development of music), which are considered to increase the likelihood of the goosebumps occurrence. Cold stimuli for 7.0 s was provided. Also, so as to confirm the cold stimulation, the surface temperature of the neck in contact with the Peltier device was measured. We used PowerLab 16/35 (PL35/16, AD Instruments) in order to measure the physiological evaluation. We measured pulse wave, GSR (Galvanic Skin Response), respiration in closed eyes at the time of listening to music, we instructed to press the button for answering subjective response.

Figure 3(c) shows that GSR increased for all 3 cold stimuli onsets. Participants reported experiencing frisson and goosebumps by pressing a button. Therefore, it was suggested that provision of the cold stimuli while listening to music may induce a sensation of goosebumps and amplify the emotional experience of the musical piece. No other physiological change was observed.
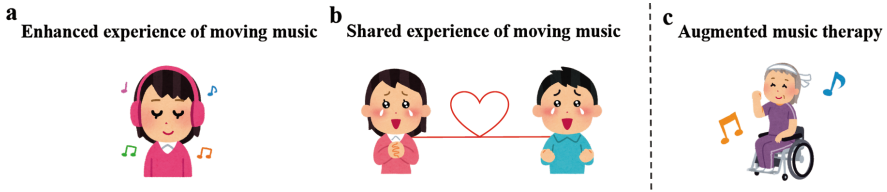
Fig. 4. Applications using the Thermal Feedback Influencer

We are envisioning the following three applications of the Thermal Feedback Influencer. The first application is the enhancement of the personal music experience (Fig. 4a). We are being really moved by listening to emotionally charged music on a

daily basis. However, the sensitivity to music depends on user's psychological and physiological condition. Since the music itself doesn't change, if we could record the timing when the frisson has occurred, it may be reproduced later. The users may be able to have goosebumps from the music over and over again. This approach can enhance the experience of music, but can be applied to many other areas such as art, musicals, movies, etc. Even when you are viewing arts with others, you might be able to produce a more first-person experience by using this device.

The second application is sharing the emotionally moving experience of music (Fig. 4b). If user can record when and at what timing the goosebumps have occurred, he or she can not only know which part of a music piece was emotionally moving for them, but also can share the experience with other people. Using such devices at a cinematographic festivals or music live performances, it would be possible to provide common feelings at the same time between the attendees in a non-verbal cross-language and cross-cultural manner.

The third application is augmented music therapy. In previous study, physiological reactions such as activation of the reward system area, and dopamine release in the midbrain limbic system, occur together with the sensation of frisson and goosebumps when listening to music [4]. There are many people suffering from the lack of dopamine, e.g. in conditions such as schizophrenia and Parkinson's disease. If we could use this device in order to enhance the emotional experience of music, the reward system of the cerebrum and the midbrain limbic system which was suppressed due to certain conditions may be re-activated. This effect might be able to improve patients' clinical condition in schizophrenia and Parkinson's disease. Even though solid scientific evidence of music therapy using fMRI and EEG still requires more research, it is still possible to test whether it has any effect or not on these clinical conditions. If increased activation of the brain regions of interest would occur when cold stimulus is provided along with a music piece, our system may provide or even increase the positive effect of the music therapy. In the future, we will investigate all these applications for better understanding of the emotional experiences caused by music.

Ethical Approval. All procedures performed in studies involving human participants were in accordance with the Ethical Committee of Human Experiment at Keio University, Shonan Fujisawa Campus and with the 1964 Helsinki declaration and its later amendments or comparable ethical standards.

Informed Consent. Informed consent was obtained from all individual participants included in the study.

References

1. Yamazaki, Y., Mitake, H., Oda, R., Wu, H.H., Hasegawa, S., Takekoshi, M., Tsukamoto, Y., Baba, T.: Hapbeat: single DOF wide range wearable haptic display. In: Proceeding of ACM SIGGRAPH 2017 Emerging Technologies Article No. 12 (2017)
2. WOOJER Homepage. https://www.woojer.com/. Accessed 14 Aug 2018
3. Akiyama, S., Sato, K., Makino, Y., Maeno, T.: ThermOn: thermos-musical interface for an enhanced emotional experience. In: Proceeding of the 2013 International Symposium on Wearable Computers, Zurich, Switzerland, pp. 45–52 (2013)
4. Salimpoor, V.N., Benovoy, M., Larcher, K., Dagher, A., Zatorre, R.J.: Anatomically distinct dopamine release during anticipation and experience of peak emotion to music. Nat. Neurosci. **14**, 257–262 (2011)
5. Panksepp, J.: The emotional sources of "chills" induced by music. Music Percept. **13**, 171–207 (1995)
6. Stevens, J.C., Choo, K.K.: Temperature sensitivity of the body surface over the life span. Somatosenssory Motor Res. **15**, 13–28 (1998)
7. Mori, K., Iwanaga, M.: Music-induced chills as a strong emotional experience. Shinrigaku Kenkyu **85**, 495–509 (2014)
8. Grewe, O., Nagel, F., Kopiez, R., Altenmüller, E.: Listening to music as a re-creative process: physiological, psychological, and psycho acoustical correlates of chills and strong emotions. Music Percept. **24**, 297–314 (2007)

Seesaw Type Actuator for Haptic Application

Kahye Song, Jung-Min Park, and Youngsu Cha[(✉)]

Center for Intelligent and Interactive Robotics,
Korea Institute of Science and Technology,
Hwarangro 14gil 5, Seongbuk-gu, Seoul 02792, Republic of Korea
givemong@kist.re.kr

Abstract. In this study, we propose a seesaw type actuator, and we investigate its actuation to determine the most efficient structure. When a high voltage input is applied between the L-shaped actuator and metal plate at the bottom substrate, another panel rises due to reaction of the electrostatic attraction. And it leads to tactile stimulation. In addition, we add a round cap to the edge of the panel of the actuator for more effective stimulation delivery. Various types of actuators experiments showed that the actuator with the largest radius of motion was an actuator with a narrow angle and a long length, and the axis of rotation coincided with the axis of gravity. This is because narrower angles between actuators increase the movable radius of motion and longer actuators can induce electrostatic attraction of larger forces and lose balance if the center of gravity axis does not match. Both gravity and electrostatic attraction are utilized for the operation of the actuator, and this actuator generates strong tactile stimulation without the risk of electric shock to users by separating the user contact part from the electrostatic force region. We expect that this new actuation mechanism is adapted to various haptic devices in the future to help the human-computer interaction.

Keywords: Seesaw type actuator · Electrostatic attraction · L-shaped actuator

1 Introduction

The human desire to feel virtual or augmented reality directly with his/her skin has provoked remarkable developments in tactile and haptic displays over the past 15 years [1]. By the recent developments, tactile and haptic displays have been more robust, smaller and easier to use. These advanced tactile and haptic devices are installed on state-of-the-art equipment, such as cell phones, watches, sportswear, and game controllers, helping users realize real-world, state-of-the-art equipment. Also, we can find their applications in automotive and augmented reality implementations, including rehabilitation robots, service robots, food-processing automation and surgery [2–4]. The important things in constructing these devices are small size, light-weight, low-cost, low-power, and high force output.

In this study, we developed a new concept actuator that can give strong and fast stimulation continuously to the fingers in accordance with the requirements of the haptic actuator [5]. Unlike previous studies, the cap was attached to the L-shaped actuator to make it a haptic device.

2   Results

One of the most important aspects of a haptic application is to deliver stimulus to the user more reliably. Therefore, we developed L-shaped actuator. The rounded cap covers the narrow, cornered L-shape, which allows the actuator to perform well as a haptic application (CA) (Fig. 1a).
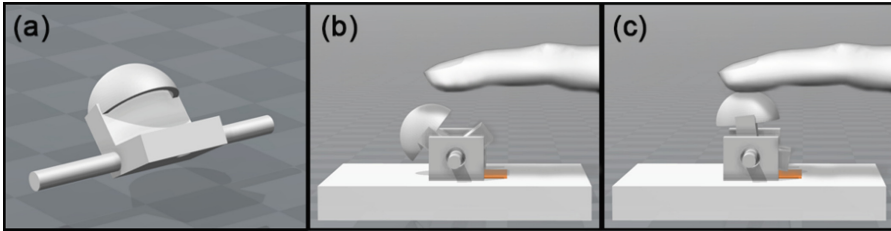
Fig. 1. L-shaped actuators with cap and its application (a) Image of L-shaped actuators with cap. (b) When power is off. (c) When the power is applied to the floor.
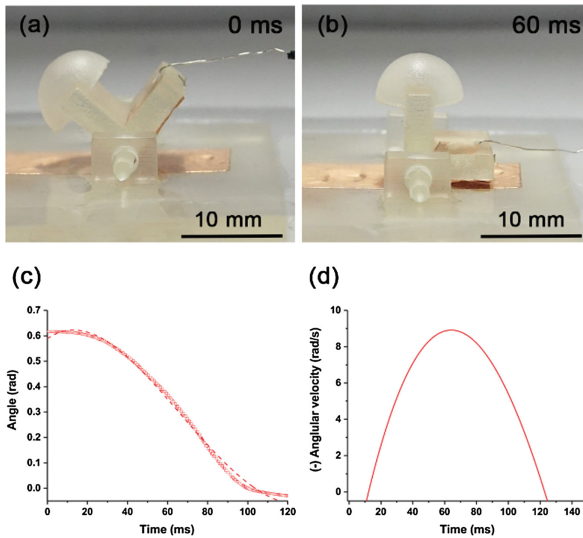
Fig. 2. Optimized type of actuator (a–b) The movement of the CA_{opt} that was made by synthesizing the most efficient length and the position of the angle axis in the previous experiment. (c) The actual angular changes tracked at 0.5 ms intervals and fitting line. The sample moved over 0.6 rad for 120 ms. (d) Angular velocity is calculated and depicted as a graph.

When the L-shaped with cap actuator which is in equilibrium is attached to the floor by the electrostatic attraction, the position of the cap part is high and it can stimulate the finger (Fig. 1b). Moreover, since the center of gravity is positioned in the panel with the cap, it is more suitable for haptic applications that require on/off to easily return to the equilibrium state, not touching the fingers. The series of experiments are conducted to find the most effective structure.
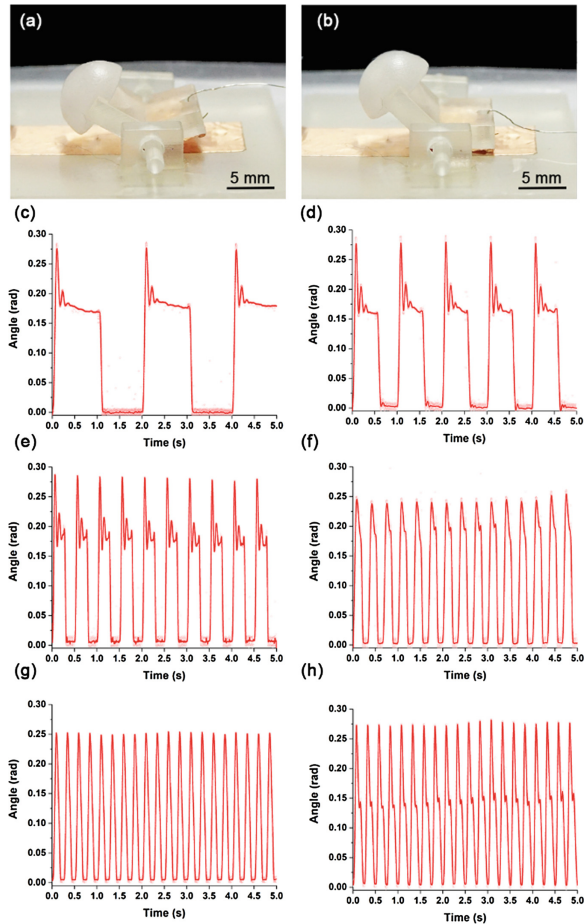
Fig. 3. On/off actuator (a–b) CA_{re} was fabricated with 8.5 mm length, 135° angle and the axis locate sight lower than the center. Voltage difference was 5 kV (high 5 kV, low 0 kV), however, different periods of electricity were applied. The actual angular changes in 0.5 Hz (c), 1 Hz (d), 2 Hz (e), 3 Hz (f), 4 Hz (g) and 5 Hz (h) tracked at 0.5 ms intervals and depicted as dots. Based on data, local regression method LOWESS (locally weighted scatterplot smoothing) were used to draw fitting line. As shown in graphs, it can be turned on/off within 1 s repeatedly with fast response speed.

And based on these experimental results, we fabricated the most effective actuator (CA_{opt}) for dynamic movement (Panel length (l) = 10 mm, Angle between two panels (θ_s) = 90°, Position of rotation axis (x_p) = 1.4 mm away from center diagonally) (Figs. 2a–b). CA_{opt} requires 1.5 times longer time for motion than L-shaped actuator because the weight is heavier than L-shaped actuator and the center of gravity is on the cap side. However, the angle changes by 0.7 rad, which is much larger than other structures (Fig. 2c). Furthermore, the maximum instantaneous velocity is larger than 9 rad/s (Fig. 2d) and the blocking force of CA_{opt} is measured as 669.1 mN.

Moreover, as mentioned above, since the center of gravity is behind the cap, it is possible to return to the original position. The experiment was carried out by making an efficient sample for return (CA_{re}). (l = 8.5 mm, θ_s = 135°, x_p = 1.4 mm away from center diagonally) (Figs. 3a–b).

At first, the supplied power difference was adjusted from 1 kV to 5 kV. Surprisingly, it was possible to drive the sample about 0.2 rad sufficiently even at 1 kV voltage difference. It means that the efficiency is high due to the lightweight and simple circuit configuration.

After that, the applied voltage difference was fixed at 5 kV (high 5 kV, low 0 kV) and the period was changed. From 0.5 Hz to 5 Hz, the CA_{re} moves up to about 0.2 rad without any difficulty with fast speed (Figs. 3c–h). Therefore, the on/off of the motion is possible in a period of several seconds.

3   Conclusion

In this study, we proposed a new type of actuator for haptic application and conduct experiment to find motion optimized structure. The CA_{opt} with a round cap showed the movement of over 0.6 rad, which is sufficient for haptic device use. Also CA_{re} exhibited rapid response time in various voltage. The range of motion can be controlled by modifying the CA's path or shape depending on the application.

The CA proposed in this study can make various sizes and are very light and easy to make. It is a compact device with very effective at delivering stimuli. Moreover, since the circuit configuration is very simple, it can be applied to various devices. The high voltage is supplied to actuator for operation, but the cap that actually touches the user is a nonconductive object. Thus, this actuator can be used safely. In addition, including proposed haptic application, it can also be used as a valve or an optical pick-up head actuator. Likewise, we expect that these developments will lead to an advanced haptic application.

References

1. Jones, L.A.: Perspectives on the evolution of tactile, haptic, and thermal displays. Presence (Camb) **25**(3), 247–252 (2016)
2. Scott, J., Gray, R.: A comparison of tactile, visual, and auditory warnings for rear-end collision prevention in simulated driving. Hum. Factors **50**(2), 264–275 (2008)
3. Lee, M.H., Nicholls, H.R.: Review Article Tactile sensing for mechatronics—a state of the art survey. Mechatronics **9**(1), 1–31 (1999)
4. Eltaib, M., Hewit, J.: Tactile sensing technology for minimal access surgery—a review. Mechatronics **13**(10), 1163–1177 (2003)
5. Song, K., Lee, H., Cha, Y.: A V-Shaped actuator utilizing electrostatic force. Actuators **7**(2), 30 (2018)

A Two-DOF Impact Actuator for Haptic Interaction

Sangyoon Kim[1], Bukun Son[1], Yongheon Lee[2], Hyunwoong Choi[1],
Woochan Lee[3], and Jaeyoung Park[2(✉)]

[1] Seoul National University, Seoul, Korea
{oiei0806,nucktu,alfredl224}@snu.ac.kr
[2] Korea Institute of Science and Technology, Seoul, Korea
{lovl223,jypcubic}@kist.re.kr
[3] Incheon National University, Incheon, Korea
wlee@inu.ac.kr

Abstract. This paper presents a new actuator mechanism that can create a planar two-DOF impact and vibrotactile stimuli with wide frequency bandwidth. The proposed device utilizes one permanent magnet and two different sets of solenoids, direction controlling solenoids and a central solenoid. The direction controlling solenoids are two sets of facing solenoid pair, which attract the permanent magnet from a neutral position toward the housing, to create an impact. The central solenoid increases the magnet's potential energy, resulting in a faster movement toward the outside of the neutral position and thus increasing the amount of impact. The central solenoid can be utilized to create an attractive force to move the magnet back to the neutral position after the impact. When creating an impact in an arbitrary orientation, two sets of solenoid pair are used to decide the initial force direction, which is parallel to the magnet's trajectory until an impact. The actuator can be used as a tactor by controlling the impact cycle.

Keywords: Two DOF · Impact actuator · Solenoid

1 Introduction

Recent growth in virtual reality industry calls for new means to create more immersive experiences in the virtual environment. To meet with the demand, haptic actuator technologies are required to provide a user with diverse tactile sensation. In the view of mobile and game interfaces, however, most of commonly used actuators have their own drawbacks in creating tactile feedback. Typical haptic actuators are categorized into eccentric motors, piezo actuators and linear resonant actuators (LRA) [1]. An eccentric motor can readily generate vibrotactile stimuli by rotating asymmetrical mass but has several disadvantages including the difficulty in controlling vibrational force and generating low-frequency signals. A piezoelectric actuator utilizes piezo-ceramic material's characteristic that expands or contracts by the magnitude of applied electrical charges. Due to the fast response time and wide frequency bandwidth, the piezo actuator is used widely in a variety haptic applications but exerts relatively weak

vibration force. An LRA creates vibratory force with the magnetic force between a permanent magnet and a solenoid and shows a fast response time. Vibration force generated by an LRA is weak when the actuation frequency is outside of its resonance frequency. Also, the residual vibration can occur after the actuation. Actuators mentioned above have their own advantages but are limited in delivering diverse haptic feedback, in terms of vibratory frequency bandwidth or the degrees of freedom in stimulus direction.

The objective of this paper is to propose an actuator mechanism that can provide diverse tactile feedback for haptic interaction. To achieve the goal, we focused on creating tactile signal with wide frequency bandwidth and more degree of freedom in the stimulus direction. A solenoidal impact generator can be a candidate for such an actuator in that it can provide such diverse tactile sensations to a user. Yang and Kim developed miniature solenoidal impact actuators in a series of studies by utilizing an unstable structure [1–3]. With the unstable structure, the residual vibration occurring in an LRA does not happen since the mass is attached to the house after an impact. The unstable mechanism can also generate vibrations with a wide frequency range by creating impacts repeatedly and controlling impact frequency. However, such a mechanism can create an impact in only one direction. Also, there is no neutral position for a mass to return after an impact, which makes it difficult to control the magnitude and direction of a stimulus. To overcome the drawbacks of the unstable impact generator while preserving its advantage of wide frequency bandwidth, we propose a new type of impact actuator mechanism. Our actuator mechanism can create an impact in an arbitrary direction on a plane (2-DOF) without having the problem of the residual vibration of an LRA.

2   Design of a Two-DOF Impact Actuator and Its Working Principle

Figure 1 shows the overall structure of our two-DOF impact actuator. The actuator consists of a part enclosing four solenoids creating a magnetic field for a directional impact and one central solenoid that generates an attractive or repulsive force around the neutral position. A permanent magnet is installed inside a housing between the four direction-controlling solenoids and a central solenoid. An impact is generated as the permanent magnet collides with the housing. The actuator's overall size is 45 mm in diameter and 30 mm in height. The permanent magnet is a cylinder, and its size is 17.5 mm in diameter and 4.95 mm in height. Each solenoid coil for the direction control is wound 1500 times and its inductive reactance is 13 Ω. The central solenoid is wound 4000 times, having the inductive reactance value of 45 Ω. Inside of the central solenoid is a ferromagnetic core which enforces the attractive/repulsive force applied to the permanent magnet. In the neutral state, the permanent magnet is supposed to be attached to the central solenoid's magnetic core. The distance between the magnetic core and the permanent magnet is short to ensure strong enough attachment to withstand an external force.
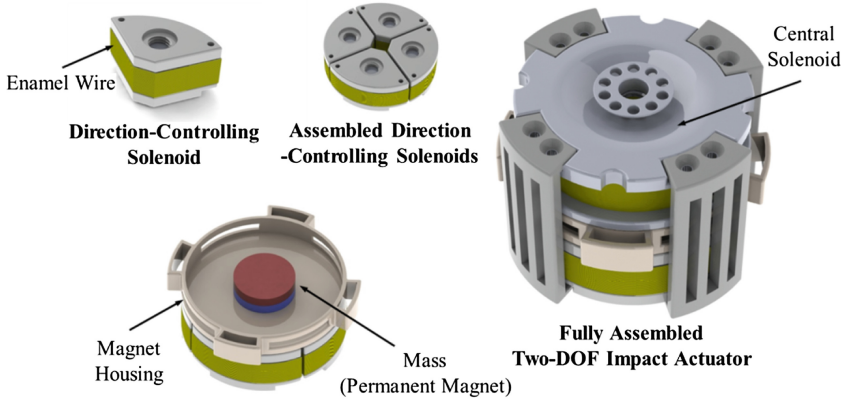
Fig. 1. Component and structure of two-DOF impact actuator and its fully assembled figure.

Figure 2 shows the working principle of the two-DOF impact actuator. For a pair of solenoids facing each other, (i.e., (1, 3) and (2, 4) as shown in Fig. 2(a)), the same amount of current flows but the direction of the current is opposite by winding coils in opposite directions. This causes two facing solenoids to have opposite magnetic polarities. Figure 2(b) shows how an impact is generated by controlling the magnetic fields of the actuator. In an initial neutral state, the permanent magnet sticks to the magnetic core of the central solenoid. For generating an impact toward the direction of the solenoid 1, electric current is applied to induce the north polarity to the solenoid, which produces an attractive force and lowers the magnetic potential energy around the solenoid. Also, by inducing north polarity to the central solenoid, repulsive force is produced, which increases the magnetic potential energy at the neutral position. Therefore, the permanent magnet moves along the potential energy's gradient until it collides with the housing around the solenoid 1. When the electric current breaks off for all solenoids, the permanent magnet returns to the neutral position being attracted by the magnetic core of the central solenoid. For the ease of the magnet's return to the neutral position, the central solenoid can exert additional attractive magnetic force.

Figure 3 shows how the two-DOF impact actuator can create an impact vector in an arbitrary direction on a plane. The combination of a force vector generated by the solenoid pair (1, 3) and the solenoid pair (2, 4) forms a force vector in a particular direction on a plane. The net vector decides the force initially applied to the permanent magnet at the neutral position and thus the magnet's travel trajectory until the impact. As the magnet moves, its path slightly deviates from the linear path parallel to the initial force vector, but the degree of deviation is negligible due to the short travel time.
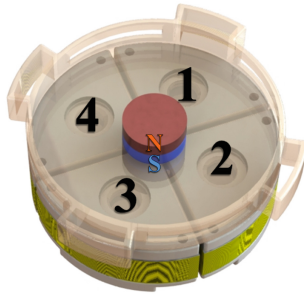
(a) Top view of the actuator without the central solenoid. Numbers indicate the direction controlling solenoids' indices.
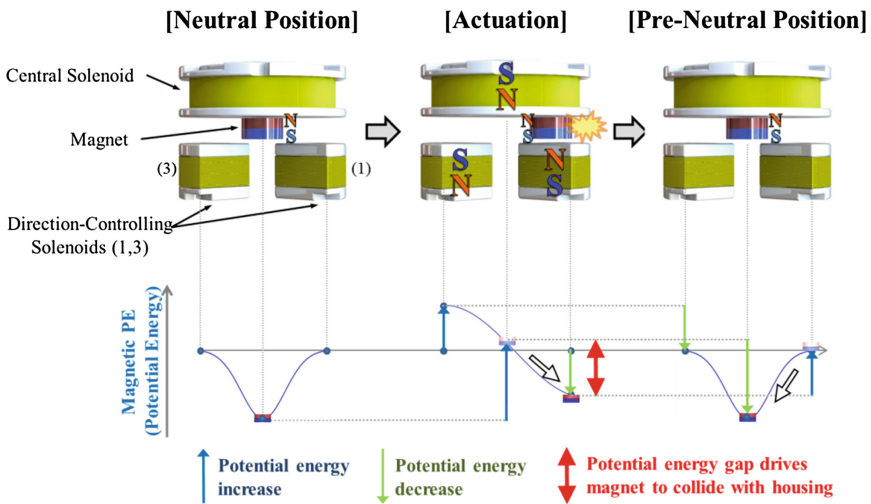
(b) (i) In the neutral position, the magnetic potential energy (PE) is low. (ii) When an electric current is applied, the magnetic PE is increased. Then, the magnet moves toward solenoid 1 to lower the magnetic PE and makes an impact. (iii) In pre-neutral position, central solenoid core exerts attractive force to retrieve the magnet to the neutral position.

Fig. 2. The working principle of the two DOF impact generator.
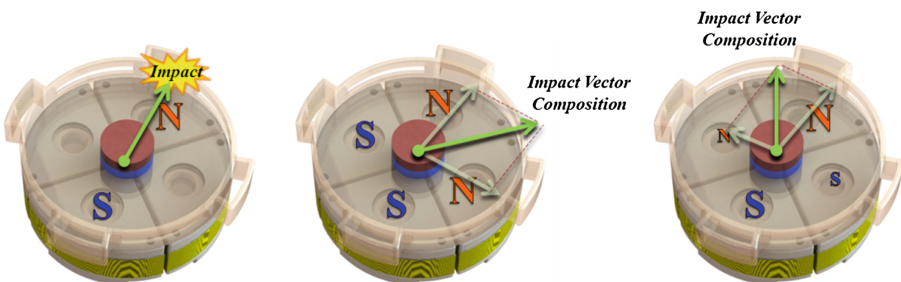
Fig. 3. Impact vector composition of two pairs of direction-controlling solenoids.

3   Conclusion

In the present paper, we propose an actuator mechanism that can create a two-DOF impact in an arbitrary direction on a plane. When used as a vibrotactile actuator, the actuator has the advantage of wide frequency bandwidth and minimal residual vibration. In our future work, our proposed mechanism will be further explained in terms of controlling strategy and applications such as virtual reality and path guidance. Moreover, the proposed actuator can be used for hand-held device applications to create two-DOF impacts.

References

1. Kim, S.Y., Yang, T.H.: Miniature impact actuator for haptic interaction with mobile devices. Int. J. Control Autom. Syst. **12**(6), 1283–1288 (2014)
2. Yang, T.H., Pyo, D., Kim, S.Y., Cho, Y.J., Kwon, D.S.: A new subminiature impact actuator for mobile devices. In: IEEE World Haptics Conference, pp. 95–100 (2011)
3. Yang, T.H., Pyo, D., Kim, S.Y., Kwon, D.S.: Development and evaluation of an impact vibration actuator using an unstable mass for mobile devices. Int. J. Control Autom. Syst. **14** (3), 827–834 (2015)

A Novel Haptic Interface for the Simulation of Endovascular Interventions

Hafiz Rashidi Ramli[1(✉)], Norhisam Misron[1], M. Iqbal Saripan[1],
and Fernando Bello[2]

[1] Faculty of Engineering, Universiti Putra Malaysia,
43400 Serdang, Selangor, Malaysia
`hrhr@upm.edu.my`
[2] Imperial College London, Center for Engagement and Simulation Science,
London SW10 9NH, UK

Abstract. Endovascular interventions are minimally invasive surgical procedures that are performed to diagnose and treat vascular diseases using flexible instruments known as guidewire and catheter. A popular method of developing the skills required to manipulate the instruments successfully is through the use of virtual reality (VR) simulators. However, the interfaces of current VR simulators have several shortcomings due to limitations in the instrument tracking and haptic feedback design. A major challenge in developing training simulators for endovascular interventional procedures is to unobtrusively access the central, co-axial guidewire for tracking and haptics. In this work, we designed a haptic interface using novel approaches to both. Instrument tracking is performed using a combination of an optical sensor and a transparent catheter. Haptic feedback is supplied by both off-the-shelf actuators and a bespoke electromagnetic actuator embedded within the catheter hub. Initial test results by expert interventionists have shown positive responses and further development is ongoing.

Keywords: Haptic interface · Endovascular interventions · Simulator training

1 Introduction

Cardiovascular disease (CVD) is the number one cause of death around the world. The projected estimation is that the annual death count attributed to CVDs will reach 23.3 million by 2030 as it continues to be the single leading cause of death in the future [1]. The seriousness of the situation led to the introduction of a new form of minimally invasive surgery over two decades ago, which enables the diagnosis and treatment of many major vascular diseases and has become a vital part of vascular health care today [2]. Unlike traditional open surgery, these endovascular interventions involve the use of long, thin and tubular specialised instruments, called catheters and guidewires, that are inserted into the patient's vascular system via a small incision in the groin or arm. With this approach, patients suffer much less trauma, leading to faster recovery, reduced risk of infection and lower treatment costs since they can usually be performed as day cases.

A popular method to develop the skills required to manipulate the instruments successfully is through the use of virtual reality (VR) simulators [3]. VR simulators

have the potential for significant development as computational technology improves. Unconstrained by any physical factors, training in the virtual realm offers many different possibilities. This includes the ability to offer a number of training scenarios, featuring a variety of anatomical models on which to operate, with different types and levels of pathology. Advancements in haptic technology help to ensure the tactile aspect of the procedures can be experienced in the simulators through the use of bespoke haptic interfaces.

There are several design issues in current haptic interfaces for the simulation of endovascular interfaces that may negatively affect the validity of the simulation experience and its effectiveness. These include: limited instrument range of movement, loss of instrument position information and unrealistic haptic feedback. The design issues are mostly due to the fact that, during endovascular interventions, the guidewire is positioned concentrically within the catheter while it is navigated within the blood vessels. This significantly reduces the line of sight and point of contact to the guidewire and is the main design challenge, referred here as "concentric occlusion". In this work, we present a novel haptic interface design aiming to addresses this issue.

2 Methodology

The haptic interface is equipped with two separate, but equally important systems that work in parallel during the simulation: instrument tracking and haptic feedback. Each of these systems is now described in more detail.

2.1 Instrument Tracking

The requirements for instrument tracking are relatively simple. The system needs to track the translational and rotational movements of both the guidewire and catheter to a resolution of 1 mm. Previous interface designs have utilised either optical or mechanical sensors to detect and track instrument movements [4, 6, 7]. The sensors are normally spaced apart and dedicated to one specific instrument. A problem occurs when the catheter is advanced past the guidewire's sensor, thus blocking and disrupting the guidewire tracking. In the proposed design, movement of the catheter is still tracked by an off-the-shelf optical sensor, but a slightly different approach is used to enable concentric tracking of the guidewire. It combines a transparent catheter and a second optical sensor (Fig. 1). Thus, the transparent catheter provides a line of sight for the guidewire to be detected by the second optical sensor.
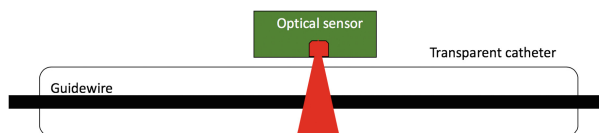
Fig. 1. Illustration of the optical sensor setup for concentric guidewire tracking

2.2   Haptic Feedback

Similar to the sensor configuration, previous interfaces have implemented separate haptic actuators spaced out and assigned to a certain instrument [5–7]. The actuators used are typically servo motors or electromagnetic clamps. In our design, a servo motor is used to apply force to the catheter, whilst a bespoke electromagnetic actuator was designed to apply force to the guidewire.

The concept was to embed the custom actuator inside the catheter hub in order to address the concentric occlusion problem. The catheter hub refers to the plastic case that forms the entrance at the proximal end of the catheter (Fig. 2 Left). It has a unique cylindrical shape measuring 8 mm × 20 mm (Diameter × Length) with 'wings' extruding from the sides. During operation, the guidewire will always pass through the catheter hub to enter the catheter tubing. Therefore, by placing an actuator within the hub, it will have direct contact with the guidewire at any time without requiring or causing any movement restrictions.
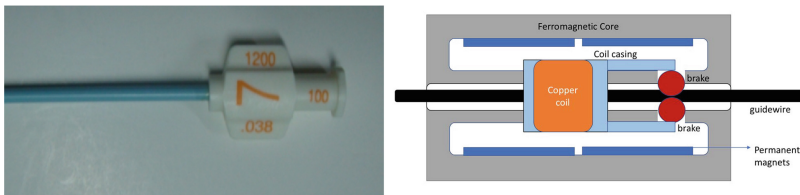
Fig. 2.   Left – Catheter Hub; Right – Bespoke actuator activated and its components

An electromagnetic actuator approach was selected due to the minimal parts required that are relatively simple to miniaturise, easy to obtain and with the potential for producing varying levels of resistance. Figure 2 (Right) shows the design of our electromagnetic actuator. When haptic feedback is required, current is supplied to the copper coil producing an electromagnetic field that reacts with the electromagnetic field of the surrounding permanent magnets, pushing the coil casing (3D printed) and activating the sphere brakes. The "arms" of the coil casing will push the brakes towards the guidewire (passing through the channel inside the ferromagnetic core) applying certain amount of resistance.

2.3   Prototype Integration

Both the tracking and haptic feedback systems are integrated within the prototype interface shown in Fig. 3. The prototype featured two ports for interaction with two different sets of instruments to allow for the simulation of different stages of the intervention. The tracking sensors and haptic feedback actuators are controlled by an Arduino board that communicates with a 3D virtual simulator environment (Fig. 4). Movement of the instruments inserted into the haptic interface by an operator is tracked and mirrored by the virtual instruments. Collision between the instruments and vasculature in the virtual environment causes the actuators to feed back the corresponding force onto the operator.
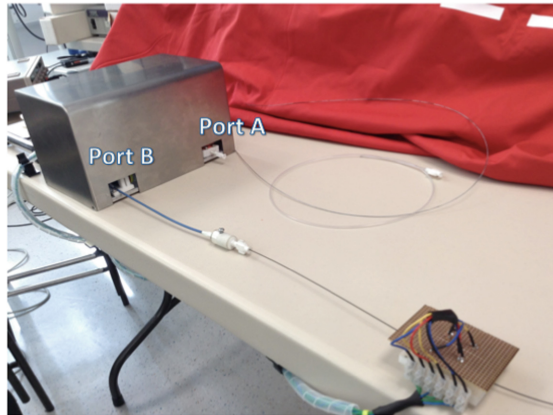
Fig. 3. Prototype interface device setup for testing

Fig. 4. 3D generated virtual environment with simulated vasculature and set of guidewire and catheter

3   Results and Discussion

The prototype system was presented to an interventional cardiologist at the London Heart Hospital for testing of the proof of concept. Ethics approval was obtained from the Imperial College Research Ethics Committee (Ref ICREC_13_6_12). Informed consent was obtained from all study participants.

During the testing stage, the cardiologist was asked to perform simple tasks using the haptic interface, including advancing the guidewire and catheter from one end of the virtual vessel to the other. This includes manipulating the instruments to navigate

past a narrowing in the vessel, which activates the actuators to recreate the feeling of resistance through the collisions between the virtual instruments and the vessel. After 15 min of testing the prototype, the cardiologist was asked to complete a questionnaire evaluating the tracking and haptics systems, as well as the general concept.

The cardiologist reviewed the tracking system and scored it highly in terms of responsiveness and accuracy, with the movements of the real-life instruments being adequately translated into the virtual environment. The haptic feedback system was said to be effective for both the catheter and guidewire. The resistance effect produced on the guidewire using the new hub actuator was highlighted as being subtler than that in current interfaces. This could be an advantage of using the bespoke actuator. Use of transparent catheters instead of the regular blue colored catheters was deemed acceptable, as long as they felt the same when manipulated. However, embedding the actuator within the catheter hub has increased its size and changed its handling. It was suggested that future iterations of the actuator will need to be miniaturized further to minimise disruption to the operator. Lastly, the concept of using more than one port during the simulation was not as well received and needs further consideration.

4   Conclusion

We have presented a novel haptic interface for the simulation of endovascular interventions designed to address the shortcomings of current interfaces. The tracking and haptic feedback systems were tested in a proof of concept prototype that was positively reviewed by an interventional cardiologist. Future work will include miniaturization of the actuator hub and further testing by subject matter experts.

References

1. World Health Organization: Global status report on noncommunicable diseases 2010 Geneva. http://www.who.int/mediacentre/factsheets/fs317/en/. Accessed 17 June 2018
2. Darzi, S.A., Munz, Y.: The impact of minimally invasive surgical techniques. Ann. Rev. Med. **55**, 223–237 (2004)
3. Coles, T., Meglan, D., John, N.: The role of haptics in medical training simulators: a survey of the state of the art. IEEE Trans. Haptics **4**(1), 51–66 (2011)
4. Betrisey, S., Vecerina, I., Zoethout, J.: Device for determining the longitudinal and angular position of a rotationally symmetrical apparatus. Patent EP 1574825 (2005)
5. Vecerina, I., Betrisey, S., Zoethout, J.: Actuator for an elongated object for a force feedback generating device. Patent US 20070063971 (2007)
6. Chui, C., Chen, P., Yaoping, W., Ang Jr., M.H., Yiyu, C., Mak, K.-H.: Interventional radiology interface apparatus and method. Patent US6538634 (2003)
7. Ohlsson, F.: Interventional simulation device. Patent US7520749 (2009)

Encounter-Type Haptic Feedback System Using an Acoustically Manipulated Floating Object

Takuro Furumoto[✉], Yutaro Toide, Masahiro Fujiwara,
Yasutoshi Makino, and Hiroyuki Shinoda

The University of Tokyo, Chiba 277-8561, Japan
{furumoto,toide}@hapis.k.u-tokyo.ac.jp,
Masahiro_Fujiwara@ipc.i.u-tokyo.ac.jp,
{yasutoshi_makino,hiroyuki_shinoda}@k.u-tokyo.ac.jp

Abstract. This paper proposes a novel encounter-type haptic feedback system for virtual reality (VR) utilizing a balloon that can move around in three dimensional space. By locating a balloon at a position corresponding to that of virtual object, the user wearing a head mounted display feels a contact sensation when his or her hand touches a virtual object. The balloon is remotely actuated by applying acoustic radiation pressure. The users can touch a VR object directly by their hands or via controllers or rods. We constructed a prototype system and conducted a preliminary experiment.

Keywords: Encounter-type haptic feedback · Airborne ultrasound · Floating object · Virtual reality

1 Introduction

A contact sensation is indispensable for virtual reality (VR) for its users to naturally interact with its contents. Many approaches have been proposed to achieve a natural contact sensation.

Encounter-type haptic feedback [1–3] is one approach to present a natural contact sensation of an object in a virtual world or in a remote place. Encounter-type device presents a contact sensation by controlling a real proxy object so that it touches the user only when he or she touches a virtual object. Conventionally, a proxy object is controlled by a robot arm [1, 2] or is implemented in an exoskeleton [3].

In this paper, we propose a novel encounter-type haptic feedback system utilizing a balloon whose position is synchronized with the position of a virtual object (Fig. 1). The balloon is manipulated in three dimensional space using airborne ultrasound. Therefore, the proposed system can present a contact sensation anywhere in three dimensional space without mechanical actuation.

The feature of the system is that it does not require users to wear special haptic devices. This allows a user to move their hands in a wide range. In comparison with midair haptics using ultrasound [4–6] or air flow [7], the proposed system requires only several small devices to cover a large workspace.
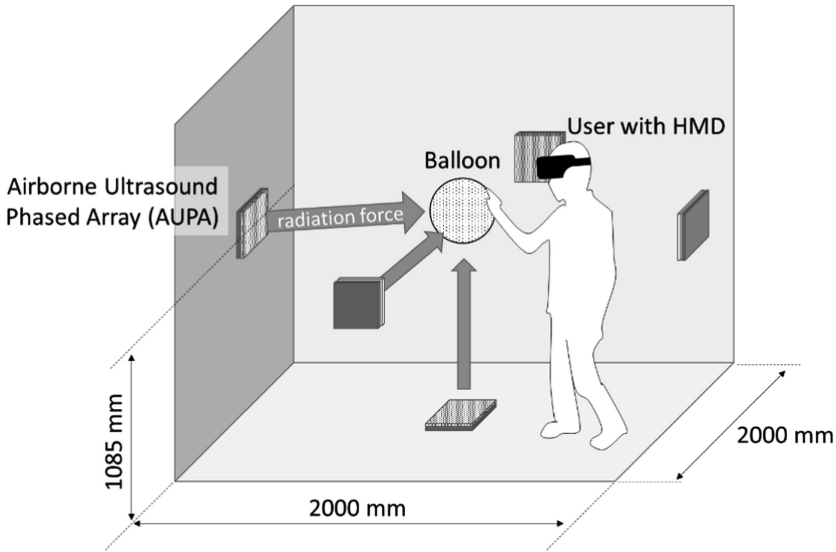
Fig. 1. System overview.

2   System Configuration

The proposed system presents a contact sensation consistent with VR image by controlling a position of a balloon to the corresponding position of the virtual object. The proposed system consists of two subsystems: a VR image output subsystem and a floating object position control subsystem (Fig. 2). The VR image output subsystem renders a virtual world and user's virtual hands using Unity and Leap Motion, and displays the virtual world to the users through a head mounted display (HMD). The floating object control subsystem deliver the balloon to the position corresponding to that of the virtual object. It actuates the balloon using acoustic radiation pressure generated by airborne ultrasound phased array devices [4]. The balloon is stabilized by a PID feedback controller based on its position observed by Kinect v2. To synchronize a balloon and a virtual object, the position of the virtual object is transformed from VR space coordinates to real space coordinates and is send to the position control subsystem in real time. Through the above process, a user gets a contact sensation from a floating object when he or she touches a virtual object image displayed by the HMD at an arbitrary 3D position.

We constructed a prototype and conducted a preliminary experiment in which the user interacted with a spherical object in VR space (Fig. 3). All procedures performed in the experiment involving human participants were in accordance with the ethical standards of the institutional research committee and with the 1964 Helsinki declaration and its later amendments or comparable ethical standards. Informed consent was obtained from all individual participants included in the study. The figure demonstrates that the user encountered a balloon when he approached to the virtual sphere.
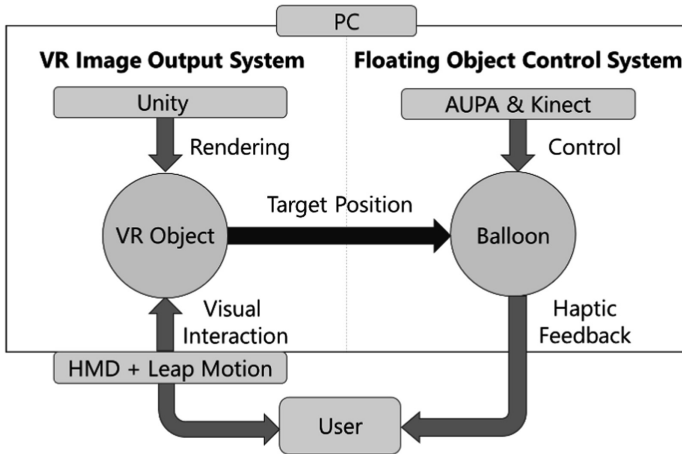
Fig. 2. System configuration.

Fig. 3. Haptic feedback by the proposed system.

References

1. McNeely, W.A.: Robotics graphics: a new approach to force feedback for virtual reality. In: Proceedings of IEEE Virtual Reality Annual International Symposium, pp. 336–341 (1993)
2. Tachi, S., Maeda, T., Hirata, R., Hashimoto, H.: A constriction method of virtual haptic space. In: Proceedings of the 4th International Conference on Artificial Reality and Tele-Existence, pp. 131–138 (1994)

3. Nakagawara, S., Kajimoto, H., Kawakami, N., Tachi, S., Kawabuchi, I.: An encounter-type multi-fingered master hand using circuitous joints. In: Proceedings of the 2005 IEEE International Conference on Robotics and Automation, pp. 2667–2672 (2005)
4. Hasegawa, K., Shinoda, H.: Aerial vibrotactile display based on multiunit ultrasound phased array. IEEE Trans. Haptics **11**(3), 367–377 (2018)
5. Hoshi, T., Takahashi, M., Iwamoto, T., Shinoda, H.: Noncontact tactile display based on radiation pressure of airborne ultrasound. IEEE Trans. Haptics **3**(3), 155–165 (2010)
6. Carter, T., Seah, S.A., Long, B., Drinkwater, B., Subramanian, S.: UltraHaptics: multi-point mid-air haptic feedback for touch surfaces. In: Proceedings of the 26th Annual ACM Symposium on User Interface Software and Technology (UIST 2013), pp. 505–514. ACM, New York (2013)
7. Poupyrev, R.S., Glisson, M., Israr, A.: AIREAL: interactive tactile experiences in free air. ACM Trans. Graph. **32**(4), 134 (2013)

Development of a Rigidity and Volume Control Module Using a Balloon Filled with Dilatant Fluid

Saizoh Kojima[✉], Hiroaki Yano, and Hiroo Iwata

University of Tsukuba, 1-1-1 Tennodai, Tsukuba, Ibaraki, Japan
s_kojima@vrlab.esys.tsukuba.ac.jp

Abstract. In this paper, a rigidity and volume-changing device is proposed for presenting the shape and rigidity of a virtual object in the real world. This device comprises a balloon filled with a dilatant fluid and two syringes connected to electric linear actuators. The electric linear actuators enables controlling the volume of the balloon by allowing the user to change the amount of dilatant fluid in the balloon. Moreover, when the amount of fluid (water) contained in the balloon changes, the rigidity of the balloon changes in proportion to the composition of the fluid (ratio of the amount of water and starch). In this study, a prototype system was developed, and the performance of the system was evaluated by measuring the rigidity of the balloon at different volumes.

Keywords: Virtual reality · Haptic display · Dilatant fluid

1 Introduction

In the process of object recognition, a human identifies an object through visual and auditory information and haptic sensation. Haptic sensation conveys information regarding the shape, texture, and rigidity of the object, which is essential for realizing that the object physically exists. Various devices/interfaces have been developed to produce haptic sensations. In our laboratory, studies on three-dimensional shape-changing haptic interfaces using a balloon array have been conducted, and it is possible to control the outer surface and rigidity distribution of the balloon array for representing a three-dimensional virtual object in the real world. As the smallest units of the shape-changing interface were spherical balloons, the outer shape of the interface tended to become corrugated. To solve this issue, it is possible to form a smooth outer shape by covering the balloon array with a sheet made of elasticated silicone gel. However, as the rigidity of the sheet cannot be changed, creating an arbitrary uniform rigidity distribution inside the balloon array is difficult. In this study, we assumed that uniform rigidity and the smooth outer shape of a virtual object could be achieved by combining a thin elastic balloon and dilatant fluid with a device to control the volume of fluid in the balloon. Moreover, a user can deform the outer shape of the balloon, and the outer shape can be maintained by reducing the amount of water in the dilatant fluid. A prototype system was developed, and its performance was evaluated by measuring the rigidity of the balloon at each volume.

2   Basic Principle of Rigidity and Shape Presentation

Interacting with a virtual object in the real world is the most natural way to determine its physical characteristics, such as shape and rigidity. Through related studies that dealt with providing the shape and rigidity of a virtual object in the real world, uneven surface displays such as Feelex [1] and Inform [2] were proposed. In addition, a method using a balloon array system was proposed such as Volflex [3]. In particular, Takizawa et al. proposed a balloon array system that could simultaneously change its shape and rigidity [4]. However, as balloons have a spherical shape, the overall outer surface of the balloon array becomes corrugated. To smooth the surface, an elasticized thin sheet, such as an elastic balloon, can be applied to cover the outer shape of the balloon array. By using a thin sheet, the shape of the inner balloon array can be directly perceived by touching it (smooth shape). On the contrary, using a thick sheet, the rigidity of the sheet itself can be perceived by a user. Then, the user may perceive that he/she is touching a soft object containing other objects. In both cases, a virtual object with uniform rigidity cannot be represented (rigidity control). To solve this issue, magnetorheological [5] or electrorheological [6] fluids can be used to control rigidity. As another choice, jamming, in which the ratio of the amount of air and powder is controlled to change the resistance, can be applied [7]. However, these methods do not produce repulsive forces but plastic deformation. In addition, as powders tend to clog in narrow spaces, maintaining uniformity of the air and powder is difficult. To overcome these issues, an elastic thin sheet, like an elastic balloon filled with a dilatant fluid, was used in this study. The dilatant fluid comprised starch and water. When a force, such as squeezing by a hand, is exerted to a dilatant fluid, the water is squeezed from the fluid, increasing the fluid viscosity. Herein, it was supposed that the rigidity of the sheet could be controlled by changing the ratio of the repulsive force of the elastic sheet to the rheological resistance of the dilatant fluid. In this study, a prototype system
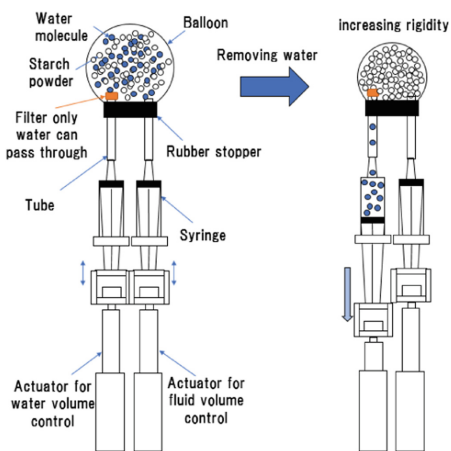
Fig. 1. Basic principle of rigidity and volume change
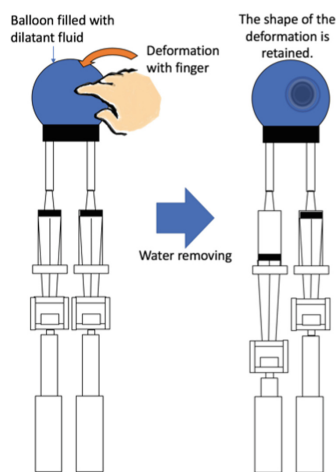
Fig. 2. Shape change by a user

was developed. The system comprises an elastic balloon and two electrically controlled syringe pumps. One of the pumps has a filter that can squeeze water from the dilatant fluid. The other controls the amount of fluid in the balloon, mainly to control the balloon volume. The pump with the filter can control the rigidity of the balloon (Fig. 1). Moreover, the balloon can maintain its shape by decreasing the amount of water inside the balloon while the user deforms it (Fig. 2).

3   System Configuration

The overall view of the prototype system is shown in Fig. 3. The size of the balloon is 50 mm in diameter and 40 mm in height. Its volume ranges from 0 (minimum) to 55 mL (maximum). The system can be roughly divided into a balloon component and a control computer (Fig. 3). Part of the balloon component is controlled by a linear actuator (ELC2F10-KP made by Orientalmotor) connected to syringes to adjust the flow of water and fluid. The stroke of the linear actuator is 100 mm, and it can move the syringe with 0.01 mm precision using the control computer.
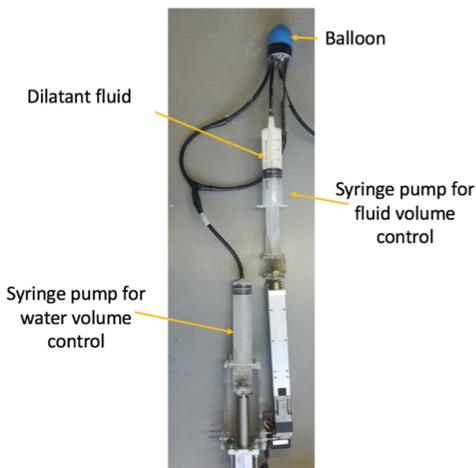
Fig. 3. Overall view of the prototype system
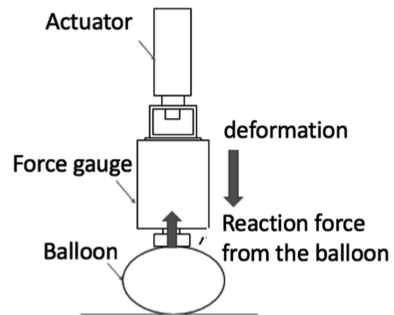
Fig. 4. Measurement of reaction force

4   Performance Evaluation of the Device

To evaluate the ability of the device to change the rigidity of the balloon by controlling the amount of water in the balloon, the reaction force from the balloon was measured using a digital force gauge with a computer-controlled linear actuator (Fig. 4). When the tip of the digital force gauge was pushed against the fluid-filled balloon, the maximum force was measured for every 1 mm of motion of the actuator up to 20 mm.

The relation between the displacement of the tip and the reaction force was measured (Fig. 5). The initial volume of the balloon was 65.45 mL. The volumes of water in the balloon were 2, 4, 6, 8, 10, 12, 14, 16, 18, and 20 mL. The spring constant, i.e. the ratio of the reaction force to the displacement of the tip of the sensor, were estimated for each condition by the least-squares method, and the estimated values are plotted in Fig. 6. For water contents greater than 8 mL, although the reaction force was proportional to the displacement, the value of the spring constant became very low, since the repulsive force caused by the elasticity of the balloon was dominant. For water contents less than 8 mL, the values of the spring constants increased owing to the resistance caused by the increasing density of the powder. In particular, when the water content was 2 mL, the reaction force increased like a plastic deformation when the displacement was larger than 17 mm. It is assumed that as the powder nearly fully occupied the space in contact with the sensor tip, a constant resistant force from the powder was mainly exerted.
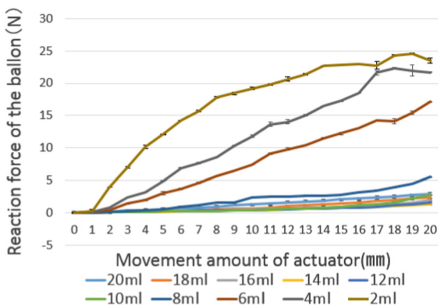
Fig. 5. Relationship between the displacement and the reaction force of the balloon
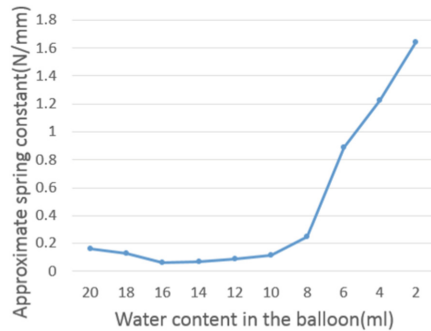
Fig. 6. Spring constant of each water content in the balloon

5   Discussion

It was confirmed that the proposed system can control the rigidity and volume of its shape. It was observed that the value of the spring constant of the balloon was proportional to the ratio of water to the amount of powder of dilatant fluid in the balloon. However, with an exerted force of over 20 N with a 2 mL water content, it behaved like a plastic object. A test subject reported that the balloon became very hard, and he felt that it was difficult to deform the balloon. For a lower water content, the balloon at times became non-uniformly rigid because the powder clogged near the filter of the syringe pump when the syringe moved quickly. A new circulation method of the fluid, such as one with a vibrating filter, should be developed for resolving the non-uniformity of the fluid.

As a future prospect, as the deformation of the balloon is completely dependent on the external force, a balloon array system will be placed inside the balloon such that the outer shape of the balloon can be controlled using the balloon array (Fig. 7). In addition, by simultaneously changing the rigidity of the inner balloons, the system can represent a virtual object, e.g., a tumor in a virtual organ. Furthermore, as practical

aspects of this system, trade-offs between the durability, dynamic range of the rigidity and shape rendering depending on the material of the balloon, amount of liquid, flow rate, and frequency of interaction should be considered.
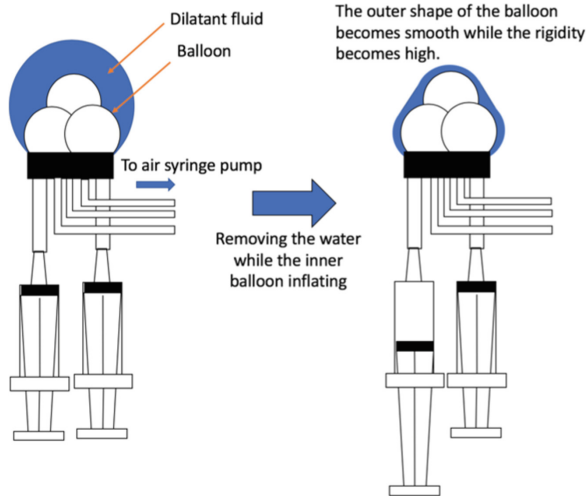
Fig. 7. Future prospect

6 Conclusion

In this study, a device capable of representing an object with arbitrary volume and rigidity in three-dimensional space has been developed. Using the dilatant fluid, it was possible to change the volume and rigidity, and the performance was evaluated by measuring the reaction force.

References

1. Iwata, H., Yano, H., Nakaizumi, F., Kawamura, R.: Project FEELEX: adding haptic surface to graphics. In: Proceeding of SIGGRAPH 2001 the 28th International Conference on Computer Graphics and Interactive Techniques, pp. 469–475 (2001)
2. Follmer, S., Leithinger, D., Olwal, A., Hogge, A., Ishii, H.: inFORM: dynamic physical affordances and constraints through shape and object actuation. In: Proceedings of UIST, vol. 13, pp. 417–426 (2013)
3. Iwata, H., Yano, H., Ono, N.: Volflex. In: Proceeding of SIGGRAPH 2005 ACM SIGGRAPH 2005 Emerging Technologies, Article No. 31 (2005)
4. Takizawa, N., Yano, H., Iwata, H., Oshiro, Y., Ohkohchi, N.: Encountered-type haptic interface for representation of shape and rigidity of 3D virtual objects. IEEE Trans. Haptics **10** (4), 500–510 (2017)

5. Kciuk, M., Turczyn, R.: Properties and application of magnetorheological fluids. J. Achiev. Mater. Manuf. Eng. **18**(1–2), 127–130 (2006)
6. Sheng, P., Wen, W.: Electrorheological fluids: mechanisms, dynamics, and microfluidics applications. Annu. Rev. Fluid Mech. **44**, 143–174 (2012)
7. Stanley, A., Gwilliam, J., Okamura, A.: Haptic jamming: a deformable geometry, variable stiffness tactile display using pneumatics and particle jamming. In: Proceedings of World Haptics Conference (WHC), 2013, pp. 25–30 (2013)

Tactile Perception Effects of Shear Force Feedback and Vibrotactile Feedback on Virtual Texture Representations

Chia-Wei Lin and Shana Smith[✉]

Department of Mechanical Engineering, National Taiwan University,
Taipei, Taiwan
{r05522631,ssmith}@ntu.edu.tw

Abstract. Nowadays, haptic feedback technology has been applied to many applications to help users acquiring more information concerning surrounding environments. In this research, a haptic feedback device was developed to combine shear force feedback and vibrotactile feedback to create realistic lateral stroking sensations to user's index fingerpad in virtual reality environments. The shear force feedback simulates the friction force which stretches the skin of the fingerpad during stroking on an object's surface, and the vibrotactile feedback simulates the surface texture information of the object in the real world. The user test shows that adding shear force feedback can increase the realism and accuracy of the virtual texture discrimination, compared with only vibrotactile feedback presented.

Keywords: Haptic feedback · Shear force feedback · Vibrotactile feedback

1 Introduction

1.1 Background

Haptic sensation is an important information for humans to explore external environments. Haptic feedback is not only important in the physical world but also in a virtual world. In a virtual reality environment, rendering realistic haptic feedback can increase the realism and immersiveness of the applications.

In the real world, when lateral stroking a physical object, human's fingerpads receive both vertical and tangential stimulation. Vertical stimulation is related to object surface texture which stimulate mechanoreceptors in human skin with vibration signals. Tangential stimulation is related to the skin stretch caused by the surface friction force.

Some prior research was conducted to simulate skin stretch caused by object weight or surface texture sensations in a virtual reality environment. For example, Minamizawa et al. [1] developed a wearable haptic device to display the weight of a virtual object. Their device can create shear force to finger when lifting a virtual object. Ikei [2] used a vibration device made by several piezoelectric actuators to simulate the texture of a virtual surface.

1.2   Motivation and Purpose

Although there was much research used vibrotactile feedback to simulate the texture of a virtual surface, the effectiveness of simulation was not consistent. For example, in Ikei's research [2], the virtual surface textures of melon and wallpaper were difficult to perceive, but lines and triangles can be perceived almost 100%. Previous research showed that some surface textures were difficult to be distinguished if only vibrotactile feedback was provided. The purpose of this research was to increase the tactile perception for similar surface textures by adding shear force feedback, in addition to the vibrotactile feedback.

2   System Architecture

In this research, a handheld device was developed for users to explore virtual surface textures with lateral stroking motions, as shown in Fig. 1. The haptic feedback device contained two modules, the shear force feedback module and the vibrotactile feedback module. The Leap Motion controller was used for tracking human hand motions. The hand motion information was used to create control signals to control the shear force feedback module and the vibrotactile feedback module. The control signals included the vibration frequency and the shear force direction.
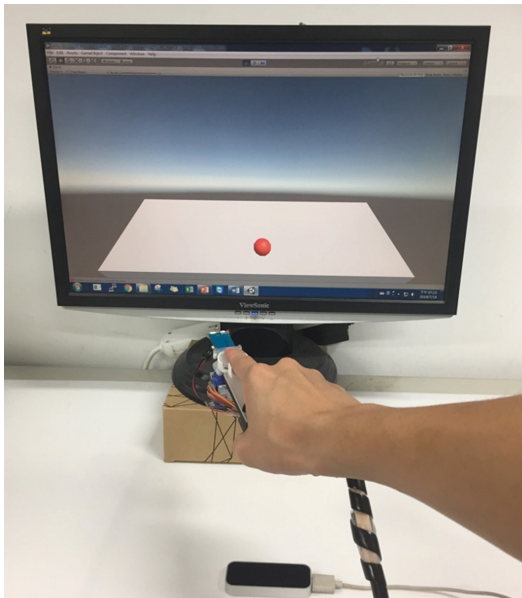
Fig. 1. The force feedback device

3   Conclusions

Two user tests were conducted. One was rendering vibrotactile feedback only, and the other one was rendering both vibrotactile feedback and shear force feedback. The user test results showed that adding shear force feedback could increase the realism and accuracy of the virtual texture discrimination, compared with only vibrotactile feedback presented. In the future, the noises of the servo motors need to be eliminated to increase the simulation accuracy.

Ethical Approval: All procedures performed in studies involving human participants were in accordance with the ethical standards of the institutional and/or national research committee and with the 1964 Helsinki declaration and its later amendments or comparable ethical standards.

Informed Consent: Informed consent was obtained from all individual participants included in the study.

References

1. Ikei, Y.: Development of realistic haptic presentation media. In: Shumaker, R. (ed.) International Virtual and Mixed Reality, VMR 2009. Lecture Notes in Computer Science, vol. 5622. Springer, Heidelberg (2009)
2. Minamizawa, K., Fukamachi, S., Kajimoto, H., Kawakami, N., Tachi, S.: Gravity grabber: wearable haptic display to present virtual mass sensation. In: ACM SIGGRAPH 2007 Emerging Technologies, Article No. 8. San Diego, CA, U.S. (2007)

Thermal-Radiation-Based Haptic Display—Laser-Emission-Based Radiation System

Satoshi Saga[✉]

Kumamoto University, Kumamoto 8608555, Japan
saga@saga-lab.org
http://saga-lab.org

Abstract. When a human places his/her hands over a source of heat, his/her hands become warm owing to thermal radiation. I propose a novel haptic display, which employs thermal radiation to display a virtual shape. A person tends to avoid a heated region at a nociceptive temperature. Using this 3 dimensional thermal control, the system displays the virtual 3-dimensional region. In this paper, I propose the laser-emission-based thermal radiation system for farther range and precise projection.

Keywords: Thermal radiation · Haptic display · Laser projector

1 Introduction

Recent years, many haptic displays are commercialized. Vibration-based haptic displays are becoming popular worldwide. Several haptic displays in mid-air are also developed. For example, Hoshi et al. [1] employed an ultrasonic phased array to produce responsive force feedback in mid-air. However, the perceptible intensity is still weak for displaying 3-dimensional region.

Fig. 1. Laser-emission-based thermal radiation system

I propose novel haptic-like display system in mid-air by using thermal-radiation. By controlling the direction and focus of this radiation, my system conveys thermal energy to a user's hand and induce nociceptive sensation (Fig. 1). Because the system uses radiation of light only, it has high controllability, displaying without any attachment on the user, larger size region display compared to conventional researches employing air-jets or ultrasonics.
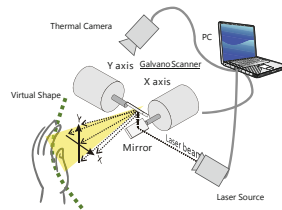
2 Thermal-Radiation-Based Haptic Display

Our system stimulates the temperature of hand around 45 °C. Therefore, the temperature adaptation occurs easily. Compared to the temperature adaptation, the pain sensation does not adapt to the stimulus [2]. By employing the difference of adaptation, I can construct a kind of haptic display.

In the first prototype, I have employed halogen lamp for the radiation source. However, the diffusive light limits the displayable range and preciseness of projecting shape. In this paper, I propose to employ laser emission for the radiation source to resolve the range and precision problem. Jun et al. [3] have researched the laser-emission-based haptic display. However, these system does not aim at showing continuous haptic information in wide range, the displayable range is limited.

Fig. 2. Area-scanning of projected laser ray

3 Laser Controlling Method

A regular laser projector emits the laser light by scanning the ray by two galvano mirrors. Based on the similar control, my system scans the thermal radiation ray and casts the ray to the displaying area (the user's palm).

This time I employed 7 W of infrared semiconductor laser emitter, which has 808 nm of wavelength. The amplitude of the emmission can be controlled by input voltage. Further, the mirrors also can be controlled by other input voltages. Here I developed a projection controller with Arduino Uno and MCP4922. By using NTSC-like interlaced scan, I realized constant heating in the squared area (Fig. 2). One scanning period of the squared area takes 40.1 ms. It is fast enough to heat up the user's palm compared to the responsiveness of human.

4 Conclusion

I research about a displaying method which employs thermal radiation to realize mid-air haptic interface. In this paper, I proposed to employ laser emmission for thermal radiation source. By using laser projection method, I developed a laser-emission-based thermal radiation display system.

References

1. Hoshi, T., Takahashi, M., Iwamoto, T., Shinoda, H.: Noncontact tactile display based on radiation pressure of airborne ultrasound. IEEE Trans. Haptics **3**(3), 155–165 (2010)
2. Zhang, X., McNaughton, P.A.: Why pain gets worse: the mechanism of heat hyperalgesia. J. Gen. Physiol. **128**(5), 491–493 (2006)
3. Jun, J.-H., Park, J.-R., Kim, S.-P., Bae, Y.M., Park, J.-Y., Kim, H.-S., Choi, S., Jung, S.J., Park, S.H., Yeom, D.-I., Jung, G.-I., Kim, J.-S., Chung, S.-C.: Laser-induced thermoelastic effects can evoke tactile sensations. Sci. Rep. **5**(11016), 1–16 (2015)

Spatiotemporal Tactile Display with Tangential Force and Normal Skin Vibration Generated by Shaft End-Effectors

Takumi Shimada[1(✉)], Yo Kamishohara[1], Vibol Yem[1],
Tomohiro Amemiya[2], Yasushi Ikei[1], Makoto Sato[1],
and Michiteru Kitazaki[3]

[1] Tokyo Metropolitan University, Hachioji, Tokyo, Japan
{shimada,yem,ikei,mkt.sato}@vr.sd.tmu.ac.jp
[2] NTT Communications Science Laboratories, Kyoto, Kanagawa, Japan
[3] Toyohashi University of Technology, Toyohashi, Aichi, Japan

Abstract. While rubbing a material, both shear force and vibration spatiotemporally occur on the skin of our finger pad. To reproduce various kind of rubbing sensation, we developed a tactile display using shaft end-effectors to spatiotemporally drive the skin of finger pad. Each shaft was connected to a DC motor and to a voice coil. When the shaft is rotated by a DC motor, the friction of the shaft tangentially move the skin. In addition, the voice coil was used to vibrate the shaft perpendicularly to the skin. There are six shafts in our present study. We conducted preliminary test to reproduce rubbing sensation of three sample materials, hemp, leather and Teflon. In the demo, participants can experience our display reproducing these material sensation. They also can adjust the amplitudes and the frequencies of tangential and normal skin vibration by comparing to the sensation of the real materials.

Keywords: Tactile display · Shaft end-effector · Tangential force · Normal vibration

1 Introduction

When we rub a material surface, the reaction force from the material stimulates our skin spatiotemporally in both tangential and normal directions. Various kinds of tactile display were developed to reproduce the rubbing sensation. A pin array and an electrotactile display can create the skin perception with normal direction [1, 2]. These devices are being used principally for providing shape sensation. However, the lack of sensation of tangential force greatly reduces the tactile information of rubbing. Actuators with high temporal resolution such as voice coil are popularly used to reproduce various kind of tactile sensation [3, 4]. Although the combination of many voice coils

can provide high spatiotemporal resolution of vibration, we considered that a shear force and tangential vibration with high spatial resolution are also required to provide tactile information of rubbing a material.

This paper introduces our tactile display that can generate shear force distribution, and tangential and normal vibration with high temporal resolution to the skin. We used six shafts as an end-effector to spatially drive the skin. Our previous studies [5, 6] investigated the characteristic sensation produced by shaft end-effectors, and the present study developed a new version of our tactile display.

2   Tactile Display

Figures 1 and 2 show the overview of our display and how the shaft end-effectors drive the skin. There are six shafts made of brass, 1 mm in diameter. The adjacent distance between each shaft is 2 mm. Each shaft is rotated by a DC motor (Maxon 260272) via an universal joint. Since a DC motor can produce high fidelity vibration [7], our display can generate spatial shear force and tangential vibration. Moreover, each shaft was also connected to a voice coil (LF040P1-S, Lead sound Corp.) in which we designed the vibration direction to be almost perpendicular to the skin. Therefore, our tactile display can spatiotemporally generate shear force, and tangential and normal vibration simultaneously.
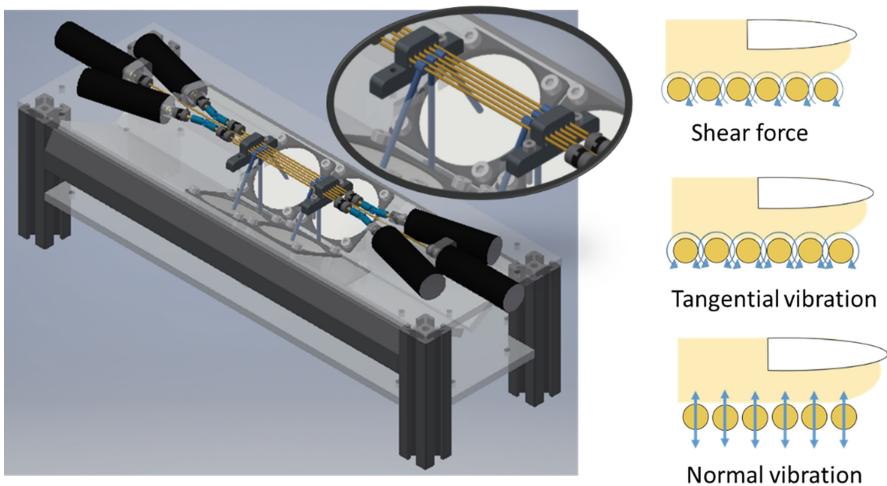
Fig. 1.   Design of our tactile display (left), and three modes for driving the skin (right)
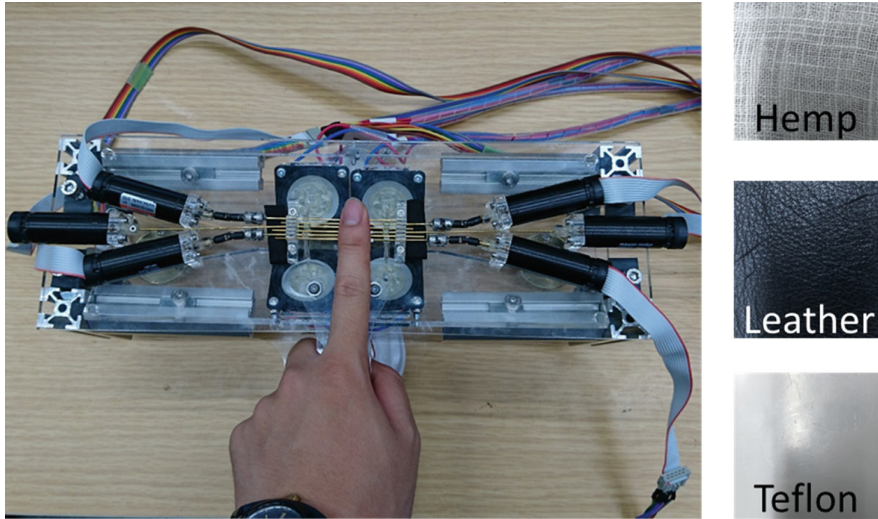
Fig. 2. Overview of demo experience (left), and three sample materials that we used in the experiments for reproducing rubbing sensation

3   Demo Experience and Conclusion

We developed a tactile display using shaft end-effectors to spatiotemporally drive the skin of finger pad in tangential and normal directions. Each shaft was connected to a DC motor and a voice coil to generate shear force as well as tangential and normal vibration. In the demo, participants can experience the rubbing sensation of at least three sample materials that were reproduced by our tactile display (Fig. 2). They can also adjust the amplitudes and the frequencies of tangential and normal skin vibration by comparing to the sensation of the real materials. Our future work will include a psychological experiment for reproducing various kinds of materials.

References

1. Wall, S.A., Brewster, S.: Sensory substitution using tactile pin arrays: human factors, technology and applications. J. Signal Process. **86**(12), 3674–3695 (2006)
2. Kajimoto, H.: Design of cylindrical whole-hand haptic interface using electrocutaneous display. In: EuroHaptics 2012, 12–15 June, vol. 2, pp. 67–72 (2012)
3. Yao, H.Y., Hayward, V.: Design and analysis of a recoil-type vibrotactile transducer. J. Acoust. Soc. Am. **128**, 619–627 (2010)
4. Minamizawa, K., Kakehi, Y., Nakatani, M., Mihara, S., Tachi, S.: TECHTILE toolkit: a prototyping tool for design and education of haptic media. In: Proceedings of the ACM Virtual Reality International Conference (VRIC 2012) (2012)

5. Yamaguchi, T., Kanai, R., Ikei, Y.: Basic characteristics of shear tactile stimulus generated by rotating contactors. In: Proceedings of ASIAGRAPH (2010)
6. Kamishohara, Y., Ikei, Y., Sato, M.: A study on a tactile display with tangential force and normal vibration. In: Proceedings of ASIAGRAPH (2017)
7. Yem, V., Okazaki, R., Kajimoto, H.: Vibrotactile and pseudo force presentation using motor rotational acceleration. In: Proceedings of Haptics Symposium, pp. 47–51 (2016)

A Haptic Feedback Touch Panel

Seung Mo Jeong[1] , Dongbum Pyo[2], Ki-Uk Kyung[1(✉)] ,
and Sungryul Yun[2]

[1] Korea Advanced Institute of Science and Technology, Daejeon,
Republic of Korea
{seungmoj,kyungku}@kaist.ac.kr
[2] Electronics and Telecommunications Research Institute, Daejeon,
Republic of Korea
{pyodb,sungryul}@etri.re.kr

Abstract. We present a haptic feedback touch panel. This actuator is capable of generating haptic stimulations, and thus can be used as a vibrotactile display. It is composed of two layers, a touch panel and a glass panel, each coated with ITO electrode. Unlike conventional vibration motors, it does not require an additional mass. The application of voltage induces electrostatic forces and consequently creates vibration. Through voltage control, vibration patterns of varying intensity and frequency can be generated. The demonstrated actuator exhibits stimulations of fast response time, and strong vibration acceleration of 5 G and normal displacement of 100 μm.

Keywords: Haptics · Vibrotactile display · Electrostatic actuator · Touch panel

1 Introduction

Haptics is a crucial technology that is embedded in most handheld devices. Taking a closer look into haptics, vibrotactile display is emerging as one of the most effective tool for stimulation. For creating such vibrotactile perception, linear electromagnetic actuators and rotary electromagnetic actuators are widely used. However, there exist drawbacks such as the need for a moving mass, and rendering constraints [1].

For these issues, devices of different actuation principles have been proposed such as Vibration Touch by Kawakami et al. [2], and SHIFT by Lee et al. [3]. One possible solution, that compensates previously mentioned drawbacks, is using electrostatic force. Given two closely placed electrodes, when voltage is input, the two electrodes attract each other due to electrical potential. Therefore, with voltage control, movement can be induced and subsequently, vibration can be generated as well [4].

We demonstrate a haptic feedback touch panel interface using electrostatic force. This interface is composed of two electrode-coated plates with air gap in between. Due to electrostatic force, when voltage is applied, the upper plate is attracted to the lower plate. Using this phenomenon, we have simulated haptic sensations of fast response and strong vibration acceleration level of 5 G.

2   Device Design and Performance

2.1   Design and Interface

The presented electrostatic actuator is composed of two layers, a top layer and a bottom layer. The top layer is a 10.1″ touch panel, with its lower side doped with a transparent electrode, indium tin oxide (ITO). The bottom layer is a glass with its upper side doped with ITO. The thicknesses of each layer are 1.5 mm and 0.7 mm, respectively. In between the two layers, spacers are placed on the boundary to prevent the layers from staying in contact. The distance between the layers is measured as 0.9 mm. For electrostatic force induction, the layers are placed so that electrode areas face each other. Figure 1 shows the overall design of the actuator. The touch panel is integrated to work with the display below. The actuator's electrodes are connected to a high voltage amplifier, which is connected to a host PC through a NI DAQ board.
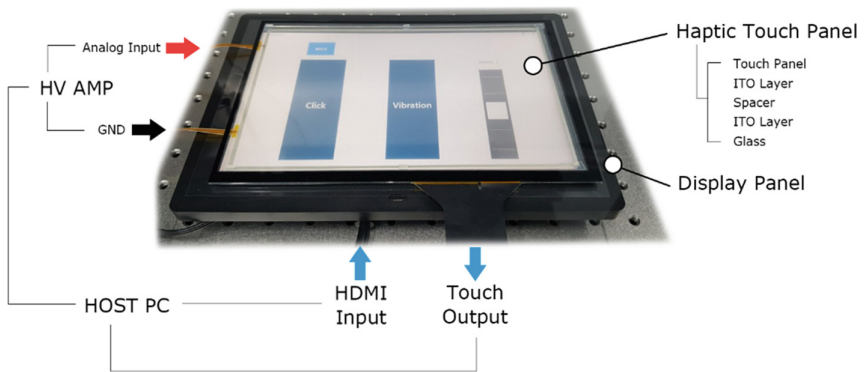
Fig. 1. Overall design of the haptic feedback actuator mounted on a conventional display panel.

The haptic interface is composed of three elements. A click button, vibration button, and intensity control slider. When a user touches one of these elements, the electrostatic actuator simulates a click or vibration with varying intensity through input voltage control. For demonstration purpose, five feedback intensity levels are chosen.

2.2   Performance

The device performance parameters are measured and shown below in Table 1.

Table 1. Measured haptic feedback actuator performance under input voltage of 4 kV.

Response time	Max. vibration acceleration	Max. vibration acceleration (@4.5 kV)	Max. vibration acceleration under 1.5N loading	Max. normal displacement amplitude
<2 ms	5 G	6 G	3 G	100 μm

The fabricated actuator has a fast response time that is less than 2 ms. The maximum vibration acceleration is reported to be 6 G at 4.5 kV input. Even under 1.5 N loading, which is a similar condition to fingertip interaction, the actuator can exert up to 3 G. In addition, the actuator undergoes maximum normal displacement amplitude of 100 μm. It is reported that human's skin has constant absolute perception thresholds of about 5 μm of deflection regardless of frequency [1]. Therefore, the haptic feedback actuator provides enough stimulus.

3   Conclusion

The fabricated device exhibits fast and strong haptic stimulations. Under 4 kV of voltage input, it has a response time of less than 2 ms, maximum vibration acceleration of 5 G, and maximum displacement of 100 μm. The actuator exerts enough force, over human's perception threshold, does not require moving mass, and renders vibration in accordance with input. Thus, the proposed interface is suitable for vibrotactile applications. Nonetheless, the haptic feedback interface has its limitations. Thus, in the future, we will work on improving electrical insulation and reducing working voltage.

References

1. Choi, S., Kuchenbecker, K.: Vibrotactile display: perception, technology, and applications. In: Proceedings of the IEEE, vol. 101, no. 9, pp. 2093–2104. IEEE (2013)
2. Kawakami, M., Mamiya, M., Nishiki, T., Tsuji, Y., Okamoto, A., Fujita, T.: A new concept touch-sensitive display enabling vibro-tactile feedback. In: Johnson, H., Nigay, L., Roast, C. (eds.) People and Computers XIII, HCI 1998, pp. 303–312. Springer, London (1998)
3. Lee, J., Lim, J.M., Shin, H., Kyung, K.U.: SHIFT: interactive smartphone bumper case. In: Isokoski, P., Springare, J. (eds.) EUROHAPTICS 2012, LNCS, vol. 7283, pp. 91–96. Springer, Heidelberg (2012)
4. Park, S., Kyung, K.U., Yun, S.R., Kim, Y.S., Lee, J.U., Park, B.J.: Film haptic system having multiple operation points. US9996199B2 (2012)

A Wearable Hand Haptic Interface to Provide Skin Stretch Feedback to the Dorsum of a Hand

Hyunwoong Choi[1], Bukun Son[1], Sangyoon Kim[1], Yonghwan Oh[2], and Jaeyoung Park[2(✉)]

[1] Seoul National University, Seoul, Korea
{alfredl224, nucktu, oiei0806}@snu.ac.kr
[2] Korea Institute of Science and Technology, Seoul, Korea
{oyh, jypcubic}@kist.re.kr

Abstract. This paper presents a glove type haptic interface that can provide cutaneous feedback to the dorsum of a user's hand. The interface consists of flex sensors, a position tracker and skin stretch modules which provides cutaneous feedback to the hand. Global position of the wrist is tracked with the position tracker and the finger posture is estimated with the flex sensors. Two skin-stretch modules installed on the dorsum of the hand behind the MCP joint of the thumb, and the middle of the index and middle fingers. Whenever there is a contact between a fingertip and a virtual object, the skin-stretch module provides cutaneous feedback by rotating a contact element toward the wrist. The skin-stretch emulates the strain of the skin occurring when a finger is pushed away by touching a real object.

Keywords: Skin stretch · Wearable · Haptic interface · Dorsum

1 Introduction

The growth of virtual reality (VR) market is prominent due to the advancements in computer vision and tracking technologies. Accordingly, there are increasing demands for a natural and intuitive user interface that can provide diverse information on VR environment. In this context, haptic interfaces are required not only to provide tactile feedback effectively but also to function in harmony with current vision/tracking technologies. So far, many of haptic researchers have focused on increasing the amount and the diversity of tactile information to a user. Such efforts have given birth to new types of haptic devices including recently introduced cutaneous haptic interfaces [1–3]. Most of the cutaneous interfaces are worn on a user's fingertip whose haptic sensitivity is highest within the human hand [4]. Thus, the fingertip haptic interface has the advantage of providing more tactile information to a user, as well as the portability as a wearable user interface. However, such fingertip haptic interfaces can be cumbersome and thus can prevent finger motions and cause fatigue. Also, the installation of a haptic device around a fingertip can hinder tracking the finger's pose with an optical sensor such as an IR sensor or an infrared LED, which is widely used in current VR

applications. Therefore, a haptic interface that can provide tactile feedback and work along with optical tracking methods is necessary considering the context of current VR technologies.

In this paper, we propose a new glove type haptic interface that can provide cutaneous feedback to the dorsum of a user's hand. As Edin and Johansson demonstrated, the skin strain sensed by SA2 type mechanoreceptors produces perceived finger posture and movement [5]. Noting this, we built a haptic interface that creates a skin stretch stimulus when a finger is bent and in contact with a virtual object. Then, the stimulus indicates a user that there is a contact between his/her fingertip and a virtual object.

2   Hand Haptic Interface to Provide Skin Stretch Feedback to the Dorsum of a Hand

In this section, we describe our proposed hand haptic interface to provide skin stretch to the dorsum of a user's hand while s/he interacts with a virtual object. Figure 1 shows the overview of the wearable haptic device where two skin stretch modules are installed right behind the metacarpophalangeal joints of thumb and the middle of index and middle fingers. We decided to install the skin stretch interface for the three fingers since they are most often used for manual object perception and manipulation [6]. A VIVE tracker (HTC, Taiwan) is installed on the device to track the position of a user's wrist and fingertip posture is estimated with a flex sensor (Spectrasymbol, U.S.A). Then, the user's fingertip position is calculated from the wrist position in the virtual space and the finger bending. When there is a contact between the virtual fingertip and a virtual object, the skin-stretch module provides a tactile feedback to indicate the user on the contact information.

Figure 2 shows the components of the skin-stretch module. A skin-stretch module was designed to stretch the skin on hand dorsum to along with/backward the direction of a finger with a servomotor (DES281BB MG, Graupner). The skin-stretch module is in the dimension of $33 \times 28 \times 26$ mm and consists of the servomotor, a pair of gears and a contact element (end effector) with silicone rubber to be in contact with the skin. The servo motor is installed on a base which is tightly fixed on the glove (Fig. 2(a)). The rotation of the servo motor is converted to the skin-stretch between a contact element and the skin (Fig. 2(b)). The nominal motion range of the contact element is 10.75 mm. The contact element (Fig. 2(c)) of the skin-stretch module is in an asymmetric shape whose radius in the direction toward the finger is larger than that in the direction toward the wrist. The asymmetry helps the fixture between the module and the skin and prevents the slip with the skin, as the contact element stretches the skin.

Figure 3 shows the skin-stretch mechanism by the contact/non-contact state between a user's fingertip avatar and a virtual object. When there is a contact between the fingertip avatar and a virtual object, the contact element is rotated backward and the skin is stretched toward the wrist, which emulates the strain of the skin when a finger is stretched by a contact with a real object.
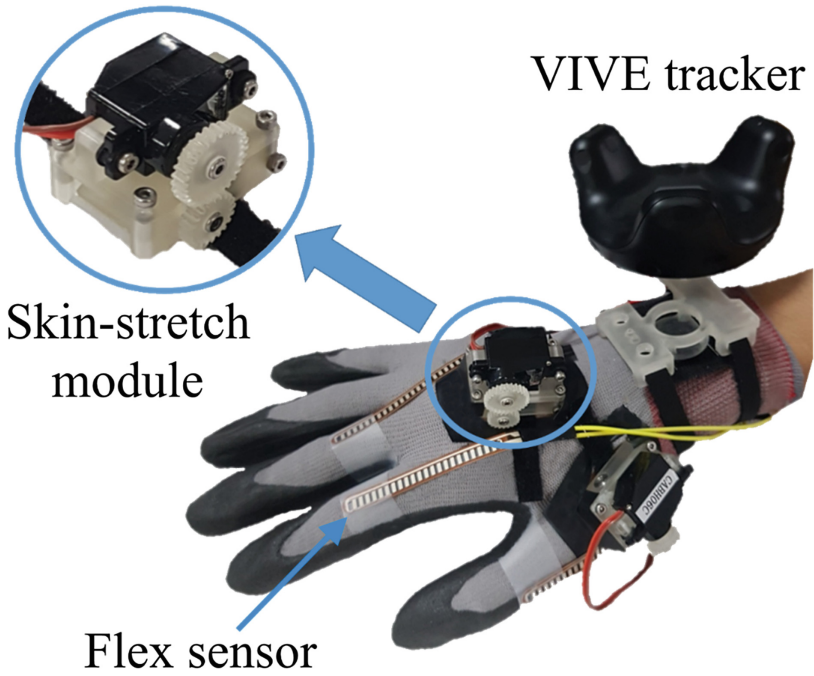
Fig. 1. A wearable skin-stretch interface to provide skin-stretch feedback to the dorsum of a hand.

(a) Trimetric view   (b) Side view   (c) Contact element
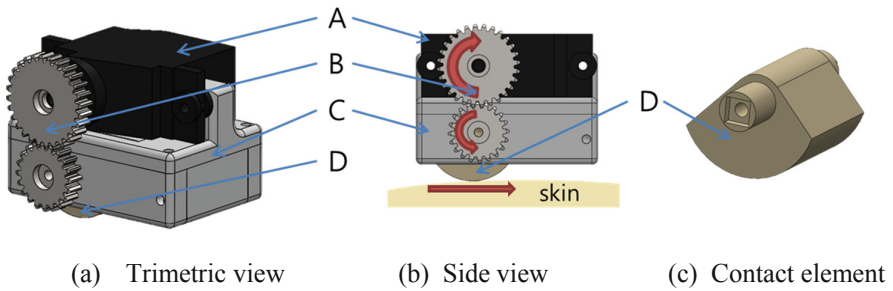
Fig. 2. The mechanical structure of a skin-stretch module to provide tactile feedback to the dorsum of a user's hand.

(a) Non-contact state   (b) Contact with a virtual object
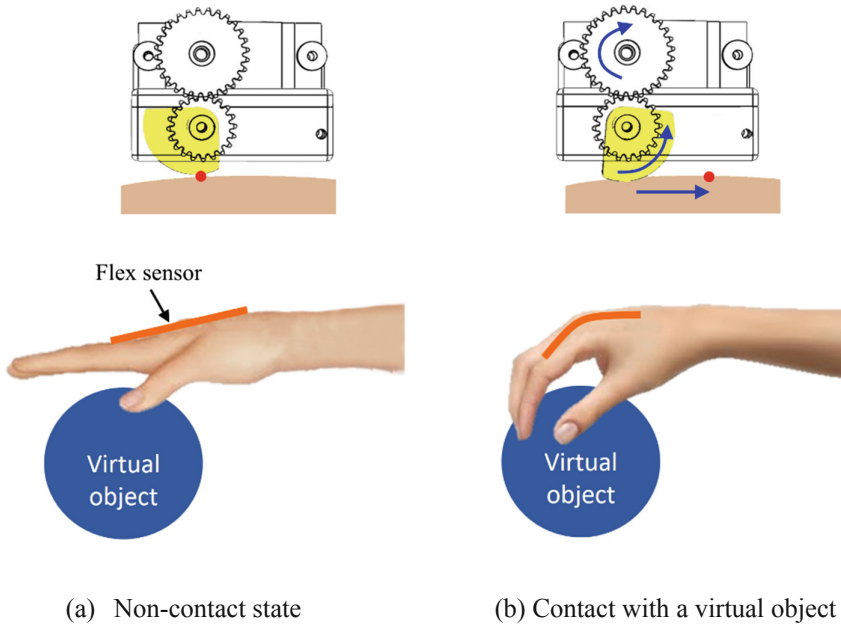
Fig. 3. Skin-stretch mechanism with/without a contact between a virtual object and a fingertip. Red circle indicates an initial contact point between the contact element and the skin.

3   Conclusion

In this paper, we proposed a glove type haptic interface which provides skin-stretch feedback to the dorsum of a user's hand. While our current design used VIVE tracker to estimate the position of the user's wrist position, we will use optical sensor to track the finger postures. Also, the effect of skin stretch feedback will be further analyzed with human subject experiment by comparing its effect with other type of haptic cues, including force feedback.

References

1. Leonardis, D., Solazzi, M., Bortone, I., Frisoli, A.: A 3-RSR haptic wearable device for rendering fingertip contact force. IEEE Trans. Haptics **10**(3), 305–316 (2017)
2. Chinello, F., Pacchierotti, C., Malvezzi, M., Prattichizzo, D.: A three revolute-spherical wearable fingertip cutaneous device for stiffness rendering. IEEE Trans. Haptics **11**(1), 39–50 (2018)

3. Yem, V., Otsuki, M., Kuzuoka, H.: Development of wearable outer-covering haptic display using ball effector for hand motion guidance. In: AsiaHaptics 2014, LNEE 277, pp. 85–89 (2014)
4. Vallbo, Å.B., Johansson, R.S.: Properties of cutaneous mechanoreceptors in the human hand related to touch sensation. Hum. Neurobiol. **13**(1), 3–14 (1984)
5. Edin, B.B., Johansson, N.: Skin strain patterns provide kinaesthetic information to the human central nervous system. J. Physiol. **487**(1), 243–251 (1995)
6. Bergamasco, M., Avizzano, C.A., Frisoli, A., Ruffaldi, E., Marcheschi, S.: Design and validation of a complete haptic system for manipulative tasks. Adv. Rob. **20**(3), 367–389 (2006)

Drone Based Kinesthetic Haptic Interface for Virtual Reality Applications

Muhammad Abdullah[1,2], Ahsan Raza[1,2], Yoshihiro Kuroda[1,2(✉)], and Seokhee Jeon[1,2]

[1] Department of Computer Science and Engineering, Kyung Hee University, Seoul, Republic of Korea
{abdullah,ahsanraza,jeon}@khu.ac.kr
[2] Graduate School of Engineering Science, Osaka University, Suita, Japan
ykuroda@bpe.es.osaka-u.ac.jp

Abstract. A drone is capable of actively generating kinetic energy and can apply force in a required direction. If a drone can interact physically with a user in a well-controlled manner, it can effectively become a haptic force feedback device. In this demonstration we will highlight the capabilities of a drone based haptic device through a bouncing ball application. Here the user can play with a virtual ball and the drone renders the impact force of the ball on the user's hand. For the scope of this demonstration during free fall, the ball is assumed in ideal 1D motion and only the force of gravity acts on the ball. The ground impact is calculated for an immovable surface and the rebound force is based on the energy conservation factor.

Keywords: Haptic interfaces · Encountered-type · Drone · Kinesthetic · Virtual reality

1 Introduction

Many conventional haptic interfaces are always tethered, either to a surface i.e. grounded or to the user i.e. ungrounded, to exert force. In case of grounded devices, the workspace is fixed and limited in space due to the mechanical restrictions of the device. Ungrounded haptic devices are connected directly to the user's body and use it for reaction support. However, this means only the "relative-force" between different parts of the body can be harnessed and passive haptic feedback is present from wearing/holding the interface. The usability of the device is remarkably decreased in both cases. To transcend the above-mentioned limitations, these design goals have to be realized:

1. The device should not be connected to the user or grounded, thus removing the need for user augmentation and mobility limitations.

2. It maintains haptic transparency in the absence of contact with virtual objects, by providing an encounter type interaction.
3. The device can be capable of furnishing an unlimited workspace, so the user can interact with a VR or AR environment without any restrictions.

An ideal drone based haptic device can achieve these goals [1–5]. There are many benefits of this concept. Mainly the system is not required to be affixed elsewhere to provide grounded-force. If the user and the drone can be tracked together, the system can provide an encountered-type interface by becoming a suitable end effector. This means it will only be coupled to the subject's hand when required and can produce absolute transparency. Since the drone is untethered, there is the possibility to create an infinite workspace, potentially increasing the usability of the system.

(a) The user feeling the impact force of the virtual ball, rendered in the upwards the user.

(b) The virtual environment as seen by direction by the drone.
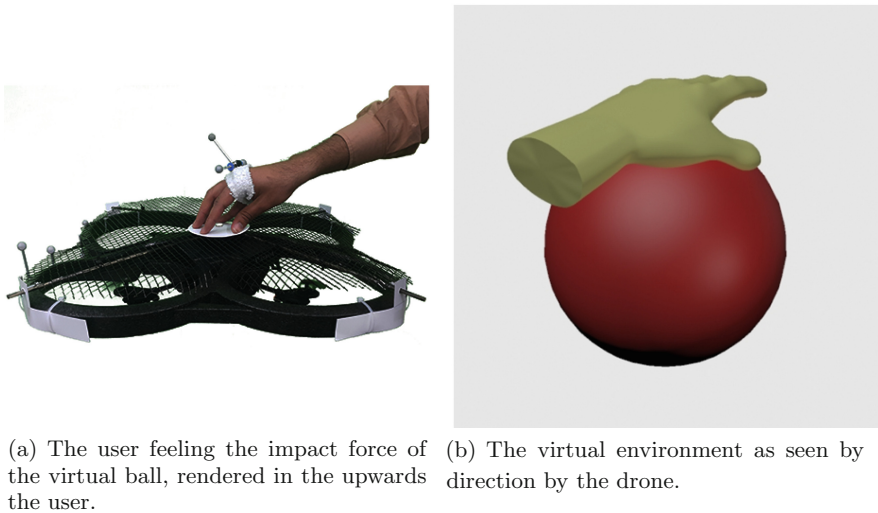
Fig. 1. The bouncing ball applications is developed by utilizing the force feedback from the device.

2   Implementation

The AR Drone 2.0 from Parrot is used in this application. The upwards motion is utilized to develop force in the respective direction. Equations developed in [1] are employed to control the force output of the drone. A safety cover designed from aluminum mesh protects the user during the interaction. The user wears an Oculus Rift headset to experience the virtual reality application. The HMD, drone and the participant's hand is tracked using the Optitrack V120 Trio motion capture system. The virtual environment is created using Unity 3D.

3   Demonstration

The demonstration explores the capabilities of a drone based haptic device. The basic concept of the bouncing ball application is shown in Fig. 1. The user is told to gently push the ball, this initiates the simulation. In the virtual environment the user can see the ball fall, hit the ground and rebound. In the real world the drone assumes a slightly lower position, waiting for the rebound phase of the simulation. Near the end of the rebound phase, the drone approaches the users hand and applies an instantaneous force based on a physics model. As the simulation ends, the drone again returns to its lower position while the ball falls away. The user may reset the simulation by touching a virtual button.

Variables such as energy conservation on ground impact, mass of the ball and value of gravity can be customized to create a unique simulation. These variables can be used to create a variety of different balls and even balloons. The bouncing ball model is a classic example of physics and is taught in many high school and undergraduate classes. By placing a force sensor on the drone, we can even measure and adjust the simulation based on the user's force.

References

1. Abdullah, M., Kim, M., Hassan, W., Kuroda, Y., Jeon, S.: HapticDrone: an encountered-type kinesthetic haptic interface with controllable force feedback: initial example for 1D haptic feedback. In: Adjunct Publication of the 30th Annual ACM Symposium on User Interface Software and Technology, pp. 115–117. ACM (2017)
2. Abdullah, M., Kim, M., Hassan, W., Kuroda, Y., Jeon, S.: HapticDrone: an encountered-type kinesthetic haptic interface with controllable force feedback: example of stiffness and weight rendering. In: 2018 IEEE Haptics Symposium (HAPTICS), pp. 334–339 (2018). https://doi.org/10.1109/HAPTICS.2018.8357197
3. Gomes, A., Rubens, C., Braley, S., Vertegaal, R.: BitDrones: towards using 3D nanocopter displays as interactive self-levitating programmable matter. In: Proceedings of the 2016 CHI Conference on Human Factors in Computing Systems, pp. 770–780. ACM (2016)
4. Knierim, P., Kosch, T., Achberger, A., Funk, M.: Flyables: exploring 3D interaction spaces for levitating tangibles. In: Proceedings of the Twelfth International Conference on Tangible, Embedded, and Embodied Interaction, pp. 329–336. ACM (2018)
5. Yamaguchi, K., Kato, G., Kuroda, Y., Kiyokawa, K., Takemura, H.: A non-grounded and encountered-type haptic display using a drone. In: Proceedings of the 2016 Symposium on Spatial User Interaction, pp. 43–46. ACM (2016)

Pneumatic Actuated Haptic Glove
to Interact with the Virtual Human

Aishwari Talhan[(✉)], Hwangil Kim, Sanjeet Kumar, Ahsan Raza,
and Seokhee Jeon[(✉)]

Department of Computer Science and Engineering, Kyung Hee University,
Deogyeong-daero, Giheung-gu, Yongin-si, Gyeonggi-do, Republic of Korea
{aishwari99,ahsanraza,jeon}@khu.ac.kr,
ghkddlf95@gmail.com, sanjeetfeb15@gmail.com

Abstract. Realistic haptic feedback of virtual human avatars would
make the virtual world more alive. In the direction of this goal, we focused
on making pneumatic actuated haptic glove to augment the perception
of human skin response. We have designed a pneumatic controlled actua-
tion with silicone-made cavities (end-effectors), which are situated at the
fingertips and the center of the palm embedded within the glove. Various
positive air pressure is used to inflate the chambers to perceive soft skins
with different shape, stiffness, and homogeneity. The palm actuator is to
provide feedback for a grasping interaction, whereas the fingertip actu-
ators are used to generate finger-based touch, e.g., pinching with two
fingers. The VR environment with the HMD is designed to improve the
immersive experience. Altogether, the system is controlled wirelessly. In
this work, we will demonstrate the various scenario of human body parts
in which the user can interact with and touch the human to perceive the
natural haptic feedback from the skin.

Keywords: Pneumatic glove · Soft haptics · Skin display ·
Augmented reality · Wearable interfaces

1 Introduction

The natural kinesthetic and tactile feedback perception through the interaction
with a virtual human body could open the new dimension in several indus-
tries, such as medical, education, and entertainment. However, creating realistic
human touch responses are complex in nature due to significant reasons: (1)
in-homogeneous structure of human body, (2) area-based nature of contact for
better realism.

Our solution in this paper is to utilize the concept of haptic augmented reality,
i.e., mixing virtual and real haptic sensation. For instance, the most important
factor for realistic skin feeling is the feeling of very gentle and smooth distribution
of pressure that surrounds the whole fingertip or palm area. Generating this kind
of feedback using currently available haptic device is very challenging since they
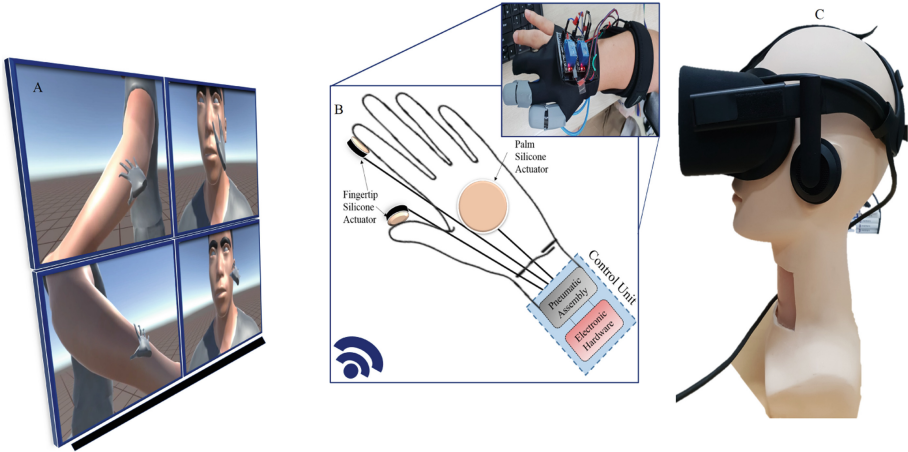
Fig. 1. Illustration of Wi-Fi enabled system architecture: (A) VR scenes (B) Haptic glove assembly (C) HMD.

usually provide point-based and tool-mediated feedback. Our approach is to completely replace the contactor or end-effector of the haptic device with skin-like material that exhibits very similar deformation characteristics as real skin, and make it only in contact with human skin when needed as a glove type. In addition, the haptic properties of the skin-like end-effector can be controllable, where we can flexibly provide different stiffness based on the internal contact dynamics simulation.

To change the haptic property of the end-effector and to control the contact force to the finger, our implementation uses pneumatic actuation with a silicone-based bladders. We also combined this actuation setup with a glove. This haptic glove is, to our best knowledge, the first attempt that is specialized for the interaction with soft skin.

2 Methodology

The most haptic gloves (including commercial) for the VR environment uses actuation techniques such as electromagnetic [1] and DC motor [2]. However, such actuation techniques may lead to unrealistic tissue-like haptic response. In the previous work [4,5], it has proven that silicone-made bladder with pneumatic actuation is capable of providing tissue like haptic feedback with realism and high-fidelity. Also, the advantages of pneumatic actuation in haptics domain are summarized in [3]. Therefore, in this project, we have designed and developed the small size, and silicone-made actuators to produce a soft response like natural skin feeling. These actuators can be embedded at the fingertips of the hand-glove to characterize the touch, palpation, and pinch. In addition, an actuator is placed at the center of the palm to represent the grasp on the human body (such as a wrist grip).

With the capability of controlling the size of the pores with variable pneumatic pressure, the system can produce soft and stiff body conditions. Moreover, the inclusion of VR scene with a head-mounted display (HMD) that is similar real human body would improve the immersiveness to the human skin touch.

2.1 System Architecture

To achieve control mentioned above, we have designed and developed a preliminary system comprising a pneumatic actuated haptic glove, a standard pneumatic and electronic hardware assembly, VR scene, and a HMD. The system is operated wirelessly. The overall components of the system are shown in Fig. 1.

3 Demonstration

Currently, the haptic glove consists of only three actuators. One is in the middle of the palm and two are at the thumb and an index finger. VR environment is created using Unity 5 and Oculus HMD. In the demonstration, we provide the real and classified skin scenarios (such as different body parts) with normal and abnormal skin conditions. The participants would able to experience immersive human touch at the various human site with the capability to perceive the natural kinesthetic and tactile feedback.

4 Future Work

In this paper, we are intended to demonstrate the preliminary system to augment the human touch using mixed reality. In the near future, we will improve the effectiveness of kin touch with precise tissue feedback such as different muscles, and stiffness like a bone. Moreover, we will characterize the system.

References

1. Avtarvr. https://www.neurodigital.es/avatarvr/
2. Sarakoglou, I., Tsagarakis, N.G., Caldwell, D.G.: A compact tactile display suitable for integration in VR and teleoperation. In: 2012 IEEE International Conference on Robotics and Automation, pp. 1018–1024, May 2012. https://doi.org/10.1109/ICRA.2012.6225248
3. Talhan, A., Jeon, S.: Pneumatic actuation in haptic-enabled medical simulators: a review. IEEE Access **6**, 3184–3200 (2018). https://doi.org/10.1109/ACCESS.2017.2787601
4. Talhan, A., Jeon, S.: Prostate tumor palpation simulator based on pneumatic and augmented haptics. Haptic Interact. Sci. Eng. Des. **432**, 353 (2017)
5. Talhan, A., Jeon, S.: Programmable prostate palpation simulator using property-changing pneumatic bladder. Comput. Biol. Med. **96**, 166–177 (2018). https://doi.org/10.1016/j.compbiomed.2018.03.010. http://www.sciencedirect.com/science/article/pii/S0010482518300611

A Novel Fingertip Tactile Display for Concurrently Displaying Texture and Orientation

Harsimran Singh[1(✉)], Sang-Goo Jeong[2], Syed Zain[2], and Jee-Hwan Ryu[2]

[1] Institue of Robotics and Mechatronics in the German Aerospace,
Wessling, Germany
harsimran.singh@dlr.de
[2] Department of Mechanical Engineering, KOREATECH,
Cheonan, Republic of Korea
{jsg1215z,zainmehdi,jhryu}@koreatech.ac.kr,
http://robot.kut.ac.kr

Abstract. Although there have been numerous researches recently on tactile device, unfortunately, research on small size finger-tip tactile device has been limited, and researches on the device that simultaneously transmit texture and orientation information of rendered objects has been even more limited. The wearable tactile device presented in this paper can transmit rotational and vibrational cues at the same time and can alleviate the spatial limitations.

Keywords: Finger-tip haptic · Tactile device · Ferrofluid · Solenoid · Neodymium magnet · Wearable

1 Introduction

The sense of touch is distributed throughout the human body and not concentrated in a specific area. Without the sense of material (texture, weight and compliance) or geometric (curvature, orientation, size) information, it would be difficult to even perform even the smallest of daily tasks. Therefore, it would be advantageous to have a tactile feedback which would enhance the human experience and also make the tasks more immersive and easier to perform, especially for applications such as telemanipulation, robotic minimally invasive surgery, virtual reality, video games.

Various haptic devices such as pin array type tactile devices [1–4] and vibration feedback devices [5–7] have been proposed. Also tactile devices that uses some mechanism to apply two or three dimensional vector force at one or more

contact points [8,9]. However, limited researches has been done on haptic devices that can be lightweight, portable and wearable at the same time, display textures and geometric information simultaneously, also exhibit high bandwidth, minimum delay and drag.

2 Design of the Ferro-Fluid Based Tactile Display

A neodymium magnet was placed inside a thin leak proof enclosure which was filled with ferro-fluid and attached to the base of human finger using Velcro. The ferro-fluid stuck to the magnet and surrounded it due to its ferrous properties, we term this neodymium magnet enclosed by ferro-fluid (NMEF). The casing was covered up using nitrile rubber keeping its flexibility and availability. In order to deliver orientation and vibrational feedback to the user an external magnetic field was required. To serve the purpose we introduced two additional actuators to our design:

- An external neodymium magnet with the same dimensions as NMEF, mounted on a small DC motor.
- A solenoid wound around the casing.
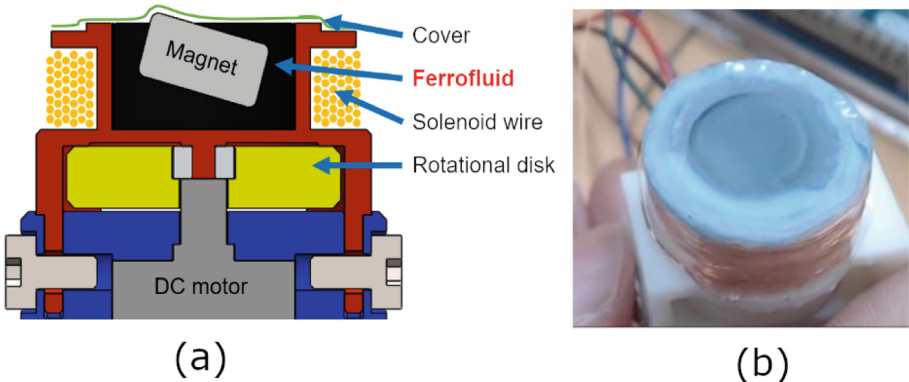
Fig. 1. Experimental prototype of ferro-fluid based tactile display.

Figure 1 shows the schematic and prototype fabricated for the ferro-fluid based wearable tactile display. Fabricated prototype has a light weight cylindrical 3D printed thin casing whose dimensions are 1.2×0.8 cm. The casing encloses a disc neodymium magnet, whose diameter is 0.8 cm and height 0.5 cm, and ferro-fluid. The orientation and vibration of the NMEF causes deformation to the user's fingertip to cue tangential shear force and texture feedback.

References

1. Yang, T., Kim, S., Kim, C.H., Kwon, D., Book, W.J.: Development of a miniature pin-array tactile module using elastic and electromagnetic force for mobile devices. In: World Haptics 2009 - Third Joint EuroHaptics Conference and Symposium on Haptic Interfaces for Virtual Environment and Teleoperator Systems, pp. 13–17 (2009)
2. Yang, G.-H., Kyung, K.-U., Srinivasan, M.A., Kwon, D.-S.: Quantitative tactile display device with pin-array type tactile feedback and thermal feedback. In: Proceedings 2006 IEEE International Conference on Robotics and Automation, ICRA 2006, pp. 3917–3922 (2006)
3. Velazquez, R., Pissaloux, E.E., Wiertlewski, M.: A compact tactile display for the blind with shape memory alloys. In: Proceedings 2006 IEEE International Conference on Robotics and Automation, ICRA 2006, pp. 3905–3910 (2006)
4. Moy, G., Wagner, C., Fearing, R.S.: A compliant tactile display for teletaction. In: Proceedings 2000 ICRA, Millennium Conference, IEEE International Conference on Robotics and Automation, Symposia Proceedings (Cat. No. 00CH37065), vol. 4, pp. 3409–3415 (2000)
5. Gemperle, F., Ota, N., Siewiorek, D.: Design of a wearable tactile display. In: Proceedings of the Fifth International Symposium on Wearable Computers, pp. 5–12 (2001)
6. Nara, T., Takasaki, M., Tachi, S., Higuchi, T.: An application of SAW to a tactile display in virtual reality. In: 2000 IEEE Ultrasonics Symposium, Proceedings, An International Symposium (Cat. No. 00CH37121), vol. 1, pp. 1–4 (2000)
7. Akhter, S., Mirsalahuddin, J., Marquina, F.B., Islam, S., Sareen, S.: A smartphone-based haptic vision substitution system for the blind. In: 2011 IEEE 37th Annual Northeast Bioengineering Conference (NEBEC), pp. 1–2 (2011)
8. Solazzi, M., Frisoli, A., Bergamasco, M.: Design of a cutaneous fingertip display for improving haptic exploration of virtual objects. In: 2010 IEEE RO-MAN, pp. 1–6. IEEE (2010)
9. Prattichizzo, D., Chinello, F., Pacchierotti, C., Malvezzi, M.: Towards wearability in fingertip haptics: a 3-DoF wearable device for cutaneous force feedback. IEEE Trans. Haptics **6**(4), 506–516 (2013)

Spatial Haptic Feedback Virtual Reality Controller for Manipulator Teleoperation Using Unreal Engine

Jae Min Lee[✉], Dong Yeop Kim, and Jung-Hoon Hwang

Korea Electronics Technology Institute,
Bucheon-si, Gyeonggi-do 14502, Republic of Korea
qhrhtm2000@keti.re.kr
http://www.keti.re.kr

Abstract. Virtual reality (VR) gives immersion to operators in teleoperated robot system, and many researchers have studied its possibility for better performance. We have studied the vision system for teleoperation, and tried to transfer visual information to the operators. In this paper, we suggested other information channel methodologies. One is haptic feedback for pinching of human operator. It presents the force of the slave robot gripper. The other is vibration motors on our hand set and elbow orthesis. They give spatial information incorporating with virtual walls. We merges these haptic feedbacks with VR Tracker, and every information is integrated to Unreal Engine for virtual reality.

Keywords: Virtual reality · Haptic feedback · Vibration cue · Teleoperation · Master (controller)

1 Introduction

Head mount display copes with many limitations of flat panel display in robot teleoperation. We have expressed it with immersion to remote space. It can give three dimensional visual information to the operator intuitively through VR system [1,2]. The information can be briefly expressed with 3D mesh (i.e. $[x, y, z, R, G, B]$).

Additionally, we add two more information on the VR controller for better usability in robot teleoperations. First, we applied haptic feedback mechanism inspired from robotic surgical systems between the thumb and forefinger. It can give the gripping information of the slave robot. Second, we embedded vibration motors on our handset and elbow orthesis. The motors gives contact information between slave robot and virtual walls.

[3] shares inspiration with us. On the other hand, its approach differs from ours, because [3] tried to transfer haptic information through inside of the hand. Our system give directional information from hand to outside space where the contact point of the robot is mapped. Accordingly, the vibration feedback is only presented when the robot contact to obstacles or other objects.

In this paper, we suggested our spatial haptic feedback controller used in VR system, and introduced its design. The main target robot is a vertical articulated robot such as UR3 of Universal Robots.

2   System Configuration

Our controller has a handset with first VIVE Tracker [4] (Fig. 1(a)), second VIVE Tracker on elbow (Fig. 1(b)), and elbow orthesis (Fig. 1(c)). The first VIVE tracker transfers six Degree of Freedom (DoF) of operator hand to end-effector of the slave robot. The vector from the second tracker to the first one is used as the approaching vector for the slave robot control. Six vibration motors cooperate each other to generate continuous spatial vibration cue.
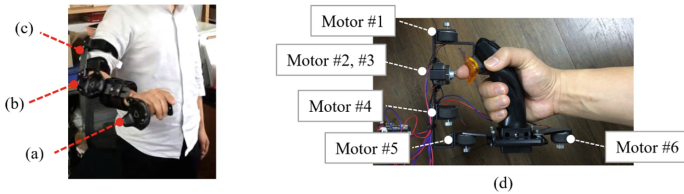
Fig. 1. (a) VIVE Tracker gives six Degree of Freedom (DoF) of operator's hand. It indicates the DoF of the slave gripper. (b) Second VIVE Tracker perceive the DoF of elbow, and it is used for redundant DoF of manipulator. (c) Elbow orthesis constraints mechanical relationship between two VIVE Trackers. (d) Six vibration motors presents haptic cue for contacting between the slave robot and virtual walls.

In the handset in Fig. 2, there is a motor mechanism to present force feedback to operator's the thumb and forefinger. We got inspired from robot surgical systems. When the slave robot grips something, the motor in the handset generates torque. The operator in virtual space recognises the object size in the gripper of the slave robot.

3   Experiments

We tested our spatial VR controller in Unreal Engine [5]. The 12 DoF from two VIVE tracker are transfered to UR3. In constrast to previous controller, there is no unintended mechanical friction (Fig. 3).

Ethical Approval. There was no participate involved subjective study.

(a)   (b)

Fig. 2. The handset of spatial haptic feedback has force feedback mechanism for operator's pinch (between the thumb and forefinger).
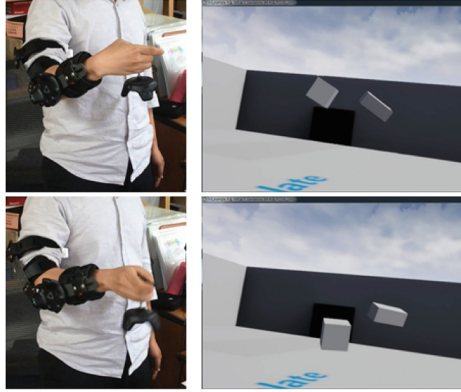
Fig. 3. Unreal Engine perceive the six DoF of the two VIVE tracker (totally, 12 DoF), and they can be used as manipulator motion input.

4   Conclusion

Spatial haptic feedback of our VR controller means that the combination of vibration motors can give the relationship information between the slave robot and virtual walls. Pinch haptic feedback is correlated with the position of gripper jaws. Two VIVE Trackers gives 12 DoF of operator's arm, and they are used for solving redundant robot kinematics problem.

References

1. Jung, Y., Kim, D.Y., Hwang, J.-H.: Realtime 3D object detection visualization using point cloud clustering in unreal engine for efficient remote robot arm control. In: Korean Society for Precision Engineering 2017 Autumn Conference, p. 308, December 2017
2. Kim, D.Y., Shin, D.-I., Hwang, J.-H., Kim, Y.-O.: Methodological comparison of visualization for tele-operated robot visual guidance. J. Inst. Control Robot. Syst. **22**(11), 877–882 (2016)
3. Ooka, T., Fujita, K.: Virtual object manipulation system with substitute display of tangential force and slip by control of vibrotactile phantom sensation. In: 2010 IEEE Haptics Symposium, pp. 215–218 (2010)

4. HTC VIVE Tracker Homepage. https://www.vive.com/us/vive-tracker/. Accessed 14 Aug 2018
5. Unreal Engine Homepage. https://www.unrealengine.com. Accessed 14 Aug 2018
6. Yang, G.-H., Jin, Y., Kang, S.: Development of vibrotactile cradle for smart cellphone providing spatial and directional cues. In: RO-MAN 2012, pp. 259–264. IEEE (2012)

2D Braille Display Module Using Rotating Latch Structured Voice Coil Actuator

Joonyeong Kim, Byung-Kil Han, and Dong-Soo Kwon[✉]

Korea Advanced Institute of Science and Technology, Daejeon,
Republic of Korea
{kimjy09l, bkhan, kwonds}@kaist.ac.kr

Abstract. A braille system for visually impaired people is valuable for acquiring information by using only tactile sense of the fingertips. However, the information can be expressed by braille is limited as characters, it's difficult to display two-dimensional information or more. In this paper, we propose a braille display module based on electromagnetism principle, and propose possibility as a portable braille pad. The module has minimized size compared to the conventional braille actuator. While satisfying dimensions of braille standards, the braille pins are arranged at equidistant intervals to be able to express two-dimensional information. In addition, the proposed module has a rotating latch structure, which minimizes the power consumption and can be applied to portable device.

Keywords: Portable braille device · 2D scalability · Miniaturization ·
Latch structure

1 Introduction

Braille is a tactile writing and reading system for visually impaired people. It is composed with embossed dots and its simple notation makes it the best way for the visually impaired people to express the characters. However, Braille actually has a low literacy rate due to its some dis-advantages: bulky and not refreshable [1]. Although refreshable braille displays have been developed for decades, they failed to popularize due to their high cost and low utilization. Because of the nature of braille which is specialized only in reading the characters, they could not express information more than one dimension. In this paper, we aim to develop a novel type of Braille display for the visually impaired people to provide the convenience of braille and to broaden the opportunity of information acquisition. The conventional braille display provided only one-dimensional information through a cell-type Braille module, we aim to develop a braille display that provides more various information of two-dimensional form by equally spacing braille pin arrays. Moreover, we propose the utilization of the module to the portable device for the visually impaired people. Although pin-array displays have been developed for decades with various principle, they do not have proper power consumption and size for portable devices [2–4]. In this paper, we propose latch structure to and demonstrate a simple array module that can be expandable as a pad display to express more various information.

2 Design and Operating Mechanism

Proposed braille display module is based on the electromagnetism principle, a voice coil and a magnet are used for operating one braille pin. Figure 1 describes the structure of the module and two states of a pin extruded and inserted. The magnet is inserted in a spin structure that can rotate vertically above the voice coil. The spin structure rotates eccentrically from the center of the steel core, allowing the magnet to effectively receive torque from the voice coil and determine the state of the pin above. The extruded structure of steel core in voice coil allows a certain distance with magnet to efficiently apply torque to the magnet. Figure 2 shows the overall appearance of braille display module of 4 by 4 array. Totally 16 pins are in a module and it is infinitely expandable. The pin-to-pin distance is 2.5 mm to meet the braille standards, the thickness of module is 5.5 mm. The regularly arranged pins can express not only the characters with braille system, also the two-dimensional information.
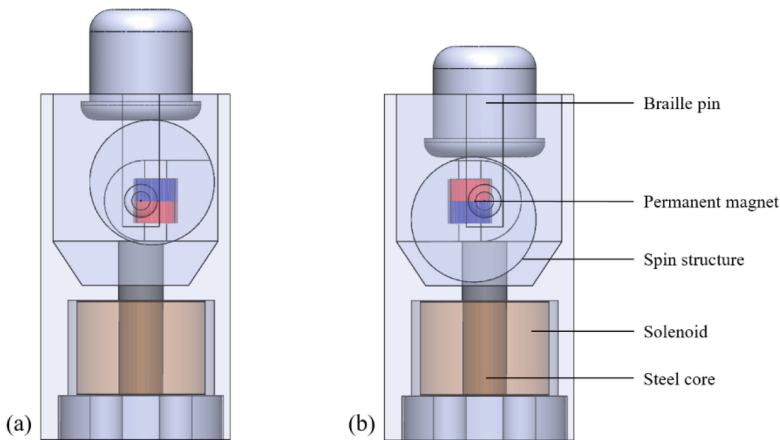
Fig. 1. Detailed structure of braille display module (a) extruded state (b) intruded state
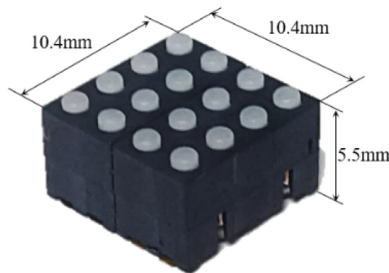
Fig. 2. Overall appearance of braille display module

3 Conclusion

In this paper, we introduced a novel braille display module that can provide two-dimensional information with equally arranged braille pins. The electromagnetism-based braille actuator with rotating latch structure has lower power consumption that it is expected to be used as a portable braille pad for the visually impaired people.

References

1. American Printing House for the Blind: Facts and Figures on Americans with Vision Loss. American Foundation for the Blind (2008)
2. Kim, S.C., et al.: Small and lightweight tactile display (SaLT) and its application. In: World Haptics 2009. Third Joint Eurohaptics Conference, 2009 and Symposium on Haptic Interfaces for Virtual Environment and Teleoperator Systems, pp. 69–74. IEEE (2009)
3. Wall, S.A., Brewster, S.: Sensory substitution using tactile pin arrays: human factors, technology and applications. Signal Process. **86**(12), 3674–3695 (2006)
4. Linvill, J.G., Bliss, J.C.: A direct translation reading aid for the blind. Proc. IEEE **54**(1), 40–51 (1966)

Conceptual Design of Soft Thin Self-sensing Vibrotactile Actuator

SiHo Ryu , Dong-Soo Choi , and Sang-Youn Kim$^{(\boxtimes)}$

Interaction Laboratory of Advanced Technology Research Center,
Korea University of Technology and Education, Cheonan, South Korea
sykim@koreatech.ac.kr

Abstract. This paper proposed a conceptual design of a soft thin self-sensing vibrotactile actuator, which can measure applied pressure and can generate haptic information. The proposed self-sensing actuator is composed of two electrodes and a bi-convex patterned PVC gel. A PVC gel, which is one of the dielectric electro-active polymers (EAPs), was fabricated by solution-casting with a wavy-patterned mold to improve sensing and vibrotactile actuation performances. The results show that the proposed self-sensing actuator effectively measures applied pressure, and generates vibration force to stimulate human mechanoreceptors.

Keywords: Multi-functional elastomer · Wearable device · Transducer

1 Introduction

Smart materials that can be deformed and responded by external stimuli such as magnetic field, temperature, electric field or light have been widely and actively studied as sensors or actuators. Among the various smart materials, ionic and non-ionic electroactive polymers (EAPs), which are observed large deformation according to an input voltage, can be a candidate for fabricating soft sensors or soft actuators [1–4]. Especially, the solvent inside the ion EAPs changes the volume of the ion EAPs while moving between the polymer electrolytes by the input voltage [5, 6]. The operating principle of the ion EAPs require a low input voltage, but they have some disadvantages such as solvent evaporation. So, unfavorably, it is not easy to implement sensors or actuators by using the ionic EAPs because of their short lifespan. On the other hand, a dielectric EAP (dEAP) as one of the non-ionic electroactive polymers have been received great attention due to fast response, high operation efficiency and particularly nonvolatile characteristics [7, 8]. Generally, the dEAPs are compressed in the thickness direction by the electrostatic pressure formed when a voltage is applied to the two compliant electrodes, which causes the dEAPs to expands in a parallel direction. Furthermore, as soon as the applied voltage is removed, the dEAPs return to its original shape. Besides, in a structure having two compliant electrodes and a dEAP, capacitance change is observed according to applied pressure. Due to these capabilities of dEAPs,

self-sensing actuators based on dEAPs have been developed. Jung *et al.* proposed a self-sensing method for dielectric elastomer based actuators [9]. Rosset *et al.* fabricated a tunable grating with self-sensing capable using an acrylic elastomer (3M VHB) [10]. Rizzello *et al.* suggested a self-sensing algorithm for better operation of dielectric EAP actuators [11]. However, these self-sensing actuators are demanded compliant electrodes and pre-stretching process. In order to overcome these problems, we propose a new soft, thin, self-sensing vibrotactile actuator without any compliant electrode or pre-stretching process. The proposed self-sensing actuator not only measure applied pressure but also convey haptic information to users.

2   The Proposed Self-sensing Vibrotactile Actuator

Figure 1 shows a schematic illustration of the proposed soft, thin self-sensing vibrotactile actuator, which can measure applied pressure and can generate haptic information. The proposed self-sensing actuator is composed of a bottom layer, a top layer with planner springs, a flexible spacer and a bi-convex patterned PVC gel as shown in Fig. 1(a). The top layer has an electrode (10×10 mm^2) and eight planar springs (Fig. 1(b)). The spacer, which has a sticky layer at both sides constantly, maintains a gap between the two electrodes. The bi-convex patterned PVC gel is used as a dielectric EAP and is fabricated by a solution casting method using Poly (vinyl chloride) (PVC) powder and acetyl tributyl citrate (ATBC) plasticizer. Each part was stacked and attached using the flexible spacer as shown in Fig. 1(b) and (c). Pressure can be measured as capacitance changing because the distance between the two electrodes (top and bottom) becomes closer than the initial state. Bi-convex patterning makes the stiffness of the PVC gel lower and influences the sensitivity and restoring behavior of the self-sensing actuator. The electrostatic force between two electrodes and the electrical-induced deformation cause vibration in the proposed self-sensing actuator.
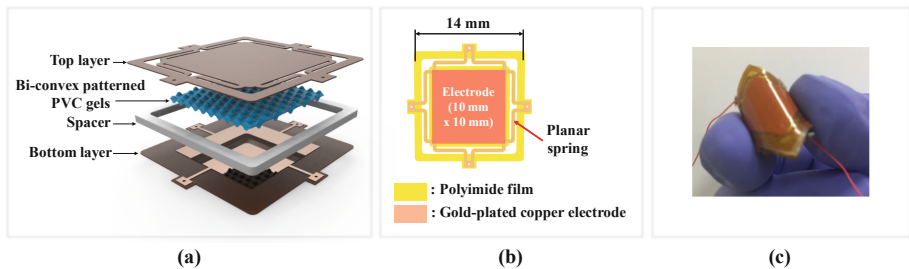
Fig. 1. The proposed self-sensing vibrotactile actuator.

3   Conclusion

In this paper, we proposed the concept of a soft, thin integrated sensor and actuator that can act as a pressure sensor or a vibrotactile actuator. If the proposed self-sensing actuator is embedded into consumer electronic devices or wearable devices, the devices not only recognize a user's input (2D or 3D touch information) but also create haptic information.

References

1. Xue, B., Qin, M., Wang, T., Wu, J., Luo, D., Jiang, Q., Li, Y., Cao, Y., Wang, W.: Electrically controllable actuators based on supermolecular peptide hydrogels. Adv. Func. Mater. **26**(48), 9053–9062 (2016)
2. Tas, S., Zoetebier, B., Sukas, O.S., Bayraktar, M., Hempenius, M., Vancso, G.J., Nijmeijer, K.: Ion-Selective Ionic Polymer Metal Composite (IPMC) actuator based on crown ether containing sulfonated poly(arylene ether ketone). Macromol. Mater. Eng. **302**(4), 1600381 (2017)
3. Bhandari, B., Lee, G.Y., Ahn, S.H.: A review on IPMC material as actuators and sensors: fabrications, characteristics and applications. Int. J. Precis. Eng. Manuf. **13**(1), 141–163 (2012)
4. Lee, H.K., Choi, N.J., Jung, S., Park, K.H., Jung, H., Shim, J.K., Ryu, J.W., Kim, J.: Electroactive polymer actuator for lens-drive unit in auto-focus compact camera module. ETRI J. **31**(6), 695–702 (2009)
5. Brunetto, P., Fortuna, L., Graziani, S., Strazzeri, S.: A model of ionic-metal composite actuators in underwater operations. Smart Mater. Struct. **17**(2), 025029 (2008)
6. Bae, J.W., Shin, E.J., Jeong, J., Choi, D.S., Lee, J.E., Nam, B.U., Lin, L., Kim, S.Y.: High-performance PVC gel for adaptive micro-lenses with variable focal length. Sci. Rep. **7**(1), 2068 (2017)
7. Duduta, M., Clarke, D.R., Wood, R.J.: A high speed robot based on dielectric elastomer actuators. In: 2017 IEEE International Conference on Robotics and Automation (ICRA), pp. 4346–4351. IEEE (2017)
8. Choi, D.S., Jeong, J., Shin, E.J., Kim, S.Y.: Focus-tunable double convex lens based on non-ionic electroactive gel. Opt. Express **25**(17), 20133–20141 (2017)
9. Jung, K., Kim, K.J., Choi, H.R.: A self-sensing dielectric elastomer actuator. Sens. Actuators A **143**(2), 343–351 (2008)
10. Rosset, S., O'Brien, B.M., Gisby, T., Xu, D., Shea, H.R., Anderson, I.A.: Self-sensing dielectric elastomer actuators in closed-loop operation. Smart Mater. Struct. **22**(10), 104018 (2013)
11. Rizzello, R., Naso, D., York, A., Seelecke, S.: A self-sensing approach for dielectric elastomer actuators based on online estimation algorithms. IEEE/ASME Trans. Mechatron. **22**(2), 728–738 (2017)

Conceptual Design of Soft and Transparent Vibrotactile Actuator

Dong-Soo Choi and Sang-Youn Kim[✉]

Interaction Laboratory of Advanced Technology Research Center,
Korea University of Technology and Education, Cheonan, South Korea
sykim@koreatech.ac.kr

Abstract. This paper reports a soft and transparent vibrotactile actuator which can be easily embedded into small wearable devices. When AC voltage is applied to the actuator, the electroactive polymer gets charged and then generates vibration. Vibration mechanism and experiment results for suggested vibrotactile actuator are explained.

Keywords: Dielectric elastomer · Wearable device · Electroactive polymer

1 Introduction

Recently, the paradigm of electronic devices is shifting from rigid devices to flexible and deformable devices for their advantages, such as bendable, conformal shaped, elastic, light weight, and etc. To successfully shifting from current rigid devices to flexible and deformable devices, a flexible touch screen, a flexible electronics, and a flexible battery have been recently introduced and developed, and furthermore, flexible and deformable devices have been being studied to provide better affordance to users by altering their shapes. Such the deformable and flexible devices can be more easily shaped into any desired form if vibrotactile actuators should be designed to have good flexibility. Thus, flexible and bendable vibrotactile actuators can highlight the strength of the deformable and flexible devices.

One of the promising candidate materials for flexible and bendable vibrotactile actuators is electroactive polymers [1–4]. There are two types of EAPs which are divided into ionic and non-ionic EAPs. In an ionic EAP, the mobility or diffusion of ions inside the polymer causes its actuation. Even though the ionic EAP requires low input voltage to induce the actuation, it needs to maintain wetness. In other words, ionic EAP requires additive protective layers in order to be operated in open-air conditions. Another disadvantage is that its actuation force is not sufficient to stimulate human's mechanoreceptors and its response time is too slow to create haptic sensation in real-time.

To create strong force in real-time in open-air condition, many researchers have turned their eyes on non-ionic EAPs. It has fast response and can create relatively large actuation forces. Furthermore, it can hold strain under DC voltage input and it has high

operation efficiency [5–7]. A non-ionic EAP (dEAP) consists of a thin dielectric film sandwiched between two compliant electrodes. When a voltage is applied to the electrodes of the dEAP, the generated electrostatic pressure compresses the dielectric film in the thickness direction, and thus the dEAP expands in planar directions. Furthermore, the dEAP returns to its original shape as soon as the applied voltage is removed. In this paper, we propose a new flexible and bendable vibrotactile actuator based on an IPN-VHB.

2 The Proposed Soft Vibrotactile Actuator

The soft vibrotactile actuator based on an IPN-VHB was fabricated by the following procedure. At first, a VHB film was stretched to 1600% (400% × 400%) using a jig, which can be extended to XY axis, and was attached to a rectangular frame. After that, trimethylolpropane trimethacrylate (TMPTMA) solution was sprayed onto both sides of the pre-stretched film. The prepared film was cured at 85 ˚C for 5 h in vacuum oven to obtain the soft vibrotactile actuator (Fig. 1).
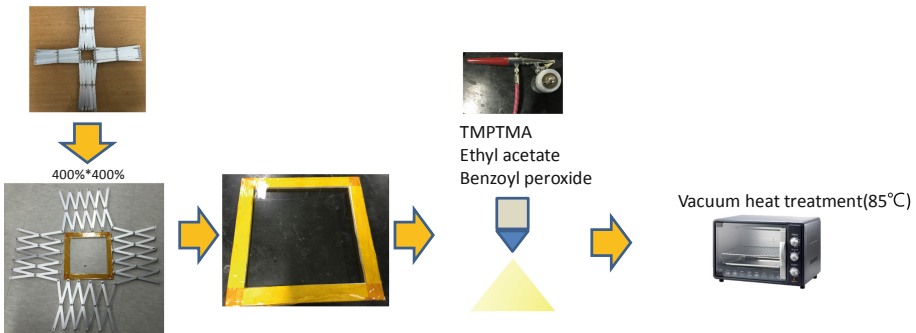
Fig. 1. The proposed self-sensing vibrotactile actuator.

We conducted a performance test in order to obtain vibrational force according to the frequency. For obtaining vibrotactile behavior of the proposed actuator, sinusoidal AC input voltage signal from a function generator was amplified by 1000 times through a high voltage amplifier. The amplified voltage was applied to the proposed vibrotactile actuator with a wide range of frequency (1 to 300 Hz). Vibration acceleration was measured with an additional 100 g mass added on the actuator. Figure 2 shows the acceleration magnitude of the proposed actuator in the frequency range of 1 to 300 Hz. The best vibration output is 0.74 g at 70 Hz.
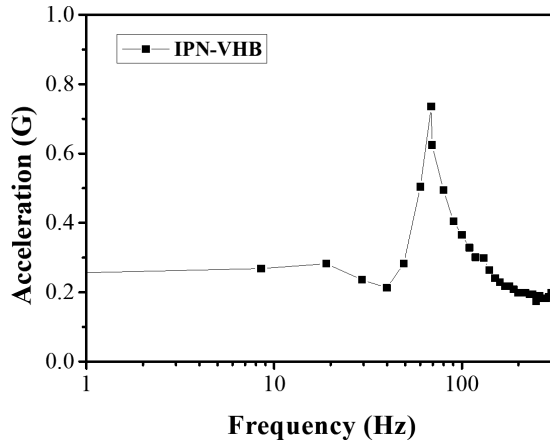
Fig. 2. The vibrotactile behavior of the proposed actuator

3 Summary

The soft and thin haptic actuator based on the IPN-VHB was suggested and its experimental results were explained. Since this vibrotactile actuator is able to vibrate with various frequencies, various haptic sensations can be generated. The suggested vibrotactile actuator based on the IPN-VHB film can be candidate for commercial haptic actuator for wearable device by improving its acceleration performance.

References

1. Xue, B., Qin, M., Wang, T., Wu, J., Luo, D., Jiang, Q., Li, Y., Cao, Y., Wang, W.: Electrically controllable actuators based on supermolecular peptide hydrogels. Adv. Funct. Mater. **26**(48), 9053–9062 (2016)
2. Tas, S., Zoetebier, B., Sukas, O.S., Bayraktar, M., Hempenius, M., Vancso, G.J., Nijmeijer, K.: Ion-selective ionic polymer metal composite (IPMC) actuator based on crown ether containing sulfonated poly (Arylene Ether Ketone). Macromol. Mater. Eng. **302**(4), 1600381 (2017)
3. Bhandari, B., Lee, G.Y., Ahn, S.H.: A review on IPMC material as actuators and sensors: fabrications, characteristics and applications. Int. J. Precis. Eng. Manuf. **13**(1), 141–163 (2012)

4. Lee, H.K., Choi, N.J., Jung, S., Park, K.H., Jung, H., Shim, J.K., Ryu, J.W., Kim, J.: Electroactive polymer actuator for lens-drive unit in auto-focus compact camera module. ETRI J. **31**(6), 695–702 (2009)
5. Duduta, M., Clarke, D.R., Wood, R.J.: A high speed robot based on dielectric elastomer actuators. In: 2017 IEEE International Conference on Robotics and Automation (ICRA), pp. 4346–4351. IEEE (2017)
6. Kim, U., Kang, J., Lee, C., Kwon, H.Y., Hwang, S., Moon, H., Koo, J.C., Nam, J.-D., Hong, B.H., Choi, J.-B.: A transparent and stretchable graphene-based actuator for tactile display. Nanotechnology **24**(14), 145501 (2013)
7. Akshita, Sampath, H., Indurkhya, B., Lee, E., Bae, Y.: Towards multimodal affective feedback: interaction between visual and haptic modalities. In: Proceedings of the 33rd Annual ACM Conference on Human Factors in Computing Systems, CHI 2015, pp. 2043–2052. ACM (2015)

Collaborating Through Magic Pens: Grounded Forces in Large, Overlappable Workspaces

Soheil Kianzad$^{(\boxtimes)}$ and Karon E. MacLean$^{(\boxtimes)}$

Department of Computer Science, University of British Columbia, Vancouver, Canada
{skianzad,maclean}@cs.ubc.ca

Abstract. We demonstrate a grounded, planar force feedback device (the Magic Pen) via applications in collaborative task coordination and learning. The pen's ballpoint drive achieves force-feedback grounding through rolling frictional contact on an arbitrary 2D surface. Its current tether provides communications and power, to be replaced in the near future with wireless and battery respectively. The ballpoint drive can render virtual features such as constraints and active guidance with no restriction on 2D workspace size or location. Together, these features give Magic Pens unique capabilities: multiple users can use them flexibly in either co-located or remote collaboration, e.g., reaching in and around one another to access the same point; and (untethered) they will be fully nomadic force feedback devices [8].

We will demonstrate a pair of Magic Pens in two collaborative scenarios:

Virtual Jigsaw Puzzle: Working together to complete a task, users experience *constraints* (e.g., board edge; repelled from a partner's piece); and *guidance* (e.g., one user can direct a partner's attention to another piece).

Virtual Electrostatic Lab: The Pen conveys electrostatic forces between charges. Multiple users can place and drag point charges in the same field, and feel the changing attractive/repulsive forces to understand their inverse square relation to separation.

Keywords: Grounded force feedback · Large workspace · Haptic stylus · Computer-supported collaborative work · Ballpoint drive · Nomadic interface

1 Introduction and Motivation

Most haptic devices must be anchored to a base in order to transfer reaction forces to the ground, via mechanical arms or cables. This static grounding constricts mobility and restricts the device's working area, for a given cost and stiffness [4].
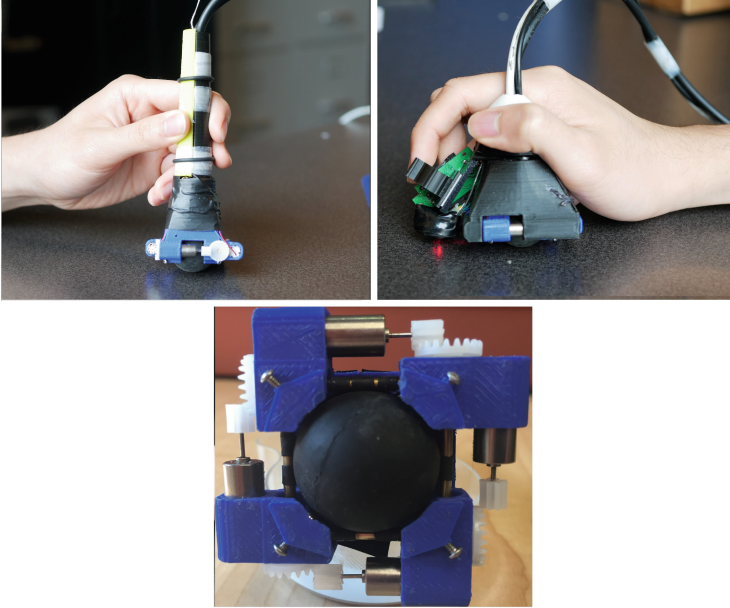
Fig. 1. Ballpoint force feedback devices. *Left:* Ball point drive; localization via a Blackberry trackball system, orientation from BNO055 (blended accelerometer, magnetometer and gyroscope data fused in three-axis roll/pitch/yaw Euler orientation output – Adafruit.com). *Right:* Version with optical mouse sensor for localization, pointing and clicking. *Center:* Four motors work in opposing pairs to roll the mouse trackball in 2D, generating velocity and/or force.

We present the Magic Pen (Fig. 1), a potentially nomadic [8] grounded force feedback device which supports large movements with local precision using a ballpoint drive mechanism [6]. This haptic stylus can generate directional 2-degree of freedom forces via frictional rolling contact on an arbitrarily large, grounded two-dimensional surface; the surface need not be flat, and the generated forces are independent of the end-effectors' location. Magic Pens are intrinsically low-cost devices, targeted originally at minimally resourced secondary school classrooms. They are comprised of 3D printed parts and low cost motors and gear drives [6].

A context where this capability will be valuable is collaborative work and joint learning, in part because multiple users can move across a large workspace and even reach across one another while feeling mutually relevant forces. In this demo, we convey this new device's capabilities in multi-user settings.

In one definition of computer-supported collaborative work (CSCW) related to collaborative *learning* (CSCL), individuals try to construct, negotiate and share meanings in a cooperative action [3]. A necessary condition is the ability to attend to and monitor joint activity. This can become a problem when the environment (e.g., a graphical user interface, or GUI) is too immersive or cluttered with excessive visual cues [10].
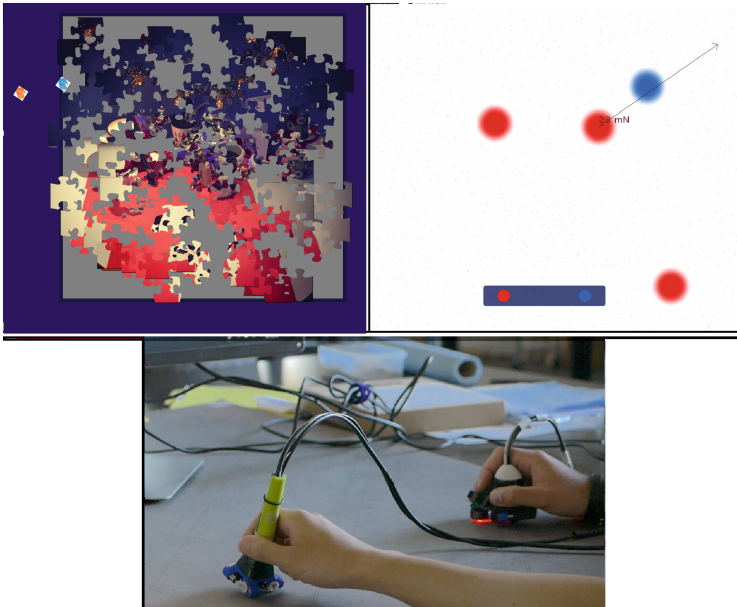
Fig. 2. Haptic-enabled collaborative learning activities. *Left: Virtual Jigsaw Puzzle (screenshot).* Each avatar (blue and orange hand icons) represents one user. Each can grab and move puzzle pieces to complete a joint task (finishing the puzzle). In this image, one user (blue hand) is placing one piece in the right place while the second user (orange hand) is being guided to the right position. *Right: Electrostatic Virtual Lab (screenshot).* Each dot shows a single point charge, negative (blue) or positive (red) which has been placed by a user. Users can select positive/negative from the menu at the screen's lower edge. In this view, one user is "holding" a red charge, while another drags a blue charge away from it, experiencing the changing force field as the distance grows. *Center: Devices.* Multiple users can use Magic Pens in large overlappble workspaces.

In such a situation, haptic feedback can be an unobtrusive channel to increase awareness of partners' presence and actions, and receive or give help [9]. It can center one or a group of users' attention around a certain manipulation location, and lower cognitive effort through unobtrusive GUI-provided constraints, particularly as the GUI changes due to partner activity.

Presentation History: The Magic Pen mechanism was first presented (oral, full paper) at HAPTICS 2018 [6], and demonstrated there in a single-user configuration with Virtual Electrostatic Lab. It has been further engineered for force feedback quality and robustness, extended to a multi-user configuration, renderings improved, and developed with additional applications.

2   Demonstration Description

Our two demonstrations (Fig. 2) are based on theories of tangible user interfaces in CSCL [1]. They are intended to show mechanisms by which Magic Pens could:

– *Motivate* students to construct an example which other classmates can experience;
– Assist students in *comprehending* a constraint or relationship;
– Promote *communication* through which students can jointly achieve the same learning goal or conclusion; and
– Enable *distribution* of roles, information and controls.

2.1   Virtual Jigsaw Puzzle

The "Jigsaw technique," introduced by Aronson et al. [2], is an accepted instantiation of CSCL where each participant has access to one aspect of a total pool of information needed to solve a task. Participants must work together to finish a task – in this case, to solve a jigsaw puzzle.

Our haptic-enabled virtual jigsaw puzzle emphasizes collaboration rather than learning gain. We constructed our jigsaw GUI using Sprite, a library that supports 2D image manipulation [7]; and for device interfaces we employed a modified version of hAPI, Gallacher et al.'s open-source tool [5].

Each participant can feel constraints (e.g., cannot pass the GUI environment's edges or acquire a partner's part). Using a non-haptic mouse, a "teacher" can apply directional forces to nudge students towards a useful place.

2.2   Virtual Electrostatic Lab

Users are asked to construct a physics example, in order to experience Coulombs law, governing attractions between point charges. One user can construct the model and move the placed charges, while the second can control the main charge with the visual information about the force (Fig. 2, *Right*: the red charge with an arrow).

To encourage negotiation between partners and thus establish a common conceptual understanding, we make it easy for them to trade roles. They can do this either by exchanging their physical pens, or swapping the position of their digital avatars.

References

1. Antle, A.N., Wise, A.F.: Getting down to details: using theories of cognition and learning to inform tangible user interface design. Interact. Comput. **25**(1), 1–20 (2013)

2. Aronson, E.: Building empathy, compassion, and achievement in the jigsaw classroom. In: Improving Academic Achievement: Impact of Psychological Factors on Education, pp. 209–225 (2002)

3. Dillenbourg, P.: What do you mean by collaborative learning? In: Cognitive and Computational Approaches, pp. 1–19. Elsevier, Oxford (1999)

4. Dominjon, L., Perret, J., Lécuyer, A.: Novel devices and interaction techniques for human-scale haptics. Vis. Comput. **23**(4), 257–266 (2007). https://doi.org/10.1007/s00371-007-0100-4

5. Gallacher, C., Ding, S.: hAPI library, February 2017. https://github.com/HaplyHaptics/hAPI. Accessed 15 Aug 2018

6. Kianzad, S., MacLean, K.E.: Harold's purple crayon rendered in haptics: large-stroke, handheld ballpoint force feedback. In: 2018 IEEE Haptics Symposium (HAPTICS), pp. 106–111, March 2018. https://doi.org/10.1109/HAPTICS.2018.8357161

7. Lager, P.: Sprite library, October 2015. http://www.lagers.org.uk/s4p/ref/index.html. Accessed 15 Aug 2018

8. Lapoehn, S., Schieben, A., Hesse, T., Schindler, J., Köster, F.: Concept of controlling the usage of nomadic devices in highly automated vehicles. IET Intell. Transp. Syst. **9**(6), 599–605 (2015). https://doi.org/10.1049/iet-its.2014.0208

9. Sallnäs, E.L., Rassmus-Gröhn, K., Sjöström, C.: Supporting presence in collaborative environments by haptic force feedback. ACM Trans. Comput.-Hum. Interact. **7**(4), 461–476 (2000). https://doi.org/10.1145/365058.365086

10. Slater, M., Wilbur, S.: A framework for immersive virtual environments (five): speculations on the role of presence in virtual environments. Presence: Teleoperators Virtual Environ. **6**, 603–616 (1997)

Haptic Application

Baby Touch: Quantifying Visual-Haptic Exploratory Behaviors in Infants of Sensory-Motor Development

Kazuki Sakurada[1(✉)], Akari Oka[1], Ritsuko Kiso[1],
Leina Shimabukuro[1], Aoba Ueno[1], and Masashi Nakatani[1,2]

[1] Environment and Information Studies,
Keio University, Tokyo, Kanagawa, Japan
{tl5435ks,mn2598}@sfc.keio.ac.jp
[2] JST PRESTO, Fujisawa, Japan

Abstract. We propose a method to quantify an infant's exploratory behavior by taking a video of his/her actions and analyzing them. Exploratory behaviors of infants are known to be necessary for the development of cognitive functions and language acquisition. Multiple studies on exploratory behaviors have been conducted; however, exploratory behaviors of infants have been commonly classified and quantified manually, requiring ample efforts. Advances in computer vision research using machine learning in recent years have made it possible to automatically analyze captured videos and register movements of the human body. In this study, we developed a measurement system that enables the quantification of exploratory behaviors of infants by combining OpenPose, OpenFace, and a computer vision library. First, we created a video-capturing environment suitable for capturing an infant's behavior. Second, we integrated the computer vision library to analyze infants fixating on and touching objects placed in front of them. As a result, we are now able to quantify some aspects of infants' exploratory behavior. Our measurement system will be useful for investigating the exploratory behavior of six to fifteen-month old children using visual-haptic modalities, and also it will also be valuable in comprehending the developmental stages of each child.

Keywords: Exploratory procedures · Child psychology · OpenPose · OpenFace

1 Introduction

An infant's exploratory behavior is known to be necessary for the development of cognitive functions and language acquisition. Developmental psychologist Jean Piaget defined representative actions that are subjectively related to the environment and objects, and infants simply exhibit these actions during the sensorimotor stage (ages: 0–2 years old) [1, 2] (Table 1). Some studies reported how exploratory behavior changes according to the development [3–7]. Ruff also showed that tactile information such as geometric and texture information object identification in infants [3, 4] (Fig. 1).
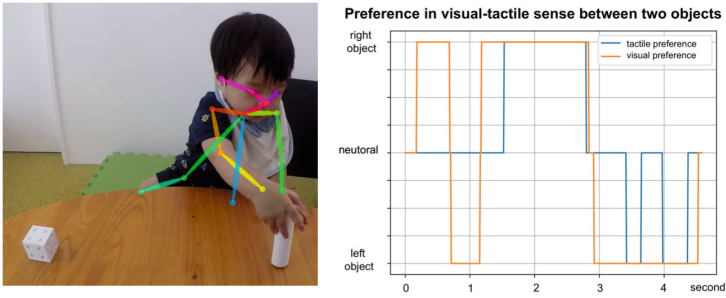
Fig. 1. Quantified exploratory behavior data using our developed system

However, when investigating these exploratory behaviors, it was necessary to classify and quantify an infant's activities by using the eyes and hands, which generated excessive workloads. Although a motion capturing system has enabled us to quantitatively evaluate daily behaviors [8], there is a concern that an infant's attention may be interrupted by optical markers that are attached to the body in a conventional optical motion capturing system.

Table 1. Sensory-motor stages proposed by Piaget [2].

Stage	Years	Acquired ability
1st stage	birth ~ 1 month	**Reflexive** … Simple reflex activity; example: kicking.
2nd stage	1 month ~ 4.5 months	**Primary Circular Reactions** … Reflective behavior becomes elaborated and coordinated; example: eye follows hand movements.
3rd stage	4.5 months ~ 9 months	**Secondary Circular Reactions** … Repeats chance actions to reproduce an interesting change or effect; example: kick crib, doll shacks, so kick crib again.
4th stage	9 months ~ 12 months	**Coordination of Secondary Schema** … Acts become clearly intentional; example: reach behind a cushion for the ball
5th stage	12 months ~ 18 months	**Tertiary Circular Reactions** … Discovers new ways to obtain the desired goal; example: pull a pillow nearer in order to get toy resting on it.
6th stage	18 months ~ 24 months	**Invention of New Means through Mental Combinations** … Invents new ways and means; example: use a stick to reach the desired object.

If a method that can automatically quantify an infant's exploratory behaviors would be developed, the difficulties faced during previous studies could be easily overcome. Since digital devices such as touch panels and smartphones are now widely used in kids raring situations, such change in the way how infants play during their childhood may affect learning process as well as manual dexterity of hands. Also if our proposed method would be achieved, we could discuss the role of kids playing in their cognitive development in both quantitatively and qualitatively.

The advancement of computer vision technology accompanied by machine learning in recent years has made it possible to quantify bodily movement by analyzing captured videos without markers [9]. By using this technique, exploratory behaviors can be quantified without impairing the infants' focus and attention.

In this study, we propose a method to quantify infant exploratory behaviors by analyzing a video automatically with computer vision.

2   System Developments

In order to quantify the exploratory behaviors of infants, we first conceived an environment to record a video. Then we developed a software system for quantifying exploratory behaviors of infants during their playing to judge whether infants while playing to determine whether infants are touching (Fig. 2 left) or looking (Fig. 2 right) at a toy.

In the environment, we have developed a filming system that shoots the behavior of infants from two angles: the front and the top. In our software, we developed the system which judges whether an infant is watching a toy or touching it.
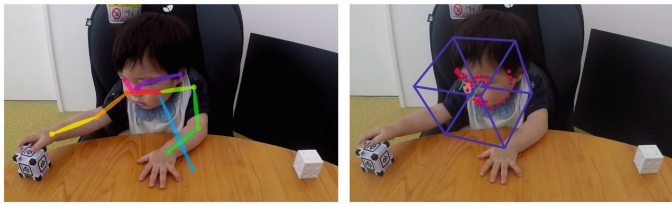
Fig. 2. Data analysis result using OpenPose (left) and OpenFace (right).

2.1   Capturing System

We used two cameras in order to capture eye gaze direction and haptic exploratory behaviors: Sony FDR-X3000 4K Action Cam for the front and Sony HDR-AS50 Action Cam for the top. The tripods were SLIK minipro 7N for the front and HUSKY #1004 four steps tripod, SIRUI sliding arm HA-77 for the top. Figure 3 shows the spatial configuration of our capturing system.
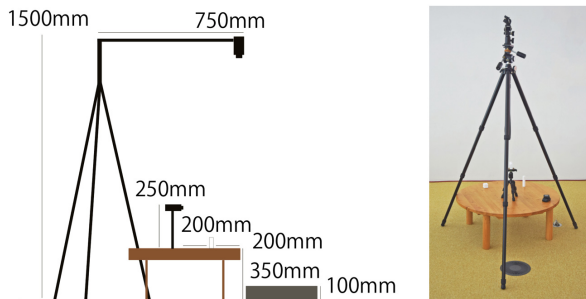
Fig. 3. Video capturing environment

2.2   Analysis Software System

In our quantification, we used OpenPose [9–11] and OpenFace [12], OpenCV [13] libraries. Data obtained from OpenPose and OpenFace was combined with the target information through OpenCV in order to determine whether an infant was taking a look at or reaching out their hand for a certain object. The specification of our PC environment was following: Intel Core i7-7820X, NVIDIA GeForce GTX1080Ti 11 GB, and Ubuntu 16.04.

3   Preliminary Experiment

We conducted a preliminary experiment to test whether our developed measurement system was capable of measuring exploratory behaviors in infants.

Experimental Apparatus
We employed similar experimental apparatus as used by Ruff [3, 4]. Based on previous study, we replicated experimental apparatus using a 3D printer (Creator Pro, FLASHFORGE) with a Poly-Lactic Acid (PLA) filament. We prepared three different cubes (concave, convex, flat) and three different cylinders (rough-textured; smooth-textured light-weighted and smooth textured heavy-weighted) for this experiment.

Task
A preferential looking method was employed in the experiment; In this method, infants had freely interacted with two experimental objects that were presented for one minute. After free exploration, an experimenter hid these objects behind a black cardboard and changed one of the two experimental objects. Subsequently, the experimenter removed the black cardboard and infants were allowed to explore the experimental objects again for 10–30 s. Based on literature, infants tend to preferentially look at a novel object rather than an old one [1].

During the experiment trials, we made a video recording of infants' exploratory behavior. The captured video was utilized offline for classifying and quantifying exploratory behavior into visual (eye directions) and tactile (hand positions) exploration.

Result
Figure 4 shows our preliminary results. Using a developed analysis software system, we were successfully able to quantify visual and tactile exploratory activities without human supervision. In this example, visual exploration started with an object on the right side and then moved into the left side, and then moved back and forth a few times. Haptic exploration followed visual exploration on the right side and then changed into an object on the left in this trial.

Ethical Approval
All procedures preformed in studies involving human participants were in accordance with the Ethical Committee of Human Experiment at Keio University, Shonan Fujisawa Campus and with the 1964 Helsinki declaration and its later amendments or comparable ethical standards.
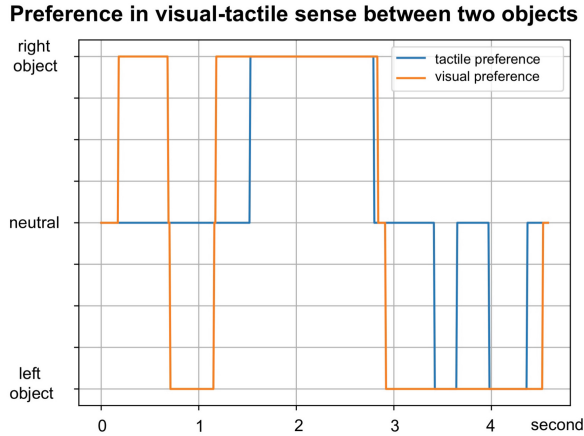
Fig. 4. An example of quantification of an infant's exploratory behaviors

4   Future Work

In this study, we reported our experimental setup and procedures for quantifying visual-tactile exploratory behavior in infants at the sensory-motor stage. We conceived a video capturing setup and confirmed that our proposed system served as an automatic annotation system by integrating open source libraries (i.e., OpenPose and OpenFace). Although it required some improvements, we believe our proposed system is capable of analyzing exploratory behavior in infants, at least for a certain experimental paradigm.

Following three items can be achieved through using our behavior capturing system. First, it is possible to investigate what type of exploratory behavior was observed in infants of six to fifteen months old. A previous study proposed that exploratory behavior is necessary for not only for perception but also cognitive development [3, 4]. Infants tended to touch and fixate an object that captured their attentions, but dominancy of visual or tactile information has not been well-studied yet. This is because it requires a lot of workloads to classify exploratory behavior of infants using manual annotation. A previous study adopted manual annotation procedures, but it has not been popular because of troublesome data analysis, and manipulation of subjective data was a concern. Our proposed system employed computer vision using machine classifications. It can guarantee a consistent analysis criteria once neural network was established. Due to its consistency, we are able to study individual differences of exploratory behavior in infants quantitatively. This technical advancement is going to facilitate the understanding of child development in cross-sectional and longitudinal studies. Some of the literature discussed that children who vigorously explore touchable objects with both vision and touch have higher Intelligence Quotient (IQ), but its mechanism is still elusive. Using our developed system, we plan to classify exploratory behavior into visual and tactile explorations and investigate whether there is a difference between infants in visual and tactual dominancy in exploratory behavior.

We plan to apply our system for several purposes. First, it's possible to quantitatively determine the development stage of each child; this is currently determined subjectively by nursery or kindergarten teachers. Second, we may be able to propose suitable playing toys based on the developmental stage. Third, it would be also possible to assist teachers in kindergartens to verbalize the developmental status of each child based on quantitative data generated by artificial neural network. As a result, we may be able to decrease the working hours of nursery or kindergarten teachers. It may be also possible to understand the developmental stage of a child at home by capturing daily playing behaviors with a webcam. With accumulating information on exploratory behavior, we may be able to understand the importance of tactile exploratory behaviors in infancy.

Contributions. K.S. and M.N. developed observation system and K.S. implemented computer vision analysis system. All authors conducted experiments and data analysis. K.S. and M.N. conceived the experiments and wrote this paper.

References

1. Vauclair, J.: Le développement du jeune enfant. Belin Sup Psycho (2004)
2. Stephens, W.B.: Piaget and inhelder—application of theory and diagnostic techniques to the area of mental retardation. Educ. Training Mentally Retarded **1**(2), 75–86 (1966)
3. Ruff, H.A.: Role of manipulation in infants' responses to invariant properties of objects. Dev. Psychol. **18**(5), 682 (1982)
4. Ruff, H.A.: Infants' manipulative exploration of objects: effects of age and object characteristics. Dev. Psychol. **20**(1), 9 (1984)
5. Ruff, H.A.: The differentiation of activity in infants' exploration of objects. Dev. Psychol. **28**(5), 851 (1992)
6. Kretch, K.S., et al.: The organization of exploratory behaviors in infant locomotor planning. Dev. Sci. **20**(4), e12421 (2017)
7. Wagner, B.S., Frost, J.L.: Assessing play and exploratory behaviors of infants and toddlers. J. Res. Child. Educ. **1**(1), 27 (1986)
8. Moeslund, T.B., et al.: A survey of computer vision-based human motion capture. Comput. Vis. Image Unders. **81**(3), 231 (2001)
9. Cao, Z., et al.: Realtime multi-person 2D pose estimation using part affinity fields. arXiv preprint arXiv:1611.08050 (2016)
10. Simon, T., et al.: Hand keypoint detection in single images using multiview bootstrapping. In: CVPR, vol. 1 (2017)
11. Wei, S.-E., et al.: Convolutional pose machines. In: Proceedings of the IEEE Conference on Computer Vision and Pattern Recognition (2016)
12. Amos, B., et al.: OpenFace: a general-purpose face recognition library with mobile applications. CMU-CS-16-118, CMU School of Computer Science, Technical report (2016)
13. Bradski, G.: The openCV library. Dr. Dobb's J. Softw. Tools **25**, 120 (2000)

Human-Agent Shared Teleoperation: A Case Study Utilizing Haptic Feedback

Affan Pervez[1], Hiba Latifee[2(✉)], Jee-Hwan Ryu[2], and Dongheui Lee[1,3]

[1] Department of Electrical and Computer Engineering,
Technical University of Munich (TUM), Munich, Germany
{affan.pervez,dhlee}@tum.de
[2] Department of Mechanical Engineering,
Korea University of Technology and Education, Cheonan, South Korea
{hibalatifee,jhryu}@koreatech.ac.kr
[3] Institute of Robotics and Mechatronics, German Aerospace Center (DLR),
Weßling, Germany

Abstract. Even though teleoperation has been widely used in many application areas including nuclear waste handling, underwater manipulation and outer space applications, the required mental workload from human operator still remains high. Some delicate and complex tasks even require multiple operators. Learning from Demonstration (LfD) through teleoperation can provide a solution for repetitive tasks, but in many cases, one task can be a combination of repetitive and varying motion. This paper introduces a shared teleoperation method between human and agent, trained by LfD through teleoperation. In the proposed method, human takes charge of uncertain or critical motion, whereas more mundane and repetitive motion could be carried out through the assistance of the agent. The proposed method has exhibited superior performance as compared to the human-only teleoperation for a peg-in-hole task.

Keywords: Teleoperation · Human-agent shared teleoperation · Cooperative teleoperation · Dynamic Movement Primitive · Learning from Demonstrations · Haptic feedback

1 Introduction

Imitating a task through observations is inherently easy for humans, but surprisingly challenging for robots. Usually, a robot has to be pre-programmed for performing different tasks. A slight change in a task or the environment requires re-programming of the robot, which can be a tedious and time-consuming process [2]. Learning from Demonstrations (LfD) provides an intuitive way to readily transfer new repetitive skills to the robots [1–3,9].

On the other hand, in shared teleoperation among multiple operators, the control authority of a slave robot is distributed among multiple operators. This provides a decrease in cognitive workload of each operator and a reliable execution of the task [5]. The issue of dividing the control authority among multiple operators with multiple Field-of-Views (FOVs) is addressed by [11]. That way, an operator can always take over partial or full authority over the task, whenever and wherever a need arises. However, utilizing multiple human operators is an economically expensive solution. Autonomous execution of a task on a robot relaxes the workload of a human operator, but the efficiency and safety in critical tasks [4,7], like performing surgeries, are thoroughly ensured when both a human and an autonomous artificial agent leverage from each other's capabilities in a shared teleoperation setting.

2   Human-Artificial Agent Shared Teleoperation

The artificial agent in our study is based on Dynamic Movement Primitive (DMP). DMP is a way to learn motor actions [10]. It can encode discrete and rhythmic movements. A separate DMP is learned for each considered Degree of Freedom (DOF). In the DMP framework, a canonical system acts as a clock. For synchronized motion of multiple DOFs, each DMP is driven by a common clock signal. The canonical system drives the second order transformed system:

$$\dot{v} = \tau\alpha_x(\beta_x(g - x) - v) + \tau a\mathcal{F}(s) \tag{1}$$
$$\dot{x} = \tau v$$

The learning of forcing term $\mathcal{F}(s)$ allows arbitrarily complex movements. For encoding the forcing terms of the autonomous DOFs, we utilize the learning approach presented in [8], as it can handle the large spatial and temporal variations intrinsic to teleoperated demonstrations for learning.

In this paper, we show that if the operator has a distorted visual perspective in certain DOFs, then those DOFs can be encoded by LfD, while the motion of the remaining DOFs can be controlled by the operator. Also, if there are certain DOFs which are highly critical for the execution of a task, then those could be assigned to the operator while the motion of other DOFs can be autonomously generated. The control flow of the proposed human-agent shared teleoperation architecture can be visualized in Fig. 1, where, for a given task, a human synchronizes his/her motion with the autonomous agent's DOFs by utilizing the visual and haptic feedback.

3   Results

3.1   Experimental Setup

Our proposed approach is evaluated using a peg-in-hole task rig with a master-slave teleoperation system. It consists of two 3-DOF Phantom haptic devices
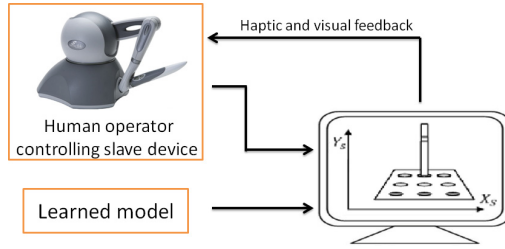
Fig. 1. Human-agent shared teleoperation.
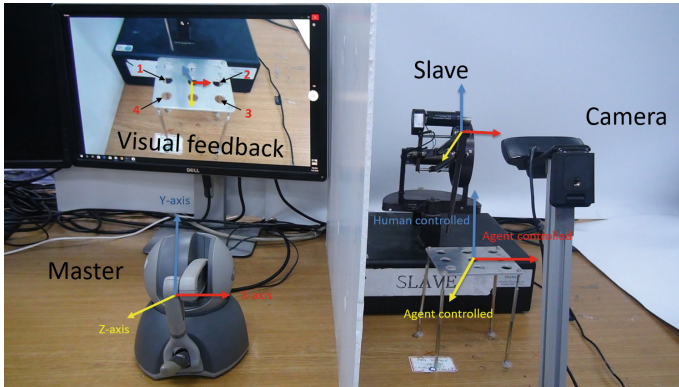
Fig. 2. Perspective distortion due to the camera position on the slave side.

(Fig. 2). A web-camera streams the visual feedback from the slave environment to the human operator with a perspective distortion, thereby inhibiting a clear visual perception to the human. The human operator controls the motion of the slave device in y-axis, whereas the artificial agent, implemented on the slave device, controls both the x and z axes of the motion. One execution cycle constitutes insertion of the slave robot end-effector into the four holes in clockwise direction, while starting and ending above the same hole.

All procedures performed in studies involving human participants were in accordance with the ethical standards of the institutional and/or national research committee and with the 1964 Helsinki declaration and its later amendments or comparable ethical standards. Moreover informed consent was obtained from all individual participants included in the study.

3.2   Discussion

For encoding the DMP, our dataset consists of slave's Cartesian positions recorded for four teleoperated demonstrations. In order to evaluate the performance of our proposed shared teleoperation approach, nine subjects participated in performing four trials of the two experiments, i.e. human-only teleoperation

and human-agent shared teleoperation. In these experiments, we evaluate the execution time, the rate of collision and the overall workload index using NASA-TLX [6] for the two settings. The plots in Fig. 3 clearly show that our human-agent teleoperation architecture slightly reduces the total execution time of the task, decreases the rate of collision and eases the mental and physical workload of the operator (NASA-TLX assessment) as compared to the human-only teleoperation.

(a)   (b)   (c)
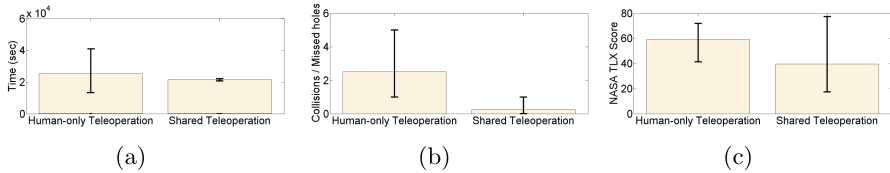
Fig. 3. Average (a) execution time, (b) rate of collision/missed holes, and (c) overall workload index of the peg-in-hole task for the two teleoperation experiments. Error bars indicate the minimum and maximum values in each experiment.

4   Conclusion

In this work, we have proposed a human-agent shared teleoperation architecture. The agent is learned through teleoperated demonstrations. The proposed approach shows significant performance improvement in circumstances where FOV deficiency as well as task's intricacy can deteriorate the efficiency when utilizing the human-only teleoperation.

References

1. Argall, B.D., Chernova, S., Veloso, M., Browning, B.: A survey of robot learning from demonstration. Robot. Auton. Syst. **57**(5), 469–483 (2009)
2. Billard, A., Calinon, S., Dillmann, R., Schaal, S.: Robot programming by demonstration. In: Springer Handbook of Robotics, pp. 1371–1394 (2008)
3. Calinon, S., Lee, D.: Learning control. In: Vadakkepat, P., Goswami, A. (eds.) Humanoid Robotics: A Reference. Springer, Heidelberg (2018)
4. Dragan, A.D., Srinivasa, S.S.: Assistive teleoperation for manipulation tasks. In: Proceedings of the Seventh Annual ACM/IEEE International Conference on Human-Robot Interaction, pp. 123–124. ACM (2012)
5. Gromov, B., Ivanova, G., Ryu, J.H.: Field of view deficiency-based dominance distribution for collaborative teleoperation. In: 2012 12th International Conference on Control, Automation and Systems (ICCAS), pp. 1990–1993. IEEE (2012)
6. Hart, S.G., Staveland, L.E.: Development of NASA-TLX (task load index): results of empirical and theoretical research. In: Advances in Psychology, vol. 52, pp. 139–183. Elsevier (1988)

7. Medina, J., Lorenz, T., Lee, D., Hirche, S.: Adaptive risk-sensitive optimal feedback control for haptic assistance, pp. 3639–3645 (2012)
8. Pervez, A., Ali, A., Ryu, J.H., Lee, D.: Novel learning from demonstration approach for repetitive teleoperation tasks. In: 2017 IEEE World Haptics Conference (WHC), pp. 60–65. IEEE (2017)
9. Pervez, A., Lee, D.: Learning task-parameterized dynamic movement primitives using mixture of GMMs. Intell. Serv. Robot. **11**(1), 61–78 (2018)
10. Schaal, S.: Dynamic movement primitives-a framework for motor control in humans and humanoid robotics. In: Adaptive Motion of Animals and Machines, pp. 261–280. Springer (2006)
11. Usmani, N.A., Kim, T.H., Ryu, J.H.: Dynamic authority distribution for cooperative teleoperation. In: 2015 IEEE/RSJ International Conference on Intelligent Robots and Systems (IROS), pp. 5222–5227. IEEE (2015)

Liquid-VR - Wetness Sensations for Immersive Virtual Reality Experiences

Kenichiro Shirota, Makoto Uju, Roshan Peiris$^{(\boxtimes)}$, and Kouta Minamizawa

Keio University Graduate School of Media Design, Yokohama, Japan
{aratanal,ujyu,roshan,kouta}@kmd.keio.ac.jp

Abstract. We propose Liquid-VR, a system that simulates wetness and liquid sensations for the whole body by providing a combination of thermal and vibrotactile stimuli from the user's face and across the upper body to the lower body. A head mounted display with thermal and vibrotactile modules simulates the wetness sensations on the face with the displayed visuals. These sensations are carried through out the body by using an array of vibrotactile modules placed on the collarbones and the feet actuated to simulate moving phantom sensations. We demonstrate this experience through virtual reality application scenarios such as being in a shower or being in side a glass of liquid.

Keywords: Wetness · Virtual reality · Liquid · HMD haptics · Full body haptics

1 Introduction

Recent research has been looking at new methods to combine multisensory feedback stimuli to enhance the immersive experiences for virtual reality applications. For example, ThermoVR [3] and AmbioTherm [4] have explored thermal and wind sensations for virtual reality scenarios.

Similarly, our previous research titled LiquidReality [2] explored presenting wetness feelings on the user's face for immersive applications. In this work, we used the neurophysiological principles that indicate that our perception of wetness sensations are through a combination of thermal (cooling) and tactile sensations [1]. As such, in LiquidReality, we used thermal and vibrotactile feedback modules integrated on a head mounted display to present co-located visual and haptic feedback for wetness sensations.

In this demonstration, we present Liquid-VR (Fig. 1), where the users are able to enjoy wetness stimuli with virtual reality. Furthermore, we introduce additional tactile modules placed on the collarbones of the user and at the feet that are able to simulate moving phantom sensations to further enhance this
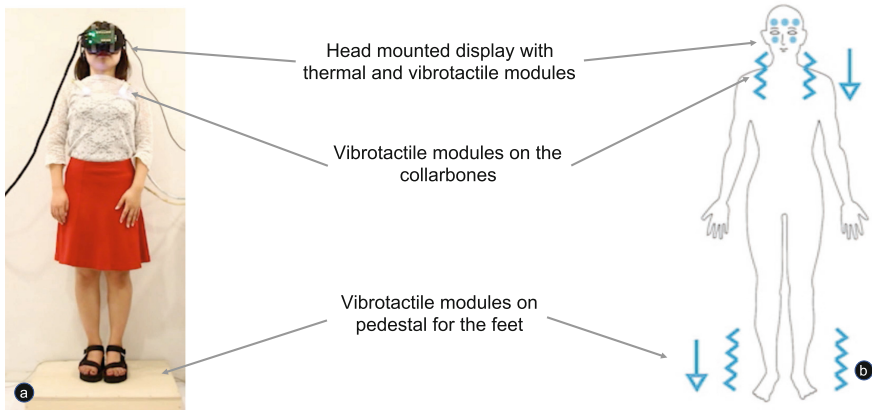
Fig. 1. (a) A user with the Liquid-VR system. (b) Combination of thermal and moving phantom vibrotactile stimuli carry out the immersive experiences for the user

experience. We identify that the combination of the thermal feedback on the face together with the vibrotactile sensations moving across from the face across the body to the feet would create the illusion of moving wetness sensations on the whole body.

2   Liquid-VR System

As depicted in Fig. 2, we used feedback provided on the face, the collarbones and the feet. For the face, we used the thermal head mounted display previously introduced in LiquidReality as the main haptic and visual feedback device. This head mounted display consists of four thermal modules that directly contacts the wearer's face. Each module is controlled by a temperature controller implemented on an Arduino Mega microcontroller[1]. In addition, we integrated two $HAPTIC^{TM}$ $Reactor$ vibrotactile[2] modules to provide tactile stimuli to the user's face through the headm mounted display as stipulated by in the LiquidReality research.

In addition, we used two of the same $HAPTIC^{TM}$ $Reactor$ modules as the actuators upperbody that were driven through Techtile toolkit amplifiers. These are encased in a 3D printed mount and attached to the collarbones of the user for maximum effect. Next, for the feet, we used two modules of the Clark Synthesis TST239 Silver Tactile Transducer[3] actuators to provide effective tactile feedback to the feet. The use of audio based tactile transducers presents the advantages of driving the actuators through relevant audio signals such as sounds of liquid streams and flows. In addition, we used two thermal modules placed on the ankles to provide thermal feedback for the feet.

---

[1] https://www.arduino.cc/en/Main/arduinoBoardMega.
[2] http://www.alps.com/prod/info/E/HTML/Actuator/.
[3] http://clarksynthesis.com/clark-synthesis-products/tactile-sound-transducers/.
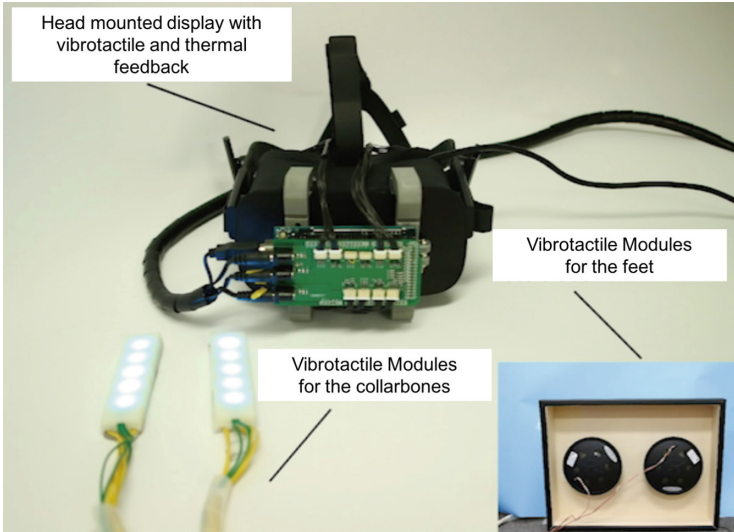
Fig. 2. The system setup of Liquid-VR consists of a head mounted display with thermal feedback modules that provide the wetness sensations, and vibrotactile modules for the collarbone and feet that provide the moving tactile sensations

3   Demonstration Experience

During our demonstration, participants will be provided various wetness scenarios such as being under a shower or (Fig. 3(a)), being inside a body of water (glass of water) (Fig. 3(b)), etc. All these scenarios are prepared in Unity3D[4] where the user will be able to interactively engage with the virtual content. The stimuli for these scenarios are synchronized with the visual content.

For the purpose of the demonstration, we will provide cold thermal stimuli to induce the wetness perception while the vibrotactile stimuli will be used to simulate events such as the splash impact on the face and flow of liquid across the body.

All procedures performed in studies involving human participants in this work were in accordance with the ethical standards of the institutional and/or national research committee and with the 1964 Helsinki declaration and its later amendments or comparable ethical standards. Informed consent was obtained from all individual participants included in this work.

---

[4] https://unity3d.com/.
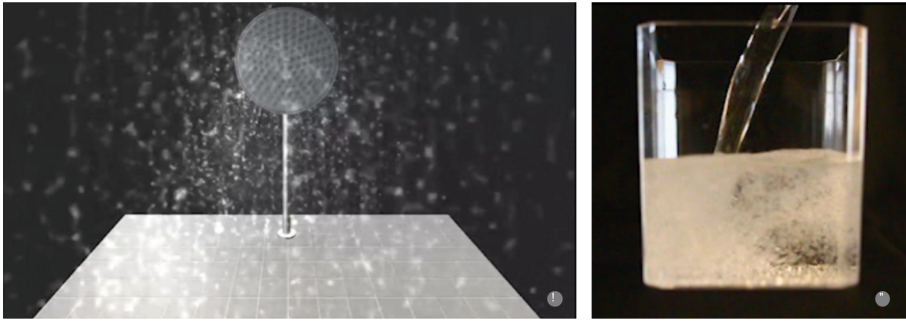
Fig. 3. Liquid-VR scenarios: (a) Shower scenario: user is able to experience a virtual shower inside a virtual bathroom scenario; (b) Soda scenario: user can experience unusual experiences such as being inside a glass of soda with the bubbles running through them

References

1. Filingeri, D., Fournet, D., Hodder, S., Havenith, G.: Why wet feels wet? A neurophysiological model of human cutaneous wetness sensitivity. J. Neurophysiol. **112**(6), 1457–1469 (2014)
2. Peiris, R.L., Chan, L., Minamizawa, K.: LiquidReality: wetness sensations on the face for virtual reality. In: Prattichizzo, D., Shinoda, H., Tan, H.Z., Ruffaldi, E., Frisoli, A. (eds.) Haptics: Science, Technology, and Applications, pp. 366–378. Springer, Cham (2018)
3. Peiris, R.L., Peng, W., Chen, Z., Chan, L., Minamizawa, K.: ThermoVR: exploring integrated thermal haptic feedback with head mounted displays. In: Proceedings of CHI 2017 (2017)
4. Ranasinghe, N., Jain, P., Tolley, D., Karwita, S., Yilei, S., Do, E.Y.L.: AmbioTherm: simulating ambient temperatures and wind conditions in VR environments. In: Proceedings of the 29th Annual Symposium on User Interface Software and Technology, UIST 2016 Adjunct, pp. 85–86. ACM, New York (2016). https://doi.org/10.1145/2984751.2985712

Deformation and Friction: 3D Haptic Asset Enhancement in e-Commerce for the Visually Impaired

Hong Jian Wong[1(✉)], Wei Kang Kuan[1], Andrew Jian Yue Chan[1], Samuel John Omamalin[1], Kian Meng Yap[1], Alyssa Yen-Lyn Ding[1], Mei Ling Soh[1], and Ahmad Ismat Bin Abdul Rahim[2]

[1] Sunway University, 5, Jalan Universiti, Bandar Sunway, 47500 Subang Jaya, Selangor, Malaysia
hjwongdrl@gmail.com,
{wei.k334,11070273,16090037}@imail.sunway.edu.my,
{kmyap,alyssad,meilings}@sunway.edu.my
[2] Telekom Research & Development Sdn. Bhd. (TM R&D), TM Innovation Centre, Cyberjaya, Malaysia
drismat@tmrnd.com.my

Abstract. The availability of Internet resources is currently restricted for the visually impaired (VI) due to the primarily visual-based information transfer methods afforded by modern connectivity devices. A haptic device was suggested in enabling the VI to feel the shape of the assets with a stylus, gaining a more concrete perception of formerly purely visual depictions of said assets. This paper describes the trials of an e-commerce website, which enables the use of this haptic technology to feel products of which VI users intend to purchase. Additional features that were recently implemented include the ability to deform products where appropriate, and frictional surfaces depending on the surface material. A majority of VI testers provided positive impressions towards the direction of development with fine-tuning necessary to improve asset deform and friction quality, while giving additional feedback for further improvements to the website.

Keywords: Visually impaired · e-Commerce · Instant force feedback · Haptics · Deformation · Friction · H3D

1 Introduction

The human brain utilizes several methods in recognizing its surroundings and the physical objects within it, one being the sense of touch. Such haptic sensations that the human somatosensory system can detect are primarily tactile and kinaesthetic sensations. Tactile sensations are the feelings of direct contact from the skin to the physical object, while the awareness of the position and movements through the stimulation of muscles and joints falls under the category of kinaesthetic sensation [1].

In the real physical world, tactile sensations can be easily initiated when human skin encounters the physical asset; while in the virtual environment, collision between virtual assets has to be detected and simulated with a haptic device, with the inclusion of friction. Furthermore, these virtual assets would have to have deformable surfaces in order to simulate kinaesthetic sensations for non-rigid physical objects, giving way in a natural manner to provide further information on their material, such as in practicing breast tumour palpation for medical training [2].

One method to simulate these sensations is with a dedicated haptic device. A haptic device provides an avenue for bidirectional-actuated human-machine interaction within a virtual environment [3]. Through the interaction between human and machine, the device acts as a medium to allow users to touch and feel 3D assets in a virtual environment in addition to manipulating them. This haptic transmission system provides utility to a broad range of fields such as medicine, education, research and training [4, 5].

However, research and products on haptic feedback interaction in e-commerce, specifically for the VI community using the haptic device, is currently in scarcity. To supplement that, we visited multiple local VI organizations and talked to IT proficient VI individuals on ways to improve website accessibility for VI individuals. With this knowledge, we customized an e-commerce site allowing VI individuals to perform transactions online, with minimal guidance from non-VI persons, and haptic-audio feedback interaction. The assets were shaped and coloured with simple material while additional deformation and friction was applied for trialing purposes.

2   Configuration

The JomJe website is a simple e-commerce site specifically catered to the VI community as seen in Fig. 1 (Left), built for compatibility with current web technology and standards. It functions as an ordinary website with accessibility-friendly features for the VI, such as meaningful URLs for screen readers, and product catalogues which have support for haptic devices. The website groups the products into categories for easy navigation, with a description in text to be read to the user via screen reader (NVDA, JAWS etc.).
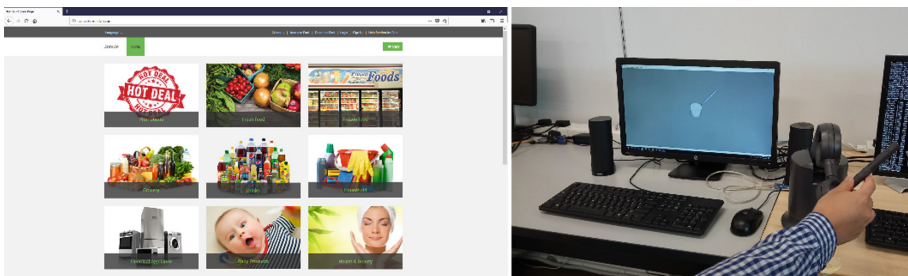
Fig. 1. Left: Layout of the JomJe website; **Right:** Set up of haptic device with H3DViewer displaying the asset and stylus representation

Each 3D asset was stored in the JomJe website in an X3D file format, to be down-loaded into the PC for rendering via H3DAPI. When opened, a 3D Systems® Touch model haptic 3D stylus (1000 Hz servo loop with 3.4 N maximum force feedback) would receive coordinate data relayed from the H3DAPI, with both the asset and a virtual representation of the stylus displayed in a H3D Viewer window as shown in Fig. 1 (Right). The Ruspini renderer was selected to ameliorate effects of micro gaps in rendering on the stylus, with a sphere (default proxy radius of 0.0025 m) as a contact point [6].

Previously, all items displayed - and tested upon - in JomJe were rigid assets. Plastic or elastic deformation in Fig. 2 (scaled from 0 to 1, or rigid to fully deformable) as well as constant frictional forces (scaled from 0 to 1, or smooth to maximum 3.4 N resistance) were subsequently introduced in this new version, using a simple Gaussian function to form the deformation profile as shown in Eq. (1). In the case of small or slender assets, a weak spring effect helped guide the user to the asset surface.

$$f(x) = DeformAmplitude\left(e^{-\left(\frac{(x-DeformCenter)^2}{DeformWidth^2}\right)}\right) \tag{1}$$
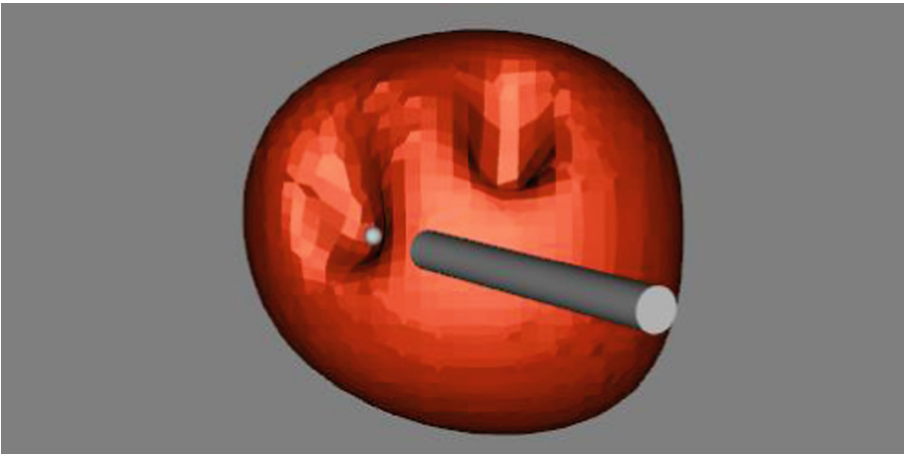
Fig. 2. Example of plastic deformation on plasticine asset

3   Testing

The testing was divided into three stages:

- **First Stage:** Evaluation on the JomJe e-commerce website, getting familiar with the website before being given tasks to perform on the website as a gauge of effective usage, such as searching for and completing purchases of items.
- **Second Stage:** Interaction with rigid 3D assets, followed by deformable and friction-applied assets, gauging accuracy of responses within a two-minute limit in determining the object shape and material of construction.

- **Third Stage:** Collection of opinions as feedback for future improvements.

The items provided for evaluation included a headset for hearing the screen reader, a PC with H3D preinstalled, Internet connection and a keyboard with the standard US QWERTY layout, and the aforementioned model of touch stylus.

At the time of writing, 52 volunteer members (42 male and 10 female) from the VI community within Malaysia performed evaluations on the website (First Stage), each hailing from different backgrounds. Of these, 10 were below 18 years of age and 18 were between 18 to 20 years of age, while 5 were around 35 years of age, with the rest evenly distributed between the ages of 17 and 62. Within this sample, 9 individuals (8 male and 1 female) performed evaluations on the 3D assets with different characteristics (Second Stage). These belonged to the age group below the age of 18. As for the Third Stage, all 52 participants took part in the collection of opinions.

4   Outcomes

The results of the post-testing surveys determined that 81.6% of participants found the website enjoyable to use. 71.1% also stated that the website has a straightforward method of use, with the same proportion recommending its usage to other colleagues. Conversely, the inadequacies of error messages during operational failure was marked at 65.8%. Overall, 78.9% of participants declared that the development of a "website with haptic technology" as above is important to them, as shown in Fig. 3.
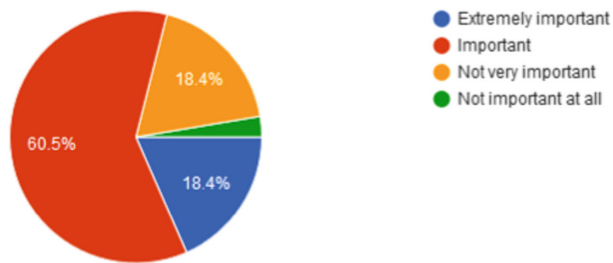
Fig. 3. Participant responses on the importance of a website with haptic technology

In addition, participants tested on the Second Stage provided unanimously positive reviews regarding the recent implementation of deformation and friction, due to the ability to feel texturing rather than solely shape. However, the accuracy in feeling the shape and texture of each asset stood at an overall 37.0% and 44.4% respectively, with some suggesting that texturing made it difficult to determine the shape of the asset.

A more detailed breakdown of results was organized in Table 1. As such, the exaggeration of asset characteristics, such as sharper angles and increased friction may be necessary to provide the information necessary in determining assets accurately. Further issues include unsteady force feedback, deformation limited by polygon resolution and individual GPU capability, and fine-tuning of characteristics to match real physical objects.

Table 1. Accuracy of participants in determining asset characteristics

Assets	Shape	Texture
Solid ball	66.7%	44.4%
Elastic beach ball	22.2%	33.3%
Plastic plasticine sphere	22.2%	55.6%

Using further participant feedback, features that have been or are being implemented included resizable fonts and theme customization for those with visual capability, enhanced item descriptions, and sound and texture support for 3D items. Some implementations require additional linked files as opposed to the current single X3D file download method, suggesting that reconfiguration of the method for handling X3D files on the client side may be beneficial.

In terms of 3D image resolution, the quality of each asset had to be balanced with the specification of individual machines. 3D images with high polygon densities would place a greater strain on the graphics component, more so should quality deformation and physics be implemented for every asset. Scalable resolution for each asset could be considered to fit the capability of future clients.

5   Conclusion

The JomJe website was conceptualized primarily to provide accessibility to VI individuals, and has since received a majority of positive responses from its testing sample size. Improvements upon assets such as deformation and friction effects have successfully been implemented, however fine-tuning of asset characteristics to balance texturing and shape recognition for VI usage would be necessary for practical application.

In the future, after further iterations of feedback and improvement as described in this report, it is desired that a deployment-ready version of the JomJe would become available, allowing the VI to benefit in the transacting segment of the Internet, and provide inspiration in promoting availability of the Internet to the VI as a whole.

Ethical Approval: All procedures performed in studies involving human participants were in accordance with the ethical standards of the Sunway University Research Ethics Committee (Ethics Approval Code: SUREC 2018/046) and with the 1964 Helsinki declaration and its later amendments or comparable ethical standards.

Informed Consent: Informed consent was obtained from all individual participants included in the study.

References

1. Demain, S., Metcalf, C.D., Merrett, G.V., Zheng, D., Cunningham, S.: A narrative review on haptic devices: relating the physiology and psychophysical properties of the hand to devices for rehabilitation in central nervous system disorders. Disabil. Rehabil. Assistive Technol. **8**(3), 181–189 (2013)
2. Jeon, S., Choi, S., Harders, M.: Rendering virtual tumors in real tissue mock-ups using haptic augmented reality. IEEE Trans. Haptics **5**(1), 77–84 (2011)
3. Sreelakshmi, M., Subash, T.D.: Haptic technology: a comprehensive review on its applications and future prospects. Mater. Today Proc. **4**(2), 4182–4187 (2017)
4. Liu, L., Li, W., Dai, J.: Haptic technology and its application in education and learning. In: 2017 10th International Conference on Ubimedia Computing and Workshops, pp. 1–6. IEEE, New York (2017)
5. Husman, M.A., Maqbool, H.F., Awad, M.I., Abouhossein, A., Dehghani-Sanij, A.A..: A wearable skin stretch haptic feedback device: towards improving balance control in lower limb amputees. In: 2016 38th Annual International Conference of the IEEE Engineering in Medicine and Biology Society (EMBC), pp. 2120–2123. IEEE, New York (2016)
6. Ruspini, D.C., Kolarov, K., Khatib, O.: The haptic display of complex graphical environments. In: Proceedings of the 24th Annual Conference on Computer Graphics and Interactive Techniques, pp. 345–352. ACM Press/Addison-Wesley Publishing Co., New York (1997)

Human Rendezvous via Haptic Suggestion

Gianluca Paolocci[1,2]($\boxtimes$), Tommaso Lisini Baldi[1], and Domenico Prattichizzo[1,2]

[1] Department of Information Engineering and Mathematics, University of Siena,
Via Roma 56, 53100 Siena, Italy
`paolocci@diism.unisi.it`
[2] Department of Advanced Robotics, Istituto Italiano di Tecnologia,
Via Morego 30, 16163 Genova, Italy
`gianluca.paolocci@iit.it`

Abstract. In this work we propose a wearable system to guide humans in structured or unstructured environments, with the aim of reaching simultaneously a rendezvous point. Directional and rhythmic cues are provided using wearable haptic interfaces placed at the subject's ankles. The walking pace guidance is achieved through the synchronization of the user's step cadence with the rhythm suggested by tactile cues. Directional hints are provided using different vibro-tactile patterns when reaching predefined locations called *checkpoints*. Here the estimated walking parameters are updated. The user retains complete access to audio and visual information from the environment, thus he/she is ready to react to unexpected events (*e.g.*, moving obstacles). Exploitation of the proposed approach are assistive and rescue scenarios, human-human collaboration, as well as rehabilitation.

Keywords: Human guidance · Haptic communication ·
Cadence suggestion

1 Introduction

Human body guidance is exploited in several contexts, ranging from rescue procedures to training and rehabilitation [1,3,5]. Novel and promising technologies allow to track and guide individual limbs, as well as complex movements requiring high coordination [8,9].

In this work, we focus on a fundamental human activity: locomotion. In particular, we want to address the problem of guiding humans in structured and unstructured environments. The aim is suggesting walking pace to multiple users to reach the goal destination at the same time.

Over the years, haptic stimuli have been found an effective, yet non-intrusive way for suggesting directions and pace cues to users [4,7]. They represent an interesting way to provide information when audio and visual modalities are not available or overloaded (*e.g.*, vision is temporarily impaired).

A representative scenario of the demo is depicted in Fig. 1, where two participants (*User1* and *User2*) are guided, by means of haptic interfaces, to reach at the same time a shared goal location.

Our method exploits the sensory-motor entrainment to suggest a specific walking cadence [2,10]. It is known that the frequency of a cyclic movement, such as walking and running, can be affected by rhythmic sensory inputs and can smoothly converge to the input rhythm. For example, when people walk while listening to music, their step cycle gradually conforms to the rhythm of the music.

We showed in our previous work [6] that subjects adapt to the rhythm provided by the haptic interfaces with very low effort and without overloading other sensory input channels (visual and auditory). Two different body locations were tested to assess which was the most suitable to convey the walking pace. Experimental results and questionnaires showed subjects to prefer the rhythmic cues displayed at the ankles instead of the wrist positioning. Vibrations provided at the forearms were considered as disturbances for manipulation tasks, and the proximity of the haptic stimulus with the foot during the heel strike let subjects synchronize more easily with the external rhythm.

2   Materials and Methods

Our solution relies on flexible vibro-tactile interfaces placed at the ankles, providing cadence and direction suggestions to the users. In Fig. 2 the haptic devices are described. In the experiments, subjects were asked to adapt their walking cadence to the rhythm proposed by the wearable interfaces.

2.1   System Overview

The desired cadence is suggested to the users through rhythmic vibrations provided by remotely controlled elastic haptic bands. Each wearable haptic interface is composed by two water-proof vibro-motors. Whenever a trigger is sent to a haptic device, the motors vibrate for 0.1 s at a frequency of 250 Hz, delivering a haptic stimulus to the wearer. The vibration frequency has been selected with respect to the user's maximal sensitivity, achieved around 200–300 Hz [11] (the human perceptibility range is between 20 Hz and 400 Hz). A pressure sensor is placed under the right heel to detect contact with ground and count the number of steps. The step count is necessary for post-experimental analysis, and is a valid tool to update walking parameters (*i.e.*, the estimated step-length) in unstructured environments. An ad-hoc algorithm is used to control the haptic interfaces through external devices (laptop, smartphone). Information about the path and the time to complete the rendezvous are entered to calibrate the
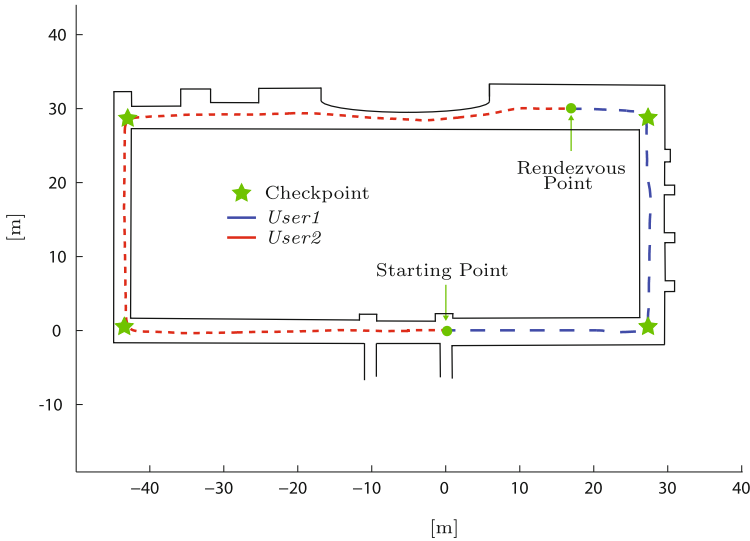
Fig. 1. Cadence is suggested to the users via two vibro-tactile elastic bands placed on the ankles. To reach a predefined point at the same time, users have to adapt their walking pace. The rhythm is updated at specific points in the map, called *checkpoints*. Here, the user also receives direction information through repeated vibrations in the steering side. In this representative scenario, *User1* is closer to the goal point than *User2*. To reach the rendezvous point at the same time, *User1* has to keep a slow pace, while *User2* has to increase the walking cadence. Different rhythms are depicted with different spacing in the dashed line representing the users' path. In this example, *checkpoints* are defined at every corner.

(a)   (b)
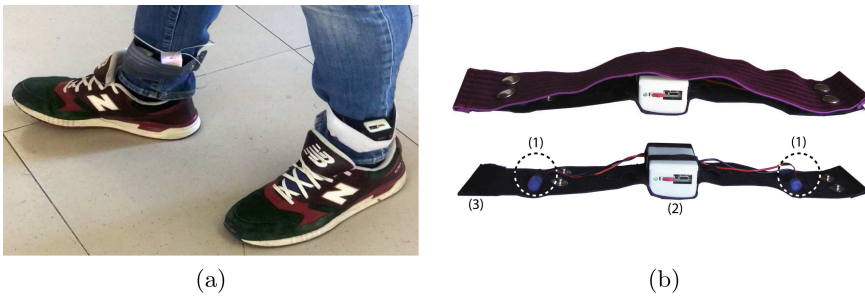
Fig. 2. Cadence cues are provided to the users via two vibro-tactile elastic bands placed on the ankles (a). The haptic bands (b) are composed of two vibrating motors (1) attached to an elastic wristband (3). A Li-Ion battery is in charge of power and an Arduino board controls the interface (2).

system. The communication is realized with an RN-42 Bluetooth antenna connected to a 3.3 V ATmega328 microcontroller, which is also in charge of the motors activation and timing.

2.2   Experimental Procedures

Before starting the experiment, the subjects' average step length at comfortable cadence is estimated. We select two paths toward the meeting point and choose the checkpoint locations. The time to reach the rendezvous point depends on the estimated step length and the average cadence we want to achieve.

In a structured environment it is not difficult to track the users along the path. Thus the arrival at checkpoints can be monitored automatically by the algorithm, which computes the remaining time and distance, and adapts the output cadence.

In an unstructured environment we decide to rely on operators for preliminary experiments. A ghost operator is in charge of following each subject at a 5 m distance to supervise the experiment. At each checkpoint, the step length estimation is automatically updated according to the number of steps from the last checkpoint (all the distances are known). This process allows to update the step-cadence reference to reach the destination on time. The trial ends when both users reach the rendezvous point. In both cases informed consent is obtained from all individual participants included in the study.

2.3   Live Demonstration

The experiment becomes self explanatory by recruiting two volunteers to perform the rendezvous trial along different paths. The meeting point is placed at different distances, so that the algorithm will have to estimate different cadence values to provide to the users. Considering the wide space needed to perform this live demonstration, we propose two possible alternatives. Both involve two subjects, who will have to reach simultaneously the meeting point through a physical or virtual path.

In case there is enough space to plan two different paths toward the meeting point, we will perform the trials regularly. Two routes of different (known) length will be defined and the users will have to synchronize to the step cadence suggested by the vibro-tactile interfaces. Before the trial begins, subjects will be required to walk a 30 m pathway at their own comfortable speed, to estimate the subject's average step-length. The initial desired cadence for each user will be determined by the overall distance they will have to travel and the estimated step length. A ghost operator will follow each subject with a smartphone to indicate the arrival at checkpoints. After reaching each checkpoint, the step length will be refined on the basis of the number of steps walked, and the desired cadence will be updated. During the trial, the suggested cadence will vary depending on the subjects' synchronization ability: users able to keep the external pace will see low variation of the step-cadence, while low synchronization rate will result in bigger cadence variations. The performance parameter will be the difference

in time between the two arrivals to the meeting point. If the necessary space is not available, we will simulate the virtual paths with gym-steps: users will climb virtual stairs by stepping on and off, covering a different number of stairs. We will keep track of the trial progresses via display representation of the step count. This method doesn't take into consideration the user's step length, which may be simulated with steps of different height. Cadence will vary with respect to remaining time and stairs, and the users will have to adapt their stepping frequency to the stimulus rhythm. In this case, the trial ends when both the subjects reach the virtual meeting point.

2.4 Conclusions

In this demonstration we present a system to guide users on time to the rendezvous point. It relies on information as path length and subjects locomotion parameters to estimate the adequate cadence and provide it to the user through vibro-tactile interfaces placed at the user's ankles. The users have to adapt their walking pace to the one suggested by the haptic interfaces. The rhythm is updated at specific points, called *checkpoints*, where the user also receive direction information through repeated vibrations in the steering side. In future works, we will further investigate the users adaptability at high-varying frequencies, and how the step-length depends on the provided cadence. Possible application scenarios are human-human and human-robot collaboration, training and rehabilitation.

References

1. Cosgun, A., Sisbot, E.A., Christensen, H.I.: Guidance for human navigation using a vibro-tactile belt interface and robot-like motion planning. In: Proceedings of IEEE International Conference on Robotics and Automation, pp. 6350–6355. IEEE (2014). https://doi.org/10.1109/ICRA.2014.6907796
2. Delcomyn, F.: Neural basis of rhythmic behavior in animals. Science **210**(4469), 492–498 (1980). https://doi.org/10.1126/science.7423199
3. Van Erp, J.B.F., Van Veen, H.A.H.C., Jansen, C., Dobbins, T.: Waypoint navigation with a vibrotactile waist belt. ACM Trans. Appl. Percept. **2**(2), 106–117 (2005). https://doi.org/10.1145/1060581.10605805
4. Karuei, I., Maclean, K.E.: Susceptibility to periodic vibrotactile guidance of human cadence. In: Proceedings of IEEE Haptics Symposium, pp. 141–146. IEEE (2014). https://doi.org/10.1109/HAPTICS.2014.6775446
5. Lindeman, R.W., Sibert, J.L., Mendez-Mendez, E., Patil, S., Phifer, D.: Effectiveness of directional vibrotactile cuing on a building-clearing task. In: Proceedings of ACM International Conferecne on Human Factors in Computing Systems, p. 271. ACM (2005). https://doi.org/10.1145/1054972.1055010
6. Lisini Baldi, T., Paolocci, G., Prattichizzo, D.: Human guidance: suggesting walking pace under manual and cognitive load. In: International Conference on Human Haptic Sensing and Touch Enabled Computer Applications, pp. 416–427 (2018). https://doi.org/10.1007/978-3-319-93399-3_36
7. Lisini Baldi, T., Scheggi, S., Aggravi, M., Prattichizzo, D.: Haptic guidance in dynamic environments using optimal reciprocal collision avoidance. IEEE Robot. Autom. Lett. **3**(1), 265–272 (2018). https://doi.org/10.1109/LRA.2017.2738328

8. Lisini Baldi, T., Scheggi, S., Meli, L., Mohammadi, M., Prattichizzo, D.: GESTO: a glove for enhanced sensing and touching based on inertial and magnetic sensors for hand tracking and cutaneous feedback. IEEE Trans. Hum.-Mach. Syst. **47**(6), 1066–1076 (2017). https://doi.org/10.1109/THMS.2017.2720667

9. Lugo-Villeda, L.I., Frisoli, A., Sandoval-Gonzalez, O., Padilla, M.A., Parra-Vega, V., Avizzano, C.A., Ruffaldi, E., Bergamasco, M., et al.: Haptic guidance of light-exoskeleton for arm-rehabilitation tasks. In: Proceedings of IEEE International Symposium in Robot and Human Interactive Communication, pp. 903–908, September 2009. https://doi.org/10.1109/ROMAN.2009.5326057

10. Miyake, Y., Miyagawa, T.: Internal observation and co-generative interface. In: Proceedings of IEEE International Conference on Systems, Man, and Cybernetics, vol. 1, pp. 229–237. IEEE (1999). https://doi.org/10.1109/ICSMC.1999.814095

11. Riener, A.: Sensor-Actuator Supported Implicit Interaction in Driver Assistance Systems, vol. 10. Springer (2011). https://doi.org/10.1007/978-3-8348-9777-0

Controlling Robot Vehicle Using Hand-Gesture with Mid-Air Haptic Feedback

Tao Morisaki$^{(\boxtimes)}$, Masahiro Fujiwara, Yasutoshi Makino,
and Hiroyuki Shinoda

Graduate School of Frontier Sciences, The University of Tokyo,
5-1-5 Kashiwanoha, Kashiwa-shi, Chiba 277-8561, Japan
`morisaki@hapis.k.u-tokyo.ac.jp`,
`Masahiro_Fujiwara@ipc.i.u-tokyo.ac.jp`,
`{yasutoshi_makino,hiroyuki_shinoda}@k.u-tokyo.ac.jp`

Abstract. In this paper, we improve the usability of hand-gesture control system of robot vehicle using mid-air haptic feedback. The system notifies a user of three states of the system with haptic feedback: (A) the user's hands exists in a recognition range of the system, (B) the robot vehicle is controllable and (C) the user is controlling the robot vehicle. As a result, haptic feedback improved the usability and the variation of haptic feedback was not perceived completely.

Keywords: Mid-air haptic feedback · Hand-gesture control · Usability

1 Introduction

In order to facilitate remote control of robot vehicles, many intuitive interfaces have been published. Young et al. [1] proposed a dog-leash like interface where users pull the leash connected to the robot vehicle. In the system proposed by Ishii et al. [2], users instruct courses to a robot vehicle by drawing the route with a laser pointer. Among these interfaces, hand-gesture is a promising interface requiring no devices taken by users. Richarz et al. [3] proposed controlling a robot by pointing to the destination with a finger. Dennis et al. [4] proposed a method using hand-gesture accompanied by voice commands. However, current hand-gesture methods have a common problem: the lack of the sense on the control state. A user's hand motion shows a vehicle route during a certain time and has no meaning at other times. The user continuously wants to sense and confirm which state the user's hand is in. It is also a problem how to inform the system of the state switch. These senses and intention transmission are managed by haptic feedback in conventional tangible controller as a joystick [5].

In this research, we propose a gesture control method accompanied by mid-air ultrasound haptic feedback. In the initial phase, the midair haptic stimulation notifies users of the recognition range of a hand-tracking system: whether the system is recognizing the user's hand or not. In the recognition range, the user can switch into a route-teaching mode by a predefined hand gesture and confirm the mode change by a haptic feedback. After that, the robot vehicle follows the hand trajectory while the hand is in the route-teaching mode. The system enables gesture control of a robot vehicle as intuitive as a touchable interface.

2 Mid-Air Haptic Feedback Using Airborne Ultrasound

For midair haptic feedback, there are two typical methods, AIREAL [6] using air cannon and Airborne Ultrasound Tactile Display (AUTD) [7] using ultrasound. The authors chose AUTD shown in Fig. 1 because AUTD can produce a high-pressure area in the air with high spatial resolution.
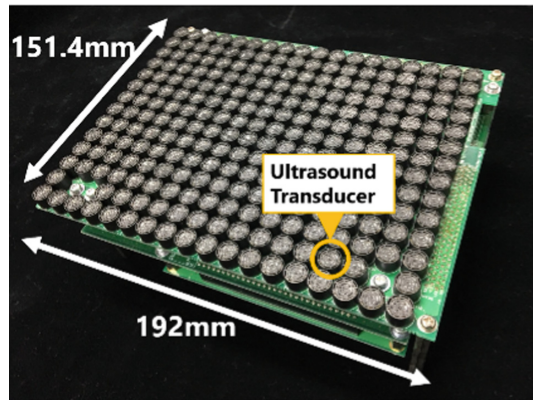
Fig. 1. Airborne ultrasound tactile display

An AUTD unit used in this research has 248 ultrasound transducers and produces noncontact haptic feedback by using acoustic radiation pressure. Acoustic radiation presser P [pa] is calculated by

$$P = \alpha E = \alpha \frac{p^2}{\rho c^2} \tag{1}$$

where p [pa] is an effective value of sound presser of ultrasound, ρ [kg/m^3] is volume density of the air, c [m/s] is sound velocity in the air, and α [-] is determined according to a reflective condition of an object.

AUTD controls the phase of ultrasound transducers to produce a high-presser focal point at a certain point that creates haptic stimulation.

3 Control System of a Robot Vehicle Using Hand-Gesture with Mid-Air Haptic Feedback

3.1 System Configuration

A control system of a robot vehicle is shown in Fig. 2. The system is separated into two parts: a robot and a controller. The robot is a 3WD Omni Wheel Robot (NEXSUS robot) with a wireless communication module named Xbee. The robot moves forward,
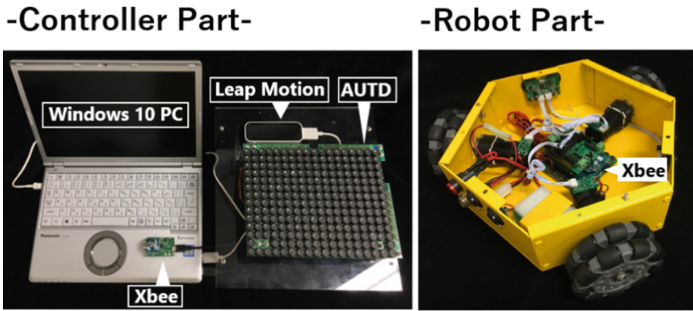
Fig. 2. System configuration

backward, right and left. The controller is composed of Leap Motion which detects hand motion, AUTD which creates mid-air haptic feedback with ultrasound, Xbee and windows 10 PC (Let's Note CF-SZ6).

3.2   Interface Design

We classify the states of the control system by three classes (A) the user's hand exists in recognition range of the system, (B) the robot vehicle is controllable, and (C) the users are controlling the robot vehicle.

The detailed system states are summarized in Fig. 3. (1) The system watches and waits while a user's hand exists out of the recognition range. (2) When a user's hand moves into the recognition range, the system notifies with intermittent haptic feedback on fingertip (state A). (3) When a user makes a fist, the system stimulates the center of the fist with continuous haptic feedback and enables controlling the robot vehicle (state B). Making a fist is an intuitive gesture to enable control of a robot vehicle. (4) Users can control the robot vehicle by moving more than 100 mm (state C). The vehicle robot moves in the same direction as the user's hand at a constant velocity. In this mode, haptic feedback becomes stronger. (5) The robot vehicle is suspended when users open the hand or put a fist back in the original position and, returns to the state (2) or (1).
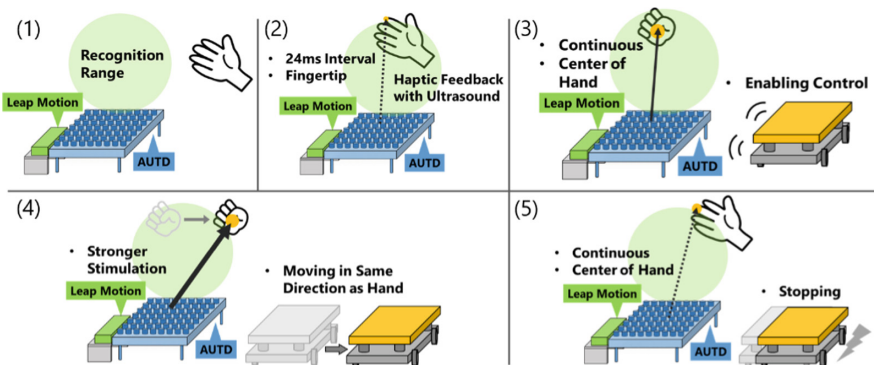
Fig. 3. System states

4   Demonstration

In the demo, the participants experience this robot control system. In the experiment in the laboratory, the midair haptic feedback improved the usability of control system. However, some users reported they did not perceive variation of haptic feedback completely. We will improve the variation of haptic feedback and evaluate the usability in the conference venue.

Ethical Approval: All procedures performed in studies involving human participants were in accordance with the ethical standards of the institutional and/or national research committee and with the 1964 Helsinki declaration and its later amendments or comparable ethical standards.

Informed Consent: Informed consent was obtained from all individual participants included in the study.

References

1. Young, J.E., Kamiyama, Y., Reichenbach, J., Igarashi, T., Sharlin, E.: How to walk a robot: a dog-leash human-robot interface. In: Proceedings of IEEE International Workshop Robot and Human Interactive Communication, pp. 376–382 (2011)
2. Ishii, K., Zhao, S., Inami, M., Igarashi, T., Imai, M.: Designing laser gesture interface for robot control. In: Gross, T., Gulliksen, J., Kotzé, P., Oestreicher, L., Palanque, P., Prates, R. O., Winckler, M. (eds.) INTERACT 2009. LNCS, vol. 5727, pp. 479–492. Springer, Heidelberg (2009). https://doi.org/10.1007/978-3-642-03658-3_52
3. Richarz, J., Scheidig, A., Martin, C., Müller, S., Gross, H.M.: A monocular pointing pose estimator for gestural instruction of a mobile robot. Int. J. Adv. Robot. Syst. **4**(1), 139–150 (2007). SPEC. ISS.
4. Perzanowski, D., Schultz, A.C., Adams, W., Marsh, E., Bugajska, M.: Building a multimodal human-robot interface. IEEE Intell. Syst. Appl. **16**(1), 16–21 (2001)
5. Cornelio Martinez, P.I., De Pirro, S., Vi, C.T., Subramanian, S.: Agency in mid-air interfaces. In: Proceedings of 2017 CHI Conference on Human Factors in Computing Systems - CHI 2017, pp. 2426–2439 (2017)
6. Sodhi, R., Poupyrev, I., Glisson, M., Israr, A.: AIREAL: interactive tactile experiences in free air. ACM Trans. Graph. **32**(4), 134 (2013)
7. Hoshi, T., Takahashi, M., Iwamoto, T., Shinoda, H.: Noncontact tactile display based on radiation pressure of airborne ultrasound. IEEE Trans. Haptics **3**(3), 155–165 (2010)

Improvement of Walking Motivation by Vibratory Display Powered by an Ankle-Worn Generation Device

Minatsu Sugimoto[✉], Hiroo Iwata[✉], and Hiroya Igarashi[✉]

University of Tsukuba, 1-1-1 Tennodai, Tsukuba, Ibaraki 305-8577, Japan
m_sugimoto@vrlab.esys.tsukuba.ac.jp,
iwata@kz.tsukuba.ac.jp,
igarashi.hiroya.fw@u.tsukuba.ac.jp

Abstract. We propose an ankle-worn power generation device that supplies power to a vibration speaker to improve walking motivation. With the walking motion of the user, the vibration speaker is driven. In this paper, we propose an interface of a wearable generator that obtains electric power from ankle movement during walking by means of attaching a device with power generation functions to the ankle, and we report the performance evaluation result of the ankle-worn power generation device. In addition, as a part of investigating factors that improve walking motivation, we also describe the results of a questionnaire on walking and its considerations, and the approach to the design-oriented aspects assuming scenarios for future use.

Keywords: Vibration speaker · Wearable harvester · Walking motivation

1 Introduction

A smart wearable system (SWS) for health care applications can constantly monitor heartbeat, blood pressure, and other metrics by wearing the device. In addition, it can be used in daily life by wearing it on the body; its continuous monitoring can be used in telemedicine and other purposes. These features provide a new means of medical treatment, with a role in quickly discovering diseases and injuries and reducing risk. With an SWS with these merits, energy supply to the SWS is a major design consideration. Most current SWS devices use batteries as the energy supply source, but batteries have the risk of running out of charge and the user's forgetting to recharge them; in addition, batteries can be heavy and bulky. In an SWS where continuous monitoring over time is important, a power supply source that can continuously supply electric power is required. As a means for providing a continuous power supply for a long time, a wearable generator can generate electricity from the wearer's daily activities. Compared with that of a battery, the supplied electricity amount is small, but it is expected to be sufficient to drive a sensor, and by using it together with a conventional battery, it can be expected to extend the battery life. The development of a wearable generator that the user can use for a long time in everyday life is more important in SWS devices for health care requiring long-term observation with weak electric power.

Walking provides opportunities for people to exercise more frequently in their lives, and some studies have attempted to generate electricity from walking motion. However, the proposed devices that attempt to generate electricity from walking tend to fatigue the user. It is anticipated that lowering voluntary walking motivation is a problem; for example, a method of generating electricity by attaching a gear-type electric power generator to the side of the knee has been proposed [2]. On the other hand, in a study to generate electricity by an electromagnetic coil incorporated in the sole of a shoe [3], it is more difficult to walk because of the thickness of the shoe soles; a problem of the structure makes it difficult to walk when the size of the coil exceeds 15 mm. The difficulty in walking is expected to result from a feeling of fatigue caused by using a device that forces the user to take on a large burden in walking. In addition, Hashimoto et al. proposed a system [4] that presents a tactile sense to the sole of the foot as research on providing sensation during walking.

Therefore, in this research, we developed a vibratory display powered by an ankle-worn generation device with the aim of developing a power generating device that does not fatigue the user during walking, so as to increase the walking motivation of the user, and of establishing a fitting method. In addition, we developed a wearable power generator that does not disturb walking by designing a wearing position focused on the bluntness of skin sensation in the shin and a mechanism capable of generating electricity with weak force. In addition to the development of wearable power generation equipment to examine awareness and motivation regarding walking, we also considered the elements of the application to promote walking motion.

2   Ankle Power Generating Device

2.1   Design Guideline

In response to the above-mentioned problems, we solved the problem of foot fatigue caused by the power generator with the following approach based on a previous study [5] that showed that relaxing the feeling of fatigue of the foot increased the motivation of walking [5]:

(1) Reduction of cognitive load in the senses
(2) Reduction of load on motor function
(3) Power generation mechanism that generates power with low labor

For the design guideline (1), it is perceived than the feeling of pressure or discomfort comes from actually feeling the installed wearable generator. The designed generators are made small so as to reduce the fatigue feeling of the foot. In the present research, this is realized by attaching a wearable generator fixed to a belt on the shin [6] with a dull sensation on the skin and on the instep of the foot while wearing shoes. For design guideline (2), in addition to being between the above-mentioned shin and foot instep, the motion of a large ankle-worn device [6] with large motor function is used as a power source. For the design guideline (3), we developed a power generation device that can generate electricity with little effort; here we used a power generation vibrating element that generates power by vibrating or bending.

2.2   Structure of the Ankle Power Generation Device

Figure 1(a) shows the mechanism of power generation, which combines a mechanism that generates electricity without hindering the bending and stretching motion of the joint and a mechanism that generates electricity by vibration using the force escaping to the ground when the heel lands on the ground. In the mechanism, a vibration-type power generating element is used, capable of generating electric power by using a sheet-type vertical vibration of 20 mm and a horizontal vibration of 75 mm with bending and stretching. The configuration of the ankle power generating device includes a mechanism on the anterior side of the ankle that generates electric power by bending and stretching the vibration generating element sheet according to the bending and stretching motion of the ankle while walking, and a mechanism for swinging the heel on the ground during walking. It consists of two mechanisms, including a mechanism behind the ankle that generates power by vibration of the sheet. Figure 1(b) shows the developed ankle power generating device.
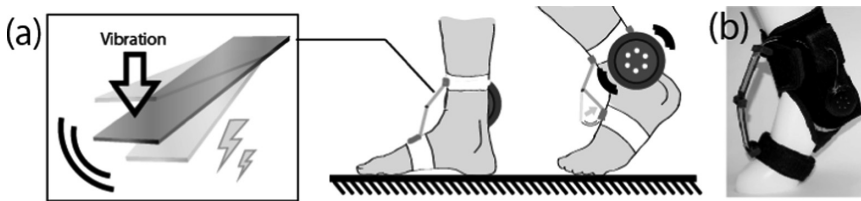
Fig. 1. (a) Structure of the ankle generation device. (b) Prototype of the device.

As a feature of this mechanism, we focused on the shin, on which the sensation on the skin is dull, as a location for mounting the power generator fixture. The point that we used was intended for a low-power stiffness vibration power generation sheet as a power generation mechanism to weakly suppress the wearer's force. There is a point at which it uses the bending and stretching exercise and the shock that escapes to the ground when the heel is swung down to the ground for power generation.

In addition, this mechanism uses a lightweight seat-type power generation mechanism along the joint; the size of the power generation device using a conventional electromagnetic coil is proportional to the amount of power generation. In view of the structure of the shape and a circle, there was a problem in which the entire device including the fixture became heavy and bulky when worn on the body. However, in this mechanism, the structure called for a thin sheet shape for power generation by the vibration and the bending operation. Because a vibration generating sheet having these characteristics is used, a space-saving apparatus along the body such as around the joint is possible, and the apparatus itself is thin and lightweight. This makes it possible to reduce the load on the user due to wearing it, and fatigue relief can be expected.

2.3   Vibratory Display

In order to improve walking motivation, we developed a vibratory display powered by the ankle generation device. To improve walking motivation, we propose a device that transforms ankle movement into haptic feedback. By wearing the device on top of one's shoes, the device detects movement of the ankle while walking and generates electricity from the movement. This system is composed of an energy harvester and a vibratory display. The energy harvester is built from two vibration power generation elements. It generates electricity through the bending and stretching movement induced by the ankle during walking. The harvested energy powers the vibratory display. The vibratory display is driven in conjunction with the bending and stretching motion of the ankle during walking. Figure 2(a) shows the concept of the vibratory display powered by the ankle generation device and a prototype of the system that was built. As an application, the ankle generation device generates electricity as a user walks. The vibratory display plays a sound by its power. Our prototype emits different sounds depending on how the user walks. Therefore, the user will try various ways of walking thanks to the improved walking motivation provided by the device.
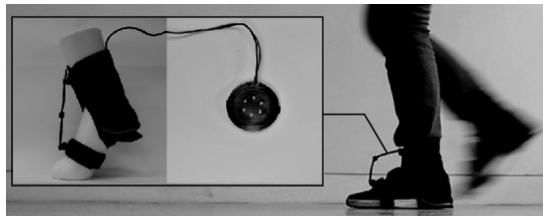
Fig. 2.   Structure of ankle generation device and a prototype of the device

3   Evaluation of the Ankle-Worn Power Generation Device

3.1   Evaluation Method

On the basis of the approaches described in the design guidelines, we developed an ankle-worn power generation device and evaluated its performance. We measured the amount of power generated by the device, and we conducted a questionnaire survey on the motivation of walking. In addition to measuring the amount of electricity generated by the ankle power generating device, by conducting a survey on the motivation of walking, which is the power source of the ankle-worn power generating device in parallel, it is possible to acquire further knowledge such as the factors that reduce the motivation of walking, We aimed to establish a fitting method and help to ease the subjective feeling of fatigue.

3.2   Electricity Generation Measurement

The amount of electricity generated by the developed ankle power generating device was measured. When the vibration generating element sheet used for the ankle power generating device was vibrated, the generated voltage was recorded at a maximum of

50 V, and the power generation amount was 0.025 W. In addition, the voltage obtained when the ankle power generating device was attached to one foot during walking was 1.7 V.

3.3   Survey on Walking Motivation

A questionnaire survey was conducted on a total of 40 male and female subjects on walking to develop a factor to consider in a method to promote walking motion, which is the power source of the ankle-worn power generating device. Table 1 shows the results the average of the responses to the questions. Question A is "The time spent walking in one day," B is "The time you want to walk in one day," C is "The distance walked in one day," and D is "The distance you want to walk in one day."

Table 1. Average time and distance in a day.

Sex	A	B	C	D
	Time [min]	Time [min]	Distance [km]	Distance [km]
Male	74	149	4.8	6.0
Female	82	139	10.6	83.7

4   Evaluation Results and Discussion

It was found from the voltage measurement of the ankle power generating device that a voltage of 1.7 V can be obtained step by step. Thus, by using the SWS using a battery or a rechargeable SWS and the ankle power generation device, it is possible that the device can avoid running out of charge while the SWS device is in use.

In addition, on the basis of the results of the survey on walking conducted to develop a factor to consider in a method for further promoting walking by the user, "the amount that we want to walk" is larger than the "walking amount," by a factor of 7.9 in terms of distance and a factor of 1.7 in terms of time. For men, the factor was 1.3 for distance and 1.7 in terms of time. From these results, it was observed that women wanted to increase their walking distance, and men wanted to increase their walking time. Accordingly, when considering a method such as an application for further promoting walking by a user, women use an application focused on walking distance, and men combine an application focused on walking time with an ankle power generating device. We proposed an assumption that walking motivation can be improved more effectively by suggestion.

5   Approach in Terms of Industrial Design

For a wearable device assumed to be used daily, the design aspect of the device itself is regarded as important. In the wearable device research being performed in design studies and fashion fields, there are also many previous studies on wearable devices of

the shoe type, such as Click Sneaks and Heelys Hack [7]. These devices have a simple attachment method, a design that blends in with daily life, and the durability to withstand daily walking. As shown in Fig. 2, the ankle power generation device developed in this research consists of a cloth belt and a vibration power generation element sheet, which is lightweight and easy to attach and detach. In addition, we plan to enhance the design in consideration of durability in the future.

6   Conclusion and Future Prospects

In this study, we developed a vibratory display powered by an ankle-worn generation device with the aim of developing a power generator that does not increase the user's fatigue during walking, so as to increase the walking motivation of the user, and of establishing a mounting method. In addition, we describe the performance evaluation of the ankle power generation device aiming to supply power to the SWS. For the performance evaluation, we describe the results of measurements of the amount of electric power generated by the ankle power generation device during walking. The results show the possibility of preventing battery depletion by walking with the ankle power generating device, thereby overcoming a problem of conventional SWSs. The elements of the application to raise walking motivation by gender were also shown.

In the future, from the viewpoint of a design-oriented approach, we will consider improvements designed considering the design aspect and durability, examining concrete applications that increase walking motivation, and improving the design to obtain even more power generation.

References

1. Chan, M., et al.: Smart wearable systems: current status and future challenges. Artif. Intell. Med. **56**(3), 137–156 (2012)
2. Donelan, J.M., et al.: Biomechanical energy harvesting: generating electricity during walking with minimal user effort. Science **319**(5864), 807–810 (2008)
3. Ylli, K., et al.: Human motion energy harvesting for AAL applications. J. Phys: Conf. Ser. **557**(1), 012024 (2014)
4. Sakai, K., Hachisu, T., Hashimoto, Y.: Sole tactile display using tactile illusion by vibration on toenail. In: Hasegawa, S., Konyo, M., Kyung, K.-U., Nojima, T., Kajimoto, H. (eds.) AsiaHaptics 2016. LNEE, vol. 432, pp. 95–97. Springer, Singapore (2018). https://doi.org/10.1007/978-981-10-4157-0_16
5. Manabe, Y., et al.: Improvement of rehabilitation by foot care. J. Showa Hosp. **4**(1), 007–010 (2007)
6. Penfield, W.G.: Motor and Sensory Homunculus (1950)
7. Seymour, S.: Fashionable technology: The intersection of design, fashion, science and technology. Springer, New York (2009)

TouchPhoto: Enabling Independent Picture-Taking and Understanding of Photos for Visually-Impaired Users

Yongjae Yoo[(✉)] , Jongho Lim , Hanseul Cho, and Seungmoon Choi

Pohang University of Science and Technology,
Gyeongbuk, Pohang 37673, South Korea
{dreamseed,lcdplayer,johanseul,choism}@postech.ac.kr
http://hvr.postech.ac.kr

Abstract. Photographs are a powerful medium for recording moments and sharing them with others. However, visually-impaired users have quite limited access to photograph's benefits. In this paper, we present an integrated system TouchPhoto, which provides visual-audio-tactile assistive features to allow visually-impaired users to take and understand photographs independently. A user can take photographs with auditory guidance and record several audio tags to aid recall of the photograph's content. For comprehension, a user can listen to the audio tags embedded in a photograph and also touch the photograph using an electrostatic friction display. The latter is done after salient features in the photograph, e.g., human faces, are extracted to facilitate tactile recognition.

Keywords: Blind photography · Assistive technology · Multimodal interaction · Electrovibration

1   Introduction

Photography enables users to visually capture the moment, preserve it, and share it with others. However, approximately 250 millions of visually-impaired users hardly benefit from photo-related activities, although most of them are frequently exposed to such situations [3]. They have to seek help from sighted people, and if no help is available, they hold on or give up the task [10].

Several applications have been developed to support photo-related activities for visually-impaired users, mostly relying on sensory substitution. Their goals include assisting photo taking [9], recording ambient sounds and explanations with photos [3], and describing and reading the content of pictures [4]. However, attempts to directly transmit the graphical contents of photos by means of haptic exploration, as is done in tactile graphics, have not been made. This approach

might turn out to be an effective modality for understanding the content of photos and reminding related memories and experiences.

In this paper, we present an integrated system of TouchPhoto, which is envisioned as an integrated system providing visually-impaired users with multimodal assistance to assist their independent undertaking of photo-related activities. TouchPhoto provides multimodal sensory feedbacks–visual, audio, and haptic stimuli–to deliver information. For haptic interaction, we use an electrostatic friction display for its wide applicability to regular touchscreen devices such as tablet PCs, as well as its convenience of use.
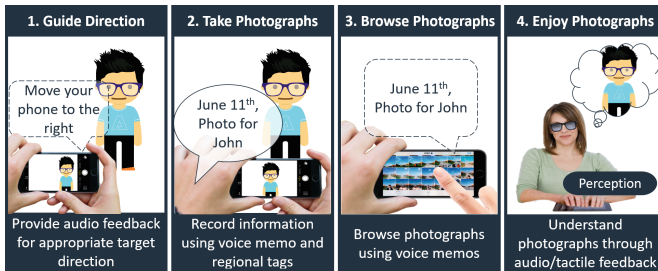
Fig. 1. Use scenario of Touchphoto.

2   Implementation of TouchPhoto

In this section, we present an overview and general design of TouchPhoto. At present, the main features of TouchPhoto support only photographs of people. This emphasizes the social and emotional function of photography, as a way to remember people and related events. Reviving such personal and emotional memories via audio-haptic multimodal interaction is our first goal, which also agrees to the general nature of the tactile sense [8]. Figure 1 shows the use scenario of TouchPhoto.

2.1   Apparatus

As shown in Fig. 2, TouchPhoto uses a regular smartphone to take photographs. We made an application running on Android with the support of Google Talk-Back. The application has two main functions, a camera and a photo album for visually-impaired users. The portrait photographs taken are processed to extract facial features of a nose, eyebrows, eyes, lips, and a face contour using an external API (Face++, Face Landmark) [2]. Each photograph is augmented with the coordinates of regional tags, and facial features, and audio data recorded by the camera app. The photographs are uploaded to a cloud storage service (Amazon S3; simple storage service).

Fig. 2. The structure and data flow of Touchphoto.

We learned from visually-impaired users that they prefer a large workspace (15–17 inches; as large as a laptop PC) for the exploration of tactile graphics. Such large electrostatic display have not been adopted to commercialized products yet, so we built a large electrostatic display by attaching a transparent electrocon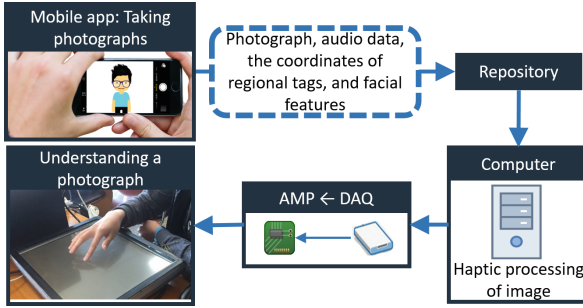ductive film (3M, SCT3250) onto a 17-inch LCD monitor. An IR (infrared radiation) frame (E&T Tech Inc., Model T17) was mounted on the display for finger tracking. A PC downloads the photographs and controls the display using a data acquisition card (National Instruments; NI-6251) and a high-voltage amplifier (Piezodrive; MX200b).

2.2   Photo-Taking

While taking a picture, the Android app of TouchPhoto detects human faces in the photograph using OpenCV (Fig. 3, the left panel). Then, it provides speech guidance to help the visually-impaired user move the detected face to the center of the screen, for example, "(Move your phone) to the right." During camera aiming, ambient sound was also recorded.

After taking a photograph, the user can record a voice message about the photograph. This voice memo augments the photograph with the user's own memories and experiences, which are valuable for the user's better recollection. The voice memo is also used as an auditory index in the photo album.

TouchPhoto supports another type of auditory tags, named as regional tags. By pinching on a certain region in the photograph, a user can set a regional tag and record a voice message specific to that region. Regional tags are designed to be added by a friend, but some low-vision users can do that by themselves. This is useful for pictures with a number of people or objects; later visually-impaired users can easily recognize the content of the photograph by touching the regional tags and listening to the voice memos. To our knowledge, regional auditory tags are a new feature to TouchPhoto.
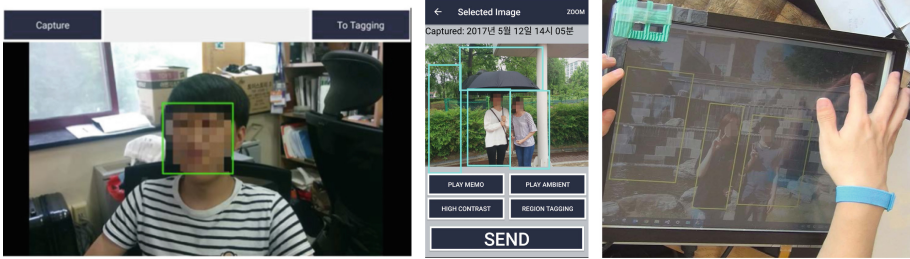
Fig. 3. Picture-taking, browsing, and understanding interface of Touchphoto.

2.3 Browsing and Understanding

Browsing and understanding the contents of photos can be done in both the Android app and tactile display. If s/he selects a photo in the album, menus for high-contrast image, regional tags, ambient sound, and sending the photo to tactile display are appeared on the screen (Fig. 3, the middle panel). When the user selects 'Send' menu at the bottom of the screen, the contents would be sent to the tactile display controlled by a program running on a PC (Fig. 3, the right panel). The photograph sent from the Android app is displayed on the 17-inch LCD screen with rectangles representing audio-tagged regions.

The screen also shows two buttons. One button toggles regional audio tags. When the regional tag function is toggled on, rectangular representations are shown on the screen, and the user can find them by scanning on the screen and perceiving simple electrovibration rendered when a tagged region is touched. A regional audio tag is played back when the user taps on the area. The other button controls the magnifier function. While the magnifier function is toggled on, the region of the human face is zoomed for easier tactile exploration. The user can perceive the 3D geometries and textures of important face features, like a nose, eyebrows, eyes, lips, and face contour, by touch.

3 Tactile Rendering

3.1 3D Rendering

In graphics, 3D features are often presented on a 2D display. We tried the similar approach using a surface haptic display. Since a human face consists of several 3D features, height rendering might be essential for highly informative presentation.

The first step of our tactile rendering is to extract the 2D coordinates of facial features in the photograph. We use an external API (Face++, Landmark Analysis) [2], which finds the positions of facial features, such as a nose, eyebrows, eyes, lips and the face contour, in a photograph. Then we fit a 3D face model (CANDIDE-3 model [1]) to the extracted facial features to obtain the height coordinates. These 3D coordinates of the facial features are used for tactile rendering.
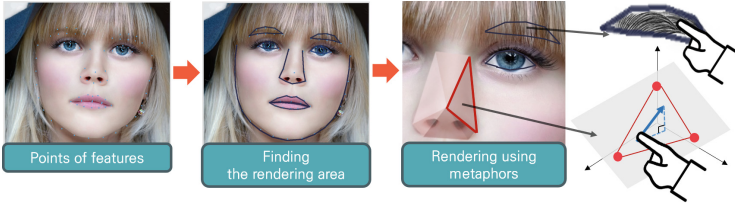
Fig. 4. Tactile rendering procedure.

The literature showed the feasibility of height rendering on an electrostatic friction display using gradient-based lateral force modulation [5,7]. We apply this method to render the 3D features in a face. If a user's finger scans the surface of tactile display, the position of contact was tracked by the infrared touchscreen frame that is attached on the display in real time. When the position of contact was inside the region of facial features, we calculated a 2D vector $\vec{v} = (x_2 - x_1, y_2 - y_1)$, by differentiating the two consequent input coordinates of (x_1, y_1) and (x_2, y_2). The height difference, $\Delta z = z_2 - z_1$, obtained from the fitted 3D face model, were calculated by interpolations in the plane which is being touched (Fig. 4). The tangential component, $\frac{\Delta z}{||v||}$ decided the output voltage. If it exceeds 2.0 $(\tan(63.5^\circ))$, it was clipped to 2.0, due to the amplifier's voltage limitations. The amplitude of output signal was calculated as $A = 20 \times \frac{\Delta z}{||v||} + 10.0$ (V), where 10.0 is the approximated AL point of our display's electrovibration. Thus, the output waveform was $A \times \sin(2\pi ft) + A$ or $A \times sgn(\sin(2\pi ft)) + A$, where A is the DC offset component. The frequencies (f) for the corresponding facial landmarks were determined by iterative procedures (Table 1).

Table 1. Tactile rendering parameters for textures.

	Eyebrow	Eye	Nose	Lip	Face contour
Target texture	Hair	Glass	Skin	Soft	Embossed carving
Waveform	Square	Sine	Sine + Square	Sine	Square
Frequency (Hz)	40	550	100	50	100
Amplitude (V)	80	80	40	60	80

3.2   Texture Rendering

Changing the frequency and amplitude of vibration provides the sensations of textures with different roughnesses [6]. For better identification of facial features, we render different textures for the major facial landmarks using the parameter values shown in Table 1. The parameter values are tuned to build analogies to the features. For example, eyes were rendered by high-frequency, smooth vibrations, while lips were by a bit rougher vibrations, albeit not too much. Hairy parts such as eyebrows were rendered using low-frequency, rough textures. The tactile rendering procedure is illustrated in Fig. 4.

4   Conclusions

In this paper, we have presented TouchPhoto, an integrated system to assist visually-impaired users to take, manage, and understand photographs independently. Visually-impaired users can take photographs with auditory guidance, as well as record several audio tags to aid recall of the photograph's content. For comprehension, a user can listen to the audio tags embedded in a photograph and also touch the photograph using an electrostatic friction display. We also implemented a tactile rendering algorithm of human faces that allows users to perceive height and texture using gradient-based lateral force modulation. We envision that the outcomes of this study could contribute to a better design of accessible photography apps for visually-impaired users. As a future work, we will improve haptic devices and rendering methods for understanding photographs, while not sacrificing the small and handy device form factor.

References

1. Ahlberg, J.: CANDIDE-3-an updated parameterised face. Linŏping University, Technical report (2001)
2. FacePlusPlus Inc.: Face++ cognitive services (2015). http://www.faceplusplus. com/
3. Harada, S., Sato, D., Adams, D.W., Kurniawan, S., Takagi, H., Asakawa, C.: Accessible photo album: enhancing the photo sharing experience for people with visual impairment. In: Proceedings of the 31st SIGCHI Conference on Human Factors in Computing Systems (CHI 2013), pp. 2127–2136 (2013)
4. Jayant, C., Ji, H., White, S., Bigham, J.P.: Supporting blind photography. In: Proceedings of the 13th International ACM SIGACCESS Conference on Computers and Accessibility (ASSETS 2011), pp. 203–210 (2011)
5. Kim, S.C., Israr, A., Poupyrev, I.: Tactile rendering of 3D features on touch surfaces. In: Proceedings of the 26th Annual ACM Symposium on User Interface Software and Technology (UIST 2013), pp. 531–538 (2013)
6. Klazky, R.L., Lederman, S.J., Hamilton, C., Grindley, M., Swenesen, R.H.: Feeling texture through a probe: effects of probe and surface geometry and exploratory factors. Percept. Psychophys. **65**(4), 613–631 (2003)
7. Osgouei, R.H., Kim, J.R., Choi, S.: Improving 3D shape recognition with electrostatic friction display. IEEE Trans. Haptics **10**(4), 533–544 (2017). https:// ieeexplore.ieee.org/abstract/document/7937894
8. Paterson, M.: The Senses of Touch: Haptics. Affects and Technologies. Bloomsbury Academic, London (2007)
9. Vázquez, M., Steinfeld, A.: An assisted photography framework to help visually impaired users properly aim a camera. ACM Trans. Comput.-Hum. Interact. (TOCHI) **21**(5), 25:1–25:29 (2014)
10. Voykinska, V., Azenkot, S., Wu, S., Leshed, G.: How blind people interact with visual content on social networking services. In: Proceedings of the 19th ACM Conference on Computer-Supported Cooperative Work & Social Computing (CSCW 2016), pp. 1584–1595 (2016)

A Ball-Type Haptic Interface
to Enjoy Sports Games

Takuya Handa[✉], Makiko Azuma, Toshihiro Shimizu,
and Satoru Kondo

NHK (Japan Broadcasting Corporation),
1-10-11 Kinuta, Setagaya-ku, Tokyo, Japan
handa.t-es@nhk.or.jp

Abstract. We have developed a ball-type haptic interface that enables users to enjoy watching sports games more actively. For a game such as beach volleyball, the viewer manipulates the ball-type device on the surface of a table where the court is displayed. The ball impact is presented as a vibration when he/she moves the device to where the player is hitting the ball. In this demonstration, we propose a viewing style to enjoy the speed and impact of sports games more actively.

Keywords: Haptics · Impact vibration · Human interface · Sports

1 Introduction

We are working to develop haptic interfaces for intuitive expression of developments in sports games, and we are striving to present intensity, which is the real thrill of sport. In this research, we have developed a ball-type haptic interface that uses beach volleyball 3D tracking data recorded by the object tracking system [1] to provide a more-active way to enjoy sports games. This system gives users a vicarious experience of being an athlete by coupling the experience with their body movements.

2 Haptic Interface for Enjoying Sports Games

Figure 1 shows external and internal views of the ball-type haptic device and examples of using the haptic interface for sports games. The device is covered with a 90-mm sponge ball, and it contains a vibration device, an active speaker, and a wireless charging adapter. We prototyped two devices, colored blue for the left audio channel and yellow for the right audio channel, corresponding to the colors of the team uniforms in the beach volleyball game. Figure 2 shows a schematic diagram of the interface. The left half of the figure shows the object tracking system [1]. This system analyzes video from four cameras placed around the court, recording the 3D position of the ball in each frame of the video in CSV format. Our interface is composed of the elements on the right half of Fig. 2. The control PC receives the data recorded by the object tracking system. Changes in the acceleration of the ball are computed from the position data and used to detect events such as when players hit the ball. Pre-set

simulated audio signals based on these events, such as a received sound, are sent to the devices via Bluetooth communication. The ball-type devices present the received audio signals as vibrations, and these devices also play them back as sounds. An Xperia Touch (SONY G1109 Android 7.0), which is a smart device with an LCD projector supporting touch operations on the projection surface, is connected to the control PC via Wi-Fi. The control PC outputs vibration signal on the right channel when the ball is in the area covered by the yellow device, and the PC outputs to the left channel when the ball is not in that area. According to the impression of the users who tried this system, the intervals between two strikes helped to understand situations such as attacks, sets, and missed receptions.

Fig. 1. External and internal views of the ball-type haptic device and practical examples.

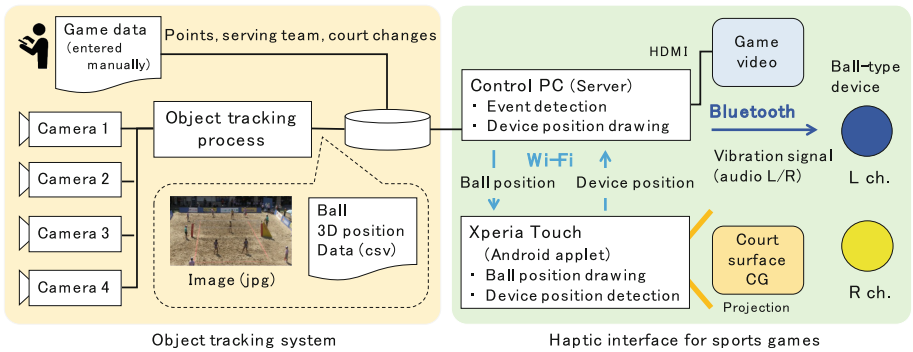
Fig. 2. Schematic diagram of object tracking system and haptic interface for sports games.

3   Conclusion

We proposed a viewing style to enjoy the speed and impact of sports games more actively. This interface is able to associate haptic information with real video of sports games such as beach volleyball using 3D ball location data obtained from video with object tracking technology.

Ethical Approval and Informed Consent
All procedures performed in studies involving human participants were in accordance with the ethical standards of the institutional committee and with the 1964 Helsinki declaration and its later amendments or comparable ethical standards. Informed consent was obtained from all individual participants included in the study.

Reference

1. Takahashi, M., Ikeya, K., Kano, M., Okubo, H., Mishina, T.: Robust volleyball tracking system using multi-view cameras. In: Proceedings of the 23rd International Conference on Pattern Recognition, WePT.9, pp. 2741–2746 (2016)

Exciting but Comfortable: Applying Haptic Feedback to Stabilized Action-Cam Videos

Daniel Gongora[✉], Hikaru Nagano, Masashi Konyo, and Satoshi Tadokoro

Graduate School of Information Sciences, Tohoku University,
6-6-01 Aramaki Aza Aoba, Aoba-ku, Sendai, Miyagi, Japan
{daniel,nagano,konyo,tadokoro}@rm.is.tohoku.ac.jp

Abstract. Videos recorded with action cameras let viewers experience extreme activities from a safe environment. Unfortunately, these videos can be uncomfortable to watch due to intense camera shaking, and video stabilization limits the experience of motion. Here we propose using vibrotactile feedback to preserve the feeling of motion in first-person view videos that have been stabilized. First, we created vibrations from camera motion estimates for two vibrotactile actuators that emphasize the feelings of turns and jumps. Then, we conducted a pilot user study to assess viewers perception of motion in stabilized videos with and without vibrotactile feedback. We observed that motion vibrations added to a stable video did not preserve the motion intensity ratings of a raw video without vibrations. We also observed that motion vibrations had a significant effect on comfort and satisfaction, and that video stabilization did not have a significant effect on the perceived synchronization between a stable video and vibrations generated from the original video.

Keywords: Vibrotactile · Video stabilization · Camera motion

1 Introduction

First-Person View (FPV) videos captured with action cameras open the doors for viewers to places and activities otherwise unreachable or too dangerous. These kind of videos often exhibit considerable amounts of trembling due to the intense nature of the activities being recorded. On the one hand such intense trembling can lead to headaches or even nausea in viewers [4] but on the other hand smoothing the movements in the video can altogether distort the original activity and instill in viewers a sense of lacking.

Camera trembling also plays a role in inducing a sense of self motion in viewers. In fact, a sense of self motion, or vection, starts sooner and lasts longer with vertical viewpoint trembling when compared to displays without trembling [7]. Therefore, preserving the feeling of movement while creating a comfortable experience requires an approach different to video stabilization alone.
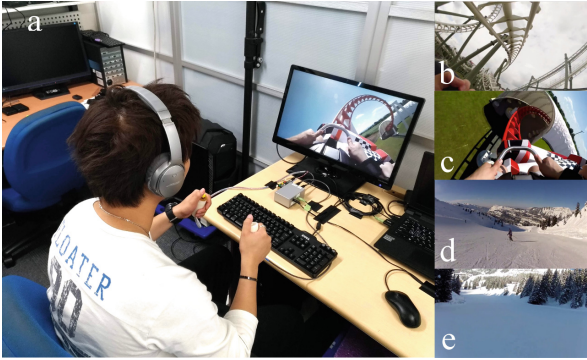
Fig. 1. (a). Participant watches a video while holding a vibrator on each hand. The videos show a rollercoaster (b and c) or downhill snowboard (d and e).

Here we propose using vibrotactile feedback for preserving the feeling of motion in stabilized videos. We use vibrotactile feedback because previous research has shown that vibrations are effective for modulating vection [1], and for improving the experience of watching videos [3]. We generate vibrotactile feedback for a video using the method we proposed in [2]. In our method, panning motion is felt as vibrations that travel from one hand to the other in the direction of motion in the video, and bumps or jumps are felt as short exponentially decaying vibrations on both hands. Our method uses the speed and acceleration of the movement between consecutive frames to modulate constant frequency vibrations in light of research that suggests that, when moving your finger sideways, vibrations to the fingertip proportional to the speed and acceleration of the finger affect the perception of physical parameters, such as viscosity and inertia [6]. Our method has proven to be effective in increasing the perceived realism and satisfaction of First-Person View (FPV) action videos.

2   User Study

This study consists of six feedback conditions resulting from the combination of two types of visual feedback and three types of vibrotactile feedback. Vibrotactile feedback is delivered on both hands and it is random (*random*), generated by our method (*motion*), or absent (*none*). The videos are either raw (*raw*), i.e. in its original form, or stabilized (*stable*) using [5] distributed with FFmpeg (https://www.ffmpeg.org/). Note that in this experiment random vibrations refer to vibrations that have no obvious connection with the video instead of vibrations generated from a random signal.

We used a four-question questionnaire to assess motion intensity, synchronization between video and vibrations, comfort, and satisfaction, see Table 1. Each question was followed by a seven-point Likert scale.

2.1   Participants and Procedure

Six male graduate students aged between 22 and 28 years ($M = 24.3$, $SD = 1.97$) were recruited. All of them signed informed consent prior to taking part in this experiment. The following experimental protocol was approved by Tohoku University's ethics committee.

Participants were instructed to sit down at about $80\,cm$ from the screen, resting their arms on the arms of the chair, Fig. 1. The study lasted for approximately $30\,min$ and it began with a brief instruction on how to fill the questionnaire. Then, to familiarize participants with the experimental conditions and to clarify what synchronism means in the context of this experiment, participants watched two $30\,s$ videos with vibrations generated by our method, and with random vibrations. Once the second video was over, participants could either replay both videos, or start the experiment. During the experiment, participants answered the questionnaire after watching $25\,s$ videos. The next video started playing $10\,s$ after the questionnaire was completed. This procedure was repeated 24 times (6 feedback conditions × 4 repetitions). For each of the four repetitions, participants were assigned to a feedback condition using a 6×6 Latin square balanced for first order carryover effects. Participants were instructed to answer Q2 with *Neither synchronized nor desynchronized* in conditions without vibrotactile feedback.

We used a different video in each of the four repetitions. The videos showed one of two scenarios from a FPV perspective: downhill snowboard, or rollercoaster. The presentation order was randomized for each participant.

Table 1. Questionnaire used in the user study.

Q1: How intense was the movement of the camera?
Q2: How much were video and vibrations synchronized?
Q3: How comfortable was your experience watching the video?
Q4: How was your experience watching this video?

2.2   Stimuli

Vibrotactile feedback was presented to the palms using Linear Resonant Actuators (Haptuator - Tactile Labs) enclosed with 3D-printed cylinders. Videos were presented using a full HD (1920×1080) 23.6-inch display. We used pink noise to block auditory feedback from biasing participant's judgments.

We created motion vibrations from vertical and horizontal displacements in the video. Vertical displacements trigger short exponentially decaying vibrations on both hands when they exceed a fixed threshold, and horizontal displacements modulate the amplitude of constant frequency vibrations, [2].

We created random vibrations for each video from the vibrations generated by our method. First, the timing of impacts in a video was randomized but the number of impacts was kept unchanged. Then, vibrations for horizontal camera movements were reversed and, left and right channels were swapped. This way, random vibrations had no deliberate spatial or temporal connection with the video but they were not conspicuously different from vibrations generated by our method.

3 Results

Participants' ratings are shown in Fig. 2. We analyzed the effects of video stabilization and vibrotactile feedback type with a significance level of $\alpha = .05$. We used a Cumulative Link Mixed Model (CLMM) with video stabilization, vibrotactile feedback type and their interaction as fixed effects, and subject as random effect. The model uses a logit link function with equidistant thresholds. Tukey-adjusted least square means pairwise comparisons are shown in Table 2.

Table 2. Tukey-adjusted least square means pairwise comparisons. Significant values are shown in gray and NA denotes comparisons that do not apply in Q2 due the absence of vibrotactile feedback.

ID	Comparison	Q1	Q2	Q3	Q4
1	motion,raw - none,raw	0.861	NA	<0.001	<0.001
2	motion,raw - random,raw	0.980	0.012	0.375	0.673
3	motion,raw - motion,stable	0.003	0.824	0.385	0.510
4	motion,raw - none,stable	0.037	NA	0.724	0.042
5	motion,raw - random,stable	0.010	0.001	0.437	0.308
6	none,raw - random,raw	0.998	NA	0.125	0.001
7	none,raw - motion,stable	<0.001	NA	<0.001	<0.001
8	none,raw - none,stable	0.001	NA	0.027	0.083
9	none,raw - random,stable	<0.001	NA	0.114	0.003
10	random,raw - motion,stable	<0.001	0.001	0.002	0.022
11	random,raw - none,stable	0.003	NA	0.993	0.684
12	random,raw - random,stable	0.001	0.751	1.000	0.993
13	motion,stable - none,stable	0.969	NA	0.012	<0.001
14	motion,stable - random,stable	0.999	<0.001	0.003	0.003
15	none,stable - random,stable	0.999	NA	0.996	0.937

Motion intensity ratings (Q1) are shown in Fig. 2. We observed a significant effect of Video Stabilization ($p < .001$). A likelihood ratio test suggests that individual differences were significant ($p < .001$). Motion intensity perception in stable videos was split between weak and strong, whereas in raw videos motion was mostly perceived as strong regardless of the type of vibrotactile feedback.
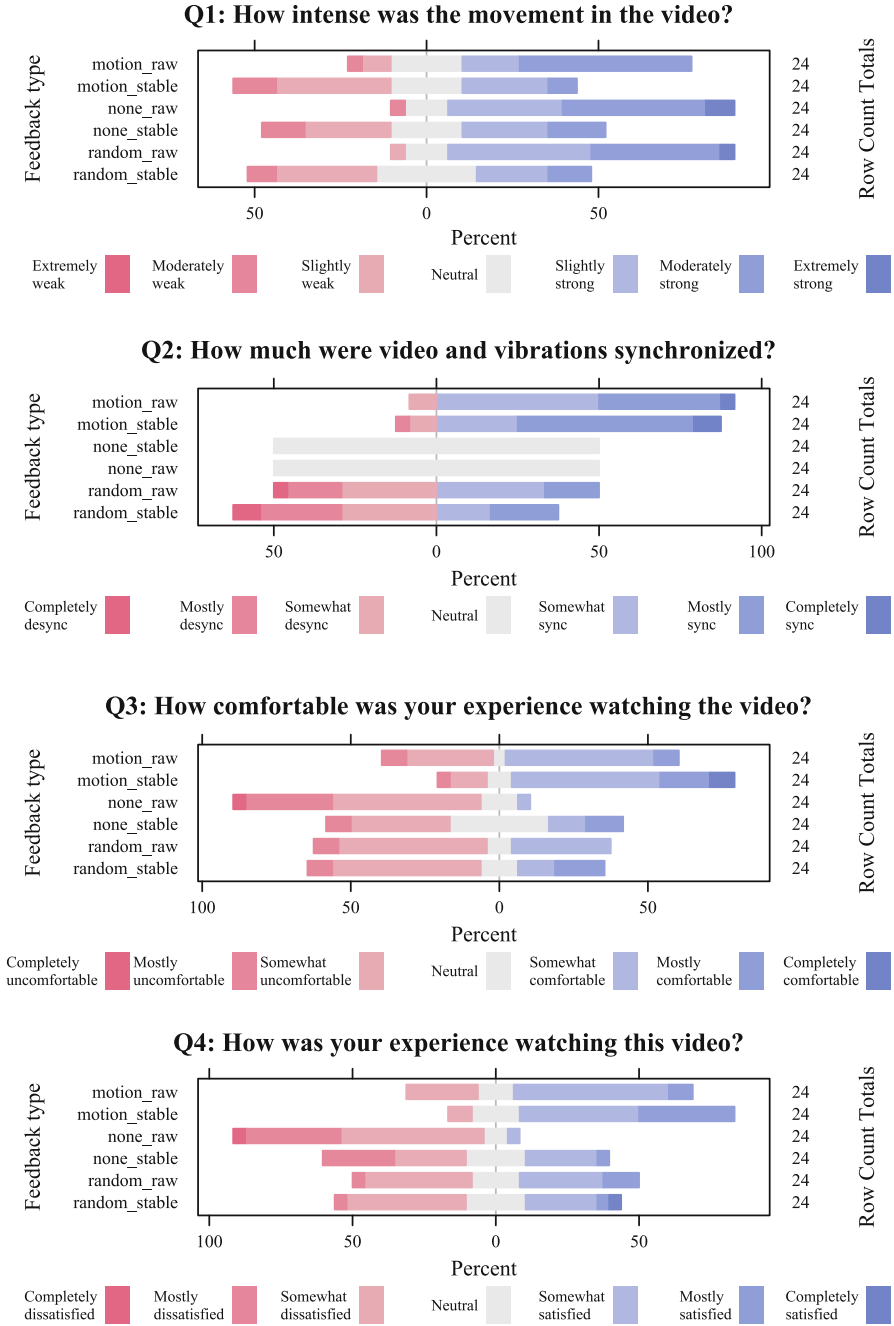
Fig. 2. Percentage of ratings for each point on the scale.

Furthermore, motion intensity ratings of a stable video with motion vibrations were significantly different from those of a raw video without vibrations (Q1: 7). A raw video without vibrations had a larger proportion of ratings describing the movement in the video as strong.

Synchronization ratings (Q2) are shown in Fig. 2. We observed a significant effect of Vibrotactile feedback ($p < .001$). A likelihood ratio test suggests that individual differences were not significant ($p = .963$). Vibrations generated by our method were mostly perceived as being synchronized with the video, whereas for random vibrations synchrony ratings were split between synchronized and desynchronized. Video stabilization had no significant effect on synchronization (Q2: 3, 12).

Comfort ratings (Q3) are shown in Fig. 2. We observed a significant effect of Vibrotactile feedback ($p < .001$) and Video stabilization ($p = .003$) on comfort ratings. A likelihood ratio test suggests that individual differences were not significant ($p = .999$). Stabilizing a video had a significant effect on comfort only when vibrations were not presented (Q3: 8). Adding motion vibrations to a video had a significant effect on comfort (Q3: 1, 13).

Satisfaction ratings (Q4) are shown in Fig. 2. We observed a significant effect of Vibrotactile feedback ($p < .001$) and Video stabilization ($p = .025$) on satisfaction ratings. A likelihood ratio test suggests that individual differences were not significant ($p = .398$). Raw videos without vibrotactile feedback were mostly associated with dissatisfaction, whereas stable videos with vibrations generated by our method were mostly associated with satisfaction. Adding vibrations generated by our method to a video had a significant effect in satisfaction (Q4: 1, 13), random vibrations had a significant effect only with raw videos (Q4: 6).

4   Conclusion

We proposed using vibrotactile feedback to compensate the lack of motion in FPV that have been stabilized and we conducted a pilot user study to assess this proposal. We observed that motion intensity ratings of a stable video with motion vibrations differed significantly from ratings obtained with a raw video without vibrations. We also observed that video stabilization did not have a significant effect on ratings pertaining to video and vibrations synchronization. Finally, we observed that motion vibrations had a significant effect on comfort and satisfaction ratings when compared to conditions without vibrotactile feedback. In future studies we will consider a broader range of vibrotactile effects to better represent camera motion, and we will characterize the feeling of motion not only in terms of intensity.

References

1. Farkhatdinov, I., Ouarti, N., Hayward, V.: Vibrotactile inputs to the feet can modulate vection. In: 2013 World Haptics Conference (WHC), pp. 677–681. IEEE (2013)
2. Gongora, D., Nagano, H., Konyo, M., Tadokoro, S.: Vibrotactile rendering of camera motion for bimanual experience of first-person view videos. In: 2017 IEEE World Haptics Conference (WHC), pp. 454–459. IEEE (2017)
3. Kim, M., Lee, S., Choi, S.: Saliency-driven real-time video-to-tactile translation. IEEE Trans. Haptics **7**(3), 394–404 (2014)
4. Kuze, J., Ukai, K.: Subjective evaluation of visual fatigue caused by motion images. Displays **29**(2), 159–166 (2008)
5. Martius, G.: Vid.stab - video stabilization library. https://github.com/georgmartius/vid.stab
6. Okamoto, S., Konyo, M., Tadokoro, S.: Vibrotactile stimuli applied to finger pads as biases for perceived inertial and viscous loads. IEEE Trans. Haptics **4**(4), 307–315 (2011)
7. Palmisano, S., Allison, R.S., Kim, J., Bonato, F.: Simulated viewpoint jitter shakes sensory conflict accounts of vection. Seeing Perceiving **24**(2), 173–200 (2011)

Configuration of Haptic Feedback Based Relief Robot System

Byung-jin Jung[1], Tae-Keun Kim[1], Geon Won[1], Dong Sub Kim[1], Jung-Hoon Hwang[1(✉)], and Jee-Hwan Ryu[2]

[1] Korea Electronics Technology Institute, Bucheon, Korea
{jbjsin, taekeunkim17, hangams,
dongsip, hwangjh}@keti.re.kr
[2] Korea University of Technology and Education, Cheonan, Korea
jhryu@koreatech.ac.kr

Abstract. This paper deals with the development of a relief robot system that can provide first aid to the injured person by remote control in disaster environment and battlefield. To perform safe first aid, relief robot has hardware and controller that can feed back the contact force while following the command of remote controller. In addition, a controller capable of maintaining system stability under the influence of time delay and packet loss due to communication state during remote control is mounted. The developed relief robot system is evaluated through experiments simulating actual first aid procedures.

Keywords: Relief Robot · Haptic feedback · Remote control ·
Series elastic actuator · Virtual Spring Damper

1 Introduction

The injured person rescue in the disaster environment and battlefield is a long - standing concern of mankind. With the development of robotic technology, robotic systems are being developed that can replace humans in various risk situations. Relief Robot is a system that provides first aid to injured person by using remote manipulation robot technology in a difficult environment such as disaster environment and battle field which is difficult to approach [1]. For successful rescue, Relief Robot requires safe interaction with surrounding environment. Specifically, the Relief Robot has a high possibility of intentional/unintentional contact between the environment and the robot. In this reason, Relief Robot should have hardware and software functions to minimize damages of robot and surrounding environment.

In this paper, we propose Relief Robot Manipulator and Remote Control System which can control the intentional contact situation by the operator and can have haptic feedback of contact force. The developed Relief Robot system adopts TDPA - based controller to secure system stability even in the presence of communication delay and packet loss.

2   Relief Robot System Configuration

The Relief Robot manipulator should be able to measure joint torque and contact force for remote manipulation and haptic feedback performance. This section deals with manipulator hardware and controller configurations for contact force and joint torque measurements.

The Relief Robot manipulator system developed in this paper can be shown as Fig. 1. The remote control unit is configured using Sigma 7 of Force Demension INC.
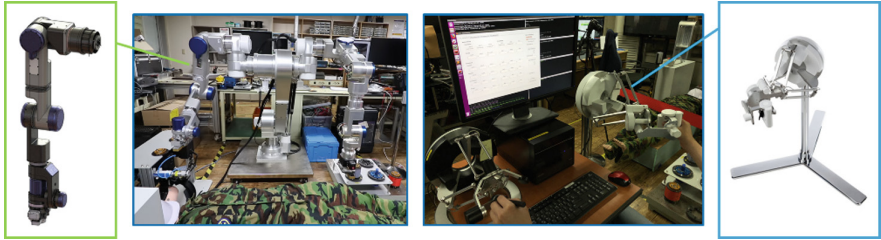

Fig. 1. Configuration of the Relief Robot system.

2.1   Contact Force Measurement and Haptic Feedback

The contact force between the external environment and the Relief Robot manipulator is measured by an F/T sensor mounted on the wrist. The F/T sensor used in the system configuration is Robotous INC. And the structure of the mounting part is the same as Fig. 2.
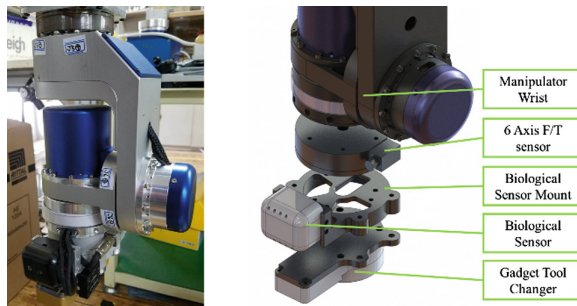

Fig. 2. Wrist F/T sensor mount structure.

The F/T sensor mounted on the wrist of Relief Robot measures the forces of three axes based on the tool coordinate system. For intuitive remote manipulation, the three axis forces measured on the tool coordinate system are converted to the robot coordinate system. Robot coordinate reference force information is converted back to the remote controller coordinate system to provide haptic feedback to the user. At this time, the feedback force is amplified or attenuated to an appropriate level through the haptic feedback gain. The process can be expressed as (1).

$$F_{fb} = K \times {}^r_b R(q_{remote}) \times {}^b_t R(q_{robot}) \times F_{measure} \tag{1}$$

In this case, ${}^b_t R$ represents the rotation transformation from the tool coordinate system to the base coordinate system, and ${}^r_b R$ represents the rotation transformation from the remote controller coordinate system to the base coordinate system. Also, K means haptic feedback gain.

2.2   Command Tracking and Joint Torque Measurement

To follow remote control commands, Virtual Spring Damper (VSD) based motion controller was applied to Relief Robot. The VSD based motion controller creates a virtual spring-damper system that connects the manipulator end-effector with the target point. At this time, the force generated by the virtual spring-damper system is converted into a joint torque command that causes the manipulator to follow the target position [2]. This process is equivalent to (2).

$$\tau_{cmd} = J^T \times \left(K_s \times (X_{des} - X) - K_v \times \dot{X}\right) + g(q) \tag{2}$$

J^T is the Jacobian transpose of the system, K_s is a virtual spring, and K_v is a virtual damper. The target point X_{des} is generated from the input of the remote control device. In order to follow τ_{cmd} at each joint of the manipulator, joint torque measurement and control are required.

Series Elastic Actuators (SEA) were applied to each joint for joint torque measurement and control. SEA is an actuator with a deformable structure between the output of the joint actuator module and the link of the robot [3]. Using the torsion and stiffness of the deformable structure located at the output of the SEA, the joint torque can be measured as (3).

$$\tau_s = K \times \left(\frac{\theta}{N} - q\right) \tag{3}$$

K is the stiffness of the deformable structure, this the position of the motor, q is the position of the link, and N is the reduction ratio. The shape of the SEA and the deformable structure used in this paper can be expressed as Fig. 3.
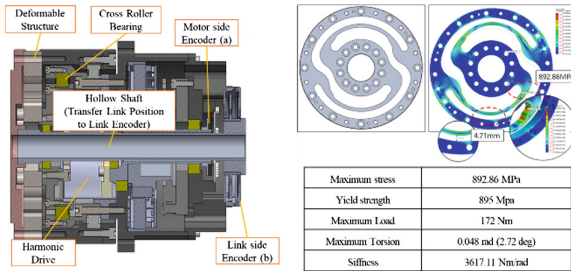

Maximum stress	892.86 MPa
Yield strength	895 Mpa
Maximum Load	172 Nm
Maximum Torsion	0.048 rad (2.72 deg)
Stiffness	3617.11 Nm/rad

Fig. 3. Structure of series elastic actuator and deformable component.

Where a is an encoder that measures the joint output and b is an encoder that measures the position of the link.

However, low joint stiffness has the disadvantage of reducing the response frequency of joint system. These disadvantages lead to degradation of the path following performance and generation of undesired joint vibrations. In this paper, the Disturbance Observer (DOB) based joint torque controller is applied to control the SEA. The DOB-based SEA torque controller considers the influence of low stiffness as a kind of disturbance and compensate it. This type of controller has proven to be stable in cases such as [4, 5].

2.3   Stability Enhancement of Remote Control

The Time Domain Passivity Approach based Remote Control algorithm is an algorithm that adjusts the input to maintain system stability even in situations of communication delay or packet loss [6]. The TDPA-based remote control algorithm can be represented as shown in Fig. 4.
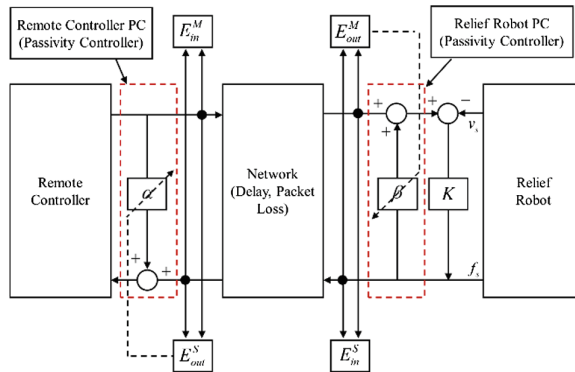
Fig. 4.   Block diagram of TDPA based remote controller.

In this case, E_{in}^{M} in is the energy input to the remote control master, and E_{out}^{M} is the energy output from the remote control master. E_{in}^{S} is the energy input to the Relief Robot, and E_{out}^{S} is the energy output from the Relief Robot. The input or output energy is calculated from the speed of the remote control master and manipulator, and the passivity observer (PO), which estimates the passivity of the system, can be configured as Eq. (4).

$$E^{M} = \Delta T \times \left(E_{out}^{M} - E_{in}^{M} \right)$$
$$E^{S} = \Delta T \times \left(E_{out}^{S} - E_{in}^{S} \right)$$

(4)

If the value of passivity observer (PO), (eq) is negative, the system is stable, but if the value is positive, there is a possibility that the system becomes unstable. When the value of passivity observer (PO) is positive, the passivity controller (PC), represented by alpha and beta in Fig. 4, keeps the system stable by shaping the output of the remote controller master and Relief Robot slave.

3   Experiment and Discussion

The experimental procedure is shown in Fig. 5. The gadget that supplies the injured person with oxygen is mounted on the end effector of the Relief Robot manipulator. The oxygen supply gadget is one of a series of gadgets developed for relief operations. The series for relief work has hemostasis, oxygen supply and injection, and its development process has been reported in [7]. The operator uses Sigma 7 of Force Dimension INC. to remotely manipulate the Relief Robot to supply oxygen to the injured person. At this time, the data communication between the remote controller and the Relief Robot is set up to generate a time delay of 300 ms and a packet loss of 30% ratio.

Fig. 5. First aid experiment for system verification.

Experimental results show that the Relief Robot manipulator successfully applied the oxygen supply gadget to the injured person according to the operation of the operator. In addition, the stability of the system was maintained even in the event of contact.

The experimental procedure and additional experiments about contact situation are described in the attached video material.

References

1. Kim, H., Park, D., Choi, T., Do, H., Kim, D., Kyung, J., Park, C.: Design of high payload dual arm robot with replaceable forearm module for multiple tasks: human rescue and object handling. J. Korea Rob. Soc. **12**(8), 441–447 (2017)
2. Arimoto, S., Hiroe, H., Ryuta, O.: A simple control method coping with a kinematically ill-posed inverse problem of redundant robots: analysis in case of a handwriting robot. Asian J. Control **7**(2), 112–123 (2005)
3. Pratt, G.A., Williamson, M.M.: Series elastic actuators. In: 1995 IEEE/RSJ International Conference on Intelligent Robots and Systems. Human Robot Interaction and Cooperative Robots, Pittsburgh, USA, pp. 399–406 (1995)
4. Paine, N., Mehling, J.S., Holley, J., Radford, N.A., Johnson, G., Fok, C.-L., Sentis, L.: Actuator control for the NASA-JSC Valkyrie humanoid robot: a decoupled dynamics approach for torque control of series elastic robots. J. Field Rob. **32**(3), 378–396 (2015)
5. Kong, K., Bae, J., Tomizuka, M.: A compact rotary series elastic actuator for human assistive systems. IEEE/ASME Trans. Mechatron. **17**(2), 288–297 (2012)
6. Ryu, J.H., Kwon, D.S., Hannaford, B.: Stability guaranteed control: Time domain passivity approach. IEEE Trans. Control Syst. Technol. **12**(6), 860–868 (2004)
7. Park, T., Jeong, C., Lee, J., Lee, S., Kim, H.: Design of special end effectors for first aid robot. In: 2017 IEEE International Symposium on Safety, Security and Rescue Robotics (SSRR), Shanghai, China, pp. 179–180. IEEE (2017)

Gravity Ball: A Virtual Trackball with Ultrasonic Haptic Feedback

Jemin Lee and Seokhee Jeon[✉]

Department of Computer Science, Kyung Hee University, Seoul, South Korea
i_jemin@hotmail.com, jeon@khu.ac.kr

Abstract. This paper presents a virtual trackball named Gravity Ball. By touching, grabbing, pushing, dragging, swiping, and scrolling the Gravity Ball, a user can conduct multi-mode manipulations on a 3D object via a single interaction medium. Physics-based haptic feedback is provided through ultrasonic-based mid-air haptic device, enabling the user more immersive interaction and more precise manipulation. Potential of the concept is demonstrated through a gun-shooting video game.

Keywords: AR · VR · Trackball · UltraHaptics

1 Concept

1.1 Virtual Haptic Interface with Real World Physics

Manipulation of virtual objects in 3D space has been gained a lot of attention. Conventional interfaces, e.g., game pad and mouse-keyboard combination, still rely on the legacy of interfaces for 2D manipulation which can't easily combined with 3D virtual environments by reduced 3D manipulation performance.

More advanced approaches such as 3D motion-based and gesture-based interfaces (e.g., Wii-mote and Kinect) have been around. These interfaces achieved great success due to their intuitiveness in 3D manipulation. They usually directly map the user's 3D motion to the objects' position and/or applied the laser-pointer metaphor to the 3D interface. However, one of the main shortcomings of this approach is that precise 3D manipulation is not very easy compared to conventional 2D-based interfaces because 3D motion-based interface has a no real-world collider, so they can't provide physical haptic feedback. Because conventional 2D-based interfaces have a real-world collider, a user know position and movable range of controller by touching or pushing without seeing it.

To overcome these shortcomings, we merge the positive aspects of both 2D and 3D interfaces. To this end, we present Gravity Ball; a 3D virtual trackball interface with mid-air haptic feedback. Our assumption is that trackball metaphor inherently increases the accuracy of controlling while 3D manipulation-ability is preserved by applying the concept of direct mapping used in 3D-based interface to the trackball.

In addition, we combined this concept with a mid-air haptic device (UltraHaptics interface), providing a user a real-world physics of the trackball, which, we believe, further improves the immersion and accuracy of manipulation. Through haptic

feedback, the user can interact with an interface without seeing it and can gauge the value of inputs through haptic channel. Furthermore, we added additional modes of control by allowing a user not only rotating, but also pushing, swiping, grabbing, and dragging the trackball.

2   Gravity Ball

2.1   Hardware and Software

We use UltraHaptics DK1 which produce haptic feedback in a free space by ultrasonic wave and Leap Motion for detecting a user's hand. We use Unity3D which contains physics engines for creating a software. We choose simple sphere shape for Gravity Ball and haptic feedback and physics model is created accordingly.

2.2   Features

A user can touch Gravity Ball in a screen, by moving user's hand (Position of hands tracked by Leap Motion). We implemented the Gravity Ball not fixed in a space, but hanged at a certain point by a spring. Thus, it can be pushed by user's hand, and Gravity Ball won't be overlapped with user's hand. Due to the spring the ball always return back to the origin position after releasing the force. The stiffness of the spring pushes back user's hand, and user can feed physical repulsive force (Fig. 1).
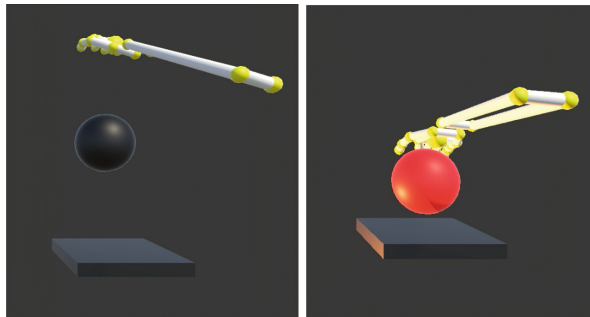
Fig. 1. Pushing the Gravity Ball

A user can grab, scroll, swipe, push, pull, press along all direction (except for pushing or pulling from bottom to up because user's hand blocks the ultrasonic feedback). Both the absolute value and relative velocity of the movement (including position and rotation) can be used as a value as an input depending on the application.

The system can detect how hard a user push by position and velocity. Based on these and physics simulation, the haptic feedback intensity is calculated. The intensity is rendered to the user haptically through UltraHaptics as well as visually by changing the color of the ball.

2.3   Types of Input

As a proof-of-concept work, present implementation only offer the following four different types of inputs: (1) wheel scrolling by X axis which imitate mouse wheel scrolling, (2) horizontal or vertical swiping by X and Z axis which imitate trackpad swiping, (3) horizontal or vertical pushing or pulling by X and Z axis, and (4) pressing down by Y axis which imitate button press. All axis values come between - 1.0 and 1.0 except pressing down input come between true or false. Note that this is examples of inputs, and more diverse application is possible.

Some of raw input values will be decreased or ignored when it is against with user's intention. For example, when user scrolling Gravity Ball, Gravity Ball will detect changes of pitch but also there are also small changes of yaw and roll. In that case, we believe yaw and roll values are not necessary. So, if Gravity Ball detects a motion and it's identified as wheel scrolling, Gravity Ball will decrease or set raw input values 0 which related to yaw and roll (Fig. 2).

Fig. 2. A user grab, press, swipe Gravity Ball

2.4   Gravity Ball Shooter Game

We created demo shooter game using Gravity Ball. Player have to stay alive by shooting Enemy AI. In this game, player can shoot or reload by pressing down Gravity Ball. Player can adjust gun rotation by swiping and scrolling Gravity Ball (Fig. 3).

Fig. 3. A user fire a gun by pressing down Gravity Ball, rotate a gun by scrolling Gravity Ball

2.5   Codes

Gravity Ball offer public method for attaching other Unity3D projects. Like Unity built-in Input methods, Gravity Ball offer these methods:

```
GravityBall.GetInputAxis("Move Axis Name"); // -1.0 ~ 1.0
GravityBall.GetInputSwipe("Swipe or Scroll Axis Name");
GravityBall.Instance.GetButton(); // true or false
```

We created public repositories for Gravity Ball [1] and shooter demo [2] on GitHub so anyone can clone the project.

References

1. Ultra-Haptics-Gravity-Ball. https://github.com/IJEMIN/Ultra-Haptics-Gravity-Ball. Accessed 17 Aug 2018
2. gravityball-shooter. https://github.com/IJEMIN/gravityball-shooter. Accessed 18 Aug 2018

SwarmGlove: A Wearable Tactile Device for Navigation of Swarm of Drones in VR Environment

Luiza Labazanova(✉), Akerke Tleugazy, Evgeny Tsykunov,
and Dzmitry Tsetserukou

Skolkovo Institute of Science and Technology, Moscow, Russian Federation
{Luiza.Labazanova, Akerke.Tleugazy, Evgeny.Tsykunov,
D.Tsetserukou}@skoltech.ru

Abstract. Navigation of the quadcopters with tactile feedback has been extensively studied for the cases of single drone. However, the operation of the swarm is a complex task, which requires intuitive interaction. We introduce wearable tactile device aimed at control of the formation with impedance interlinks. Tactile patterns representing dynamics of the swarm (extension or contraction) are proposed. The user feels the state of the swarm at the fingertips and receives valuable information, which, coupled with visual feedback, improves the controllability of the complex life-like formation. In order to demonstrate capabilities of the technology, we developed VR applications in Unity, in which user guides the swarm in the virtual city and village environments through both static and dynamic obstacles to avoid collisions.

Keywords: Human-swarm interaction · Vibrotactile glove · Swarm navigation

1 Introduction

The control of a swarm of unmanned aerial vehicles (UAVs) is increasingly investigated by researchers. There are numbers of studies that suggest different approaches to provide effective coordination, navigation, and planning of multi-robots in the cluttered environment [1, 2]. However, flying robots usually face difficulties associated with limited battery life. Additionally, control of delivery drones in the habitual areas is prohibited in most cases. These issues can be solved by navigation of robots in virtual reality (VR), which provides flexible and safe environment for conducting experiments.

Kato [3] proposed a remote navigation system for a simple telepresence robot in VR. However, it is difficult for operator to guide robots in the crowded environment and avoid obstacles simultaneously due to the limited information from robots. Additionally, while tracking multiple objects, human visual system is overloaded and the more objects are flying the more stress operator is experiencing. This paper presents a vibrotactile glove for interaction of human with a swarm of aerial robots by providing an intuitive mapping of the formation state to the human fingertips. We propose to deliver the tactile feedback about such parameters of the formation state that are hard to estimate from the visual feedback, i.e., formation state (extension or contraction) and

the direction of state propagation. This information can improve the effectiveness of swarm navigation in the unstructured environment.

2   SwarmGlove Architecture

2.1   Technology of Wearable Tactile Device

We propose to control a swarm using a wearable tactile glove. We designed a prototype of the tactile display with five ERM vibrotactile actuators attached to the fingertips as shown in Fig. 1(a). Vibration motors receive control signals from Arduino UNO; infrared reflective markers are located on the top of the unit (Fig. 1(b)). The micro-controller receives values of the formation state parameters from PC through Xbee Pro radio frequency modules and generates an appropriate vibration pattern.
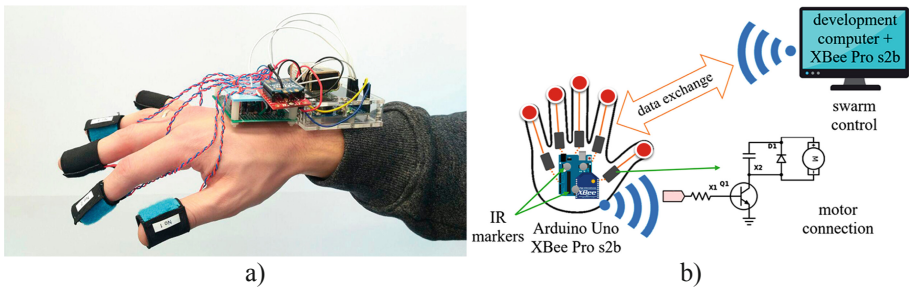
Fig. 1.   (a) Tactile glove; (b) Configuration of SwarmGlove.

2.2   Tactile Patterns

We designed tactile patterns for presenting the feeling of the swarm behavior at the fingertips. Our motivation on selection of the particular tactile pattern was to bring the valuable information that potentially can improve the quality (speed, safety, precision) of operation of the swarm. During swarm manipulation by the operator, the formation can change its shape, becoming contracted or extended (because of impedance inter-links), which can lead to the collisions [4]. The distance between drones is presented by the tactile flow propagation. If the formation is extended, the flow goes from the middle finger to the side ones (Fig. 2(a–c)), otherwise, from the side fingers to the middle one (Fig. 2(d–f)). The change of distance is presented by the gradient of vibration intensity, see Fig. 2(a, d).
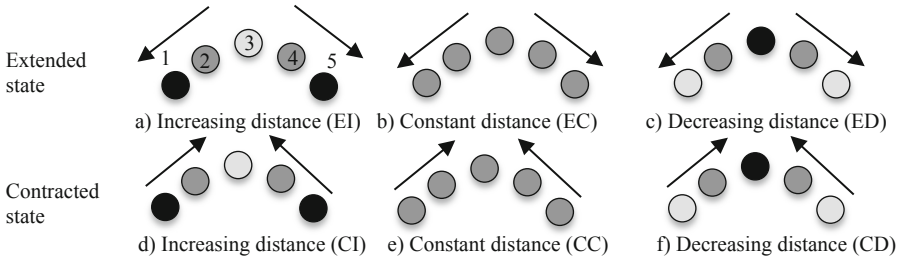
Fig. 2. Tactile patterns for representing the state of the formation in terms of drone-to-drone distance. Each circle represents finger of a right hand (view from the dorsal side of the hand). The gray scale color represents the intensity of tactor vibration.

2.3   SwarmCity VR Application

We have developed several VR applications in Unity to demonstrate the simulation of the swarm navigation in the cluttered environment. In *SwarmCity* application, user guides the swarm of three drones in the virtual city (Fig. 3(a)). A large amount of buildings creates a high risk of a collision of the swarm with them. The task is to guide the swarm with a given speed from the starting position to the finish without collisions.
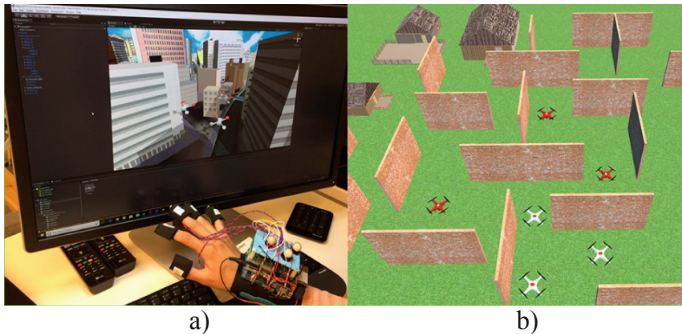
Fig. 3. (a) *SwarmCity* application; (b) *SwarmVillage* application.

2.4   SwarmVillage Application

In *SwarmVillage* application user is able to control the swarm including its velocity in the village environment (see Fig. 3(b)). There are static obstacles in the form of walls, buildings, and trees. In addition, there are patrol drones (red drones) flying through the village that poses an additional risk to the swarm. Thus, the main idea is to guide the swarm of drones (white drones) from point A to point B in a safe manner with support of tactile feedback.

2.5 Visualization Setup

For visualization of the virtual environment, we use HTC Vive VR headset. Control of the swarm by the user is implemented through HTC vive tracker attached to the user's palm (Fig. 4).
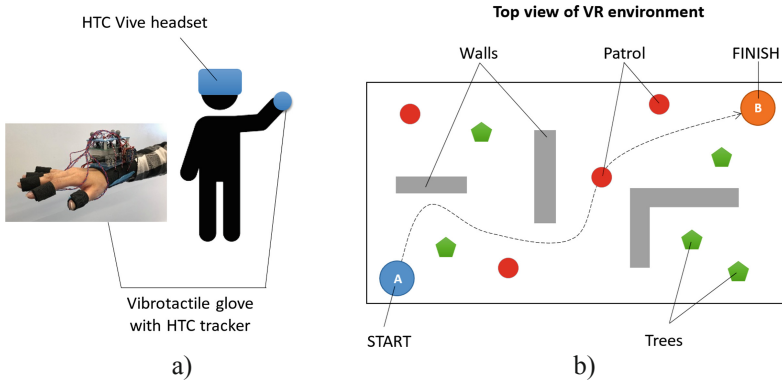
Fig. 4. (a) Configuration of the *SwarmVillage* demonstration; (b) Virtual environment layout.

3 Experiments and Results

Six right-handed volunteers participated in the experiment. Optimal sensitivity of the skin is achieved at frequencies between 150 and 300 Hz [5]. Therefore, for three vibration levels we assigned average frequency values of: 150 Hz, 200 Hz, 250 Hz (refer to three gray scale colors shown in Fig. 2). The experiment was devoted to the detection of multi-modal patterns. Each of the subjects experienced 60 stimuli (6 patterns were repeated 10 times in a random order).

All procedures performed in studies involving human participants were in accordance with the ethical standards of the institutional and national research committee and with the 1964 Helsinki declaration and its later amendments or comparable ethical standards. Informed consent was obtained from all individual participants included in the study. The results of the user study for the experiment are listed in Table 1. The

Table 1. Group percentage recognition of patterns for experiment.

Percentage, %	Example					
Actual pattern	CD	CI	CC	ED	EI	EC
Contracted state, Decreasing distance (CD)	**98.3**	0	0	0	1.7	0
Contracted state, Increasing distance (CI)	3.3	**86.7**	8.3	1.7	0	0
Contracted state, Constant distance (CC)	10.0	5.0	**85.0**	0	0	0
Extended state, Decreasing distance (ED)	1.7	0	0	**86.7**	0	11.7
Extended state, Increasing distance (EI)	3.3	3.3	0	8.3	**66.7**	18.3
Extended state, Constant distance (EC)	0	0	0	3.3	3.3	**93.3**

diagonal term of the confusion matrix indicates the percentage of the correct responses of participants. The first letter in the abbreviation of the pattern name stands for the current formation state (contraction or extension), while the second letter stands for the state propagation direction (how the drone-to-drone distance is changing: increasing, constant, or decreasing).

In order to evaluate the statistical significance of the differences between patterns, we analyzed the results of the user study using single factor repeated-measures ANOVA, with a chosen significance level of $p < 0.05$.

The results of experiment revealed that the mean percent of correct scores for each subject averaged over all six patterns ranged from 78.3 to 96.7%, with an overall group mean of 86.1% of correct answers. Table 1 shows that the distinctive patterns CD and EC have higher percentages of recognition 98.3 and 93.3, respectively. On the other hand, patterns CC and EI have lower recognition rates of 85 and 66.7%, respectively. For most participants, it was difficult to recognize pattern EI, which usually was confused with pattern EC. Therefore, it is required to design more distinctive tactile stimuli to improve the recognition rate.

The ANOVA results showed a statistically significant difference in the recognition of different patterns ($F(5, 30) = 3.09$, $p = 0.023 < 0.05$). The paired t-tests showed statistically significant differences between the EI and EC ($p = 0.015 < 0.05$), CD and CI ($p = 0.017 < 0.05$), CD and CC ($p = 0.0007 < 0.05$), CD and EI ($p = 0.019 < 0.05$). However, the results of paired t-tests between other patterns did not reveal any significant differences, thus, these patterns have nearly the same recognition rate.

4   Conclusion

The wearable tactile glove SwarmGlove was designed to allow operator to control the swarm of drones in VR environments in an intuitive and safe manner. The proposed tactile patterns deliver to the operator the state of drone formation in order to provide safe navigation of dynamic swarm. User study experiment to understand the rate of recognition of proposed patterns was conducted. ANOVA results revealed a statistically significant difference between all patterns. Paired t-test showed patterns, which users discriminate easier. The developed applications *SwarmCity* and *SwarmVillage* make it possible to learn how to navigate swarm of drones in the city and village environments safely. Future work will focus on the user study of swarm operation in VR. We would like to find out the effect of SwarmGlove on safety and effectiveness of swarm control. Moreover, we plan to develop VR applications for simulation of consumer goods delivery by swarm and tactile communication of visually impaired persons with drones.

References

1. Duarte, M., Oliveira, S., Christensen, A.: Hybrid control for large swarms of aquatic drones. In: Proceedings of the 14th International Conference on the Synthesis & Simulation of Living Systems, pp. 785–792. MIT Press, Cambridge (2014)
2. Araki, B., Strang, J., Pohorecky, S., Qiu, C., Naegeli, T., Rus, D.: Multi-robot path planning for a swarm of robots that can both fly and drive. In: 2017 IEEE International Conference on Robotics and Automation, pp. 5575–5582. IEEE (2017)
3. Kato, Y.: A remote navigation system for a simple tele-presence robot with virtual reality. In: 2015 IEEE/RSJ International Conference on Intelligent Robots and Systems, pp. 4524–4529. IEEE (2015)
4. Tsykunov, E., Labazanova, L., Tleugazy, A., Tsetserukou, D.: SwarmTouch: tactile interaction of human with impedance controlled swarm of nano-quadrotors. In: 2018 IEEE/RSJ International Conference on Intelligent Robots and Systems. IEEE (2018, in press)
5. Jones, A., Sarter, N.: Tactile displays: guidance for their design and application. Hum. Factors **50**(1), 90–111 (2008)

Haptics in Virtual Reality

Extended AirPiano: Visuohaptic Virtual Piano with Multiple Ultrasonic Array Modules

Inwook Hwang[✉] and Sungryul Yun

Electronics and Telecommunications Research Institute (ETRI),
Daejeon, Republic of Korea
{inux, sungryul}@etri.re.kr

Abstract. We developed an improved version of midair visuohaptic virtual piano utilizing multiple ultrasonic array modules. We implemented scheduling algorithm for simultaneous generation of haptic points to increase the output efficiency. Our algorithm is based on temporal switching of modulated ultrasonic signals and player draft system on multiple ultrasonic modules. With the extended AirPiano, a user can play the virtual piano in a scene shown via the HMD and can feel the haptic points on their whole fingers while touching the keys.

Keywords: Midair haptics · Virtual environment · Haptic point scheduling

1 Introduction

Mid-air haptic display allows barehand haptic interaction in a 3D space and is arising as a novel type of haptic interface. Our recent study, AirPiano showed feasibility of mid-air visuohaptic interaction using ultrasonic phased array [1]. AirPiano was developed for piano beginners to learn basic piano playing in an interesting virtual environment. Air-Piano rendered haptic feedback on user's fingertip for their keypress into focused air pressure generated by modulating ultrasound signals. In the user study, participants rated mid-air haptic feedback for their piano key stroke than the absence of haptic feedback. However, there were several limitations on the AirPiano. The haptic workspace was very small compared to the real piano. In addition, the haptic feedback was given only on fingertips, and so weak, especially when a user presses multiple keys together.

In this study, we introduce an improved version of AirPiano which was expanded using multiple ultrasonic array modules to render more number of midair haptic points simultaneously in a larger volume of workspace than those of the original AirPiano. We implemented a customized spatiotemporal scheduling to control a larger number of ultrasonic foci. Utilizing the greater number of foci, the available sites of stimuli were also enlarged from fingertips to every knuckles of fingers.

2 Generation of Multiple Haptic Points

Simultaneous representation of multiple haptic points is essential to realize natural barehand interaction in midair. However, the intensity of a haptic point is reduced with the number of concurrent haptic points. Therefore, we used two techniques based on

the characteristics of ultrasonic phased array to render more number of haptic points efficiently in a wider space at the same time.

2.1 Temporal Switching

First, we used temporal switching scheme that utilizes duty cycle of ultrasonic modulation. We drive each haptic point with ultrasonic wave modulated as on/off square wave at a frequency can be perceived as vibration (<500 Hz). The ultrasonic transducer array becomes idle during the off state, which takes the half of a cycle. We adjusted an alternating operation when we render two or more haptic points [2]. In our algorithm [3], the period of on state is reduced by the number of haptic points and the periods for each haptic point is not overlapped each other. The idle time can be removed in case of the haptic points have same modulation frequency. When the haptic points have different modulation frequencies, we adjusts the interval of on time for each haptic point to remove the overlapped on state signals between multiple points while minimizing the instant fluctuation of frequency to be below the perception threshold. The operation of temporal switching algorithm was represented in Fig. 1.
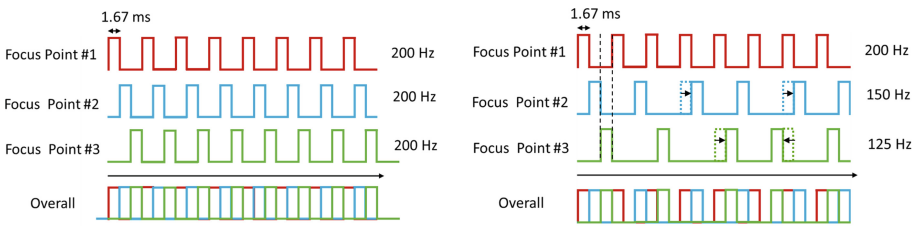
Fig. 1. Operation of temporal switching algorithm (Left: all focal points have a same modulation frequency. Right: focal points have different modulation frequencies).

2.2 Spatial Scheduling

Our previous AirPiano used a 16×16 transducer array (UHEV-1 by Ultrahaptics). The working area of the array is about 40 cm in width at 30 cm height and the stimulus intensity degrades along the distance from center on horizontal plane [4]. This workspace is not sufficient for our piano application that supports two-handed play. We tried to increase the workspace by integrating multiple transducer arrays together. Our approach is individual operation of array modules rather than a unified control of all transducers in arrays. The individual operation can reduce the computation complexity than that of the unified control method and easy to achieve the realtime performance.

Our scheme is based on a simple player draft system for haptic points in a scene [5]. In this algorithm, each transducer array module selects a haptic point with minimal rendering cost in every 'round'. The rounds continue until there is a remained point.

A cost value for every point-array pair is calculated on every update of haptic points. We used the distance between the haptic point and position for maximum output as the cost value. The form and parameters of the cost function can be modified including modulation frequency, point priority, and so on. We represented the procedure in Fig. 2. We can change the layout of transducer modules freely with the spatial scheduling.
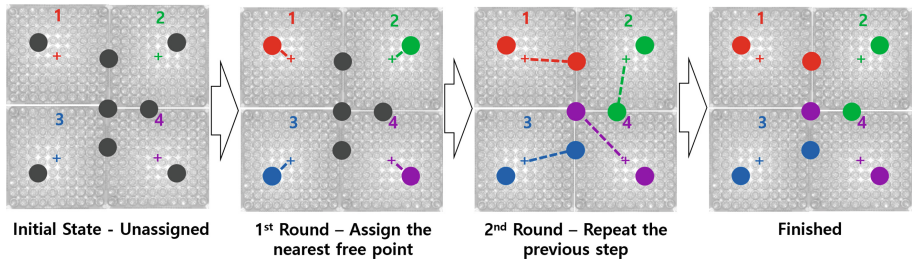

Fig. 2. An example procedure of our spatial scheduling algorithm. Colored crosses represent center of the display module.

3 Implementation

3.1 Hardware

The test system was configured with an Alienware 15″ laptop has Intel i7 CPU and Nvidia GTX1070 GPU, an Oculus Rift HMD, and four Ultrahaptics UHEV-1 ultrasonic haptic modules including a Leap Motion IR hand tracker (See Fig. 3). The haptic modules were placed on a table in 2×2 square layout to generate ultrasonic pressure in upward direction. The hand tracker was attached on the user side of the layout to capture the user's key pressing motion precisely.

3.2 Software

Virtual environments of the extended AirPiano is mostly identical to those of the original AirPiano. We used Unity 2017 to develop the virtual environment with Ultrahaptics windows SDK V2.6.0. We assigned a Unity collider on every knuckle of both hands. The update rate of virtual scene and haptic points was about 100 Hz and selected by maximum speed of hand tracking and Unity rendering. Coordinate among real world, HMD, hand tracker, and haptic modules were adjusted and calibrated.
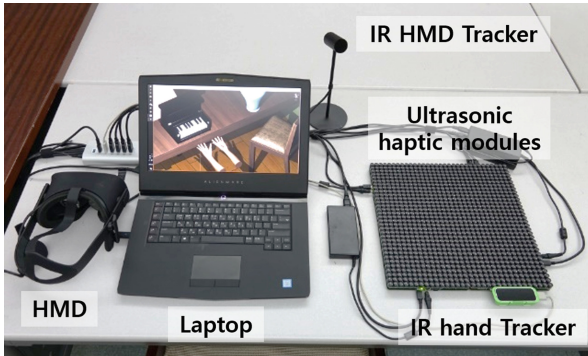
Fig. 3. Hardware setup of the extended AirPiano

4 Conclusion

We extended our previous visuohaptic virtual piano with multiple ultrasonic array modules. For the extension, we customized spatial and temporal scheduling of multiple haptic points to handle more points in a larger workspace. We do not believe that our development can fulfill the limitations of the AirPiano. The spatial scheduling is not optimal and the feedback is still too weak compared to the real keypress feeling. However, we hope that this study can show a way to improve midair haptic experience.

References

1. Hwang, I., Son, H., Kim, J.R.: AirPiano: enhancing music playing experience in virtual reality with mid-air haptic feedback. In: World Haptics Conference (WHC 2017), pp. 213–218. IEEE (2017)
2. Long, B., Seah, S.A., Carter, T., Subramanian, S.: Rendering volumetric haptic shapes in mid-air using ultrasound. ACM Trans. Graph. (TOG) **33**(6), 181 (2014)
3. Hwang, I., Seo, J.: An improved method for generating multiple focuses in non-contact ultrasonic haptic display. In: IEIE Fall Conference, pp. 831–833 (2016). (in Korean)
4. Ultrahaptics Developer site – How it works: Interaction zones and form factors. https://developer.ultrahaptics.com/knowledgebase/interaction-zones-form-factors/. Accessed 13 Aug 2018
5. Hwang, I., Seo, J.: A method for focal points scheduling on mid-air ultrasonic haptic display. In: Conference on Electronics and Information Communications, pp. 85–87 (2017). (in Korean)

Presentation of Stepping Up and Down by Pneumatic Balloon Shoes Device

Masato Kobayashi[✉], Yuki Kon[✉], and Hiroyuki Kajimoto[✉]

University of Electro-Communications,
1-5-1 Chofugaoka, Chofu, Tokyo 182-8585, Japan
{kobayashi,kon,kajimoto}@kaji-lab.jp

Abstract. In recent years, to have a realistic experience in the VR space, various study and contents employed the sense of walking. In this study, we developed a light weight shoe-type VR device for uneven height presentation using pneumatically driven balloons. While previous shoe-type walking simulation device becomes heavy, the balloon enabled light-weight wearable device. The weight of the presenting device was about 430 g on one foot and the thickness of the shoe sole when non-operation was about 1.0 cm. We report the method of presenting stepping on the stage by the shoes device.

Keywords: Locomotion device · Pneumatic balloon · Height presentation · Shoes device · VR device

1 Introduction

Virtual reality (VR) is most commonly experienced through head mounted displays (HMDs). VR contents using HMD has become common. In order to have a realistic experience in the VR space, various study and contents employed the sense of walking, by using motion platforms, tactile presentation devices or large space [1–4]. On the other hand, most of these attempts supposed to walk on a flat surface, with addition of texture feeling by vibration [5–7] or MR fluid actuator [8].

On the other hand, presentation of topographical information, such as slopes and obstacles (e.g. stairs) is quite limited. Sugihara et al. developed ALF, which presents the uneven shape of the ground by placing hexagonal actuator units on the floor [9]. Noma et al. proposed a walking device that presents slopes and steps by providing segmented stages that operate up and down in the treadmill [10]. However, in the case of such install type walking devices, there is a problem that the cost is higher compared to a simple treadmill. In contrast, Schmidt et al. developed "Level-Ups", which is a wearable device that presents differences in surface height when climbing to a stage using a mechanism that raises and lowers the sole [11]. This type of wearable device is expected to widen the range of usage, but it still has the problem of heavy weight and size of the shoe sole is excessive.

In this research, we propose a shoe-type device consisting of pneumatic balloons actuated by vacuum pumps. The pneumatic balloon enables a significant reduction in weight and sole thickness compared with conventional devices.

This paper, reports the method to present the sensation of stepping on the stage by the proposed shoes device.

2   Height Presentation Using Pneumatic Balloon Shoes

2.1   Overview of Height Presentation

Figure 1 shows the height presenting shoes using pneumatic balloons. The weight of the device was about 430 g on one foot and the thickness of the shoe sole when uninflated was about 1.0 cm, which is within the range of ordinary shoe sole. Two balloons made of thermoplastic polyurethane are arranged in the front and rear of the shoe. The balloon expands to increase the height of the shoes. On the contrary, by pulling out air with the pump, the balloon contracts and returns to its original height when air is extracted with the pump. When inflated, the shoe was approximately 5.0 cm higher without load compared with non-operation state. When loaded with 60 kg weight person, it is approximately 3.0 cm higher than the non-operation state. It took 700 ms for Balloon to expand to its maximum, which is slightly slower than normal human footsteps, but endurable for basic experiments.
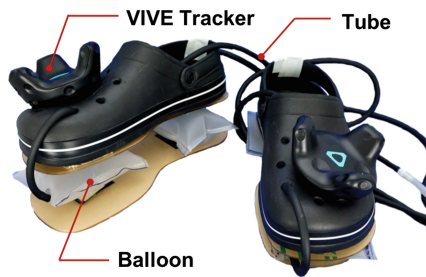
Fig. 1. Height presenting shoes using pneumatic balloons
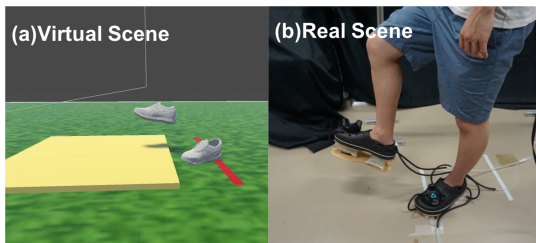
Fig. 2. State of height presentation using pneumatic balloon shoes: (a) Virtual Scene (b) Real Scene

The position and tilt of the shoe are measured using a tracking device (VIVE Tracker (2018), HTC) attached to the top of the shoe, and they are reflected to the state of foots in the VR space. The balloon is expanded at the timing when the foot comes on the stage in the VR space as shown in Fig. 2. The user perceives the height change by stepping on the inflated balloon. In the case where the foot leaves from the stage, the balloon contracts and returns to its original height.

2.2   Device Configuration

Figure 3 shows the system configuration of this device. In this system, two vacuum pumps (VP 0940, Nitto Kouki) are used for one balloon, one for exhaust and the other for intake, to achieve faster response. By controlling the solenoid valves (VX 313, SMC) connected to the vacuum pump, the state of the balloon can be changed. The inflation of the balloon is controlled by two types of atmospheric pressure sensors for positive pressure and negative pressure and a microcontroller (ESP32-DeviKitC, Espressif Systems).
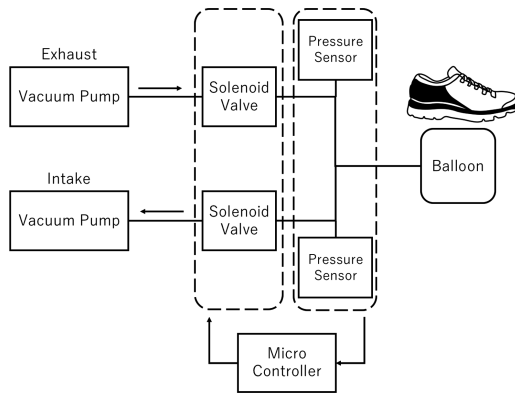
Fig. 3. System configuration of pneumatic balloon shoes

3   Conclusion

In this research, we proposed a shoe device using pneumatic balloons actuated by vacuum pumps as a method to solve the problem of excessive weight and thickness of previous shoe-type devices.

Our proposed device can present height of approximately 3.0 cm when loaded with 60 kg weight, and it is possible to dynamically present a stage in the VR experience. Current main issue is that, it takes 0.7 s to inflate the balloon to its maximum, which is a little slow for natural walking. Furthermore, we found that the softness of the balloons made the experience not realistic. Our future works include improvements of these issues, and development an application to the VR scene.

Ethical Approval. All procedures performed in studies involving human participants were in accordance with the ethical standards of the institutional and/or national research committee and with the 1964 Helsinki declaration and its later amendments or comparable ethical standards.

Informed Consent. Informed consent was obtained from all individual participants included in the study.

References

1. Iwata, H.: The torus treadmill: realizing locomotion in VEs. IEEE Comput. Graph. Appl. **19** (6), 30–35 (1999)
2. Iwata, H., Yano, H., Fukushima, H., Noma, H.: CirculaFloor [locomotion interface]. IEEE Comput. Graph. Appl. **25**(1), 64–67 (2005)
3. Virtuix Omni. http://www.virtuix.com/. Accessed 01 Aug 2018
4. Razzaque, S., Kohn, Z., Whitton, M.C.: Redirected walking. In: Proceedings of EUROGRAPHICS, vol. 9 (2001)
5. Kim, T., Cooperstock, J.R.: Enhanced pressure based multimodal immersive experiences. In: Proceedings of the 9th Augmented Human International Conference (2018)
6. Nordahl, R., Berrezag, A., Dimitrow, S., Turchet, L., Hayward, V. and Serafin, S.: Preliminary experiment combining virtual reality haptic shoes and audio synthesis. In: Kappers, A.M.L., van Erp, J.B.F., Bergmann Tiest, W.M., van der Helm, F.C.T. (eds.) International Conference on Human Haptic Sensing and Touch Enabled Computer Applications, pp. 11–16. Springer, Heidelberg (1997)
7. Visell, Y., Law, A., Cooperstock, J.R.: Touch is every where: floor surfaces as ambient haptic interfaces. IEEE Trans. Haptics **2**(3), 148–159 (2009)
8. Son, H., Gil, H., Byeon, S., Kim, S., Kim, J.R.: RealWalk: feeling ground surfaces while walking in virtual rality. In: Extended Abstracts of the 2018 CHI Conference on Human Factors in Computing Systems, D400, pp. 01–04 (2018)
9. Sugihara, T., Miyasato, T.: The terrain surface simulator ALF (ALive! Floor). In: Proceedings of VRSJ ICAT 1998, pp. 170–174 (1998)
10. Noma, H., Sugihara, T., Miyasato, T.: Development of ground surface simulator for Tel-E-Merge system. In: IEEE-Virtual reality 2000 Conference, pp. 217–224 (2000)
11. Schmidt, D., Kovacs, R., Mehta, V., Umapathi, U., Kohler, S., Cheng, L., Baudish, P.: Level-Ups: motorized stilts that simulate stair steps in virtual reality. In: Proceedings of the 33rd Annual ACM Conference on Human Factors in Computing Systems, pp. 2157–2160 (2015)

VR Training System of Step Timing for Baseball Batter Using Force Stimulus

Wataru Sakoda[1(✉)], Toshio Tsuji[1], and Yuichi Kurita[1,2]

[1] Hiroshima University, 1-4-1 Kagamiyama, Higashihiroshima City,
Hiroshima 739-8527, Japan
{watarusakoda,ykurita}@hiroshima-u.ac.jp, tsuji@bsys.hiroshima-u.ac.jp
[2] JST PRESTO, Tokyo, Japan
http://www.bsys.hiroshima-u.ac.jp/en
http://www.jst.go.jp/kisoken/presto/en/index.html

Abstract. Conventionally, correct motion in sports training and rehabilitation has been taught directly from a trainer. However, oral or gesture presentations are difficult based on what the trainer considers to be the accurate motion. We propose a motion timing presentation method using force stimulus, which has high relevance to the target motion. In this study, we developed a timing presentation training system for a baseball batter using force stimulus. The force stimulus is presented according to the pitching motion reproduced on a virtual reality (VR) system to present the timing stimulus repeatedly. The stimulus is used for presenting the timing of the initial foot step motion, which is the first phase of batting. For verification of the timing presentation effect of the training system, we measured the initial batting timing of the baseball beginner. As a result, it was found that the foot step could be started very close to the target timing using force stimulus presentation.

Keywords: Force stimulus · Motion timing presentation ·
VR training system · Baseball · Pneumatic Gel Muscle

1 Introduction

Presentation of correct motion timing is an effective method to efficiently acquire a target motion in sports training and rehabilitation. Correct motion has been taught directly by trainers, but it is difficult for trainers to teach the player exactly what he really wants to tell. Moreover, there are methods of presenting correct motion or motion timing using sensory stimulus. Fothergil [1] proposed a visual feedback method that presents the correct trajectory of the rowing motion. Yoshihiro [2] presented rhythmic auditory stimulus to Parkinson's patients to teach the correct timing for walking. Spelmezan [3] proposed a motion instruction method using a vibro-tactile suit during snowboard practice. Because the tactile stimulus is directly presented to the target site, it is possible to instruct a detailed motion compared to simple visual or auditory stimulus. Although visual,

auditory, and tactile stimuli can be presented in real time and as intended, these stimuli are not all directly related to the target motion; therefore, it is necessary for the player to consciously link the stimulus information and the target motion.

Thus, we propose a motion timing presentation method using force stimulus. In a previous study, Hayakawa et al. [4] developed a force tactile interface to prompt early acceleration by raising a driver's seat. A driver can perform the target motion naturally because the motion to foot off the accelerator and the motion raising the seat are almost the same motion. Presentation of force stimulus can directly teach the direction of a motion, so the relationship between stimulus and target motion is strong. We expect that presentation of force stimulus will provide a high learning effect in training and rehabilitation without restricting vision and hearing. Then, when stimulus presentation is used to teach motion timing, reaction time from the stimulus is an important factor. Our previous study suggested that the reaction time to force stimulus and its standard deviation are not inferior to the reaction time to other stimuli [5]. Therefore, force stimulus can be used as a motion timing presentation without problems. We developed a timing presentation training system for a baseball batter using force stimulus. The system was developed by combining force stimulation and virtual reality (VR) simulation created as shown in Fig. 1.

In this paper, we describe the overview of the system and the experiments performed.
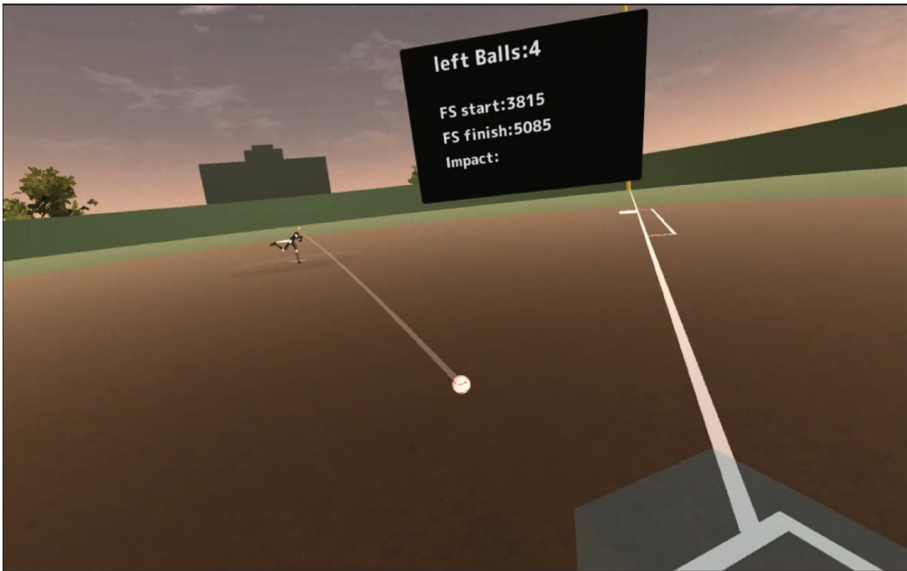
Fig. 1. VR batting simulation

2   VR Batting Simulation

2.1   Overview of VR Simulation Creation

There has been growing interest in VR training in sports. Two Japanese professional baseball teams introduced VR training systems for batting practice. These systems can select any pitcher or ball type, any number of times using accumulated data and to produce a highly immersive experience.

We also created a pitching animation using Unity (Unity 2018.2) to reproduce the same pitching motion and ball movement. The pitching animation is created using pitching motion data provided by one baseball expert who acquired pitcher data by an optical motion capture system. The release point, arrival point, and ball speed are set by a script. When the impact timing and the ball arrival time are close, a hitting animation is displayed. Impact timing is defined as the time when the bat passes between a laser and a photodiode.

2.2   Evaluation Index

Timing skill and bat control skill are important to hit a ball accurately. Timing skill enhances the time accuracy of swinging at the same time as the ball arrives and the bat control skill enhances the spatial accuracy of hitting the ball at the correct position on the bat. Among these two skills, this study focused on the timing skill. Impact time is affected by three batting timing phases: "foot step start (FS start)," "foot step finish (FS finish)" and "Swing start".

In the VR batting simulation, "FS start" is defined as the elapsed time from the start of the pitching motion until foot switches are released and "FS finish" is defined as the elapsed time from the start of the pitching motion until the switches are pushed after FS start. In this study, we did not develop a system to measure "Swing start" yet. As the first step, we decided on FS start as an evaluation index.

3   Comparison of FS Start Between Expert and Beginner

In this experiment, we compared FS start of an expert and a beginner to investigate the characteristics of start timing in both types of swings.

3.1   Method

Participants: One baseball expert (23 years old) and one baseball beginner (23 years old). Apparatus: A plastic bat (76 [cm], 250 [g]). A head mount display (HMD) and shoes with foot bottom switches. Experimental design: Measure FS start for five swings. The interval between tasks is set to 10 [s]. Before the task, we allow 5–10 practice swings. Then, we calculate the average and standard deviation (SD) of FS start for both participants. This study was conducted in accordance with the Declaration of Helsinki. We obtained informed consent, and asked the health condition in verbally by the subjects.

(a)Average of FS start
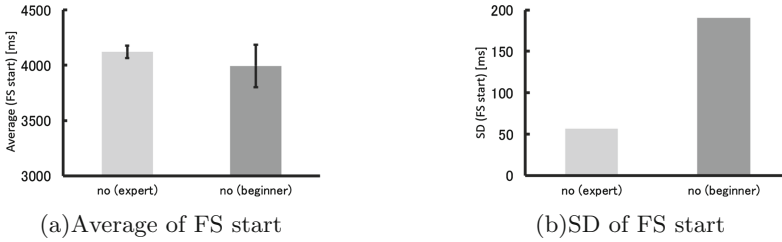
(b)SD of FS start

Fig. 2. Comparison of FS start between expert and beginner. "no" means no force stimulus is used.

3.2   Result

As shown in Fig. 2(a), the averages of FS start were approximately 4.0 [s] and there was no significant difference. The pitching motion when FS start is 4.0 [s] indicates the timing to start lowering the stepping foot. Figure 2(b) shows the beginner's SD of FS start was more than three times greater than the expert's.

3.3   Consideration

From the results, we deduce that the expert starts the swing motion from a certain fixed timing of the pitching motion. On the contrary, the beginner does not have enough batting experience, so he follows no rule on when to start the swing. Thus, we developed a training system to acquire a consistent FS start.

4   VR Training System for Batter's Timing Skill

Figure 3 shows an overview of the developed system. This system consists of the following devices: HMD, two Pneumatic Gel Muscles (PGMs) developed by Daiya Industry Co., Ltd. as actuators for the force stimulus presentation, a

(a)Overview

(b)Implementation
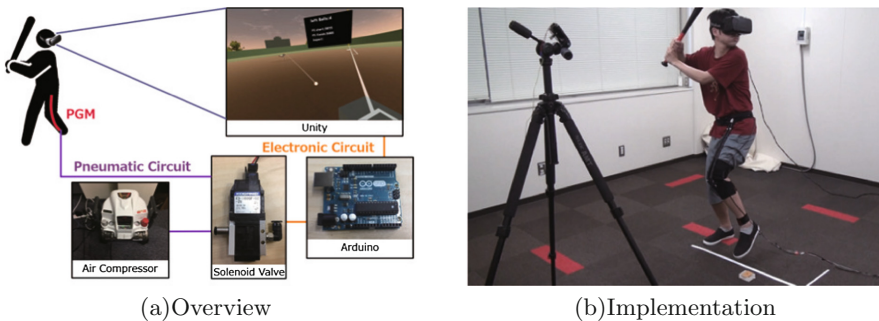
Fig. 3. VR training system

pneumatic compressor, a solenoid valve to switch the supply of air from the compressor to the PGMs, foot bottom switches, a photodiode, a laser, a microcomputer (Arduino) that controls the ON/OFF of solenoid valve using information received with Unity and transmits sensor information to Unity. The solenoid valve is opened after the set time to contract the PGMs arranged along the rectus femoris muscle. Contraction of the PGMs urges the FS start motion.

5   Evaluation of Timing Presentation Effect Using Force Stimulus

As the developed training system is aimed at improving the timing skill, it is desirable that the target motion be performed at the target timing. We measured FS start when force stimulus is presented and compared it with the usual FS start to evaluate the motion timing presentation effect of force stimulus.

5.1   Method

Participants: The same baseball beginner. Apparatus: A plastic bat. HMD and shoes with the switches. Experimental design: Measure FS start for five swings. The interval between tasks is set to 10 [s]. The force stimulus is presented 3.0, 3.2, 3.4, 3.6, 3.8, and 4.0 [s] after the start of the pitching motion. This condition is set with reference to the expert's FS start measured in the previous experiment.

(a)Average of FS start

(b)SD of FS start
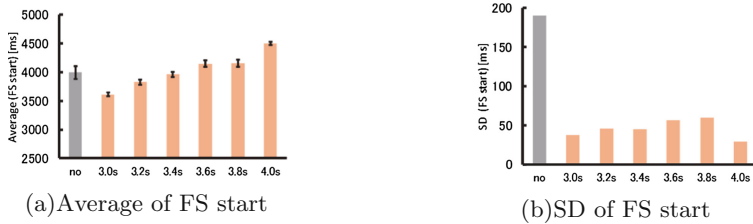
Fig. 4. Comparison of beginner's FS start between normal and force stimulus presentations. The stimulus is presented after 3.0, 3.2, 3.4, 3.6, 3.8 and 4.0 [s] from the pitching motion start.

5.2   Results

Figure 4 shows the results of the previous and current experiments. From Fig. 4(a), it is understood that the SD of FT start is reduced to approximately 75 % of the original SD by the timing presentation using force stimulus. In addition, as shown in Fig. 4(b), most FS start which presented force stimulus has achieved after approximately 500–600 [ms] from stimulus presentation.

5.3   Consideration

Based on the results of this experiment, it was suggested that by the presentation of force stimulus, a beginner can learn to swing with a stable FS start. Most FS started after approximately 500–600 [ms] from stimulus presentation. This result represents the total reaction time to the force stimulus and the movement time from the start of motion to release of the foot bottom switches. There was no large variation in reaction time to the force stimulus and movement time, and it was possible to experience a highly reproducible swing motion.

It remains a challenge for future research to examine the training effect of this system by observing any change in FS start during training and at some later point in time without further training.

5.4   Conclusion

We developed a training system for a batter's foot timing skill using force stimulus. In conclusion, the results indicate that by force stimulus presentation, a beginner's foot step could be started almost as intended. The developed training system can be expected to be effective for acquiring a stable swing for beginners who have a significant SD in FS start. In the future, we will investigate impact timing evaluation and training effects on impact timing. In addition, we plan to design a system that presents FS finish and swing start timing.

References

1. Fothergill, S.: Examining the effect of real-time visual feedback on the quality of rowing technique. Procedia Eng. **2**(2), 3083–3088 (2010)
2. Yoshihiro, M.: Interpersonal synchronization of body motion and the walk-mate walking support robot. IEEE Trans. Robot. **24**(3), 638–644 (2009)
3. Spelmezan, D.: An investigation into the use of tactile instructions in snowboarding. In: Proceedings of the 14th International Conference on Human-Computer Interaction with Mobile Devices and Services, pp. 417–426 (2012)
4. Hayakawa, M.: Haptic interface to encourage preparation for a deceleration behavior against potential collision risk. In: SICE Annual Conference (2013)
5. Sakoda, W., et al.: Investigation of efficacy of force stimuli for motion timing display -Comparison with visual, auditory, and vibration stimuli-. In: The Robotics and Mechatronics Conference (2018)

Shape and Stiffness Sensation Feedback with Electro-Tactile and Pseudo-Force Presentation When Grasping a Virtual Object

Vibol Yem[1(✉)], Yasushi Ikei[1], and Hiroyuki Kajimoto[2]

[1] Tokyo Metropolitan University, Hino, Tokyo, Japan
{yem,ikei}@vr.sd.tmu.ac.jp
[2] The University of Electro-Communications, Chofu, Tokyo, Japan
kajimoto@kaji-lab.jp

Abstract. We developed a 3D virtual reality system with electro-tactile and pseudo force stimulation for presenting sensation of shape and stiffness of an object to the tips of thumb and index finger. Our system comprises two fingertip gloves and a finger-motion capture device. Each glove provides a shape sensation via an electrode array of the electro-tactile display and pseudo-force sensation via asymmetric vibration of a DC motor. In our demo experience, participants can grasp a 3D virtual object and perceive both tactile feedback on the fingertips and visual feedback of rigid or deformable shape of the objects showing on the monitor. Our previous study confirmed that the initial vibration amplitude, which represents the reaction force when the thumb and the index finger initially contact the surface of an object, effects to the intensity of stiffness perception. In the demo, we design several kinds of initial vibration amplitude, shape, and shape deformation for different perception of shape and stiffness.

Keywords: Stiffness · Shape sensation · Pseudo force ·
Motor-rotational acceleration · VR interaction

1 Introduction

Shape and stiffness are an important material property that we always sense both of them at the same time when we grasp an object. To reproduce the sensation of grasping, a haptic device must produce a sensation of contact area sensation and a sensation of force that simulates backward extension of the fingertip. Mechanical pin array and electrode array have widely studied for presenting shape sensation [1, 2]. Electro-tactile device achieves high responsiveness and light weight by comparing to the mechanical pin array. Kajimoto [2] designed a cylindrical tactile device that can present shape sensation to the palm via an electrode array. However, the undeformable cylindrical device limits the finger's movement and the intensity of stiffness. Some techniques involved mechanical grounded actuators [3, 4] whereas others comprised wearable robotic mechanisms [5, 6] to provide a grasping feedback sensation in which the fingertips are physically pushed in a backward-extension movement. However, these devices use physical force that are often large and heavy.

Our previous study found that a DC motor could produce an illusionary rotational force sensation when the input voltage was asymmetric (i.e. saw tooth waveform) [7]. We also mounted DC motors to the backside of the thumb and index finger and confirmed that the pseudo-force sensation occurred in each finger, which can be applied for grasping sensation feedback [8]. We also confirmed that a stronger initial vibration which represented the reaction force when the thumb and index finger contacted the surface of the object, represented materials that were harder and more rigid [9]. In this study, we attempted to present both shape and stiffness of a 3D virtual object with the combination of an electrode array and pseudo-force perception produced by a DC motor.

2 System

2.1 Fingertip Glove

The fingertip glove comprises an electrode array and a DC motor (Maxon, 118396) as shown in Fig. 1 (left). The glove that is used for attaching an electrode array and the DC motor to the fingertip was made from titanium using a three-dimensional printer. More detail about the hardware of electro-tactile display and DC motor drivers can be found in [2] and [9].
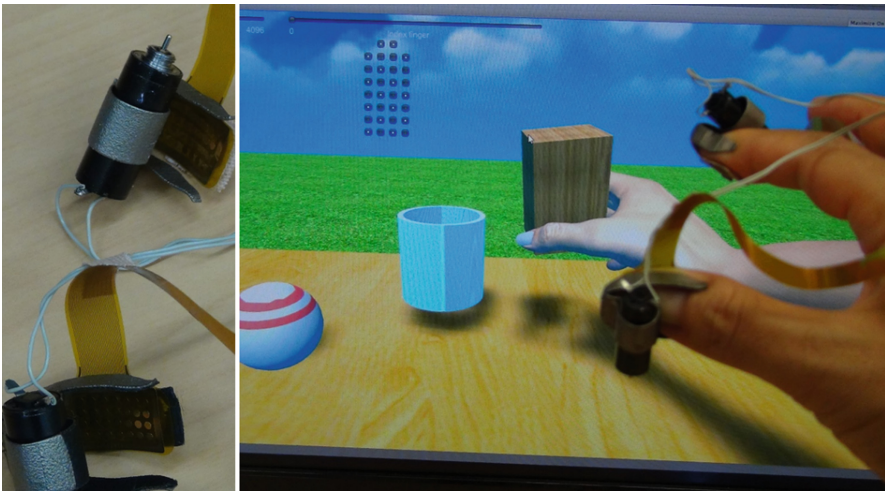
Fig. 1. Fingertip glove comprising an electrode array and a DC motors (left). A 3D virtual reality system that uses electro-tactile and pseudo-force perception via DC motor rotational acceleration to present shape and stiffness feedback sensations to the tips of the thumb and index finger during grasping of a virtual object (right).

2.2 Presentation Algorithm

In the virtual environment, we attached an invisible virtual electrode array to the tip of each virtual fingertip. When each finger touches the surface of an object, some of electrodes on the virtual fingertip contact to or get inside the surface of the virtual object. We synchronized the position of electrodes in the virtual environment to the real electrodes and we present the contact area by stimulating the contact electrodes.

When the user attempts to touch or grasp a virtual object, the user's virtual fingers can easily move inside that virtual rigid body if there is no physical force to resist the fingers. This is a common issue for every wearable haptic device because the movement of virtual fingers in a virtual environment follows the position of the fingers in the real world, as measured via a motion capture device. To solve this issue, we developed an algorithm in which we make the virtual fingers of actual position invisible and show the modified fingers moving on the surface of the object when the actual finger get inside the object (Fig. 2). We determined the strength of the force feedback on the fingertips according to the vibration amplitude of the input voltage. This amplitude is proportional to the total distance that the thumb and index finger move inside the object. The amount of deformation of the virtual surface were also proportional to this distance value. More detail about pseudo-force and visual feedback algorithm can be found in [9].

Deformation: $\Delta d = |d_b - d_a| = |D_b - D_a|$
Distance inside the object: $\Delta x = \Delta x_{index} + \Delta x_{thumb}$
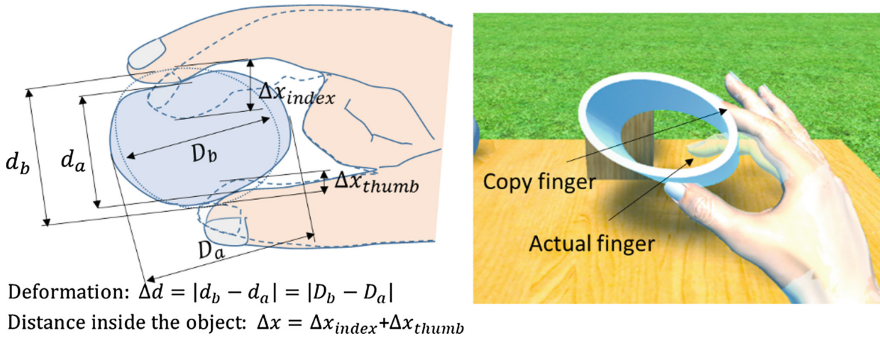
Fig. 2. The algorithm for maintaining thumb and index finger contact with the surface of the virtual object and deformation of the virtual object when grasping (left), When the user's virtual fingers entered the rigid virtual object in the virtual environment (left), we made them invisible and showed copy fingers grasping the surface of the object (right).

3 Demo Experience and Conclusion

We developed a system in which we use electrode arrays and DC motors to deliver the electro-tactile and pseudo-force sensation to the tips of the thumb and index finger. Electro-tactile stimulation is for presenting shape sensation and pseudo-force is for stiffness sensation. In the demo, participants can experience grasping sensation feedback of several virtual objects with different shape and stiffness intensity. Our future

work will conduct a psychological experiment for reveal the parameters that allow our fingertip glove to reproduce grasping sensation more realistic.

Ethical Approval. All procedures performed in studies involving human participants were in accordance with the ethical standards of the institutional and/or national research committee and with the 1964 Helsinki declaration and its later amendments or comparable ethical standards.

Informed Consent. Informed consent was obtained from all individual participants included in the study.

References

1. Wall, S.A., Brewster, S.: Sensory substitution using tactile pin arrays: human factors, technology and applications. J. Sig. Process. **86**(12), 3674–3695 (2006)
2. Kajimoto, H.: Design of cylindrical whole-hand haptic interface using electrocutaneous display. In: Euro Haptics 2012, 12–15 June, vol. 2, pp. 67–72 (2012)
3. Ma, K.Z., Ben-Tzvi, P.: RML glove - an exoskeleton glove mechanism with haptics feedback. IEEE/ASME Trans. Mechatron. **20**(2), 641–652 (2015)
4. Choi, I., Hawkes, E.W., Christensen, D.L., Ploch, C.J., Follmer, S.: Wolverine: a wearable haptic interface for grasping in virtual reality. In: Proceedings of IEEE/RSJ Intelligent Robots and Systems (IROS), pp. 986–993 (2016)
5. Liu, J., Song, A., Zhang, H.: Research on stiffness display perception of virtual soft object. In: Proceedings of IEEE International Conference Information Acquisition (ICIA), pp. 558–562 (2007)
6. Nojima, T., Sekiguchi, D., Inami, M., Tachi, S.: The SmartTool: a system for augmented reality of haptics. In: Proceedings IEEE Virtual Reality (VR), pp. 67–72 (2002)
7. Yem, V., Okazaki, R., Kajimoto, H.: Vibrotactile and pseudo force presentation using motor rotational acceleration. In: Proceedings of Haptics Symposium, pp. 47–51 (2016)
8. Sakuragi, R., Yem, V., Kajimoto, H.: Pseudo force presentation to multiple fingers by asymmetric rotational vibration using a motor: consideration in grasping posture. In: Proceedings of World Haptics Conference, pp. 305–309 (2017)
9. Yem, V., Kajimoto, H.: A Fingertip glove with motor rotational acceleration enables stiffness perception when grasping a virtual object. In: Proceedings of HCI International Conference (2018)

Whole Body Haptic Experience Using 2D Communication Wear

Kohki Serizawa[1]([✉]), Yuichi Masuda[1], Shun Suzuki[1],
Masahiro Fujiwara[1], Akihito Noda[2], Yasutoshi Makino[1],
and Hiroyuki Shinoda[1]

[1] Graduate School of Frontier Science, The University of Tokyo, Tokyo, Japan
{serizawa,masuda,suzuki}@hapis.k.u-tokyo.ac.jp,
Masahiro_Fujiwara@ipc.i.u-tokyo.ac.jp,
{yosutoshi_makino,hiroyuki_shinoda}@k.u-tokyo.ac.jp
[2] Department of Mechatronics, Nanzan University, Nagoya, Japan
anoda@nanzan-u.ac.jp

Abstract. In recent years, a two-dimensional communication (2DC) technology has been proposed which performs communication and power supply with a large number of functional sensor/actuator units attached on cloth without individual connection. It is easy to make wearable system by using the 2DC cloth. Many vibrators can be attached at any place on the sheet to realize whole body tactile displaying wear. Various tactile expressions can be achieved on the whole body such as being stroked, pressed, grabbed, and so on. In this research, we propose a VR system which enables a user to be touched his/her body synchronized with VR images by using the whole body haptic wear. Users can experience various tactile sensations to their whole body through easily wearable garment device.

Keywords: Virtual reality · Wearable device · Whole body tactile display · Two-dimensional communication

1 Introduction

In this paper, we propose a Full-body Touch Sensation System (FTSS) that enables a user to feel being touched sensation for his/her whole body (Fig. 1). In FTSS, users can intuitively control their own avatars displayed in a VR space. When an operator touch the avatar in the VR space, the user feels vibratory sensation through the whole body haptic wear. For enriching a whole body tactile experience, a variety of tactile expressions such as "stroked", "touched", "grabbed" and so on, is required. In order to realize these sensations, the sufficient spatial resolution of the vibrators is considered to be important. However, in general, attaching many vibrators on clothes need a large number of wires, which results in less comfortable for wearing.

There have been some previous studies that put many vibrators on a cloth as one of the tactile displaying methods over the whole body [1, 2]. In those cases, the cumbersome wires are connected. Some studies tried to connect vibrators through the conductive thread line on a cloth [3]. In those studies, the sensor/actuator elements
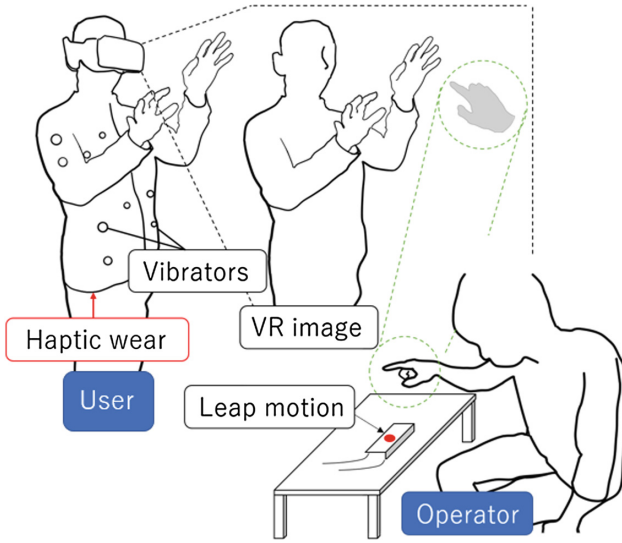
Fig. 1. System overview

must be arranged at the designated position on the cloth. In FTSS, we can attach many vibrators on a cloth without connecting individual wires by using a wearable two-dimensional communication (2DC) technology. Many vibrators attached on the 2DC wearable sheet can communicate with a host machine through the sheet. In addition, their electrical power is supplied through the same sheet [4]. In this study, we combine the wearable vibratory wear with virtual images as shown in Fig. 1. Whole body haptic experience can improve the reality of VR environment.

2   Prototype

2.1   Wearable 2DC

Figure 2 shows an example of implementation of whole body haptic wear using wearable 2DC. In the wearable 2DC, the sheet in which conductive fibers are embroidered on each surface of the base non-conductive fabric is used as a medium for communication and energy feeding. Since the conductive surfaces on each side of the sheet are insulated from each other, two independent current paths are formed on both sides of one cloth. A vibratory unit is connected to each side of the sheet by piercing like a pin badge. In this prototype, we confirmed that more than 10 vibrators can be activated independently.

2.2   Interaction with Avatar in VR Space

In our prototype, we measured user's motion by using Kinect, whose API allows to extract body skeletal information. An operator can touch this avatar in VR space by

Fig. 2. Whole body haptic wear

measuring his/her hand with Leap Motion. The user can be touched by the operator in VR space with vibratory feedback sensation through the whole body haptic wear.

References

1. Lindeman, R.W., Page, R., Yanagida, Y., Sibert, J.L.: Towards full-body haptic feedback: the design and deployment of a spatialized vibrotactile feedback system. In: Proceedings of ACM Virtual Reality Software and Technology (VRST), pp. 146–149 (2004)
2. Bloomfield, A., Badler, N.: Collision awareness using vibrotactile arrays. In: IEEE Virtual Reality Conference, pp. 163–170 (2007)
3. Schiphorst, T., Jaffe, N., Lovell, R.: Threads of recognition: using touch as input with directionally conductive fabric. In: Proceedings of the SIGCHI Conference on Human Factors in Computing Systems, Portland, Oregon, USA (2005)
4. Noda, A., Shinoda, H.: Frequency-division-multiplexed signal and power transfer for wearable devices networked via conductive embroideries on a cloth. In: 2017 IEEE MTT-S International Microwave Symposium, pp. 1–4 (2017)

Towards Automatic Synthesis of Motion Effects

Sangyoon Han[1(✉)], Jaebong Lee[2], and Seungmoon Choi[1]

[1] Pohang University of Science and Technology,
Pohang, Gyeongbuk 37673, South Korea
`{han0209,choism}@postech.ac.kr`
[2] NVIDIA, Santa Clara, USA
`jaebongl@nvidia.com`
`http://hvr.postech.ac.kr`

Abstract. Motion effects are a key component to improve users' immersiveness in 4D contents and virtual reality. However, the production of motion effects is still very labor-intensive and time-consuming. In this demonstration, we present synthesis algorithms which generate motion effects by analyzing the audiovisual content of 4D ride and films. Our synthesis algorithm provide compelling multimedia experiences to viewers while greatly improving the productivity.

Keywords: 4D film · Multi-sensory theater · Motion simulator ·
Motion cueing · Motion effects · Synthesis · Automatic generation

1 Introduction

Motion effects elicit responses from the human vestibular system to the linear acceleration and angular velocity applied to the body. Traditionally, motion effects have been used for simulators, e.g., flight simulators for pilots and astronauts, to present physically accurate vestibular feedback. At present, we have greatly wider use of motion effects for entertainment purposes, such as 4D rides in amusement parks, 4D films in theaters, and relatively new virtual reality (VR) games with head-mounted displays (HMDs) and personal platforms. However, the production of motion effects is done solely by manual authoring or coding, and this costly process prevents the faster and wider dissemination of 4D content. It is imperative to facilitate 4D effect production by providing automatic synthesis algorithms.

In this demonstration, we present automatic algorithms that generate motion effects by analyzing the audiovisual content of 4D rides and films. Such automatic algorithms can greatly facilitate 4D effects production. While watching 4D rides and films, users can experience compelling 4D effects using a motion chair.

In Sect. 2, we classify motion effects into four classes. In Sect. 3, we design synthesis algorithms for three classes which account for almost all of motion effects.

2 Taxonomy of 4D Effects

We interviewed three experienced 4D effects designers and analyzed 2278 4D effects displayed with 10 regular films. Then we classified them into the following four categories according to their characteristics.

Camera Motion Class (C): Motion effects are generated based on camera motion. On average, 20% of motion effects classified as C effects.

Object Motion Class (O): Motion effects track the movement of an object of interest in a scene. Approximately 62% of motion effects corresponded to O effects.

Impulse and Vibration Class (V): Motion effects respond to impacts or vibrations in the scene, such as gun fires, explosions, and vehicle vibrations. V class accounted for about 20% of motion effects.

Context Class (T): Sensory information does not provide direct clues for motion, but motion effects are based on the semantic understanding of the designer's scene. For example, when a scene tightly zooms in a car driver pushing the accelerator, motion feedback is provided to back to simulate the expected movement of the car. Less than 3% of motion effects were classified as T class.

Combined motion effects of multiple classes are also used frequently. For example, to simulate the motion of a gliding plane under enemy fire, impulsive V effects can be added to smooth O effects.

3 Synthesis Algorithms

Our synthesis algorithm assume that audiovisual stream of a film are segmented and the class (C, O, or V) of motion effects to make is given. Our algorithms for C and O effects use video as a source (Sects. 3.1 and 3.2) and our algorithm for V effects uses sound (Sect. 3.3). The overall flow of our synthesis algorithms is illustrated in Fig. 1. The motion effects synthesized by each algorithm are combined, and are generally high quality, even comparable to manually-made motion effects (see user studies in [3] and [2]).
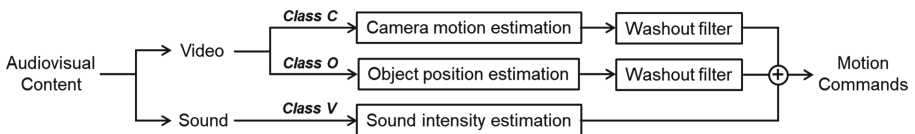
Fig. 1. Flow of the automatic synthesis algorithms.

3.1   Synthesis of Camera Motion Effects

The goal of this synthesis algorithm, Algorithm C [3], is to synthesize class C motion effects that respond to the dynamic camera motion in point-of-view shots. Algorithm C consists of two phases: estimating camera motion from video sequences and mapping the estimated camera motion to 4D chair motion. The first phase computes the relative angular velocities and linear accelerations of a virtual camera between consecutive frames using the epipolar constraint. The overall procedure is optimized to synthesize plausible motion effects for viewers. The second phase determines position and orientation commands to a 4D chair from the estimated camera motion. To this end, we use a washout filter [4], a standard high-pass filter for motion simulation with proven convergence property to the initial state.

3.2   Synthesis of Object Motion Effects

The goal of this synthesis algorithm, Algorithm O [2], is to synthesize class O motion effects that respond to the movement of an object of interest in the scene. We design Algorithm O based on viewer-centered rendering strategy which aligns the chair's motion with that of the view's visual attention. This algorithm consists of two phases: estimating the object position on the 2D screen and mapping the object position to the 4D chair motion. The first phase estimates the 2D position of an object which is selected to be tracked by 4D designers. The second phase determines position and orientation commands to 4D chair from the object movement. We also use a washout filter as described in Sect. 3.1.

3.3   Synthesis of Impulse and Vibration Effects

The goal of this synthesis algorithm, Algorithm V [2], is to synthesize class V motion effects that respond to the events that involve impulses and vibrations such as gunfire, collision, explosion, and engine vibration. These events are usually involve sound effects that are perceived rougher and louder than ambient sound or background music. So we can detect these events by analyzing the perceptual characteristics of sound. We use the computational model presented in [1] to calculate the perceptual intensity of sound and map it to motion effects. When the intensity is larger than a certain threshold, the motion effects are generated based on the intensity and duration of the detected events.

4   Conclusion

In this paper, we have presented automatic synthesis algorithms for motion effects. Our algorithms automatically generate motion effects by analyzing the direct cues from audiovisual content. The automatically generated motion effects provide guidelines for the production of motion effects, resulting in for 4D effect designers to save their time, as well as the motion effects give viewers a compelling multimedia experience. We expect that this demonstration will provide users an exciting experience with various immersive contents, including VR.

References

1. Lee, J., Choi, S.: Real-time perception-level translation from audio signals to vibro-tactile effects. In: Proceedings of the SIGCHI Conference on Human Factors in Computing Systems, pp. 2567–2576. ACM (2013)
2. Lee, J., Han, B., Choi, S.: Interactive motion effects design for a moving object in 4D films. In: Proceedings of the 22nd ACM Conference on Virtual Reality Software and Technology, pp. 219–228. ACM (2016)
3. Lee, J., Han, B., Choi, S.: Motion effects synthesis for 4D films. IEEE Trans. Vis. Comput. Graph. **22**(10), 2300–2314 (2016)
4. Nahon, M.A., Reid, L.D.: Simulator motion-drive algorithms-a designer's perspective. J. Guidance Control Dyn. **13**(2), 356–362 (1990)

Correction to: LinkGlide: A Wearable Haptic Display with Inverted Five-Bar Linkages for Delivering Multi-contact and Multi-modal Tactile Stimuli

Miguel Altamirano Cabrera and Dzmitry Tsetserukou

Correction to:
Chapter "LinkGlide: A Wearable Haptic Display
with Inverted Five-Bar Linkages for Delivering
Multi-contact and Multi-modal Tactile Stimuli" in:
H. Kajimoto et al. (Eds.): *Haptic Interaction*, LNEE 535,
https://doi.org/10.1007/978-981-13-3194-7_33

In the original version of the book, the given name and surname of the first author were identified incorrectly in chapter 33. The author's given name is Miguel and surname is Altamirano Cabrera.

The online version of the chapter has been corrected.

Author Index